Title
Observers with performance guarantees and robustness to measurement noise for linear systems

Author
Li, Yuchun

Publication Date
2016

Peer reviewed|Thesis/dissertation

UNIVERSITY OF CALIFORNIA
SANTA CRUZ

Observers with performance guarantees and robustness to measurement noise for linear systems

A dissertation submitted in partial satisfaction of the requirements for the degree of

DOCTOR OF PHILOSOPHY

in

COMPUTER ENGINEERING

by

Yuchun Li

September 2016

The Dissertation of Yuchun Li
is approved:

Professor Ricardo G. Sanfelice, Chair

Professor Gabriel H. Elkaim

Professor Dejan Milutinovic

Professor Qi Gong

Tyrus Miller
Vice Provost and Dean of Graduate Studies

Table of Contents

List of Figures vi

List of Tables viii

List of Symbols ix

Abstract xii

Dedication xiv

Acknowledgments xv

1 Introduction **1**
- 1.1 Luenberger observer and its tradeoff 7
- 1.2 An observer with extra information 11
- 1.3 Observer with intermittent information 18
- 1.4 A brief overview of Kalman filter 20
- 1.5 Contributions and organization 21

2 Preliminaries **26**
- 2.1 Graph and Networks 26
- 2.2 Hybrid Systems 27

3 Pair of Coupled Observers for Improved Performance and Robustness **31**
- 3.1 Configuration and basic properties 31
- 3.2 Design of coupled pair of observers 42
  - 3.2.1 Rate of convergence as an inequality constraint 44
  - 3.2.2 Bound of H_∞ gain as an inequality constraint 46
  - 3.2.3 Minimization of the H_∞ norm under a rate of convergence constraint 48
- 3.3 Summary 51

4 Finite-time Convergent Observer **52**
4.1 Nominal Finite-time Convergence 52
4.2 Robust finite-time convergent hybrid observer 57
4.3 Simulation results 73
4.3.1 Piecewise-constant noise with unmodeled dynamics 73
4.3.2 General noise with recursive jumps 74
4.3.3 An application to a mass-spring system 77
4.4 Summary 79

5 Distributed Estimation with Continuous Information Transmission **80**
5.1 Observer structure and basic properties 81
5.2 $\mathcal{KL}$ characterization of performance and robustness 84
5.3 Design via feasibility/optimization problems 92
5.3.1 Rate of convergence and H_∞ gain in terms of matrix inequalities 93
5.3.2 Minimization of H_∞ norm under rate of convergence constraint with fixed connectivity graph 96
5.3.3 Minimization of H_∞ norm under rate of convergence constraint with optimized connectivity graph 103
5.4 A sufficient condition guaranteeing smaller local H_∞ gain 107
5.5 Consensus of the estimates in the nominal case 111
5.6 Summary 113

6 Dynamic Consensus for Distributed Estimation **115**
6.1 A motivational example 116
6.2 A dynamic consensus algorithm for distributed state observers . . 120
6.2.1 Problem statement 120
6.2.2 Distributed consensus algorithm 122
6.3 Design using optimization formulation 125
6.3.1 Decoupled design 125
6.3.2 Joint observer-consensus design 129
6.4 Summary 133

7 Distributed Estimation with Intermittent Information Transmission **134**
7.1 Observer configuration 135
7.2 Synchronous communication events 137
7.2.1 Hybrid modeling 137
7.2.2 Design of parameters via LMIs 150
7.2.3 Robustness to measurement and communication noise . . . 158
7.3 Asynchronous and heterogeneous communication events 164
7.3.1 Hybrid modeling 164

7.3.2 Properties of solutions 167
7.3.3 Sufficient conditions for global exponential stability 168
7.3.4 Nominal design of parameters via LMIs 180
7.4 Robustness properties and design 186
7.4.1 Robustness properties with respect to small perturbations 188
7.4.2 Robustness to measurement and communication noise . . . 192
7.4.3 Robustness properties with respect to T_1^i and T_2^i perturbations 198
7.4.4 Robustness to information dropout 201
7.5 Summary 202

8 Conclusion and Future Directions **204**

Bibliography **207**

Appendix A Publications **219**

List of Figures

1.1 Trade off between the rate of convergence and the robustness. . . 8
1.2 Luenberger observer for a batch reactor 9
1.3 Comparison between interconnected observer and Luenberger observer. 14
1.4 Relationship between parameters and rate of convergence, H_∞ gain. 15
1.5 Feasible region under constraints of convergence rate and H_∞ gain. 16

3.1 Block diagram of the coupled pair of Luenberger observers. 32

4.1 Block diagram of the finite-time convergent observers. 53
4.2 Effect of noise on a finite-time convergent observer. 55
4.3 Performance with constant unmodeled dyanmics. 75
4.4 Estimation error of the finite-time convergent observer with/without unmodeled dynamics. 76
4.5 Mass-spring system 77
4.6 Finite-time convergent observer for a spring-mass system. 78

5.1 Two agents connected as a direct graph. 90
5.2 Comparisons of estimation errors of the proposed observer and that of a Luenberger observer for different measurement noises with $N = 2$. 92
5.3 Feasible regions subject to constraints. 101
5.4 Different graph structures for agent 1 with $N = 6$. 101
5.5 The influence of the number of agents on the H_∞ gain from noise m to estimation error $\bar{e}$. 106

6.1 Graph connectivity of two agents, self link is not shown. 116
6.2 Information over the network under the effect of communication noise. 117
6.3 Comparison of steady state error according to different design strategies. 121

7.1 Phase plot of planar oscillator with synchronized events. 143

7.2 Phase plot of planar oscillator with faster consensus. 144
7.3 Phase portrait and estimation errors for a 3D plant 145
7.4 Effect of measurement and communication noise. 163
7.5 Phase plot of two agents with asynchronous events 174
7.6 Phase plots of estimation errors with asynchronous events. 175
7.7 Phase portrait and estimation errors of a 3D plant with asynchronous events 176
7.8 Trajectories from three agents for a 3D plant without local reconstrucability 178
7.9 Trajectories from three agents for a 3D plant using only local measurements neighbors' estimates 179
7.10 Estimation error under different choice of perturbation $\varsigma^{\star}$. 190
7.11 Estimation error under different choice of perturbation $\varsigma^{\star}$. 191
7.12 Perturbation on event thresholds T_1 and T_2 200
7.13 Average estimation error vs data dropout rate 201

List of Tables

5.1 Comparison of estimation error ($\bar{e}$) of the observers with measurement noise of different frequencies. 92
5.2 Local H_∞ norms vs number of incoming edges 101
5.3 Comparison of global H_∞ norms from noise m to $\bar{e}$ with different number of agents under all-to-all connection. 106
5.4 Comparison of global H_∞ norms from noise m to $\bar{e}$ with different connectivity graph with $N = 3$. 107

List of Symbols

$\mathbb{C}$	The set of all complex numbers
$\mathbb{N}$	The set of all positive integers including zero, i.e., $\{0, 1, 2, \dots\}$
$\mathbb{R}$	The set of all real numbers
$\mathbb{R}_{\geq 0}$	The set of all non-negative real numbers
$\mathbb{Z}_{\geq 1}$	The set of all positive integers, i.e., $\{1, 2, \dots\}$
$\mathrm{card}(S)$	The cardinality of the set S
$\overline{\mathrm{con}}(S)$	The convex hull of a set S
$\overline{S}$	The closure of a set $S \subset \mathbb{R}^n$ defined by the intersection of all closed sets containing S
(ν, w)	Given vectors $\nu \in \mathbb{R}^n$, $w \in \mathbb{R}^m$, $[\nu^\top \ w^\top]^\top$ is equivalent to (ν, w)
1_N	The vector of N ones
$\langle u, v \rangle$	$u^\intercal v$ for $u, v \in \mathbb{R}^n$
$\lvert\nu\rvert$	The Euclidean vector norm $\lvert\nu\rvert := \sqrt{\nu^\top \nu}$
$\{v_i\}_{i=1}^n$	An orthonormal basis for $\mathbb{R}^n$, each column vector v_i contains the only nonzero element at the *i-th* entry

$\operatorname{dom} f$	The domain of a function $f : \mathbb{R}^m \to \mathbb{R}^n$ is defined as $\operatorname{dom} f := \{x \in \mathbb{R}^m : \ f(x) \text{ is defined}\}$
$\lfloor x \rfloor$	Defines the largest integer that is less than or equal to $x \in \mathbb{R}$
$\lvert m\rvert_\infty$	Given a function $m : \mathbb{R}_{\geq 0} \to \mathbb{R}^n$, $\lvert m\rvert_\infty := \sup_{t\geq 0} \lvert m(t)\rvert$ and $\lvert m\rvert_\delta := \sup_{t\in[0,\delta]} \lvert m(t)\rvert$
$\lvert y\rvert_A$	$\lvert y\rvert_A := \inf_{x\in A} \lvert x - y\rvert$ for a given point $y \in \mathbb{R}^n$ and a closed set $A \subset \mathbb{R}^n$
$\lvert\lvert G\rvert\rvert_1$	Given a Lebesgue measurable function $G(t)$, norm $\lvert\lvert G\rvert\rvert_1$ is defined by $\lvert\lvert G\rvert\rvert_1 := \int_0^\infty \lvert\lvert G(t)\rvert\rvert dt$, where $\lvert\lvert G(t)\rvert\rvert = \sup\{\lvert G(t)u\rvert : u \in \mathbb{R}^n \,\text{and}\, \lvert u\rvert \leq 1\}$ for all $t \geq 0$
$\lvert\lvert T\rvert\rvert_\infty$	$\lvert\lvert T\rvert\rvert_\infty := \sup_{\omega\in\mathbb{R}} \lvert\lvert T(j\omega)\rvert\rvert$ for a continuous transfer function $\mathbb{C} \ni s \mapsto T(s) \in \mathbb{C}$
$D^+\nu(t)$	Given a function $\nu : \mathbb{R}_{\geq 0} \to \mathbb{R}$, $D^+\nu(t) := \limsup_{h\to 0^+} \frac{\nu(t+h)-\nu(t)}{h}$
$f^+(x)$	The right limit of function f, $f^+(x) := \lim_{t\to 0^+} f(x + t)$ if it exists
$\operatorname{diag}(A, B)$	A block diagonal matrix which has A and B on the diagonal
$\operatorname{diag}_p(A)$	A diagonal square matrix which has p sub-matrices A on the diagonal with $p \in \mathbb{N}$
$\operatorname{eig}(A)$	The set contains all eigenvalues of matrix A
$\overline{\lambda}(A)$	$\max\{Re(\lambda) : \ \lambda \in \operatorname{eig}(A)\}$ for a matrix A
$\underline{\lambda}(A)$	$\min\{Re(\lambda) : \ \lambda \in \operatorname{eig}(A)\}$ for a matrix A

$\kappa(A)$	$\min\{\lvert X\rvert \lvert X^{-1}\rvert : \ A = XJX^{-1}\}$
$\mu(A)$	$\max\{Re(\lambda)/2 : \ \lambda \in \mathrm{eig}(A + A^{\top})\}$ for a matrix A
$\lvert A\rvert$	$\max\{\lvert\lambda\rvert^{\frac{1}{2}} : \ \lambda \in \mathrm{eig}(A^{\top}A)\}$
$A * B$	The Khatri-Rao product between two matrices A and B with proper dimensions
$A \otimes B$	The Kronecker product between two matrices A and B
I_N	$I_N \in \mathbb{R}^{N\times N}$ defines the identity matrix given $N \in \mathbb{N}$
$\mathrm{He}(A, B)$	$\mathrm{He}(A, B) := A^{\top}B + B^{\top}A$ for two matrices A, B with proper dimensions

Abstract

Observers with performance guarantees and robustness to measurement noise for linear systems

by

Yuchun Li

This dissertation focuses on a class of observer designs for linear-time invariant (LTI) systems, where the state variables are typically not directly measurable or may be too expensive to completely measure. Designing an observer with both fast convergence rate and robustness to noise is a well-know challenge, yet it is an essential task in many applications. To relax the generic tradeoff between fast convergence rate and robustness to perturbations in observer design with static gains, three main scenarios are considered in this thesis. With the assumption that information is accessible continuously (discretely), the first case focuses on interconnected observers over a network. It is shown to have significant advantages when comparing to a Luenberger observer. The second scenario is when the rate of convergence is prioritized. A robust observer that exhibits both continuous and impulsive behaviors is developed. With proper choice of parameters, such an observer generates estimates that converge to the state of LTI in finite-time and is robust to small perturbations. The third scenario is when measurements and information over networks are only accessible intermittently. A hybrid distributed state observer framework is established to achieve global exponential stability of the zero estimation error set. Its robustness with respect to measurement, communication noise and unmodeled dynamics is characterized in terms of input-to-state stability (ISS). In addition to providing sufficient conditions to guarantee stability and robustness of these observers, the problem of determining parameters are characterized by Linear Matrix Inequalities (LMIs) in this thesis. Constructive LMIs based on Lyapunov methods are given to efficiently design these observers. Advantages and unique properties of these observers are illustrated in many examples throughout the thesis.

To my parents Qinghui and Fengqiong

Acknowledgments

I would like to deeply express my thanks to my advisor, mentor and friend Ricardo Sanfelice, who led me with wisdom, patience, and comprehension towards the completion of my doctorate program, while giving me intellectual freedom at the same time. Your guidance has been a valuable support all along since the first day I came in United States at 2010, through my doctoral program and the writing of this thesis. It is difficult (if not impossible) to describe how much I learned from you and I really liked the time spent on discussing and transforming ideas into plans, works, results and publications. I am pretty sure I will miss all of that.

I am extremely thankful to Gabriel H. Elkaim, Dejan Milutinovic and Qi Gong for reviewing my thesis and serving as members for my doctoral committee.

Special thanks go to my friends and office mates Xiaolu, Sean and Jun. I will really miss the time spent on discussing about math and enjoying the doctoral life with you. I would like to thank also my friends Pablo, Malladi, Nathelie, Hyejin, Daniel and all members of the Hybrid Systems Lab who made me feel literally like living in a family.

I would like to deeply thank my parents who always encourage and support me, I wouldn't approach this far without you.

Chapter 1

Introduction

Observers are used to generate an estimate of the state variables of a dynamical process, in which the state variables are typically not directly measurable or too expensive to be measured. Designing an observer with both robustness to noise and fast convergence rate is one of the keys to many practical problems. For example, in advanced battery management, state of charge is typically an unknown quantity due to its invisibility to be measured directly, many algorithms are applied to estimate this quantity along with other model parameters, such as reaction rate, see, e.g. [1]. Depending on specific model choices and assumptions, variety of observers may be applied. In [2], the author compared mixed Kalman/H_∞, adaptive Luenberger and sliding mode observer for the state of charge estimation; see, e.g., [3, 4] for more details. In chemical processes, the state is usually important yet not possible to be measured directly, a moving horizon estimation (MHE) scheme has been shown to have some advantages; see, e.g., [5, 6]. Moreover, it has been applied to other situations where the relationship between state and output is highly nonlinear, see [7]. In [8], a critical comparison between extended Kalman filter and MHE is performed. Observer can also be applied to fault diagnosis for mechanical systems, see, e.g., [9, 10].

For a linear time-invariant systems of the form

$$\dot{x} = Ax, \tag{1.1}$$

$$y = Hx + m, \tag{1.2}$$

where $x \in \mathbb{R}^n$, $y \in \mathbb{R}^p$, and $m : \mathbb{R}_{\geq 0} \to \mathbb{R}^p$ denotes measurement noise, a classic observer design has the form

$$\begin{aligned} \dot{\hat{x}}_L &= A\hat{x}_L - K_L(t)(\hat{y}_L - y), \\ \hat{y}_L &= H\hat{x}_L. \end{aligned} \tag{1.3}$$

When the gain $K_L(t)$ is chosen to be a constant gain and the pair (H, A) is detectable, the design in (1.3) is called Luenberger observer and it leads to the exponentially stable error system

$$\dot{e}_L = (A - K_L H)e_L + K_L m(t) := \widetilde{A}_L e_L + K_L m(t) \tag{1.4}$$

with estimation error given by $e_L := \hat{x}_L - x$. It is well-known that, under observability conditions of (1.1), the matrix gain K_L can be chosen to make the convergence rate of (1.4) arbitrarily fast. However, due to fast convergence speed requiring large gain, the price to pay is that the effect of measurement noise m is amplified. Indeed, the design of observers, such as those in the form (1.3), involves a tradeoff between convergence rate and robustness to measurement noise [11, 12]. In fact, in [11, page 597], D. G. Luenberger makes the following remark about the error system (1.4) when (H, A) is observable:

> "Theoretically, the eigenvalues can be moved arbitrarily toward minus infinity, yielding extremely rapid convergence. This tends, however, to make the observer act like a differentiator and thereby become highly sensitive to noise, and to introduce other difficulties."

Along the same lines, the authors of [12] recognize the compromise between performance and robustness in the design of (1.3):

> "At this point we can only offer some intuitive guidelines for a choice of K to obtain satisfactory performance of the observer. To obtain fast convergence of the reconstruction error to zero, K should be chosen so that the observer poles are quite deep in the left-half complex plane. This, however, generally must be achieved by making the gain matrix K large, which in turn makes the observer very sensitive to any observation noise that may be present, added to the observed variable $y(t)$. A compromise must be found."

see [12, page 332]. Unfortunately, this issue is also at the core of every estimation algorithm for multi-agent systems.

Several observer architectures and design methods with the goal of conferring good performance and robustness to the error system have been proposed in the literature. In particular, H_∞ tools have been employed to formulate sets of linear matrix inequalities (LMIs) that, when feasible, guarantee that the $\mathcal{L}_2$ gain from disturbance to the estimation error is below a pre-established upper bound; see, e.g., [13, 14, 15, 16], to just list a few. Following ideas from adaptive control [17, 18], observers with a gain that adapts to the plant measurements have been proposed in [19, 20], though the presence of measurement noise can lead to large values of the gains. Such issues also emerge in the design of high-gain observers, where the use of high gain can significantly amplify the effect of measurement noise. Indeed, in [21, 22], it is shown that measurement noise introduces an upper limit for the gain of a high-gain observer with constant gain when good performance is desired. More recently, observers using essentially two set of gains, one set optimized for convergence and the other for robustness, have been found successful in certain settings. Such approaches include the piecewise-linear gain approach in [23] for simultaneously satisfying steady-state and transient bounds, the high gain observer with nonlinear adaptive gain in [24], and the high gain observer with on-line gain tuning in [25]. Also recently, a switching algorithm combining two observers for performance improvement was proposed in [26].

When rate of convergence is of main importance in design specifications, several observer architectures that guarantee finite time convergence of the estimates without measurement noise are available in the literature. These include those using the properties of the solutions of multiple observers, see, e.g., [27, 28, 29, 30], using measurement-based state updates [31], and those exploiting an homogeneity property, see, e.g., [32, 33, 34, 35]. However, when noise is present in the measurement of the state of the plant, a tradeoff between rate of convergence and robustness to measurement noise is also expected in finite-time convergent observers.

As recent research efforts in multi-agent systems have lead to enlightening results in distributed estimation and consensus. Distributed Kalman filtering are employed for achieving spatially-distributed estimation tasks in [36] and for sensor network in [37, 38, 39, 40, 41]. To characterize the effect of unmodeled dynamics on the consensus multi-agent system, in [42], a region-based approach is used for distributed H_∞-based consensus of multi-agent systems with an undirected graph. For dynamic average consensus, [43] proposes a decentralized algorithm that guarantees asymptotic agreement of a signal over strongly connected and weight-balanced graphs. In [44], switching inter-agent topologies are used to design distributed observers for a leader-follower problem in multi-agent systems. In [45] and [46], the estimation of the trajectories of a moving target using distributed sensor networks are studied. However, distributed estimation algorithms that systematically meet specifications of performance and robustness to measurement noise are not available.

Along with distributed estimation, consensus for distributed systems has also been extensively studied in the literature. Static consensus, which corresponds to the agreement on the initial conditions of the agents, modeled via a directed graph, are reported in [47, 48, 49]. For dynamic average consensus, [43] proposes a decentralized algorithm that guarantees asymptotic agreement of a signal over strongly connected and weight-balanced graphs. In [50], a dynamic consensus algorithm that is robust to communication time delay is proposed. In [51], an observer-type of consensus algorithm is designed for linear systems without noise. In [52], the stability and convergence properties of integral and propotional-integral consensus is thoroughly studied. On the other hand, the literature on consensus design with robustness to measurement and communication noise is not as rich. In [53], the effect of additive noise with zero mean on the variables of a consensus algorithm is discussed, while in [42], a performance region-based approach is used for the design of distributed H_∞-based consensus. In [54], Kalman filter based consensus is shown to be robust to state and input noise. In [55], the author studies consensus under random topologies with noise and link failures.

When designing observers for realistic scenario, often the measurements can only be taken at isolated events due to the limitation of sensing frequency. Within the context of multi-agent system over communication networks, the information transmission may also be restricted to an intermittent fashion. These constraints make the classic observer designs challenging and not directly applicable. When information is available periodically with constant sampling frequency, discrete-time observers can be employed. In [56], under nominal conditions and for linear time-invariant plants, a network of local observers communicating at the same time instances is designed to achieve an attractivity property (called omniscience) between the estimates and the state of the plant. In [57], the optimal linear estimation problem for discrete time-varying networked systems over a shared communication channel is considered. The work in [58] established an observer-protocol pair to asymptotically reconstruct the states of a linear time-invariant plant with multiple sensors. In [59], a distributed algorithm for observer design for linear time-invariant continuous-time systems is designed by partitioning the dynamics into disjoint areas and attaching an algorithm to each area that updates the estimates over time windows with common length.

Approaches that maintain the continuous dynamics of the plant and treat the communication events as impulsive events have also been developed. An observer-based controller for a network control system modeled as a time-varying hybrid system is proposed in [60] and its design is performed using the Lyapunov-Krasovskii functional. In [61], an emulation-like approach is used to guarantee that a robust continuous-time observer (when available) can be used for estimation in network control systems. Such general result is obtained using trajectory-based and small-gain arguments. In [44], for a second order system capturing the dynamics of a leader-follower problem, a distributed observer allowing for switching inter-agent topologies is proposed using switched systems theory.

In addition to the above deterministic continuous, discrete, and hybrid approaches for distributed estimation, the literature of network control and estimation is rich on stochastic approaches over a variety of time domains. These include information-oriented approaches. In [62], distributed Kalman-like filters with ([63]) and without communication constraints ([39, 64]), and for spatially-distributed estimation tasks [36]. Specifically, in [65], conditions guaranteeing that a continuous-time observer for a class of nonlinear systems provides states estimates with robustness to samples and delays of the measurement are provided. In particular, the main result requires an input-to-output stability of the observer-plant pair. In [66], the authors propose a method to design observers for a class of continuous-time systems with Lipschitz nonlinearities under nonuniformly sampled measurements. The approach therein consists of composing a continuous-time high-gain observer with an inter-sample output predictor. Closely related to this work and also under the name "continuous-discrete observer," [67] provides a way to design observers for a class of Lipschitz continuous-time systems of small dimensions through the computation of finite-time reachable sets. A survey of recent advances in the design of continuous-discrete observers is available [68]. A hybrid observer guaranteeing global exponential stability of the zero-estimation error under sporadic measurements is available in [69]. However, due to the challenges introduced by asynchronous and heterogeneous communication events at unknown times, extending these methods to the multi-agent case is not trivial.

1.1 Luenberger observer and its tradeoff

In this section, two examples are discussed. One is a scalar example, which clearly demonstrates the limitation of a Luenberger observer when the convergence rate and robustness are simultaneously enforced. The other one relates to an application of a unstable batch reactor where observer-based controller is a typical option, see, e.g., [70, page 213], [71, page 62] for more details.

Example 1.1.1 *To illustrate the tradeoff between robustness to measurement noise and fast rate of convergence, consider the scalar plant*

$$\dot{x} = ax, \qquad y = x + m, \tag{1.5}$$

where m denotes constant measurement noise (e.g., a bias) and $a < 0$. A standard

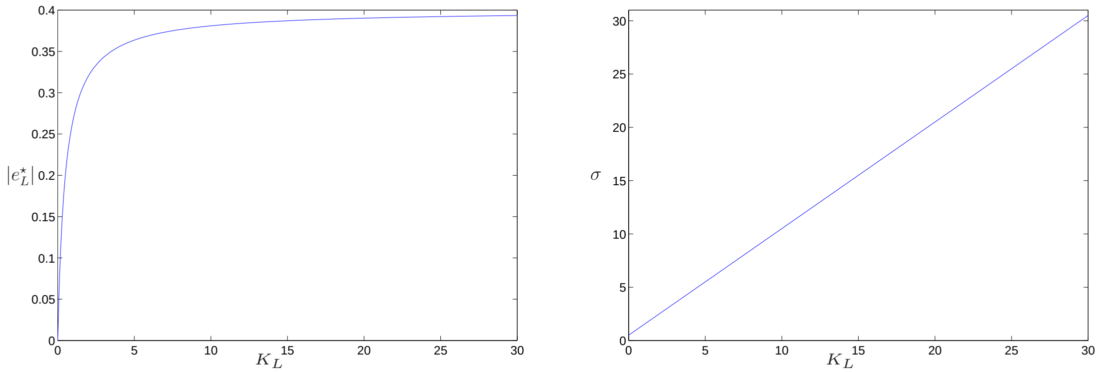

(a) The steady-state error with $|e^\star_L| = |\frac{k_L}{k_L - a} m|$, $m = 0.4$ and $a = -0.5$.

(b) Rate of convergence σ with respect to K_L.

Figure 1.1: Trade off between the rate of convergence and the robustness.

Luenberger observer for this plant is given by

$$\begin{aligned} \dot{\hat{x}}_L &= a\hat{x}_L - K_L(\hat{y}_L - y) \\ \hat{y}_L &= \hat{x}_L. \end{aligned} \tag{1.6}$$

The estimation error system is given by (1.4) *with* $\tilde{A}_L = a - K_L$. *Its convergence rate is* $\sigma = |a - K_L|$ *and its steady-state error is* $e^\star_L := \frac{K_L}{K_L - a} m$. *It is apparent that to get fast convergence, the constant* K_L *needs to be positive and large. However, with* K_L *large, the influence of measurement error is amplified as well. As suggested by Figure 1.1(a), a balance needs to be made between convergence rate and steady-state error induced by measurement noise. More importantly, if we restrict the* H_∞ *gain*[1] *from noise* m *to estimation error* e_L *to be* 0.6 *and the rate of convergence is* 2.5, *then there is no feasible gain* K_L *such that the Luenberger observer in* (1.6) *can satisfy both specifications simutanously. In Section 1.2, we will show a way to relax this tradeoff and provide feasible solutions.* $\triangle$

Next, we consider a practical problem of a unstable batch reactor.

[1]For LTI systems, the H_∞ gain from m to e_L is defined as the infinity norm of the transfer function from m to e_L.

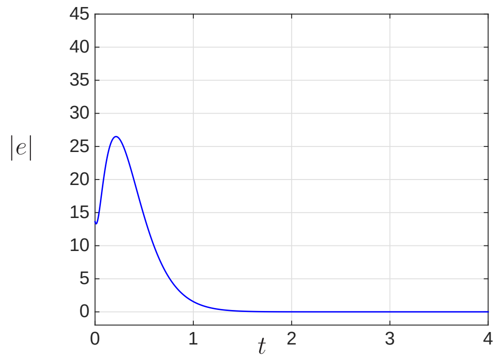

(a) The trajectory of estimation error $|e_L| = |\hat{x}_L - x|$ with zero measurement noise ($\sigma = 7$).

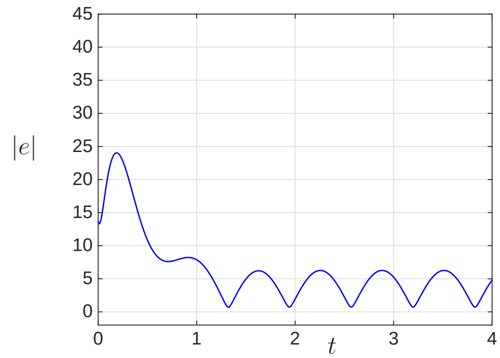

(b) The trajectory of estimation error $|e_L| = |\hat{x}_L - x|$ with measurement noise $m(t) = 2\sin(5t)$ with $\sigma = 7$.

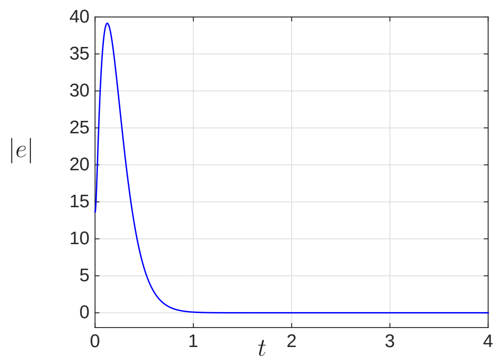

(c) The trajectory of estimation error $|e_L| = |\hat{x}_L - x|$ with zero measurement noise ($\sigma = 11$).

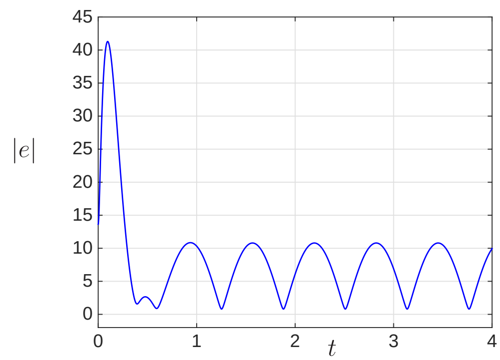

(d) The trajectory of estimation error $|e_L| = |\hat{x}_L - x|$ with measurement noise $m(t) = 2\sin(5t)$ with $\sigma = 11$.

Figure 1.2: Luenberger observer for a batch reactor subject to a convergence rate constraint.

Example 1.1.2 *Consider a linearized model for an unstable batch reactor in [70],* *which is described by the following data:*

$$A = \begin{bmatrix} 1.38 & -0.2077 & 6.715 & -5.676 \\ -0.5814 & -4.29 & 0 & 0.675 \\ 1.067 & 4.273 & -6.654 & 5.893 \\ 0.048 & 4.273 & 1.343 & -2.104 \end{bmatrix},$$

$$H = \begin{bmatrix} 1 & 0 & 1 & -1 \\ 0 & 1 & 0 & 0 \end{bmatrix}.$$

Note that the eigenvalues of A is given by $\{1.9910, 0.0635, -5.0566, -8.6659\}$, therefore, the system is unstable. Moreover, it can be verified that the pair (H, A) is observable. Then, when an observer is designed in the sense of Luenberger and the rate of convergence is required to be no less than 7, we can minimize the H_∞ gain from measurement noise m to the estimation error e_L. The resulting gain is given by

$$K_L = \begin{bmatrix} 9.7989 & -4.1385 \\ 2.6416 & 6.1663 \\ 16.1345 & -3.9715 \\ 15.7678 & -2.8363 \end{bmatrix},$$

and the corresponding H_∞ gain from measurement noise m to estimation error e_L is ≈ 3.63. If the rate of convergence requirement is 11 instead, the resulting gain *can be computed as*

$$K_L = \begin{bmatrix} 23.9485 & -29.1535 \\ 2.5002 & 11.1575 \\ 58.1575 & -5.0597 \\ 59.3809 & -17.6970 \end{bmatrix},$$

which leads to H_∞ *gain* ≈ 5.83*. Simulations for both gain matrices of this plant-observer system are shown in Figure 1.2. The initial conditions are* $x(0) = (2, 2, 2, 2)$ *and* $\hat{x}_L(0) = (15, 5, 0, 0)$*. From Figure 1.2(a) and 1.2(c), as we change the constraint for rate of convergence from* 7 *to* 11*, the estimation error converges to zero faster. However, when measurement noise exists as shown in Figure 1.2(b) and 1.2(d), the resulting effect of noise is amplified when requiring faster convergence rate.* △

Such tradeoff between convergence rate and robustness to measurement noise shown above is generic when designing Luenberger observers for linear systems, which motivates the design in the following chapters and will be discussed further.

1.2 An observer with extra information

In this section, we show that by using more than one copy of Luenberger and picking appropriate coupling between them, extra freedom is obtained to relax the tradeoff between convergence rate and the robustness to measurement noise represented by a H_∞ gain. The following example demonstrates the advantage of using more than one copy of Luenberger observers when one wants to simultaneously enforce a particular performance index (such as rate of convergence) and its H_∞ gain from measurement noise to estimation error.

Example 1.2.1 *We revisit the scalar example in* (1.5). *The tradeoff pointed out in Section 1.1 inspired the idea of interconnected observers. Here we consider a particular case which consists of a pair of coupled Luenberger observers. For the scalar plant* (1.5)*, the observer takes the form*

$$\begin{aligned}
\dot{\hat{x}}_1 &= a\hat{x}_1 - K_{11}(\hat{y}_1 - y) - K_{12}(\hat{y}_2 - y), \\
\dot{\hat{x}}_2 &= a\hat{x}_2 - K_{22}(\hat{y}_2 - y) - K_{21}(\hat{y}_1 - y), \\
\hat{y}_i &= \hat{x}_i, \quad i \in \{1,2\}, \quad \bar{x} = \frac{1}{2}(\hat{x}_1 + \hat{x}_2).
\end{aligned} \tag{1.7}$$

The coupling injections terms "$-K_{12}(\hat{y}_2 - y)$*" and "*$-K_{21}(\hat{y}_1 - y)$*" define the innovation terms of the proposed observer. Compared to* (1.6)*, with the proposed observer, a one dimensional design problem on* K_L *becomes a fourth dimensional design problem on* K_{11}*,* K_{12}*,* K_{21}*, and* K_{22}*. The output* $\bar{x}$ *of the coupled pair of observers defines the estimate of* x *as the average of the states* $\hat{x}_1$ *and* $\hat{x}_2$ *of the individual observers.*

By defining the error variables $e_i := \hat{x}_i - x$ *for each* $i \in \{1,2\}$*, the error dynamics are captured by*

$$\begin{aligned}
\dot{e}_1 &= (a - K_{11})e_1 - K_{12}e_2 + (K_{11} + K_{12})m, \\
\dot{e}_2 &= -K_{21}e_1 + (a - K_{22})e_2 + (K_{21} + K_{22})m,
\end{aligned} \tag{1.8}$$

which can be written in matrix form as

$$\dot{e} = \widetilde{A}e + \widetilde{K}m, \tag{1.9}$$

where $e = (e_1, e_2)$ *and*

$$\widetilde{A} = \begin{bmatrix} a - K_{11} & -K_{12} \\ -K_{21} & a - K_{22} \end{bmatrix}, \ \widetilde{K} = \begin{bmatrix} K_{11} + K_{12} \\ K_{21} + K_{22} \end{bmatrix}. \tag{1.10}$$

For $i, j \in \{1, 2\}$, $i \neq j$, *the steady-state error of* (1.8) *is given by*

$$e_i^\star = \frac{K_{11}K_{22} - K_{12}K_{21} - K_{ii}a - K_{ij}a}{K_{11}K_{22} - K_{12}K_{21} - K_{22}a - K_{11}a + a^2} m. \tag{1.11}$$

The estimation error of the proposed observer is given by the quantity

$$\bar{e} := \bar{x} - x \tag{1.12}$$

and has a steady-state value given by

$$\bar{e}^\star = \frac{K_{11}K_{22} - K_{12}K_{21} - (1/2)(K_{11} + K_{22} + K_{12} + K_{21})a}{K_{11}K_{22} - K_{21}K_{22} - K_{22}a - K_{11}a + a^2} m. \tag{1.13}$$

Under the condition that all eigenvalues of the matrix $\widetilde{A}$ *are stable, they can be written in the general form* $\lambda_{1,2} = -\sigma \pm j\omega$, *where* σ *is positive and* $\omega \in \mathbb{R}$ *and* $j = \sqrt{-1}$. *Then, by solving for the eigenvalues of* $\widetilde{A}$ *and comparing with the rate of convergence of the observer* (1.6), *the following conditions guarantee a faster convergence rate of the proposed observer:*

$$-\sigma = \frac{-(K_{11} - a) - (K_{22} - a)}{2} < a - K_L < 0, \tag{1.14}$$

$$((K_{11} - a) + (K_{22} - a))^2 < 4 \det(\widetilde{A}_L). \tag{1.15}$$

On the other hand, in order to assure an improvement on the effect of measurement *noise, we want to guarantee that* $|\bar{e}^{\star}| < |e_0^{\star}|$ *, which leads to the following condition:*

$$\left|\frac{K_{11}K_{22} - K_{12}K_{21} - (1/2)(K_{11} + K_{22} + K_{12} + K_{21})a}{K_{11}K_{22} - K_{12}K_{21} - K_{22}a - K_{11}a + a^2}\right| < \left|\frac{K_L}{K_L - a}\right|. \tag{1.16}$$

It can also be verified that for any given K_L*, there exist parameters* $K_{11}, K_{12}, K_{21}, K_{22}$ *of the proposed observer* (6.1) *such that conditions* (1.14)-(1.16) *hold. This observer leads to the improvement in rate of convergence and robustness suggested in Figure 1.3, where the dot dashed line denotes the state of a stable plant* (1.5)*, dashed line denotes the estimate provided by the standard Luenberger observer* (1.6)*, and the black line is the estimate from the proposed observer* (6.1).

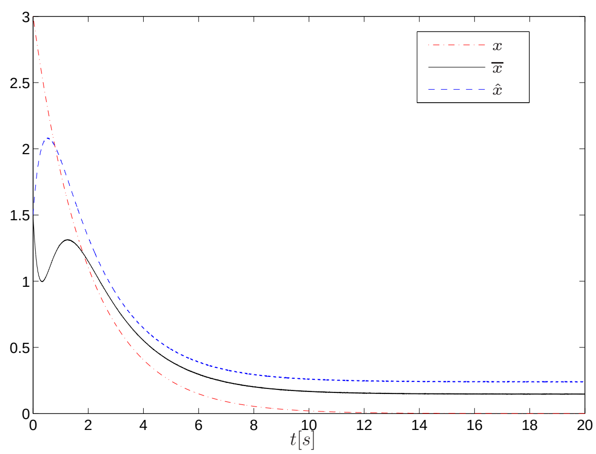

Figure 1.3: Comparison between proposed observer (black, solid) and a standard Luenberger observer (blue, dashed). The plant solution is denoted in red, dash-dot.

It should be noted that simply using two Luenberger observers without any coupling and taking the average of their estimates will not lead to both faster convergence rate and smaller steady state error. In fact, let $K_{12} = K_{21} = 0$. *Then, the system in* (6.1) *proposes a structure of two Luenberger observers without coupling. A direct calculation shows that for constant noise, the estimation error*

$\bar{e}$ *satisfies*

$$\bar{e}^{\star} = \frac{1}{2}\left(\frac{K_{11}}{K_{11}-a} + \frac{K_{22}}{K_{22}-a}\right)m.$$

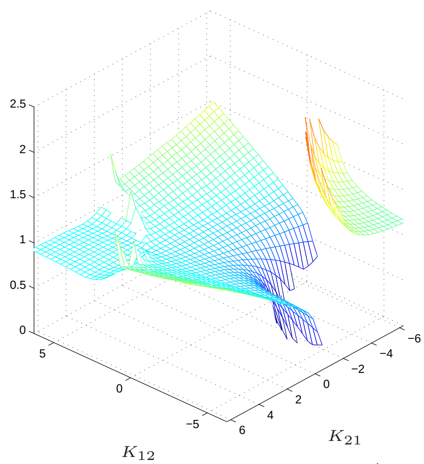

(a) H_∞ norm of proposed observer (H_∞) in (6.1) vs gains K_{12} and K_{22}.

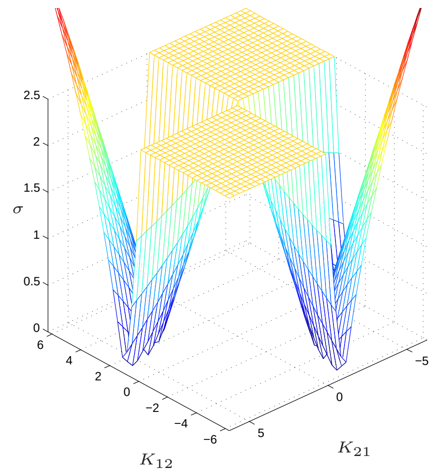

(b) Rate of convergence of proposed observer (σ) in (6.1) vs gain K_{12} and K_{21}.

Figure 1.4: Comparison between nominal observer and the proposed observer with $a = -0.5$ and $K_{11} = K_{22} = 2$.

More generally, when m *is bounded, Figure 1.1(a) shows the* H_∞ *norm from measurement noise* m *to estimation error* e_0 *for the nominal observer* (1.6) *as a function of* K_L. *On the other hand, the rate of convergence, as shown in Figure 1.1(b), also increases when* K_L *gets larger (*σ^n *and* σ *are defined as the absolute value of the real part of the dominant pole of closed-loop systems with the Luenberger observer and the coupled pair of observers, respectively). Such a tradeoff would become crucial when both rate of convergence and robustness are required. Figure 1.4(a) shows the* H_∞ *norm of the proposed observer as a function of* K_{12} *and* K_{21} *with* $K_{11} = K_{22} = K_L = 2$. *Figure 1.4(b) shows that, for* $K_{11} = K_{22} = K_L$*, the rate of convergence is also a function of* K_{12} *and* K_{21}.[2] *The figures suggest that, when a specific rate of convergence is required, instead of*

[2]Note that in Figure 1.4(a), the H_∞ grows unbounded at points on the K_{12} - K_{21} plane corresponding to the case of purely imaginary poles. This can be seen from Figure 1.4(b), where, at such points, the rate of convergence is zero.

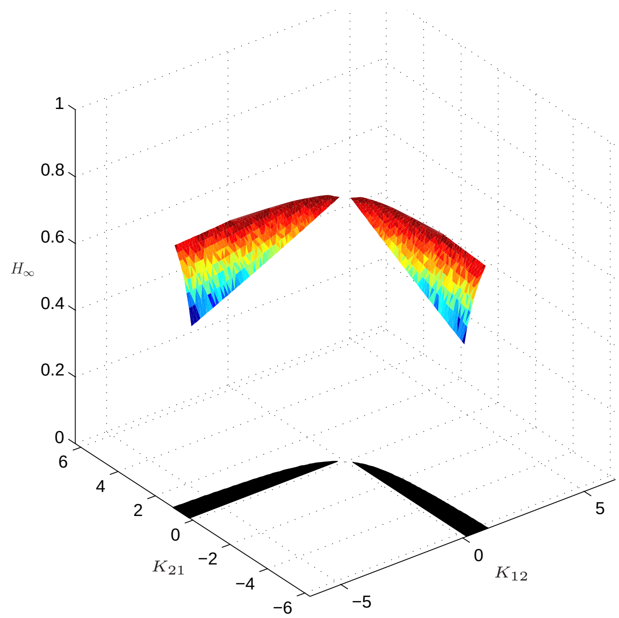

Figure 1.5: Feasible region of K_{12} and K_{21} where $H_\infty \leq H_\infty^{n,\star}$ and $\sigma^{n,\star} \leq \sigma$ for the proposed observer in (6.1) with $a = -0.5$, $K_L^\star = 2$, and particular choice of gain $K_{11} = K_{22} = K_L^\star$.

only one option (K_L) for the design of the Luenberger observer, we have more parameters for the coupled pair of observers to improve both the rate of convergence and robustness. For example, when using the observer with $K_{11} = K_{22} = K_L$, as shown in Figure 1.5, the constraint on the rate of convergence leads to a feasible area on the K_{12}, K_{21} plane while the constraint on the H_∞ norm defines an additional plane. In fact, we can show that the observer (6.1) *can have better robustness property with faster rate of convergence.* $\triangle$

Example 1.2.2 *We revisit the batch reactor system in Example 1.1.2. An interconnected observer similar as the one in* (6.1) *is considered. In particular, the* *observer has the following dynamics:*

$$\dot{\hat{x}}_1 = A\hat{x}_1 - K_{11}(H\hat{x}_1 - y) - K_{12}(H\hat{x}_2 - y) \tag{1.17}$$

$$\dot{\hat{x}}_2 = A\hat{x}_2 - K_{21}(H\hat{x}_1 - y) - K_{22}(H\hat{x}_2 - y) \tag{1.18}$$

$$y = Hx + m, \quad \bar{x} = \frac{1}{2}(\hat{x}_1 + \hat{x}_2). \tag{1.19}$$

Then, by defining estimation error $e_i = \hat{x}_i - x$ *for* $i \in \{1, 2\}$ *and* $\bar{e} = \frac{1}{2}(e_1 + e_2)$, *we further have*

$$\dot{e} = \widetilde{A}e + \widetilde{K}(\mathbf{1}_2 \otimes I_4)m \tag{1.20}$$

$$\bar{e} = \frac{1}{2}(\mathbf{1}_2^\top \otimes I_4)e, \tag{1.21}$$

where

$$\widetilde{A} = I_2 \otimes A - \widetilde{K}(I_2 \otimes H), \quad \widetilde{K} = \begin{bmatrix} K_{11} & K_{12} \\ K_{21} & K_{22} \end{bmatrix}.$$

When the design specification requires the rate of convergence to be no less than

11, *we can minimize the* H_∞ *gain from* m *to* $\bar{e}$. *The resulting gain is*

$$K_{11} = \begin{bmatrix} -24.4924 & -0.7231 \\ 6.7241 & 16.2905 \\ 159.0754 & 48.5652 \\ 123.3211 & 46.6041 \end{bmatrix}, \quad K_{12} = \begin{bmatrix} 35.3917 & 24.5557 \\ -4.6515 & 6.2317 \\ -112.6086 & -48.4871 \\ -80.9980 & -27.4796 \end{bmatrix},$$
$$K_{21} = \begin{bmatrix} 0.1234 & 9.1265 \\ 35.6030 & -10.8481 \\ -38.2258 & -27.6230 \\ -17.5271 & -31.4137 \end{bmatrix}, \quad K_{22} = \begin{bmatrix} 9.2160 & 7.5668 \\ -29.0235 & -23.0023 \\ 55.2293 & 32.9513 \\ 36.3312 & 17.6245 \end{bmatrix},$$

which leads to an H_∞ *gain* ≈ 2.97. *Under the same rate of convergence constraint, via two interconnected observers, the resulting rate of convergence is* $\approx 18.2\%$ *smaller than that from Luenberger observer (*3.63*).* △

From the examples above, it is shown that by using more information, we can design observer with faster rate of convergence and smaller H_∞ gain from the measurement noise to the estimation error. In fact, we can generalize the strategy by modeling the system as directed graph, as shown in the following chapters.

1.3 Observer with intermittent information

In realistic setting and practical scenario, the measurements and information transmitted from neighbors may not be continuously available. When information arrives periodically, we can design observers by using discrete system tools. However, when information is available only after non-periodic intervals, classic discrete system tools would not apply directly. In particular, for the plant given in (1.1), the measurements at agent i with forms in (1.2) are only available at isolated time instances $\{t_s^i\}_{s=1}^{\infty}$, namely, at agent (or sensor) i,

$$y_i(t_s^i) = H_i x(t_s^i) + m_i(t_s^i), \tag{1.22}$$

and the sequence $\{t_s^i\}_{s=1}^{\infty}$ satisfies

$$t_{s+1}^i - t_s^i \in [T_1^i, T_2^i], \tag{1.23}$$

where $0 < T_1^i \leq T_2^i$ for all i in the network. In such setting, the main challenges to the observer design mainly include the following:

1. *Asynchronous and heterogeneous communication events at unknown times:* the time instances at which agents receive information are not synchronized, meaning that each agent may receive information at different time instances. Furthermore, the amount of ordinary time elapsed between communication events for each agent can be different; for instance, an agent can receive information at a much faster rate than others. In addition, the exact event times are not known a priori.

2. *Lack of full information to reconstruct the state at each agent and at the same time:* information is not available continuously, but rather, at isolated time instances. Furthermore, none of the agents may have enough information to fully reconstruct x alone. In fact, in the nominal case, (H_i, A) may not necessarily be detectable for any i. This suggests that information must be shared among agents, but, even then, the needed information to fully reconstruct x may be available at different time instances (see item 1), which, in particular, makes detectability of $((H_1, H_2, \ldots, H_N), A)$ not very useful when solving the nominal problem.

3. *Perturbations in the dynamics, parameters, and measurements:* the lack of knowledge of the actual perturbation $\{m_i\}_{i=1}^N$ (or, for that matter, a Lipschitzness assumption) precludes from fully compensating for their effect. Furthermore, perturbations on the parameters T_1^i and T_2^i could lead to diverging estimates when the estimation algorithm has little margin of robustness to such parameters.

This motivates the work in Chapter 7, where the overall system is modeled via a hybrid system framework presented in Chapter 2. Comprehensive analysis and efficient design methods are also established.

1.4 A brief overview of Kalman filter

It is well known that the Kalman-Bucy filter is the optimal observer that minimizes the mean square estimation error [72] under certain assumptions. For the plant (1.1) (with $x \in \mathbb{R}^n$), it is given by (1.3), where $\hat{x} \in \mathbb{R}^n$ and $t \mapsto K_L(t)$ is the time-varying gain. Recall that the estimation error is $e = \hat{x} - x$, the resulting error system for the optimal observer/Kalman-Bucy filter is

$$\dot{e} = (A - K_L(t)H)e + K_L(t)m. \tag{1.24}$$

If (1.3) is initialized with $\hat{x}(0) = \bar{x}_0 := \mathbb{E}\{x(0)\}$, where $\mathbb{E}$ denotes the expected value function, then, according to [12, Theorem 4.5], for any positive definite symmetric weighting matrix function $t \mapsto W(t)$, the gain that minimizes the objective function $\mathbb{E}\{e(t)^\top W(t)e(t)\}$ for all $t \geq 0$ is $K_L(t) = Q(t)H^\top V_d^{-1}(t)$, where $t \mapsto Q(t)$ is the solution of

$$\dot{Q}(t) = AQ(t) + Q(t)A^\top - Q(t)H^\top V_d^{-1}(t)HQ(t), \tag{1.25}$$

from the initial condition $Q(0) := \mathbb{E}\{(x(0) - \bar{x}_0)(x(0) - \bar{x}_0)^\top\}$, where $t \mapsto V_d(t)$ is the (positive definite for each $t \geq 0$) covariance matrix of the measurement noise m. While the expected value of the (weighted) norm of e is minimized, the same trade off pointed out in Section 1.1 for Luenberger observers plays a key role in the design of (1.24). In fact, as [12, page 346] correctly points out, "The optimal observer provides a compromise between the speed of state reconstruction and the immunity to observation noise."

Moreover, the design of (1.24) does not permit incorporating other performance indexes in order to preserve optimality, such as the rate of convergence. Because of this nature, in the circumstance where one wants to prioritize convergence rate or to enforce extra robustness index at the same time, designing an observer based on Kalman filter might be problematic. In this thesis, we will focus on designing observers with static gains and as we will show in next section, by generating more than one copy of Luenberger and couping them, it leads to a way to formulate and solve the aforementioned problem.

1.5 Contributions and organization

In this dissertation, a generic framework of N interconnected observers design for LTI systems with static gains are proposed. Moreover, the following fundamental aspects of this class of observers are addressed:

1. Optimization in terms of LMIs for the synthesis of H_∞ gain from measurement noise to estimation error subject to convergence rate constraints and maintaining the zero estimation error set uniformly globally asymptotically stable;

2. Generating estimates that converge to the state of a plant in finite-time while

preserving robustness to small perturbations. Moreover, such finite-time convergence property is preserved under piece-wise constant measurement noises;

3. Designing consensus algorithms that enable each agent in a distributed state observer setting to have access to the global average of all local estimates across a communication network. Moreover, separated/joint design methods are developed for the distributed state observer and their consensus;

4. In distributed state observer setting with only asynchronous intermittent information and without local detectability, generating estimates that globally exponentially converge to the plant's state and rendering robustness with respect to measurement and communication noise, unmodeled dynamics and generic perturbations. Constructive LMIs are formulated for the design of parameters.

The contents of this thesis are organized into following chapters.

Chapter 2: Preliminaries

In this chapter, graph theory is briefly discussed which is essential for the modeling and analysis of interconnected observers. Moreover, a hybrid system framework and its basic properties are presented and will be used throughout the thesis.

Chapter 3: Pair of Coupled Observers for Improved Performance and Robustness

In this chapter, a pair of interconnected Luenberger observers is proposed and thoroughly discussed. Its unique advantages when comparing to standard Luenberger observer is proved analytically and validated numerically. In particular, the configuration and its basic properties are developed in (3.1). The design of parameters are formulated in LMIs based on rate of convergence constraint (3.2.1) and H_∞ gain from measurement noise to estimation error (3.2.2). Furthermore, such constructive setting enables the synthesis design in (3.2.3).

Chapter 4: Finite-time Convergent Observer

In this chapter, a hybrid observer consists of two interconnected Luenberger that evolve continuously with impulsive and periodic updates is proposed. The problem is modeled via a hybrid system framework (4.1). Even when measurement noise is present (constant or piece-wise constants), the proposed observer is robust to small perturbations and is capable of making estimates converge to the plant's state in finite-time (4.2). Numerical simulations confirm its properties and demonstrate its applicability (4.3).

Chapter 5: Distributed Estimation with Continuous Information Transmission

In this chapter, a generalization of the observer previous chapters is established. In particular, the modeling of N interconnected observer is accomplished via using directed graphs (5.1). Sufficient conditions that guarantee the uniform global asymptotic stability of zero estimation error set are presented (5.2). Moreover, the design of parameters are characterized in term of LMIs (5.3). Furthermore, it's shown analytically that such observers outperform standard Luenberger observer (5.4) under certain conditions. The last section (5.5) of this chapter briefly introduces a consensus algorithm to enable each agent has access to the global average of all local estimates.

Chapter 6: Dynamic Consensus for Distributed Estimation

In this chapter, a consensus algorithm is proposed to generate a global average of all (time-varying) local estimates from distributed state observers in the previous chapter, under communication and measurement noise in the local and global estimates. The underlying idea is illustrated in a motivational example (6.1). Characterizations of its performance and robustness in terms of $\mathcal{KL}$ bounds are established (6.2). Constructive LMIs are developed to synthesize the distributed observer and the consensus algorithm using H_∞ theory and optimization techniques in (6.3.1) and (6.3.2). The designs using these tools guarantee that the each agent agrees on the global average of all local (time-varying) estimates, asymptotically and robustly with respect to communication and measurement noise.

Chapter 7: Distributed Estimation with Intermittent Information Transmission

In this chapter, a hybrid distributed estimation framework is proposed when information is available asynchronously and intermittently over a network (7.1). Sufficient conditions are developed to guarantee global exponential stability of the zero estimation error set when information is transmitted at highly nonuniform fashion and when the agents lack local detectability (7.3). Constructive linear matrix inequalities (LMIs) are established to efficiently determine parameters (7.3.4). An in-depth robustness analysis with respect to perturbations from unmodeled dynamics, skewed clocks, measurement and communication noise is performed (7.4). In particular, ISS property with respect to measurement and communication noise is quantified by a class-$\mathcal{KL}$ function (7.4.2) and the case when random packet dropouts occur is also studied (7.4.4).

Chapter 8: Conclusion and Future Directions

In this chapter, the results in this thesis are summarized and several potential future directions are briefly discussed.

A list of publications related to this dissertation is in Appendix A.

Chapter 2

Preliminaries

2.1 Graph and Networks

In this work, we use directed graph to model the connectivity property for the overall system. In particular, a directed graph (digraph) is defined as $\Gamma = (\mathcal{V}, \mathcal{E}, \mathcal{G})$. The set of nodes of the digraph are indexed by the elements of $\mathcal{V} = \{1, 2, \ldots, N\}$, and the edges are the pairs in the set $\mathcal{E} \subset \mathcal{V} \times \mathcal{V}$. Each edge directly links two nodes, i.e., an edge from k to i, denoted by (i, k), implies that agent i can receive information from agent k. The adjacency matrix of the digraph Γ is denoted by $\mathcal{G} = (g_{ik}) \in \mathbb{R}^{N \times N}$, where $g_{ik} = 1$ if $(i, k) \in \mathcal{E}$, and $g_{ik} = 0$ otherwise. A digraph is undirected if $g_{ik} = g_{ki}$ for all $i, k \in \mathcal{V}$. The in-degree and out-degree of agent i are defined by $d^{in}(i) = \sum_{k=1}^{N} g_{ik}$ and $d^{out}(i) = \sum_{k=1}^{N} g_{ki}$. A digraph is weight-balanced if, for each node $i \in \mathcal{V}$, the in-degree and out-degree coincide. The out-degree matrix D_{out} is the diagonal matrix with the i-th diagonal entry $d^{out}(i)$, for all $i \in \mathcal{V}$. Similarly, The in-degree matrix D_{in} is the diagonal matrix with the i-th diagonal entry $d^{in}(i)$, for all $i \in \mathcal{V}$. The Laplacian matrix of the graph Γ, denoted by $\mathcal{L}$, is defined as $\mathcal{L} = D^{out} - \mathcal{G}$. The Laplacian has the property that $\mathcal{L}1_N = 0$. Therefore, 0 is an eigenvalue of the matrix $\mathcal{L}$.

Furthermore, the rest of the eigenvalues of $\mathcal{L}$ have nonnegative real parts. The set of indices corresponding to the neighbors that can send information to the i-th agent is denoted by $\mathcal{N}(i) := \{k \in \mathcal{V} : (i,k) \in \mathcal{E}\}$.

2.2 Hybrid Systems

In this paper, a hybrid system $\mathcal{H}$ has data (C, f, D, g) and is defined by

$$\begin{aligned} \dot{z} &= f(z,u) \quad z \in C, \\ z^+ &= g(z,u) \quad z \in D, \end{aligned} \tag{2.1}$$

where $z \in \mathbb{R}^n$ is the state, $u \in \mathbb{R}^p$ is the input, f defines the flow map which captures the continuous dynamics and C defines the flow set on which f is effective. The map g defines the jump map and models the discrete behavior, while D defines the jump set, from which discrete dynamics are allowed. Given an input u, a solution to $\mathcal{H}$ is given by the pair (z, u), which is parametrized by (t, j), where t denotes ordinary time and j denotes the jump time. (When the system has no input or its input is zero, its solution will be given by z.) Hybrid time domains are subsets E of $\mathbb{R}_{\geq 0} \times \mathbb{N}$ that, for each $(T, J) \in E$, $E \cap ([0,T] \times \{0, 1, \ldots J\})$ can be written in the form $\cup_{j=0}^{J-1}(I_j, j)$ for some finite sequence of times $0 = t_0 \leq t_1 \leq t_2 \leq \cdots \leq t_J$, where $I_j := [t_j, t_{j+1}]$. The t_j's define the time instants when the state of the hybrid system jumps and j counts the time of jumps. A solution to $\mathcal{H}$ is called maximal if it cannot be extended, i.e., it is not a truncated version of another solution, and it is called complete if its domain is unbounded. A solution is called Zeno if it is complete and its domain is bounded in the t direction. Two solutions are said to be (τ', ε)-close if they satisfy the following property.

Definition 2.2.1 *((τ', ε)-closeness of solutions [73, Definition 5.23]) Given $\tau', \varepsilon >$*

0, *two solutions* ϕ_1 *and* ϕ_2 *to* $\mathcal{H}$ *are* (τ', ε)*-close if*

(a) for all $(t, j) \in \operatorname{dom} \phi_1$ *with* $t+j \leq \tau'$ *there exists* s *such that* $(s, j) \in$ *dom* ϕ_2, $|t - s| < \varepsilon$, *and* $|\phi_1(t, j) - \phi_2(s, j)| < \varepsilon$;

(b) for all $(t, j) \in \operatorname{dom} \phi_2$ *with* $t+j \leq \tau'$ *there exists* s *such that* $(s, j) \in \operatorname{dom} \phi_1$, $|t - s| < \varepsilon$, *and* $|\phi_2(t, j) - \phi_1(s, j)| < \varepsilon$.

A hybrid system $\mathcal{H}$ with (C, f, D, g) is said to satisfy the hybrid basic conditions [73, Assumption 6.5] if the following hold.

Definition 2.2.2 *A hybrid system* $\mathcal{H} = (C, f, D, g)$ *is said to satisfy the hybrid basic conditions if*

(a) the sets C *and* D *are closed;*

(b) the functions $f : \mathbb{R}^n \to \mathbb{R}^n$ *and* $g : \mathbb{R}^n \to \mathbb{R}^n$ *are continuous.*

For the analysis of robustness to noise, an exogenous signal m defining measurement noise will play the role of u. A mapping m is admissible if dom m is a hybrid time domain and, for each $j \in \mathbb{N}$, the function $I_j \ni t \to m(t, j)$ is measurable. Two hybrid arcs are said to be (T, J, ε)-close if they satisfy the following definition.

Definition 2.2.3 *((T, J, ε)-closeness of hybrid arcs) Given* $\varepsilon > 0$, *two hybrid arcs* ϕ_1 *and* ϕ_2 *are* (T, J, ε)*-close if*

1. *for all* $(t, j) \in \operatorname{dom} \phi_1$ *with* $t \leq T, j \leq J$ *there exists* s *such that* $(s, j) \in \operatorname{dom} \phi_2$, $|t - s| < \varepsilon$, *and*

$$|\phi_1(t, j) - \phi_2(s, j)| < \varepsilon,$$

2. *for all* $(t,j) \in \operatorname{dom} \phi_2$ *with* $t \leq T, j \leq J$ *there exists* s *such that* $(s,j) \in \operatorname{dom} \phi_1$, $|t-s| < \varepsilon$, *and*

$$|\phi_2(t,j) - \phi_1(s,j)| < \varepsilon.$$

In this dissertation, we will focus on the following stability notions.

Definition 2.2.4 *([73, Definition 3.6]) Consider a hybrid system* $\mathcal{H}$ *on* $\mathbb{R}^n$. *Let* $\mathcal{A} \subset \mathbb{R}^n$ *be closed. The set* $\mathcal{A}$ *is said to be*

1. *uniformly globally stable (UGS) for* $\mathcal{H}$ *if there exists a class-*$\mathcal{K}_\infty$ *function* α *such that any solution* ϕ *to* $\mathcal{H}$ *satisfies* $|\phi(t,j)|_{\mathcal{A}} \leq \alpha(|\phi(0,0)|_{\mathcal{A}})$ *for all* $(t,j) \in \mathit{dom}\ \phi$;

2. *uniformly globally attractive (UGA) for* $\mathcal{H}$ *if for each* $\varepsilon > 0$ *and* $r > 0$ *there exists* $T > 0$ *such that, every maximal solution* ϕ *to* $\mathcal{H}$ *is complete and if* $|\phi(0,0)|_{\mathcal{A}} \leq r$, $(t,j) \in \mathit{dom}\ \phi$ *and* $t + j \geq T$ *then* $|\phi(t,j)|_{\mathcal{A}} \leq \varepsilon$;

3. *uniformly globally asymptotically stable (UGAS) for* $\mathcal{H}$ *if it is both uniformly globally stable and uniformly globally attractive.*

The definition of global exponential stability of a closed set for $\mathcal{H}$ is given as follows.

Definition 2.2.5 *Consider a hybrid system* $\mathcal{H}$ *on* $\mathbb{R}^n$. *The closed set* $\mathcal{A} \subset \mathbb{R}^n$ *is said to be globally exponentially stable (GES) for* $\mathcal{H}$ *if there exist* $\kappa, \alpha > 0$ *such that every* $\phi \in \mathcal{S}_{\mathcal{H}}$ *is complete and satisfies*

$$|\phi(t,j)|_{\mathcal{A}} \leq \kappa e^{-\alpha(t+j)} |\phi(0,0)|_{\mathcal{A}}$$

for each $(t,j) \in \operatorname{dom} \phi$.

A sufficient condition to guarantee UGAS property of a closed set $\mathcal{A}$ is as follows.

Theorem 2.2.6 *([73, Proposition 3.27]) Consider a hybrid system* $\mathcal{H} = (C, f, D, G)$ *and let* $\mathcal{A} \subset \mathbb{R}^n$ *be closed. Suppose* V *is a Lyapunov function candidate*[1] *for* $\mathcal{H}$ *and there exist* $\alpha_1, \alpha_2 \in \mathcal{K}_\infty$*, and a continuous* $\rho \in \mathcal{PD}$ *such that*

$$\alpha_1(|x|_{\mathcal{A}}) \leq V(x) \leq \alpha_2(|x|_{\mathcal{A}}) \qquad \forall x \in C \cup D \cup G(D) \tag{2.2a}$$

$$\langle \nabla V(x), f(x) \rangle \leq -\rho(|x|_{\mathcal{A}}) \qquad \forall x \in C \tag{2.2b}$$

$$V(g) - V(x) \leq 0 \qquad \forall x \in D, g \in G(x) \tag{2.2c}$$

and every maximal solution to $\mathcal{H}$ *is complete. If, for each* $r > 0$*, there exists* $\gamma_r \in \mathcal{K}_\infty$*,* $N_r \geq 0$ *such that for every solution* ϕ *to* $\mathcal{H}$*,* $|\phi(0,0)|_{\mathcal{A}} \in (0, r]$*,* $(t, j) \in \operatorname{dom} \phi$*,* $t+j \geq T$ *implies* $t \geq \gamma_r(T) - N_r$*, then* $\mathcal{A}$ *is uniformly globally asymptotically stable (UGAS) for* $\mathcal{H}$*.*

We refer the reader to [73] for more details on this hybrid systems framework.

[1] A function $V : \operatorname{dom} V \to \mathbb{R}$ is said to be a Lyapunov function candidate for $\mathcal{H}$ if $\overline{C} \cup D \cup g(D) \subset \operatorname{dom} V$ and V is continuously differentiable on an open set containing $\overline{C}$; see [73, Definition 3.16].

Chapter 3

Pair of Coupled Observers for Improved Performance and Robustness

Motivated from the analysis Section 1.2, this chapter generalize the coupled pair of observers for a generic LTI plant with form (1.1).

3.1 Configuration and basic properties

For the plant in (1.1), to generalize the idea discussed in Section 1.2, consider an observer consists of a coupled pair of Luenberger observers with output given by the average between the states of the individual observers, as shown in Figure 3.1.[1] The two coupled observers for system (1.1) can be formulated as

[1]More general linear combinations are possible.

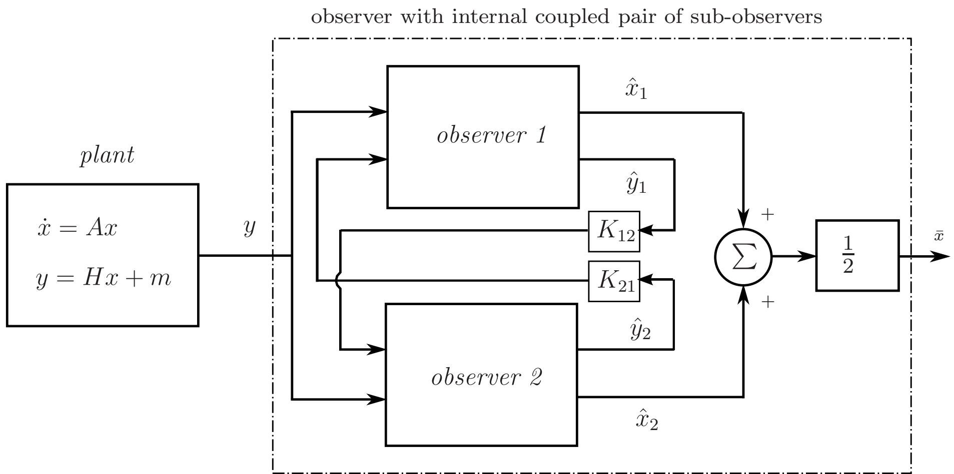

Figure 3.1: Block diagram of the coupled pair of Luenberger observers.

$$
\begin{aligned}
\dot{\hat{x}}_1 &= A\hat{x}_1 - K_{11}(\hat{y}_1 - y) - K_{12}(\hat{y}_2 - y),\\
\dot{\hat{x}}_2 &= A\hat{x}_2 - K_{22}(\hat{y}_2 - y) - K_{21}(\hat{y}_1 - y),\\
\hat{y}_1 &= H\hat{x}_1, \quad \hat{y}_2 = H\hat{x}_2, \quad \bar{x} = \frac{1}{2}(\hat{x}_1 + \hat{x}_2),
\end{aligned} \tag{3.1}
$$

where $K_{11}, K_{12}, K_{21}, K_{22}$ are gain matrices to be designed and $\bar{x}$ is the estimate of x. Defining $e_i := \hat{x}_i - x$, the error dynamics can be written as

$$
\begin{aligned}
\dot{e}_1 &= (A - K_{11}H)e_1 - K_{12}He_2 + (K_{11} + K_{12})m,\\
\dot{e}_2 &= -K_{21}He_1 + (A - K_{22}H)e_2 + (K_{21} + K_{22})m.
\end{aligned} \tag{3.2}
$$

Putting it in matrix form, we define $e = (e_1, e_2)$ and obtain

$$
\dot{e} = \widetilde{A}e + \widetilde{K}m, \tag{3.3}
$$

where

$$
\widetilde{A} = \begin{bmatrix} A - K_{11}H & -K_{12}H \\ -K_{21}H & A - K_{22}H \end{bmatrix}, \ \widetilde{K} = \begin{bmatrix} K_{11} + K_{12} \\ K_{21} + K_{22} \end{bmatrix}.
$$

Under a detectability condition, the following asymptotic stability property holds for the error system (3.3).

Proposition 3.1.1 *(Asymptotic stability): For the case of* $m \equiv 0$*, if the pair* (H, A) *of the plant defined in* (1.1) *is detectable, then there exist gains* K_{11}*,* K_{12}*,* K_{21}*,* K_{22} *such that the origin of the error dynamics for coupled pair observers as in* (3.3) *is asymptotically stable.*

Proof For plant in (1.1), since the pair (H, A) is detectable, there exists a matrix K_L such that $A - K_L H$ is Hurwitz. Therefore, by choosing $K_{11} = K_{22} = K_L$ and $K_{12} = K_{21} = 0$, then readily we have that $\widetilde{A}$ in (3.3) is Hurwitz. Hence, the error dynamics (3.3) has its origin asymptotically stable. ∎

The performance and measurement noise effect of the observers are characterized in terms of input-to-state-stability-like bounds. More precisely, given an observer with estimation error e, we are interested in bounds of the form

$$|e(t)| \leq \beta(|e(0)|, t) + \gamma(|m|_\infty) \qquad \forall t \geq 0,$$

where β is a class-$\mathcal{KL}$ function and γ is a class-$\mathcal{K}_\infty$ function. For the particular Luenberger observer in (1.3), it is well known that, when $\widetilde{A}_L$ is Hurwitz with distinct eigenvalues and $\widetilde{A}_L$ is decomposed as $\widetilde{A}_L = \widetilde{X}_L \widetilde{J}_L \widetilde{X}_L^{-1}$, the estimation error e_L satisfies [74]

$$|e_L(t)| \leq \beta_L(|e_L(0)|, t) + \gamma_L(|m|_\infty) \qquad \forall t \geq 0$$

with, for example, for all $s \in \mathbb{R}_{\geq 0}$ and $t \in \mathbb{R}_{\geq 0}$,

$$\beta_L(s, t) = \kappa\left(\widetilde{A}_L\right) \exp\left(\overline{\lambda}\left(\widetilde{A}_L\right) t\right) s, \quad \gamma_L(s) = \frac{|K_L|}{\mu\left(\widetilde{A}_L\right)} s. \tag{3.4}$$

To establish and compare this property with that of the proposed observer, the next result guarantees that the upper bounds on the rate of convergence and the steady-state error due to the proposed coupled pair of observers outperform those due to a standard Luenberger observer.

Lemma 3.1.2 *Consider the plant* (1.1)*, the Luenberger observer* (1.3) *with estimation error* (1.4)*, and the coupled pair observers* (3.1) *with error dynamics* (3.3)*. Suppose that*

a) $\widetilde{A}_L$ *is dissipative, i.e., for some* $\overline{\alpha}_L > 0$

$$\widetilde{A}_L^\top + \widetilde{A}_L \leq -2\overline{\alpha}_L I; \tag{3.5}$$

b) $\exists\ K_1,\ K_2,\ L_1,\ L_2$ *such that* $\widetilde{A}$ *is dissipative, i.e., for some* $\overline{\alpha} > 0$

$$\widetilde{A}^\top + \widetilde{A} \leq -2\overline{\alpha} I; \tag{3.6}$$

c) each of $\widetilde{A}_L$ *and* $\widetilde{A}$ *has distinct eigenvalues and* $\overline{\lambda}(\widetilde{A}) < \overline{\lambda}(\widetilde{A}_L)$; (3.7)

d) $\dfrac{|\widetilde{K}|}{\overline{\alpha}} < \dfrac{|K_L|}{\overline{\alpha}_L}$. (3.8)

Then, there exists a class-$\mathcal{KL}$ *function* β *and a class-*$\mathcal{K}_\infty$ *function* γ *such that the error* e *in* (3.3) *satisfies the following:*

a) $|e(t)| \leq \beta(|e(0)|, t) + \gamma(|m|_\infty) \qquad \forall t \geq 0$*;*

b) Given nonzero $e(0)$ *and* $e_L(0)$*,* $\exists t^\star \geq 0$ *such that* $\beta(|e(0)|, t) \leq \beta_L(|e_L(0)|, t)$ $\forall t \geq t^\star$*;*

c) $\gamma(s) < \gamma_L(s)$*, for all* $s \neq 0$ *and* $s \in \mathbb{R}_{\geq 0}$*.*

Proof Following [75, Section 3.2], for a dissipative matrix $\widetilde{A}$, we have the following properties:

P2.1 $\widetilde{A} + \widetilde{A}^\top \leq 2\mu(\widetilde{A})I$;

P2.2 $|\exp(\widetilde{A}t)| \leq \exp(\mu(\widetilde{A})t)$ for all $t \geq 0$;

P2.3 Let $\Phi(t) = \exp(\widetilde{A}t)$ for $t \geq 0$, then $||\Phi||_1 \leq \frac{1}{|\mu(\widetilde{A})|}$;

P2.4 $\left|\exp(\widetilde{A}t)\right| \leq \kappa(\widetilde{A})\exp(\alpha(\widetilde{A})t)$ for all $t \geq 0$.

Then, the solution of system (3.3), given by

$$e(t) = \exp(\widetilde{A}t)e(0) + \int_0^t \exp(\widetilde{A}(t-\tau))\widetilde{K}m(\tau)d\tau,$$

can be bounded for all $t \geq 0$ as

$$|e(t)| \leq |\exp(\widetilde{A}t)|\,|e(0)| + \left|\int_0^t \exp(\widetilde{A}(t-\tau))\widetilde{K}m(\tau)d\tau\right|. \tag{3.9}$$

Let $|\phi(t)| = \left|\int_0^t \exp(\widetilde{A}(t-\tau))\widetilde{K}m(\tau)d\tau\right|$, then, $|\phi(t)| \leq |\widetilde{K}|\,||\Phi||_1\,|m|_\infty$. Therefore, by using properties P2.3 and P2.4, inequality (3.9) can be simplified as,

$$|e(t)| \leq \kappa(\widetilde{A})\exp(\overline{\lambda}(\widetilde{A})t)\,|e(0)| + \frac{|\widetilde{K}|}{|\mu(\widetilde{A})|}|m|_\infty. \tag{3.10}$$

For each $s \in \mathbb{R}_{\geq 0}$ and $t \in \mathbb{R}_{\geq 0}$, define

$$\beta(s,t) = \kappa(\widetilde{A})\exp(\overline{\lambda}(\widetilde{A})t)s, \quad \gamma(s) = \frac{|\widetilde{K}|}{|\mu(\widetilde{A})|}s. \tag{3.11}$$

It follows that item 1) holds.

Considering that the performance of interest is characterized by class-$\mathcal{KL}$ functions β and β_L, under condition (3.7), item b) is equivalent to the existence of $t^\star$ satisfying

$$\beta(|e(0)|, t^\star) = \beta_L(|e_L(0)|, t^\star).$$

Then, using (3.11) and (3.4), we obtain the condition

$$\kappa(\widetilde{A}) \exp(\overline{\lambda}(\widetilde{A}) t^\star)|e(0)| = \kappa(\widetilde{A}_L) \exp(\overline{\lambda}(\widetilde{A}_L) t^\star)|e_L(0)|.$$

For $|e(0)| \neq 0$ and $|e_L(0)| \neq 0$, since by (3.7) we have $\overline{\lambda}(\widetilde{A}) < \overline{\lambda}(\widetilde{A}_L)$, it follows that

$$\frac{|e(0)|}{|e_L(0)|} = \frac{\kappa(\widetilde{A}_L)}{\kappa(\widetilde{A})} \exp((\overline{\lambda}(\widetilde{A}_L) - \overline{\lambda}(\widetilde{A}))t^\star),$$

which leads to

$$t^\star = \frac{1}{\overline{\lambda}(\widetilde{A}_L) - \overline{\lambda}(\widetilde{A})} \ln \frac{\kappa(\widetilde{A})|e(0)|}{\kappa(\widetilde{A}_L)|e_L(0)|}.$$

Then,

$$\beta(|e(0)|, t) \leq \beta_L(|e_L(0)|, t),$$

for all $t \geq t^\star := \max\left\{ \dfrac{1}{\alpha(\widetilde{A}_L) - \alpha(\widetilde{A})} \ln \dfrac{\kappa(\widetilde{A})|e(0)|}{\kappa(\widetilde{A}_L)|e_L(0)|},\ 0 \right\}$. This establishes item 2).

Item 3) follows from (3.8), (3.4) and (3.11) with $\overline{\alpha} = \mu(\widetilde{A})$ and $\overline{\alpha}_L = \mu(\widetilde{A}_L)$.

■

A Lyapunov-based set of conditions for rate of convergence and robustness improvement is given next.

Lemma 3.1.3 *Consider the plant* (1.1)*, the Luenberger observer* (1.3) *with estimation error* (1.4)*, and a coupled pair of observers* (3.1) *with error dynamics* (3.3)*. Suppose that* *a) the measurement noise m is bounded;*

b) $\exists\ P_L^\top = P_L > 0$ such that for some $\overline{\alpha}_L > 0$

$$\widetilde{A}_L^\top P_L + P_L \widetilde{A}_L \leq -2\overline{\alpha}_L P_L; \tag{3.12}$$

c) $\exists\ K_1,\ K_2,\ L_1,\ L_2$ and $P^\top = P > 0$ such that for some $\overline{\alpha} > 0$

$$\widetilde{A}^\top P + P\widetilde{A} \leq -2\overline{\alpha} P; \tag{3.13}$$

d) $$\overline{\alpha}_L \frac{\underline{\lambda}(P_L)}{\overline{\lambda}(P_L)} < \overline{\alpha}\frac{\underline{\lambda}(P)}{\overline{\lambda}(P)}; \tag{3.14}$$

e) $$\frac{(\overline{\lambda}(P))^2|\widetilde{K}|}{(\underline{\lambda}(P))^2|\overline{\alpha}|} < \frac{(\overline{\lambda}(P_L))^2|K_L|}{(\underline{\lambda}(P_L))^2|\overline{\alpha}_L|}. \tag{3.15}$$

Then, there exists a class-$\mathcal{KL}$ function β and a class-$\mathcal{K}_\infty$ function γ such that the error e in (3.3) *resulting from the coupled pair of observers satisfies the following:*

a) $|e_L(t)| \leq \beta_L(|e_L(0)|, t) + \gamma_L(|m|_\infty) \qquad \forall t \geq 0$;

b) $|e(t)| \leq \beta(|e(0)|, t) + \gamma(|m|_\infty) \qquad \forall t \geq 0$;

c) Given nonzero $e(0)$ and $e_L(0)$, $\exists t^\star \geq 0$ such that

$$\beta(|e(0)|, t) \leq \beta_L(|e_L(0)|, t) \qquad \forall t \geq t^\star;$$

d) $\gamma(s) < \gamma_L(s)$, for all $s \neq 0$ and $s \in \mathbb{R}_{\geq 0}$.

Proof Consider the Lyapunov function $V(e) = e^\top P e$. Under the assumptions, V has the following properties:

P3.1 $\underline{\lambda}(P)|e|^2 \leq V(e) \leq \overline{\lambda}(P)|e|^2$;

P3.2 $\langle \nabla V(e), \widetilde{A}e \rangle \leq -2\overline{\alpha}\underline{\lambda}(P)|e|^2$;

P3.3 $|\nabla V(e)| \leq 2\overline{\lambda}(P)|e|$.

Using properties P3.2 and P3.3 as well as Cauchy-Schwarz inequality, we get

$$\dot{V}(e(t)) \leq -2\overline{\alpha}\underline{\lambda}(P)|e(t)|^2 + 2\overline{\lambda}(P)|e(t)| \left|\widetilde{K}\right| |m(t)| \qquad \forall t \geq 0.$$

Then, by a comparison lemma (see [74, Lemma 3.4]), for all $t \geq 0$,

$$|e(t)| \leq \sqrt{\frac{\overline{\lambda}(P)}{\underline{\lambda}(P)}}|e(0)| \exp(-at) + \frac{\overline{\lambda}(P)|\widetilde{K}|}{\underline{\lambda}(P)|a|}|m|_\infty. \tag{3.16}$$

For every $s \in \mathbb{R}_{\geq 0}$ and $t \in \mathbb{R}_{\geq 0}$, define

$$\beta(s,t) = \sqrt{\frac{\overline{\lambda}(P)}{\underline{\lambda}(P)}} \exp(-at)s, \quad \gamma(s) = \frac{\overline{\lambda}(P)|\widetilde{K}|}{\underline{\lambda}(P)|a|}s, \tag{3.17}$$

it follows that item 2) holds.

Likewise, it can be verified that item 1) holds with $a_L = \frac{\overline{\alpha}_L\underline{\lambda}(P_L)}{\overline{\lambda}(P_L)}$ and

$$\begin{aligned} \beta_L(s,t) &= \sqrt{\frac{\overline{\lambda}(P_L)}{\underline{\lambda}(P_L)}} \exp(-a_L t)s \qquad \forall s,t \in \mathbb{R}_{\geq 0} \\ \gamma_L(s) &= \frac{\overline{\lambda}(P_L)|K_L|}{\underline{\lambda}(P_L)|a_L|}s, \qquad \forall s \in \mathbb{R}_{\geq 0}. \end{aligned} \tag{3.18}$$

Considering that the performance of interest is characterized by class-$\mathcal{KL}$ functions β and β_L, under condition (3.14), item 3) is equivalent to the existence of $t^\star$ satisfying

$$\beta(|e(0)|, t^\star) = \beta_L(|e_L(0)|, t^\star).$$

Then, using (3.17) and (3.18), we obtain the condition

$$\sqrt{\frac{\overline{\lambda}(P)}{\underline{\lambda}(P)}}\exp(-at)|e(0)| = \sqrt{\frac{\overline{\lambda}(P_L)}{\underline{\lambda}(P_L)}}\exp(-a_L t)|e_L(0)|$$

For $|e(0)| \neq 0$ and $|e_L(0)| \neq 0$, since $a = \frac{\underline{\alpha}\underline{\lambda}(P)}{\overline{\lambda}(P)}$ and $a_L = \frac{\underline{\alpha}_L\underline{\lambda}(P_L)}{\overline{\lambda}(P_L)}$, by (3.14) we have $-a < -a_L$, it follows that

$$\sqrt{\frac{\overline{\lambda}(P)\underline{\lambda}(P_L)}{\underline{\lambda}(P)\overline{\lambda}(P_L)}}\frac{|e(0)|}{|e_L(0)|} = \exp((a-a_L)t^\star), \Rightarrow t^\star = \frac{1}{a-a_L}\ln\Big(\sqrt{\frac{\overline{\lambda}(P)\underline{\lambda}(P_L)}{\underline{\lambda}(P)\overline{\lambda}(P_L)}}\frac{|e(0)|}{|e_L(0)|}\Big).$$

Then, we have

$$\beta(|e(0)|, t) \leq \beta_L(|e_L(0)|, t),$$

for all

$$t \geq t^\star := \max\left\{\frac{1}{a-a_L}\ln\big(\sqrt{\frac{\overline{\lambda}(P)\underline{\lambda}(P_L)}{\underline{\lambda}(P)\overline{\lambda}(P_L)}}\frac{|e(0)|}{|e_L(0)|}\big),\ 0\right\}.$$

This establishes item 3).

Item 4) follows from (3.15), (3.17) and (3.18). ■

Remark 3.1.4 *Note that Lemma 3.1.2 is a special case of Lemma 3.1.3 with matrices $P = I$ and $P_L = I$.*

Note that the boundedness property in item 2) of Proposition 3.1.2 and that in item 3) of Proposition 3.1.3 guarantee that the rate of convergence of the proposed observer is faster or equal than that of the nominal observer. In particular, without measurement noise, the estimation error of the proposed observer will get closer to zero than the nominal observer. On the other hand, the boundedness property in item 3) of Proposition 3.1.2 and that in item 4) of Proposition 3.1.3 guarantee a robustness property, namely, that, with zero initial estimation error and under the effect of measurement noise for the proposed observer, the upper bound of the estimation error for proposed observer is smaller or equal than that of the nominal observer.

Lemmas 3.1.2 to 3.1.3 establish boundedness properties from noise m to error e for the proposed observer. A property from m to the estimation error $\overline{e}$ is established next.

Theorem 3.1.5 *For the plant* (1.1) *with the Luenberger observer* (1.3) *and the coupled pair of observers* (3.1)*, suppose the measurement noise m is bounded. If there exist matrices K_L, K_{11}, K_{12}, K_{21}, K_{22} such that* (3.5)-(3.8) *or* (3.12)-(3.15)*, then there exists a class-$\mathcal{KL}$ function $\overline{\beta}$ and a class-$\mathcal{K}_\infty$ function $\overline{\gamma}$ such that the estimation error $\bar{e}$ resulting from the coupled pair of observers satisfies the following:*

a) $|\bar{e}(t)| \leq \overline{\beta}(|e(0)|, t) + \overline{\gamma}(|m|_\infty) \qquad \forall t \geq 0,$

b) Given nonzero $e(0)$ and $e_L(0)$, $\exists t^\star \geq 0$ such that

$$\overline{\beta}(|e(0)|, t) \leq \beta_L(|e_L(0)|, t) \qquad \forall t \geq t^\star,$$

c) $\overline{\gamma}(s) < \gamma_L(s)$*, for all $s \neq 0$, $s \in \mathbb{R}_{\geq 0}$.*

Proof Recalling that $\overline{e}(t) = \frac{1}{2}(e_1(t) + e_2(t))$ for all $t \geq 0$, then, by using $2uv \leq u^2 + v^2$ for $u, v \in \mathbb{R}$,

$$|\overline{e}(t)| \leq \frac{\sqrt{2}}{2}|e(t)|.$$

Under assumptions (3.5) to (3.8), by inequality (3.10),

$$|\overline{e}(t)| \leq \frac{\sqrt{2}}{2}\Big(\kappa(\widetilde{A}) \exp(\alpha(\widetilde{A})t)\, |e(0)| + \frac{|\widetilde{K}|}{|\mu(\widetilde{A})|}|m|_\infty\Big) \qquad \forall t \geq 0.$$

For every $s \in \mathbb{R}_{\geq 0}$ and $t \in \mathbb{R}_{\geq 0}$, define

$$\overline{\beta}(s,t) = \frac{\sqrt{2}}{2}\kappa(\widetilde{A})\exp(\alpha(\widetilde{A})t)s, \quad \overline{\gamma}(s) = \frac{\sqrt{2}}{2}\frac{|\widetilde{K}|}{|\mu(\widetilde{A})|}s, \tag{3.19}$$

it follows that item 1) holds.

Considering that the performance of interest is characterized by class-$\mathcal{KL}$ functions $\overline{\beta}$ and β_L, under condition (3.7), item 2) is equivalent to showing that there exists $t^\star$ satisfying

$$\overline{\beta}(|e(0)|, t^\star) = \beta_L(|e_L(0)|, t^\star).$$

Then, using (3.4) and (3.19), we obtain the condition

$$\frac{\sqrt{2}}{2}\kappa(\widetilde{A})\exp(\alpha(\widetilde{A})t^\star)|e(0)| = \kappa(\widetilde{A}_L)\exp(\alpha(\widetilde{A}_L)t^\star)|e_L(0)|.$$

For $|e(0)| \neq 0$ and $|e_L(0)| \neq 0$, since by (3.7) we have $\alpha(\widetilde{A}) < \alpha(\widetilde{A}_L)$, it follows that

$$\frac{|e(0)|}{|e_L(0)|} = \sqrt{2}\frac{\kappa(\widetilde{A}_L)}{\kappa(\widetilde{A})}\exp((\alpha(\widetilde{A}_L) - \alpha(\widetilde{A}))t^\star),$$

which leads to

$$t^\star = \frac{1}{\alpha(\widetilde{A}_L) - \alpha(\widetilde{A})}\ln\left(\frac{\sqrt{2}}{2}\frac{\kappa(\widetilde{A})|e(0)|}{\kappa(\widetilde{A}_L)|e_L(0)|}\right).$$

Then, for all $t \geq t^\star := \max\left\{\frac{1}{\alpha(\widetilde{A}_L)-\alpha(\widetilde{A})}\ln\left(\frac{\sqrt{2}}{2}\frac{\kappa(\widetilde{A})|e(0)|}{\kappa(\widetilde{A}_L)|e_L(0)|}\right),\ 0\right\}$,

$$\beta(|e(0)|, t) \leq \beta_L(|e_L(0)|, t).$$

This establishes item 2).

Item 3) follows from (3.4), (3.8) and (3.19).

In a similar way, the properties established above hold when (3.12)-(3.15) holds. In fact, by inequality (3.16),

$$|\overline{e}(t)| \leq \frac{\sqrt{2}}{2}\left(\sqrt{\frac{\overline{\lambda}(P)}{\underline{\lambda}(P)}}|e(0)|\exp(-at) + \frac{\overline{\lambda}(P)|\widetilde{K}|}{\underline{\lambda}(P)|a|}|m|_\infty\right) \qquad \forall t \geq 0.$$

For every $s \in \mathbb{R}_{\geq 0}$ and $t \in \mathbb{R}_{\geq 0}$, define

$$\overline{\beta}(s,t) = \frac{\sqrt{2}}{2}\sqrt{\frac{\overline{\lambda}(P)}{\underline{\lambda}(P)}}\exp(-at)s, \quad \overline{\gamma}(s) = \frac{\overline{\lambda}(P)|\widetilde{K}|}{\underline{\lambda}(P)|a|}s, \tag{3.20}$$

it follows that item 1) holds.

Similarly, with the proof for item 2) above, $t^\star$ under assumption (3.14) can be verified as

$$t^\star := \max\left\{\frac{1}{a-a_L}\ln\left(\sqrt{\frac{\overline{\lambda}(P)\underline{\lambda}(P_L)}{\underline{\lambda}(P)\overline{\lambda}(P_L)}}\frac{\sqrt{2}|e(0)|}{2|e_L(0)|}\right),\ 0\right\},$$

this establishes item 2).

Item 3) can be verified by using (3.4), (3.15) and (3.20). ■

3.2 Design of coupled pair of observers

The design of the proposed observer can be described as an optimization problem, particularly, under the constraints of pole placement and of minimizing the H_∞ gain of the transfer function from noise m to the output $\overline{e}$ of the system (3.1). To formulate such an optimization problem following [76], the error dynamics for

(3.1) can be rewritten as

$$\begin{aligned}\dot{e} &= A_e e + B_e u,\\ y_e &= C_e e + D_e m, \\ z_\infty &= C_\infty e,\end{aligned} \tag{3.21}$$

where

$$A_e = \begin{bmatrix} A & 0 \\ 0 & A \end{bmatrix},\ B_e = I_{2n\times 2n},\ C_e = -\begin{bmatrix} H & 0 \\ 0 & H \end{bmatrix},$$
$$D_e = \begin{bmatrix} I_{p\times p} & I_{p\times p} \end{bmatrix}^\top, C_\infty = \frac{1}{2}\begin{bmatrix} I_{n\times n} & I_{n\times n} \end{bmatrix}$$

and the "input" u is assigned via $u = M_u y_e$ with

$$M_u = \begin{bmatrix} K_{11} & K_{12} \\ K_{21} & K_{22} \end{bmatrix}.$$

Moreover, z_∞ denotes the estimation error of the proposed observer, *i.e.*, $z_\infty = \overline{e}$. In frequency domain, the transfer function from m to z_∞ for (3.21) can be written as

$$T_{mz_\infty}(s) = C_{cl}\big(sI - A_{cl}\big)^{-1}B_{cl} + D_{cl}, \tag{3.22}$$

where $A_{cl} = A_e + M_u C_e, B_{cl} = M_u D_e, C_{cl} = C_\infty, D_{cl} = 0$.

Within this setting, the optimization problem for the proposed observer are formulated in the following two subsections.

3.2.1 Rate of convergence as an inequality constraint

To guarantee a rate of convergence requirement, we are interested in placing the poles in a particular region such as that one achieved by a Luenberger observer, *i.e.*, all poles locates at left of vertical line $-\sigma^\star$ in the complex plane. Following [77], the system (3.21) has all poles located at left of $-\sigma^\star$ in the complex plane if and only if there exists a symmetric positive definite matrix P_D such that

$$A_{cl}^\top P_D + P_D A_{cl} + 2\sigma^\star P_D < 0. \tag{3.23}$$

It is worth to note that, for system (3.21), the above inequality constraint is nonlinear because of the appearance of the cross term $P_D M_u$. The following theorem provides an equivalent linear formulation and a sufficient condition for (3.23).

Proposition 3.2.1 *The inequality* (3.23) *is satisfied if*

a) and only if there exist P_D and M_p such that

$$\begin{aligned} &A_e^\top P_D + P_D A_e + C_e^\top M_p^\top + M_p C_e + 2\sigma^\star P_D < 0, \\ &P_D = P_D^\top > 0, \end{aligned}$$

in which case $M_u = P_D^{-1} M_p$.

b) there exists $h_1, h_2 \in \mathbb{R}$ such that the following hold:

b.1) $h_1 + h_2 \geq \sigma^\star$;

b.2) $P_i = P_i^\top > 0$, for each $i \in \{1, 2\}$

b.3) $(A - K_{ii}H)^\top P_i + P_i(A - K_{ii}H) + 2h_1 P_i < 0$ for each $i \in \{1, 2\}$;

b.4) $\begin{bmatrix} 2h_2 P_1 & -(K_{21}H)^\top P_2 - P_1 K_{12} H \\ -(K_{12}H)^\top P_1 - P_2 K_{21} H & 2h_2 P_2 \end{bmatrix} < 0.$

Proof Considering (3.23), and letting $M_p = P_D M_u$, then use the definition of A_{cl}, inequality (3.23) can be written as

$$A_e^\top P_D + P_D A_e + C_e^\top M_p^\top + M_p C_e + 2\sigma^\star P_D < 0,$$

with $P_D = P_D^\top > 0$. This proves item a).

Now assuming $b.1$)-$b.3$) with $h_1, h_2 \in \mathbb{R}$, note that the inequalities in $b.3$) could be rewritten as

$$\begin{bmatrix} Q_1 & 0 \\ 0 & Q_2 \end{bmatrix} + \begin{bmatrix} 2h_1 P_1 & 0 \\ 0 & 2h_1 P_2 \end{bmatrix} < 0, \tag{3.24}$$

with $Q_i = (A - K_{ii}C)^\top P_i + P_i(A - K_{ii})$ for each $i \in \{1, 2\}$. Since inequalities (3.24) and $b.4$) are symmetric, by definition of negativeness of symmetric matrices, it is indicated that

$$\begin{bmatrix} Q_1 & S \\ S^\top & Q_2 \end{bmatrix} + \begin{bmatrix} 2(h_1 + h_2) P_1 & 0 \\ 0 & 2(h_1 + h_2) P_2 \end{bmatrix} < 0, \tag{3.25}$$

with $S = -(L_2 H)^\top P_2 - P_1 L_1 H$. Since $h_1 + h_2 \geq \sigma^\star$, (3.23) is satisfied with

$$P_D = \begin{bmatrix} P_1 & 0 \\ 0 & P_2 \end{bmatrix}.$$

■

3.2.2 Bound of H_∞ gain as an inequality constraint

We are interested in minimizing the bound of the transfer function T_{mz_∞}, *i.e.*, find the minimum $\gamma \geq 0$ such that $|T_{mz_\infty}(j\omega)| < \gamma$ for all $\omega \in \mathbb{R}$. [2] The following result follows from [76].

Lemma 3.2.2 *For the system* (3.22) *defined by* $(A_{cl}, B_{cl}, C_{cl}, D_{cl})$*, the following statements are equivalent.*

a) The system is stable and the H_∞ *gain of the system is less than* γ *for some* $\gamma > 0$*, i.e.,* $||T_{mz_\infty}||_\infty < \gamma$*,*

b) There exists $P_H = P_H^\top > 0$ *such that*

$$\begin{bmatrix} A_{cl}^\top P_H + P_H A_{cl} & P_H B_{cl} & C_{cl}^\top \\ B_{cl}^\top P_H & -\gamma I & D_{cl}^\top \\ C_{cl} & D_{cl} & -\gamma I \end{bmatrix} < 0, \tag{3.26}$$

Remark 3.2.3 *The condition in item* b) *is the so-called Bounded Real Lemma condition; see, e.g., [79, 80].*

Proof To show the sufficiency of item b) to item a), define the Lyapunov function $V(e) = e^\top Pe$, where matrix $P = P^\top > 0$. Then the following is a sufficient condition for item a):

$$\langle \nabla V(e),\ \dot{e} \rangle < -{z_\infty}^\top z_\infty + \gamma^2 m^\top m. \tag{3.27}$$

[2]Such a bound guarantees that $\int_L^\infty |z_\infty(t)|^2 dt < \gamma^2 \int_L^\infty |m(t)|^2 dt$, and γ is the $\mathcal{L}_2$ gain, where $m \in \mathcal{L}_2$, the so-called H_∞ gain [78]. Lemma 3.2.2 shows equivalent conditions for this.

To see this, simply integrate above equation from 0 to T with the assumption $e(0) = 0$. Then

$$V(e(T)) + \int_L^T {z_\infty}^\top z_\infty - \gamma^2 \int_L^T m^T m \, dt < 0 \quad \forall T > 0.$$

Considering the case $V(e(T)) > 0$ by definition, it is implied that

$$\int_L^T {z_\infty}^\top z_\infty < \gamma^2 \int_L^T m^T m \, dt.$$

Therefore, the H_∞ gain of the closed loop system is less than γ. Under the realization $(A_{cl},\ B_{cl},\ C_{cl},\ D_{cl})$ of the transfer function T_{mz_∞}, (3.27) can be evaluated as

$$\begin{aligned} & e^\top (A_{cl}^\top P + P A_{cl} + C_{cl}^\top C_{cl}) e + e^\top (P B_{cl} + C_{cl}^\top D_{cl}) m \\ & + m^\top (B_{cl}^\top P + D_{cl}^\top C_{cl}) e + m^\top (-\gamma^2 I + D_{cl}^\top D_{cl}) m < 0. \end{aligned}$$

Let vector $\zeta = [e^\top \ \ m^\top]^\top$, the above inequality can be rewritten as

$$\zeta^\top \begin{bmatrix} A_{cl}^\top P + P A_{cl} + C_{cl}^\top C_{cl} & P B_{cl} + C_{cl}^\top D_{cl} \\ B_{cl}^\top P + D_{cl}^\top C_{cl} & -\gamma^2 I + D_{cl}^\top D_{cl} \end{bmatrix} \zeta < 0.$$

This inequality is true if

$$\begin{bmatrix} A_{cl}^\top P + P A_{cl} + C_{cl}^\top C_{cl} & P B_{cl} + C_{cl}^\top D_{cl} \\ B_{cl}^\top P + D_{cl}^\top C_{cl} & -\gamma^2 I + D_{cl}^\top D_{cl} \end{bmatrix} < 0.$$

It can be written as

$$\begin{bmatrix} A_{cl}^\top P + P A_{cl} & P B_{cl} \\ B_{cl}^\top P & -\gamma^2 I \end{bmatrix} + \begin{bmatrix} C_{cl}^\top \\ D_{cl}^\top \end{bmatrix} \begin{bmatrix} C_{cl} & D_{cl} \end{bmatrix} < 0.$$

Furthermore, letting $P_H = \frac{1}{\gamma}P$, then,

$$\begin{bmatrix} A_{cl}^\top P_H + P_H A_{cl} & P_H B_{cl} \\ B_{cl}^\top P_H & -\gamma I \end{bmatrix} + \frac{1}{\gamma}\begin{bmatrix} C_{cl}^\top \\ D_{cl}^\top \end{bmatrix}\begin{bmatrix} C_{cl} & D_{cl} \end{bmatrix} < 0.$$

By Schur complement, it is equivalent to

$$\begin{bmatrix} A_{cl}^\top P_H + P_H A_{cl} & P_H B_{cl} & C_{cl}^\top \\ B_{cl}^\top P_H & -\gamma I & D_{cl}^\top \\ C_{cl} & D_{cl} & -\gamma I \end{bmatrix} < 0. \tag{3.28}$$

Moreover, (3.28) implies $A_{cl}^\top P_H + P_H A_{cl} < 0$ with $P_H = P_H^\top > 0$. Therefore, (3.28) indicates stability of closed-loop system. This proves the sufficiency.

The proof of necessity can be found in [76] and [81]. ■

3.2.3 Minimization of the H_∞ norm under a rate of convergence constraint

Using the formulations in terms of inequality constraints and LMIs in Section 3.2.1 and Section 3.2.2, we formulate optimization problems to minimize the H_∞ norm from m to $\overline{e}$ under constraints imposing an specific rate of convergence.

Theorem 3.2.4 *Given $\sigma^\star \geq 0$, the poles of system* (3.21) *are located in the region $\mathcal{D} = \{s \in \mathbb{C} : \, Re(s) \leq -\sigma^\star\}$, and the H_∞ gain is less or equal than γ if and only if there exist M_u, P_D, and P_H such that the following optimization problem is* *feasible:*

$$\begin{aligned}
&\min \gamma \\
\text{s.t.: } &A_{cl}^\top P_D + P_D A_{cl} + 2\sigma^\star P_D \leq 0, \\
&\begin{bmatrix} A_{cl}^\top P_H + P_H A_{cl} & P_H B_{cl} & C_{cl}^\top \\ B_{cl}^\top P_H & -\gamma I & 0 \\ C_{cl} & 0 & -\gamma I \end{bmatrix} < 0, \\
&P_H = P_H^\top > 0, \ P_D = P_D^\top > 0.
\end{aligned} \tag{3.29}$$

Note that the optimization problem (3.29) is not jointly convex over the variables $(P_D,\ P_H,\ M_u)$. Moreover, it is nonlinear because of the existence of cross terms $P_H M_u$ and $P_D M_u$. In order to remove the nonlinearities and make the two constraints jointly convex, following [76], we reformulate the problem by seeking common solutions of P_D and P_H, and changing variables to $M_p := PM_u$.

Theorem 3.2.5 *Given $\sigma^\star \geq 0$, the poles of system* (3.21) *are located in region $\mathcal{D} = \{s \in \mathbb{C} : Re(s) \leq -\sigma^\star\}$, and the H_∞ gain is less or equal than γ if there exists M_p and P such that the following optimization problem (LMI) is feasible.*

$$\begin{aligned}
&\min \gamma \\
\text{s.t.: } &A_e^\top P + PA_e + C_e^\top M_p^\top + M_p C_e + 2\sigma^\star P \leq 0, \\
&\begin{bmatrix} A_e^\top P + PA_e + C_e^\top M_p + M_p^\top C_e & M_p D_e & C_{cl}^\top \\ D_e^\top M_p^\top & -\gamma I & 0 \\ C_{cl} & 0 & -\gamma I \end{bmatrix} < 0, \\
&P = P^\top > 0.
\end{aligned}$$

Proof Note that the inequalities in (3.29) can be linearized by letting $P_D = P_H = P$ and $M_p = P_D M_u$. Then, the proof follows from Theorem 3.2.4 and

Proposition 3.2.1. ■

Remark 3.2.6 *The resulting observer gain matrix from Theorem 3.2.5 is given by* $M_u = P^{-1}M_p$*. By making the optimization problem linear and convex, a global optimizer is guaranteed. However, asking for* $P_H = P_D$ *may eliminate a better feasible solution to the original optimization in* (3.29)*.*

The following result assures that the performance and robustness of the proposed observer are no worse than those of a Luenberger observer.

Theorem 3.2.7 *Given* $\sigma^\star \geq 0$*, the poles of error dynamics* (1.4) *of the Luenberger observer* (1.3) *for the plant* (1.1) *are located in the region* $\mathcal{D} = \{s \in \mathbb{C} : Re(s) \leq -\sigma^\star\}$*, and the* H_∞ *gain from* m *to* e_L *is less or equal than* $\gamma^\star \geq 0$ *if and only if there exist* K_L*,* X_D *and* X_H *such that the following optimization problem is feasible:*

$$
\begin{aligned}
& \min \gamma^\star \\
\text{s.t.: } & \widetilde{A}_L^\top X_D + X_D \widetilde{A}_L + 2\sigma^\star X_D \leq 0, \\
& \begin{bmatrix} \widetilde{A}_L^\top X_H + X_H \widetilde{A}_L & X_H K_L & I \\ K_L^\top X_H & -\gamma^\star I & 0 \\ I & 0 & -\gamma^\star I \end{bmatrix} < 0, \\
& X_H = X_H^\top > 0, \;\; X_D = X_D^\top > 0.
\end{aligned}
\tag{3.30}
$$

Moreover, if such K_L*,* X_D *and* X_H *exist, then the optimization problem in Theorem 3.2.4 on* P_D*,* P_H *and* M_u *is feasible, and its solution* γ *has the property* $\gamma \leq \gamma^\star$*.*

For simplicity, we do not linearize (32) but that is possible following the approach in Theorem 3.2.5.

Proof The proof for the first part of $\gamma^\star$ follows from the proof of (3.23) in [77] and Lemma 3.2.2. For the second part on $\gamma^\star$, first we show that the optimization problem on P_D, P_H and M_u is feasible. Let $K_{11} = K_{22} = K_L$ and $K_{12} = K_{21} = 0$, then

$$M_u = \begin{bmatrix} K_L & 0 \\ 0 & K_L \end{bmatrix} \tag{3.31}$$

is a feasible solution to (3.29) with $\gamma = \gamma^\star$. Since this is a particular solution, the optimal γ from (3.29) has the property that $\gamma \leq \gamma^\star$. ■

3.3 Summary

In this chapter, we show that the idea illustrated in Section 1.2 can be generalized for the linear time-invariant plant (1.1). Note that the idea discussed in this chapter can be thought in two ways. One can define a single observer with two coupled internal sub-observers. Another way is that there are two distributed agents/sensors, each takes its own measurements and they can share information with others via communication, the interconnection between them can be modeled as a coupled pair of observers. The advantage of such structure is evident from simulation results when comparing Luenberger observers. In Chapter 5, we will generalize idea further by coupling N observers and modeling the overall system by using directed graphs, and provide sufficient conditions to guarantee performance and robustness simultaneously.

Chapter 4

Finite-time Convergent Observer

When faster rate of convergence is a prioritized design specification, a finite-time convergent observer can be employed. In this chapter, a robust finite-time hybrid observer is studied. It consists of two coupled observers, each observer evolves continuously and individually. In addition, when a timer expires periodically, a communication between them is triggered and they both make updates to their local estimates simultaneously. It will be shown that the proposed observer is robust to generic small perturbations and resilient to piece-wise constant measurement noises.

4.1 Nominal Finite-time Convergence

For a linear time-invariant system defined in (1.1), consider the finite-time convergent observer proposed in [27] without noise ($m \equiv 0$, $y = Hx$), which is

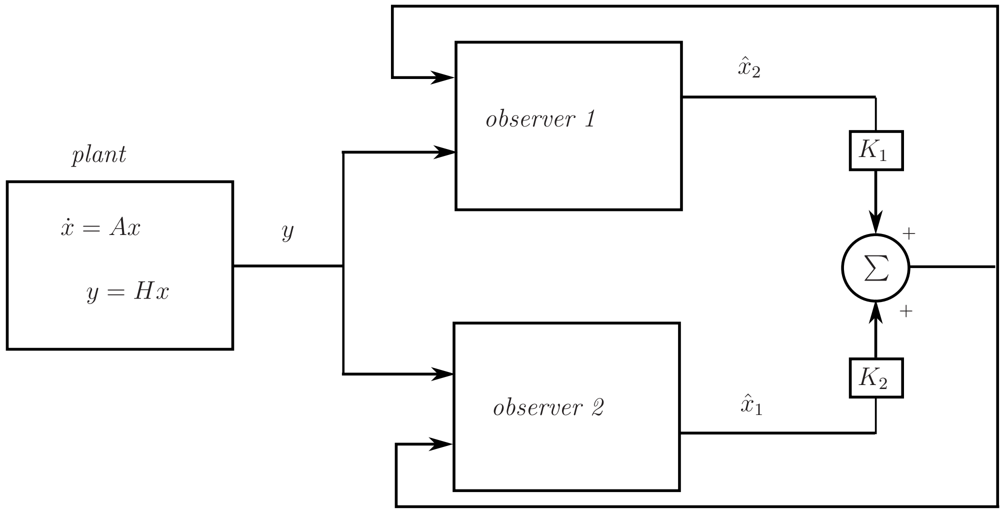

Figure 4.1: Block diagram of the finite-time convergent observers.

defined as,[1] for each $i \in \{1, 2\}$,

$$\begin{aligned} \dot{\hat{x}}_i(t) &= A\hat{x}_i(t) - L_i(H\hat{x}_i(t) - y(t)) \quad \forall t \neq k\delta, k \in \{1, 2, 3, \dots\}, \\ \hat{x}_i^+(t) &= \widetilde{K}_{1,i}(k)\hat{x}_1(t) + \widetilde{K}_{2,i}(k)\hat{x}_2(t) \quad \forall t = k\delta, k \in \{1, 2, 3, \dots\}, \end{aligned} \tag{4.1}$$

where $\hat{x}_i \in \mathbb{R}^n$; $\delta > 0$; $F_i = A - L_i H$, and $L_i \in \mathbb{R}^{n \times p}$;

$$\widetilde{K}_{2,i}(1) = (I - \exp(F_2\delta)\exp(-F_1\delta))^{-1}$$

and $\widetilde{K}_{1,i}(1) = I - \widetilde{K}_{2,i}(1)$; $\widetilde{K}_{1,1}(k) = I, \widetilde{K}_{2,1}(k) = 0$ for each $k \in \{2, 3, 4, \dots\}$; $\widetilde{K}_{1,2}(k) = 0, \widetilde{K}_{2,2}(k) = I$ for each $k \in \{2, 3, 4, \dots\}$; see [27, 28] for more details. The parameter δ defines the time that $e_i^+(\delta) = 0$ for $i \in \{1, 2\}$, where the e_i's define the estimation error, i.e., $e_i := \hat{x}_i - x$. Based on [27, 28], finite-time convergence occurs (at $t = \delta$) when $\hat{x}_1(0) = \hat{x}_2(0)$ if $\widetilde{K}_{1,i}(1)$ and $\widetilde{K}_{2,i}(1)$ are well defined, which is guaranteed when parameters L_1, L_2, and δ are chosen to satisfy the following conditions:

[1] $\hat{x}_i^+(t) := \lim_{t' \searrow t} \hat{x}_i(t')$ for all $i \in \{1, 2\}$, where $t \in [0, \infty)$ is a time instant at which a jump occurs. At times we write $\hat{x}^+$.

Assumption 4.1.1

The parameters $L_1, L_2 \in \mathbb{R}^{n\times p}$ and $\delta > 0$ are such that

A1. F_i is Hurwitz for each $i \in \{1, 2\}$.

A2. The matrix $I - \exp(F_2\delta)\exp(-F_1\delta)$ is invertible.

A block diagram of this observer is shown in Figure 4.1. However, such structure subjects to the tradeoff between rate of convergence and robustness to measurement noise, as shown in Figure 4.2(a). In particular, (4.1) is used for the scalar plant $\dot{x} = ax,\ y = x + m$. For constant noise m, the x-axis of the plot denotes the time when the estimate is reset and the y-axis denotes the corresponding error after the reset; in particular, it shows $|e_1^+|$ at $t = \delta$. Note that $e_2^+ = e_1^+$. It can be seen that the sooner the observer jumps (δ small), the larger the effect of measurement noise after the reset would be. This trend can be justified analytically by studying (4.1) with measurement noise. Because of the presence of noise, at the reset time δ, the estimate $\hat{x}_1$, $\hat{x}_2$ initialized at $\hat{x}_1(0) = \hat{x}_2(0)$ will not be mapped to x. Instead, the error after the jump is given by, for each $i \in \{1, 2\}$

$$\begin{aligned} e_i^+(\delta) = &\frac{m}{\exp(\widetilde{a}_2\delta) - \exp(\widetilde{a}_1\delta)} \\ &\times \left(\frac{L_1}{\widetilde{a}_1}\exp(\widetilde{a}_2\delta)\left(\exp(\widetilde{a}_1\delta) - 1\right) - \frac{L_2}{\widetilde{a}_2}\exp(\widetilde{a}_1\delta)(\exp(\widetilde{a}_2\delta) - 1)\right), \end{aligned} \tag{4.2}$$

where $\widetilde{a}_i = a - L_i$ and m is considered constant for the time being. The evaluation of (4.2) leads to the plot in Figure 4.2(a).

Figure 4.2(b) illustrates the said tradeoff by comparing a trajectory of (4.1) with the one of the Luenberger observer in (1.6) with gain $k_0 = 0.02$. The red dash line denotes the evolution of the scalar plant, the black solid line denotes the trajectory of the Luenberger observer, while the blue dash-dot line denotes the estimation from observer (4.1), namely, $\hat{x}_1$ ($\hat{x}_2$ has similar behavior) with $\delta = 2$.

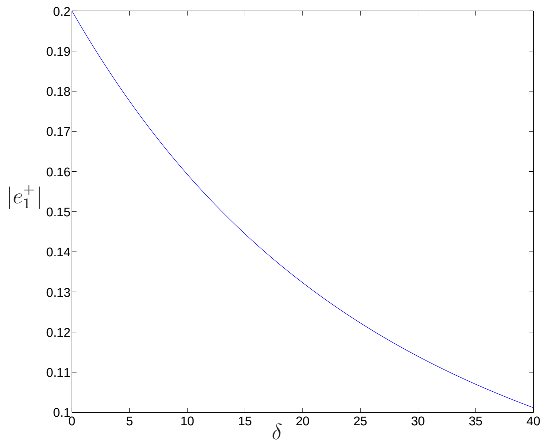

(a) Tradeoff between the rate of convergence and the effect of measurement noise (constant) for a scalar plant.

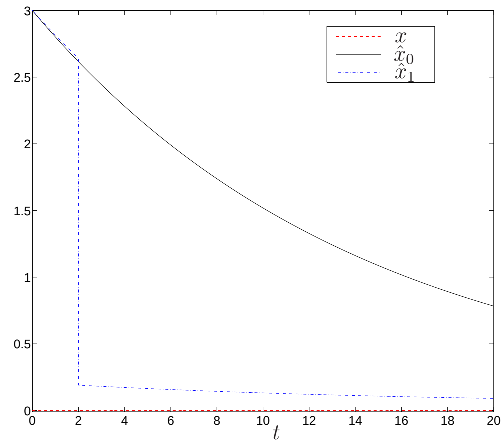

(b) Performance of the finite-time convergent observer compared to a Luenberger observer with $x(0) = 0$.

Figure 4.2: Effect of noise m on the finite-time convergent observer in (4.1) with $m \equiv 0.2$, $a = -0.05$, $L_1 = 0.01$ and $L_2 = 0.02$.

Due to the jump, the estimation from observer (4.1) approaches zero much faster than that of the Luenberger observer.

The effect of measurement noise pointed out above is generic. In fact, for a general bounded (measurable) noise signal $t \mapsto m(t)$, $e_i^+(\delta)$ can be upper bounded by $e_1^+(\delta) = e_2^+(\delta) \leq \Gamma(\delta)$, where the function $\delta \mapsto \Gamma(\delta)$ is defined as

$$\Gamma(\delta) = \left| \frac{\exp(\widetilde{a}_2\delta)}{\exp(\widetilde{a}_2\delta) - \exp(\widetilde{a}_1\delta)} \right| \frac{|L_1|}{|\widetilde{a}_1|} \sup_{t\in[0,\delta]} |m(t)| + \left| \frac{\exp(\widetilde{a}_1\delta)}{\exp(\widetilde{a}_2\delta) - \exp(\widetilde{a}_1\delta)} \right| \frac{|L_2|}{|\widetilde{a}_2|} \sup_{t\in[0,\delta]} |m(t)|.$$

Without loss of generality, let $L_2 > L_1 > 0$. Then, it follows that

$$\begin{aligned}
\lim_{\delta\to 0^+}\Gamma(\delta) &= \lim_{\delta\to 0^+}\left|\frac{\exp(\widetilde{a}_2\delta)}{\exp(\widetilde{a}_2\delta)-\exp(\widetilde{a}_1\delta)}\right|\frac{|L_1|}{|\widetilde{a}_1|}|m|_\infty \\
&\quad + \lim_{\delta\to 0^+}\left|\frac{\exp(\widetilde{a}_1\delta)}{\exp(\widetilde{a}_2\delta)-\exp(\widetilde{a}_1\delta)}\right|\frac{|L_2|}{|\widetilde{a}_2|}|m|_\infty, \\
&= \frac{|L_1|}{|\widetilde{a}_1|}|m|_\infty \lim_{\delta\to 0^+}\left|\frac{\exp(\widetilde{a}_2\delta)}{\exp(\widetilde{a}_2\delta)-\exp(\widetilde{a}_1\delta)}\right| \\
&\quad + \frac{|L_2|}{|\widetilde{a}_2|}|m|_\infty \lim_{\delta\to 0^+}\left|\frac{\exp(\widetilde{a}_1\delta)}{\exp(\widetilde{a}_2\delta)-\exp(\widetilde{a}_1\delta)}\right|, \\
&= \frac{|L_1|}{|\widetilde{a}_1|}|m|_\infty \lim_{\delta\to 0^+}\left|\frac{\exp(-(L_2-L_1)\delta)}{\exp(-(L_2-L_1)\delta)-1}\right| \\
&\quad + \frac{|L_2|}{|\widetilde{a}_2|}|m|_\infty \lim_{\delta\to 0^+}\left|\frac{1}{\exp(-(L_2-L_1)\delta)-1}\right|, \\
&= \infty.
\end{aligned}$$

Similarly, it can be shown that

$$\begin{aligned}
\lim_{\delta\to\infty}\Gamma(\delta) &= \frac{|L_1|}{|\widetilde{a}_1|}|m|_\infty \lim_{\delta\to\infty}\left|\frac{\exp(-(L_2-L_1)\delta)}{\exp(-(L_2-L_1)\delta)-1}\right| \\
&\quad + \frac{|L_2|}{|\widetilde{a}_2|}|m|_\infty \lim_{\delta\to\infty}\left|\frac{1}{\exp(-(L_2-L_1)\delta)-1}\right|, \\
&= \frac{|L_2|}{|\widetilde{a}_2|}|m|_\infty.
\end{aligned}$$

Moreover, it can be evaluated that for all $\delta \geq 0$

$$\begin{aligned}
\frac{d\Gamma}{d\delta}(\delta) &= -\frac{|L_1|}{|\widetilde{a}_1|}|m|_\infty \frac{(L_2-L_1)\exp(\widetilde{a}_2\delta)\exp(\widetilde{a}_1\delta)}{(\exp(\widetilde{a}_1\delta)-\exp(\widetilde{a}_2\delta))^2} \\
&\quad - \frac{|L_2|}{|\widetilde{a}_2|}|m|_\infty \frac{(L_2-L_1)\exp(\widetilde{a}_2\delta)\exp(\widetilde{a}_1\delta)}{(\exp(\widetilde{a}_1\delta)-\exp(\widetilde{a}_2\delta))^2} \\
&= -\left(\frac{|L_1|}{|\widetilde{a}_1|}+\frac{|L_2|}{|\widetilde{a}_2|}\right)|m|_\infty \times \frac{(L_2-L_1)\exp(\widetilde{a}_2\delta)\exp(\widetilde{a}_1\delta)}{(\exp(\widetilde{a}_1\delta)-\exp(\widetilde{a}_2\delta))^2} < 0.
\end{aligned}$$

Therefore, the function Γ is strictly decreasing. The upper bound (though it is conservative) implies the same tradeoff between the error after reset and the reset time.

For the rest of the chapter, we show a way to preserve partial finite-time convergence when measurement noise is piece-wise constant.

4.2 Robust finite-time convergent hybrid observer

This section presents our hybrid observer and its main properties. Motivated by the fact that the estimate of (4.1) is not able to converge in finite time under any nonzero noise, we propose a finite-time convergent hybrid observer for the plant in (1.1) with piecewise-constant noise. Before that, a simpler case where the noise is constant is discussed to illustrate the idea, the associated observer $\mathcal{H}_c$ has state

$$\zeta_c = (\hat{x}_1, \hat{x}_2, \xi_1, \xi_2, \hat{m}, \tau, q) \in \mathcal{X}_c := \mathbb{R}^r \times [0, \delta] \times \{0, 1\},$$

where $r = 2n + (2n+1)p$. Its flow map and jump map are

$$f_c(\zeta_c, y) = \begin{bmatrix} A\hat{x}_1 - L_1(H\hat{x}_1 - y) - L_1\hat{m} \\ A\hat{x}_2 - L_2(H\hat{x}_2 - y) - L_2\hat{m} \\ \mathrm{diag}_p(A - L_1H)\xi_1 + \widetilde{L}_1 \\ \mathrm{diag}_p(A - L_2H)\xi_2 + \widetilde{L}_2 \\ 0 \\ 1 - q \\ 0 \end{bmatrix}, \tag{4.3}$$

$$g_c(\zeta_c, y) = \begin{bmatrix} R - T(HT - I)^{-1}(HR - (y - \hat{m})) \\ R - T(HT - I)^{-1}(HR - (y - \hat{m})) \\ 0 \\ 0 \\ \hat{m} + (HT - I)^{-1}(HR - (y - \hat{m})) \\ 0 \\ 1 - q \end{bmatrix}, \tag{4.4}$$

where, for all $i \in \{1, 2\}$[2],

$$R(\hat{x}_1, \hat{x}_2) = K_1\hat{x}_1 + K_2\hat{x}_2, \quad \widetilde{L}_i = \sum_{k=1}^{p} \mathcal{I}_k^\top L_i v_k,$$
$$T(\xi_1, \xi_2) = K_1 \sum_{k=1}^{p} \mathcal{I}_k \xi_1 v_k^\top + K_2 \sum_{k=1}^{p} \mathcal{I}_k \xi_2 v_k^\top,$$

where[3] $\mathcal{I}_k \in \mathbb{R}^{n \times np}$ contains p sub-matrices of dimension $n \times n$, and the only nonzero sub-matrix among them is an identity $I_{n\times n}$ at the k-th entry. The flow set is defined by $C_c := \mathcal{X}_c$ and the jump set is given by $D_c := \{\zeta_c \in \mathcal{X}_c : \tau = \delta, q = 0\}$.

[2]For simplicity, the arguments in T and R are dropped in (4.3), and (4.4).

[3]$\widetilde{L}_i$ is a vector generated by the columns of the matrix L. $\sum_{k=1}^{p} \mathcal{I}_k \xi_1 v_k^\top$ pulls each k-th "piece" of ξ_1 and put it in the k-th column of the resulting matrix, where $\xi_i \in \mathbb{R}^{np}$.

The gains K_1 and K_2 are given by $K_1 = I - K_2$, $K_2 = (I - \exp(F_2\delta)\exp(-F_1\delta))^{-1}$. These definitions of C_c and D_c ensure that $\mathcal{H}_c$ jumps only once.

Theorem 4.2.1 *For the interconnection*[4] *between $\mathcal{H}_c$ and the plant* (1.1) *with state $z_c := (x, \zeta_c)$, assume the noise m is constant. Moreover, suppose Assumption 4.1.1 holds and that $HT(\xi_1(\delta,0), \xi_2(\delta,0)) - I$ is nonsingular. Then, for any initial condition $z_c(0,0) \in S_c := \{z_c \in \mathbb{R}^n \times \mathcal{X}_c : \hat{x}_1 = \hat{x}_2, \xi_1 = \xi_2 = 0, \tau = 0, q = 0\}$, the states $\hat{x}_1$ and $\hat{x}_2$ converge to x in finite time δ and one jump, i.e., $\hat{x}_1(t,j) = \hat{x}_2(t,j) = x(t,j)$ for all $(t,j) \in \{(t,j) \in \mathrm{dom}\ z_c : t \geq \delta, j \geq 1\}$.*

Note that the invertibility of $HT(\xi_1(\delta,0), \xi_2(\delta,0)) - I$ can be checked offline since the ξ_i trajectories have analytical expressions.

Proof For initial condition $z_c(0,0) \in S_c$, and each $(t,j) \in \mathrm{dom}\ z_c$, it follows from the definition of flow map that for $0 \leq t \leq \delta$, $j = 0$,

$$e_i(t,0) = \exp((A - L_iH)t)e_i(0,0) + \int_0^t \exp((A - L_iH)(t-\tau))L_i(m - \hat{m})d\tau,$$

and $\xi_i(t,0) = \int_0^t \mathrm{diag}_p(\exp((A - L_iH)(t-\tau)))\widetilde{L}_i d\tau$. Using the definitions of K_1 and K_2, and the fact that $\hat{x}_i = e_i + x$ and m and $\hat{m}$ are constant over $[0\ \delta]$, we get

$$R(\delta,0) = x(\delta,0) + \sum_{i=1}^{2} K_i \int_0^t \exp((A - L_iH)(t-\tau))L_i d\tau(m - \hat{m}),$$
$$T(\delta,0) = \sum_{i=1}^{2} K_i \int_0^\delta \exp((A - L_iH)(\delta-\tau))L_i d\tau,$$

[4]The hybrid observer $\mathcal{H}_c$ interconnected with the plant (1.1) defines a hybrid system $\mathcal{H} = (C, f, D, g)$ with state $z_c = (x, \zeta_c), C = \mathbb{R}^n \times C_c$, $f(z_c) = (Ax, f_c(\zeta_c, y))$, $D = \mathbb{R}^n \times D_c$ and $g(z_c) = (x, g_c(\zeta_c))$.

where we denote $R(\hat{x}_1(\delta,0),\hat{x}_2(\delta,0))$ and $T(\xi_1(\delta,0),\xi_2(\delta,0))$ by $R(\delta,0)$ and $T(\delta,0)$ respectively. Then, at the jump which occurs when $\tau=\delta$, we have

$$\begin{aligned}\hat{m}(\delta,1) &= \hat{m}(\delta,0)+(HT(\delta,0)-I)^{-1}(HR(\delta,0)-(y(\delta,0)-\hat{m}(\delta,0)))\\ &= m(\delta,0).\end{aligned}$$

which implies that $\hat{x}_1(\delta,1) = \hat{x}_2(\delta,1) = x(\delta,0)+R(\delta,0)-T(\delta,0)(m(\delta,0)-\hat{m}(\delta,0)) = x(\delta,0)$. and since $x(\delta,1)=x(\delta,0)$, we have finite time convergence of e_i's to zero. ■

The proposed observer, denoted $\mathcal{H}_o$ and with data (C_o,f_o,D_o,g_o), has state $\zeta_o=(\hat{x}_1,\hat{x}_2,\xi_1,\xi_2,\hat{m},\tau)\in\mathcal{X}_o:=\mathbb{R}^n\times\mathbb{R}^n\times\mathbb{R}^{np}\times\mathbb{R}^{np}\times\mathbb{R}^p\times[0,\delta]$ and input $y\in\mathbb{R}^p$. The first five components of the flow map f_o coincide with those of f_c and the sixth is equal to one. The first five components of jump map g_o is equal to the first five components of g_c, and the sixth is equal to zero. The flow map and jump map are given by

$$f_o(\zeta_o, y) = \begin{bmatrix} A\hat{x}_1 - L_1(H\hat{x}_1 - y) - L_1\hat{m} \\ A\hat{x}_2 - L_2(H\hat{x}_2 - y) - L_2\hat{m} \\ \mathrm{diag}_p(F_1)\xi_1 + \widetilde{L}_1 \\ \mathrm{diag}_p(F_2)\xi_2 + \widetilde{L}_2 \\ 0 \\ 1 \end{bmatrix}, \tag{4.5a}$$

$$g_o(\zeta_o, y) = \begin{bmatrix} R(\hat{x}_1, \hat{x}_2) - T(\xi_1, \xi_2)\psi(\xi_1, \xi_2)(HR(\hat{x}_1, \hat{x}_2) - (y - \hat{m})) \\ R(\hat{x}_1, \hat{x}_2) - T(\xi_1, \xi_2)\psi(\xi_1, \xi_2)(HR(\hat{x}_1, \hat{x}_2) - (y - \hat{m})) \\ 0 \\ 0 \\ \hat{m} + \psi(\xi_1, \xi_2)(HR(\hat{x}_1, \hat{x}_2) - (y - \hat{m})) \\ 0 \end{bmatrix}, \tag{4.5b}$$

respectively, where, for each $i \in \{1, 2\}$,

$$\widetilde{L}_i = \sum_{k=1}^{p} \mathcal{I}_k^\top L_i v_k, \quad R(\hat{x}_1, \hat{x}_2) = K_1\hat{x}_1 + K_2\hat{x}_2, \quad F_i = A - L_i H,$$
$$\psi(\xi_1, \xi_2) = (HT(\xi_1, \xi_2) - I)^{-1}, \quad T(\xi_1, \xi_2) = K_1 \sum_{k=1}^{p} \mathcal{I}_k \xi_1 v_k^\top + K_2 \sum_{k=1}^{p} \mathcal{I}_k \xi_2 v_k^\top,$$
$$K_1 = I - K_2, \quad K_2 = (I - \exp(F_2\delta)\exp(-F_1\delta))^{-1}$$

with $\mathcal{I}_k \in \mathbb{R}^{n \times np}$ defined by p matrices of dimension $n \times n$ in a row, of which the only nonzero sub-matrix among them is the identity matrix $I_{n\times n}$ located at the k-th entry, e.g.,

$$\mathcal{I}_k = [0_{n\times n} \quad 0_{n\times n} \ldots 0_{n\times n} \quad I_{n\times n} \quad 0_{n\times n}]$$

for $k = p - 1$. The flow set is defined by $C_o := \mathcal{X}_o$ and the jump set is given by $D_o := \{\zeta_o \in \mathcal{X}_o : \tau = \delta\}$. These definitions of C_o and D_o ensure that (possibly after the first jump) the system jumps periodically.

The hybrid observer $\mathcal{H}_o$ interconnected with the plant (1.1) defines a hybrid system $\mathcal{H} = (C, f, D, g)$ with state $z = (x, \zeta_o)$, input m, $C = \mathbb{R}^n \times C_o$, $f(z, m) = (Ax, f_o(\zeta_o, y))$, $D = \mathbb{R}^n \times D_o$ and $g(z, m) = (x, g_o(\zeta_o, y))$. For this interconnection, we have the following nominal property.

Theorem 4.2.2 *For the interconnection between $\mathcal{H}_o$ and the plant (1.1) with $z := (x, \zeta_o)$, suppose Assumption 4.1.1 holds and the measurement noise m is zero. Moreover, suppose $H \sum_{i=1}^{2} K_i \int_0^\delta \exp(F_i \tau) L_i d\tau - I$ is nonsingular. Let*

$$\mathcal{A} = \{z \in \mathbb{R}^n \times \mathcal{X}_o : x = \hat{x}_1 = \hat{x}_2\}.$$

Then, each solution to the interconnection from $z(0,0) \in S := \{z \in \mathbb{R}^n \times \mathcal{X}_o : \hat{x}_1 = \hat{x}_2, \xi_1 = \xi_2 = 0, \tau = 0, \hat{m} = 0\}$ satisfies

$$|z(t,j)|_{\mathcal{A}} \leq \rho(j) \sqrt{\frac{w_2}{w_1}} |z(0,0)|_{\mathcal{A}} \exp\left(\frac{\overline{\alpha}(Q)}{2w_2} t\right) \qquad \forall (t,j) \in \operatorname{dom} z \tag{4.6}$$

with $\rho(0) = 1$ and $\rho(j) = 0$ for each $j \in \mathbb{N} \setminus \{0\}$, $w_1 = \min\{\underline{\alpha}(P_1), \underline{\alpha}(P_2)\}$, $w_2 = \max\{\overline{\alpha}(P_1), \overline{\alpha}(P_2)\}$, for any $P_1 = P_1^\top > 0$, $P_2 = P_2^\top > 0$ such that

$$Q = \begin{bmatrix} \operatorname{He}(F_1, P_1) & 0 \\ 0 & \operatorname{He}(F_2, P_2) \end{bmatrix} < 0. \tag{4.7}$$

Proof To show the $\mathcal{KL}$-like bound in (4.6), consider a Lyapunov candidate

$$V(z) = \sum_{i=1}^{2} (x - \hat{x}_i)^\top P_i (x - \hat{x}_i),$$

where, for each $i \in \{1,2\}$, $P_i \in \mathbb{R}^{n\times n}$ is a symmetric positive definite matrix. Then, it satisfies the property

$$w_1|z|_{\mathcal{A}}^2 \leq V(z) \leq w_2|z|_{\mathcal{A}}^2 \qquad \forall z \in C \cup D \cup g(D),$$

where $w_1 = \min\{\underline{\alpha}(P_1), \underline{\alpha}(P_2)\}$ and $w_2 = \max\{\overline{\alpha}(P_1), \overline{\alpha}(P_2)\}$.

For each $z \in C$ and $\hat{m} = 0$:

$$\langle \nabla V(z), f(z)\rangle = \left[\begin{array}{cc} (x-\hat{x}_1)^T & (x-\hat{x}_2)^T \end{array}\right] Q \left[\begin{array}{c} (x-\hat{x}_1) \\ (x-\hat{x}_2) \end{array}\right],$$

with Q defined in (4.7).

The time derivative of the Lyapunov function is negative definite since by A1 in Assumption 4.1.1, the matrix Q is negative definite. Then, we have

$$\langle \nabla V(z), f(z)\rangle \leq \overline{\alpha}(Q)|z|_{\mathcal{A}}^2 \qquad \forall z \in C \text{ and } \hat{m} = 0. \tag{4.8}$$

Now, consider the change of V at jumps. For each maximal solution z to the interconnection from $z(0,0) \in S$, and each $(t,j) \in \operatorname{dom} z$ such that $(t, j+1) \in \operatorname{dom} z$, by using the definitions of K_1 and K_2, we obtain that

$$V(g(z(t,j))) - V(z(t,j)) = -V(z(t,j)) \leq -w_1|z(t,j)|_{\mathcal{A}}^2 \tag{4.9}$$

and that $g(z(t,j+1)) \in S$. Then, by direct integration and using bounds (4.8) and (4.9), for any solution of the system initialized at $z(0,0) \in S$, we have (4.6). ■

Remark 4.2.3 *The explicit $\mathcal{KL}$ bound in* (4.6) *provides a useful estimate on the overshoot during transient. Moreover, the interconnection between $\mathcal{H}_o$ and the* *plant* (1.1) *is such that every maximal solution is complete and the invertibility property of* $H\sum_{i=1}^{2}K_i\int_0^\delta \exp(F_i\tau)L_i d\tau - I$ *can be checked offline*[5]. *Furthermore, when* $z(0,0)$ *is not restricted to* S, *i.e.,* $z(0,0) \in \mathbb{R}^n \times \mathcal{X}_o$, *the bound in* (4.6) *can be extended to capture the transient due to initial conditions not in* S, *in which case, to avoid singularity, one could replace* ψ *by*

$$\psi(\xi_1,\xi_2) = \begin{cases} (HT(\xi_1,\xi_2)-I)^{-1} & \text{if } |\det(HT(\xi_1,\xi_2)-I)| > \overline{M} \\ 0 & \text{if } |\det(HT(\xi_1,\xi_2)-I)| < \overline{M} \\ \{0,(HT(\xi_1,\xi_2)-I)^{-1}\} & \text{if } |\det(HT(\xi_1,\xi_2)-I)| = \overline{M} \end{cases} \tag{4.10}$$

for each $\xi_1,\xi_2 \in \mathbb{R}^{np}$, *where* $\overline{M} > 0$ *is a small parameter such that*

$$\left|\det\left(H\sum_{i=1}^{2}K_i\int_0^\delta \exp(F_i\tau)L_i d\tau - I\right)\right| > \overline{M}.$$

Then, the following result can be verified for the nominal case and will be used for proving the main convergence property.

Lemma 4.2.4 *For the interconnection between* $\mathcal{H}_o$ *and the plant* (1.1), *assume the noise* $m : [0,T) \to \mathbb{R}^p$ *is constant where* $T \in (\delta,\infty]$. *Moreover, suppose Assumption 4.1.1 holds and* $H\sum_{i=1}^{2}K_i\int_0^\delta \exp(F_i\tau)L_i d\tau - I$ *is nonsingular. Then, for any initial condition* $z(0,0) \in S^\star$ *with* $S^\star = \{z \in \mathbb{R}^n \times \mathcal{X}_o : \xi_1 = \xi_2 = 0, \tau = 0\}$, *the states* $\hat{x}_1$ *and* $\hat{x}_2$ *converge to* x *within finite time* δ, *i.e.,* $\hat{x}_1(t,j) = \hat{x}_2(t,j) = x(t,j)$ *for all* $(t,j) \in \{(t,j) \in \operatorname{dom} z : t \in [\delta,T), j \geq 1\}$.

[5] For a scalar plant ($H=1$), $H\sum_{i=1}^{2}K_i\int_0^\delta \exp(F_i\tau)L_i d\tau - I$ reduces to $\nu_1\frac{1-\exp(F_1\delta)}{(1-\exp(-(L_1-L_2)\delta))} + \nu_2\frac{1-\exp(F_2\delta)}{1-\exp((L_1-L_2)\delta)} - 1$ with $\nu_1 = -\frac{L_1}{F_1}$ and $\nu_2 = -\frac{L_2}{F_2}$. Let $\Sigma(\delta) = \nu_1\frac{1-\exp(F_1\delta)}{(1-\exp(-(L_1-L_2)\delta))} + \nu_2\frac{1-\exp(F_2\delta)}{1-\exp((L_1-L_2)\delta)} - 1$ for $\delta \in \mathbb{R}_{\geq 0}$. Then, it can be shown that $\lim_{\delta\to 0}\Sigma(\delta) = 0$ and $\lim_{\delta\to\infty}\Sigma(\delta) = \nu_2 - 1$ where $0 < \nu_2 < 1$ for $a < 0$ and $L_2 > 0$. Moreover, $\Sigma : \mathbb{R}_{\geq 0} \to \mathbb{R}$ is continuous and monotonically decreasing. Therefore, $\Sigma(\delta)$ is invertible for any $\delta > 0$.

Proof From the initial condition $z(0,0) \in S^\star$, by definition of the flow map, we have for

$$e_i(t,0) = \exp(F_i t)e_i(\delta,0) + \int_0^t \exp(F_i(t-\tau))L_i(m-\hat{m})d\tau \qquad \forall (t,j) \in [0,\delta] \times \{0\},$$

and $\xi_i(t,0) = \int_0^t \mathrm{diag}_p(\exp((A - L_i H)(t-\tau)))\widetilde{L}_i d\tau$. When $t = \delta$ and $j = 1$, using the definitions of K_1 and K_2, and the fact that $\hat{x}_i = e_i + x$ and m and $\hat{m}$ are constant over $[0,\delta]$, we get

$$\hat{m}(\delta,1) = \hat{m}(\delta,0) + (HT(\delta,0) - I)^{-1}(HR(\delta,0) - (y(\delta,0) - \hat{m}(\delta,0))) = m(\delta,0).$$

which implies that $\hat{x}_1(\delta,1) = \hat{x}_2(\delta,1) = x(\delta,1)$. Since $x(\delta,1) = x(\delta,0)$, we have finite time convergence of e_i's to zero.

■

The following result establishes the main convergence property induced by $\mathcal{H}_o$ when piecewise-constant measurement noise is present. In the following, for a given a set $B \subset \mathbb{R}^n$, the indicator function $\chi_B : \mathbb{R}^n \to \{0,1\}$ is defined as $\chi_B(x) := 0$ if $x \notin B$, and $\chi_B(x) := 1$ if $x \in B$.

Theorem 4.2.5 *For the interconnection between the observer $\mathcal{H}_o$ and the plant (1.1) with $z = (x, \zeta_o)$, assume the measurement noise m is a piecewise-constant function defined as*

$$m(t) := \sum_k \widetilde{c}_k \chi_{B_k}(t) \qquad \forall t \in [0,\infty) \tag{4.11}$$

where, for integers $k \geq 1$, $\widetilde{c}_k \in \mathbb{R}^p$, $B_k := [\widetilde{d}_{k-1}, \widetilde{d}_k)$ with $0 \leq \widetilde{d}_{k-1} < \widetilde{d}_k$, $\widetilde{d}_k$ finite or infinite, and $\cup_k^\infty B_k = [0,\infty)$. Moreover, suppose Assumption 4.1.1 holds, $0 < \delta < \frac{1}{2}\min_{k \in \{1,2,\dots\}}\{\widetilde{d}_k - \widetilde{d}_{k-1}\}$, and $H\sum_{i=1}^2 K_i \int_0^\delta \exp(F_i\tau)L_i d\tau - I$ is nonsingular.

Then, each solution z to the interconnection with $z(0,0) \in S^\star := \{z \in \mathbb{R}^n \times \mathcal{X}_o : \xi_1 = \xi_2 = 0, \tau = 0\}$, is such that, for each $I_j \times \{j\}$ with $j \geq 1$, there exists $\widetilde{I}_j \subset (I_j \cup I_{j+1})$ with nonempty interior such that $\hat{x}_i(t,j) = x(t,j)$ for each $t \in \widetilde{I}_j$ and each $i \in \{1,2\}$.

Proof Consider the first two intervals I_0, I_1 of a solution z to the interconnection from $z(0,0) \in S^\star$. Under the assumption that $0 < \delta < \frac{1}{2}\min_{k\in\{1,2,\dots\}}\{\widetilde{d}_k - \widetilde{d}_{k-1}\}$, the measurement noise m is constant for all $t \in I_0 \cup I_1$ (Note we can rewrite m in (4.11) as a function on dom z; see [82]). Applying the jump map (4.5b), we obtain $\hat{x}_1(\delta,1) = \hat{x}_2(\delta,1)$ after the first jump. Recall that the measurement noise m is constant for each $t \in I_1$. Applying Lemma 4.2.4, it follows that there exists a nonempty sub-interval of I_2 such that $\hat{x}_1(t,j) = \hat{x}_2(t,j) = x(t,j)$ for all t belonging to that sub-interval. For any two general consecutive intervals $I_j \cup I_{j+1}$ for $j \geq 2$,

- if $\hat{x}_1(j\delta,j) = \hat{x}_2(j\delta,j) = x(j\delta,j)$, and the noise m does not change at $t = j\delta$, then, using the assumption that $0 < \delta < \frac{1}{2}\min_{k\in\{1,2,\dots\}}\{\widetilde{d}_k - \widetilde{d}_{k-1}\}$, there exists a nonempty sub-interval of I_j such that m is constant on this interval, and $\hat{x}_1(t,j) = \hat{x}_2(t,j) = x(t,j)$ for all t in that sub-interval;

- if $\hat{x}_1(j\delta,j) = \hat{x}_2(j\delta,j) = x(j\delta,j)$, and the noise m changes at $t = j\delta$, it will keep constant for $t \in I_j \cup I_{j+1}$, then it follows from an application of Lemma 4.2.4 as above that $\hat{x}_1(t,j) = \hat{x}_2(t,j) = x(t,j)$ for all $t \in I_{j+1}$;

- if $\hat{x}_1(j\delta,j) = \hat{x}_2(j\delta,j) \neq x(j\delta,j)$, it is implied that the noise m changed once in I_{j-1} and it will keep constant for $t \in I_j$. Therefore, there exists a nonempty sub-interval of I_{j+1} such that $\hat{x}_1(t,j+1) = \hat{x}_2(t,j+1) = x(t,j+1)$ for all t belongs to that sub-interval.

The claim holds by combining the arguments above. ■

The existence of the interval $\widetilde{I}_j$ for each $j \geq 1$ guaranteed by Theorem 4.2.5 implies that whenever the noise changes, the proposed observer estimates the new value of the piecewise-constant noise in finite time (within 3δ).

Remark 4.2.6 *A special case of Theorem 4.2.5, which follows from Lemma 4.2.4, is that, if the measurement noise m is constant and $H\sum_{i=1}^{2} K_i \int_0^\delta \exp(F_i\tau)L_i d\tau - I$ is nonsingular, then, for each initial condition $z(0,0) \in S^\star$ for the interconnection between the observer $\mathcal{H}_o$ and the plant* (1.1)*, $\hat{x}_1$ and $\hat{x}_2$ converge to x within 2δ.*

To analyze the robustness property to generic measurement noise m of the interconnection between the observer $\mathcal{H}_o$ and the plant (1.1), given m and $\hat{m}$ with $\mathrm{dom}\, m = \mathrm{dom}\, \hat{m}$, define $|m - \hat{m}|_{(t,j)} := \sup_{s\in[j\delta,t]} |m(s,j) - \hat{m}(j\delta,j)|$, for each $(t,j) \in \mathrm{dom}\, m$ (since $\hat{m}$ does not change over flows, $\hat{m}(s,j) = \hat{m}(j\delta,j)$) for each $s \in [j\delta,t]$ and $|m - \hat{m}|_{(t,j)} := 0$ for each $(t,j) \notin \mathrm{dom}\, m$.

Theorem 4.2.7 *For the interconnection between the observer $\mathcal{H}_o$ and the plant* (1.1) *with $z = (x, \zeta_o)$ and an admissible measurement noise m, suppose $\overline{\alpha}(F_2) < \underline{\alpha}(F_1)$ and $\overline{\alpha}(F_1) < 0$. Furthermore, suppose F_1 and F_2 are dissipative and $\overline{\mu}(F_2) < \underline{\mu}(F_1)$, and*

$$H\sum_{i=1}^{2} K_i \int_0^\delta \exp(F_i\tau)L_i d\tau - I$$

is nonsingular. Then, each solution z to the interconnection from $z(0,0) \in S^{\star\star} := \{z \in \mathbb{R}^n \times \mathcal{X}_o : \hat{x}_1 = \hat{x}_2 = 0, \xi_1 = \xi_2 = 0, \tau = 0\}$ satisfies, for each $i \in \{1,2\}$ and for all $(t,j) \in$ dom z,

$$\begin{aligned}|e_i(t,j)| \leq{}& \rho(j)\exp(\overline{\mu}(F_i)t)|e_i(0,0)| \\ &+((1-\rho(j))c\exp(\overline{\mu}(F_i)(t-j\delta))+d_i)|\max\{|m-\hat{m}|_{(j\delta,j-1)}, |m-\hat{m}|_{(t,j)}\},\end{aligned} \tag{4.12}$$

where $e_i = \hat{x}_i - x$, $\rho(j) = 1$ *if* $j = 0$ *and* $\rho(j) = 0$ *for each* $j \in \mathbb{N} \setminus \{0\}$, $d_i = \frac{|L_i|}{|\overline{\mu}(F_i)|}$, $c = c_1 + c_1 c_2(|H| c_1 + 1)$,

$$c_1 = \sum_{i=1}^{2} |K_i| \frac{|L_i|}{|\overline{\mu}(F_i)|},$$
$$c_2 = \left| \left(H \sum_{i=1}^{2} K_i \int_0^{\delta} \exp(F_i \tau) L_i d\tau - I \right)^{-1} \right|.$$

Proof Consider the interval $[0, \delta] \times \{0\}$ over which no jump occurs. By solving for the solution to the interconnection during flows, we obtain

$$|e_i(t, 0)| \leq \exp(\overline{\mu}(F_i)t)|e_i(0, 0)| + \frac{|L_i|}{|\overline{\mu}(F_i)|}|m - \hat{m}|_{(t,0)} \qquad \forall t \in [0, \delta],$$

where we use bounds in [75, Section 3.2]. At the first jump, when $t = \delta$, recalling the jump map defined in (4.5b), we have

$$|R(\hat{x}_1(\delta, 0), \hat{x}_2(\delta, 0)) - x(\delta, 1)| \leq c_1 |m - \hat{m}|_{(\delta,0)},$$

which follows from the definition of K_i, the facts that $\hat{x}_1(0, 0) = \hat{x}_2(0, 0)$ and $x(\delta, 1) = x(\delta, 0)$, and straightforward bound on $e_i(\delta, 0)$, and also that

$$\begin{aligned} |e_i(\delta, 1)| \leq\ & |R(\hat{x}_1(\delta, 0), \hat{x}_2(\delta, 0)) - x(\delta, 1)| \\ & + |T(\xi_1(\delta, 0), \xi_2(\delta, 0))| \, |\psi(\xi_1(\delta, 0), \xi_2(\delta, 0))| \\ & \times (|H||R(\hat{x}_1(\delta, 0), \hat{x}_2(\delta, 0)) - x(\delta, 1)| + |m - \hat{m}|_{(\delta,0)}). \end{aligned}$$

Note that

$$\psi(\xi_1(\delta, 0), \xi_2(\delta, 0)) = (H \sum_{i=1}^{2} K_i \int_0^{\delta} \exp(F_i \tau) L_i d\tau - I)^{-1}$$

since $\xi_1(0,0) = \xi_2(0,0) = 0$ and $\tau(0,0) = 0$. These bounds lead to $|e_i(\delta, 1)| \leq c|m - \hat{m}(0,0)|_{(\delta,0)}$. Then, it follows that for each $t \in [\delta, 2\delta]$,

$$
\begin{aligned}
|e_i(t,1)| &\leq \exp(\overline{\mu}(F_i)(t-\delta))c|m-\hat{m}|_{(\delta,0)} + \frac{|L_i|}{|\overline{\mu}(F_i)|}|m-\hat{m}|_{(t,1)} \\
&\leq \left(c\exp(\overline{\mu}(F_i)(t-\delta)) + \frac{|L_i|}{|\overline{\mu}(F_i)|}\right)\max\left\{|m-\hat{m}|_{(\delta,0)}, |m-\hat{m}|_{(t,1)}\right\}.
\end{aligned}
$$

Following the same procedure for $j > 1$, the bound on $|e_i(j\delta, j)|$ at the j-th jump is independent from the bound on $|e_i(t, j-1)|$ for each $t \in [(j-1)\delta, j\delta]$, and is given by $|e_i(j\delta, j)| \leq c|m - \hat{m}|_{(j\delta, j-1)}$. Over the flow interval $[j\delta, (j+1)\delta] \times \{j\}$, we obtain

$$
\begin{aligned}
|e_i(t,j)| &\leq \exp(\overline{\mu}(F_i)(t-j\delta))c|m-\hat{m}|_{(j\delta,j-1)} + \frac{|L_i|}{|\overline{\mu}(F_i)|}|m-\hat{m}|_{(t,j)} \\
&\leq \left(c\exp(\overline{\mu}(F_i)(t-j\delta)) + \frac{|L_i|}{|\overline{\mu}(F_i)|}\right)\max\left\{|m-\hat{m}|_{(j\delta,j-1)}, |m-\hat{m}|_{(t,j)}\right\}.
\end{aligned}
$$

Therefore, we can unify the bounds for any $(t, j) \in \text{dom } e_i$, to obtain (4.12). ■

In addition to the above results for piecewise-constant noise (Theorem 4.2.5) and to general noise (Theorem 4.2.7), the fact that the interconnection between the observer $\mathcal{H}_o$ and the plant (1.1) satisfies the hybrid basic conditions, as stated next, enables us to establish a general robustness result.

Proposition 4.2.8 *Suppose A2 in Assumption 4.1.1 holds and the measurement noise is zero. Moreover, assume* $H\sum_{i=1}^{2} K_i \int_0^\delta \exp(F_i\tau)L_i d\tau - I$ *is nonsingular. Then, the interconnection between* $\mathcal{H}_o$ *and the plant satisfies the hybrid basic conditions.*

Next, we consider the effect of general measurement noise and unmodeled dynamics on the plant. In such a setting, the plant in (1.1) becomes

$$\begin{aligned} \dot{x} &= (A + \Delta A)x, \\ y &= (H + \Delta H)x + m. \end{aligned} \tag{4.13}$$

The proposed observer uses A and H, namely, ΔA and ΔH are not known to the observer. Due to this, the hybrid observer $\mathcal{H}_o$ interconnected with the perturbed plant (4.13) defines a hybrid system $\widetilde{\mathcal{H}} = (C, \widetilde{f}, D, \widetilde{g})$ with state $\widetilde{z} = (x, \zeta_o)$, input m, flow map and jump map given by

$$\widetilde{f}(z, m) = f(z, m) + (\Delta A x, L_1 \Delta H x, L_2 \Delta H x, 0, 0, 0, 0), \tag{4.14}$$

$$\begin{aligned} \widetilde{g}(z, m) &= g(z, m) \\ &\quad + (0, T(\xi_1, \xi_2)\psi(\xi_1, \xi_2)\Delta H x, T(\xi_1, \xi_2)\psi(\xi_1, \xi_2)\Delta H x, 0, 0, -\psi(\xi_1, \xi_2)\Delta H x, 0). \end{aligned} \tag{4.15}$$

The following robustness result relates, over a finite horizon, the solutions $\widetilde{z}$ to the system $\widetilde{\mathcal{H}}$, which includes unmodeled dynamics, to the solutions z to $\mathcal{H}$, which is the hybrid system resulting from the interconnection between $\mathcal{H}_o$ and the plant (1.1). Since to establish it we use tools from [73] for autonomous hybrid systems, we assume that the measurement noise is generated by an exosystem. Let $M > 0$ and $\Omega \subset \mathbb{R}^p$ be compact. Then, we generate the measurement noise from the differential inclusion with constraints

$$\dot{m} \in M\mathbb{B} \qquad m \in \Omega, \tag{4.16}$$

where, with some abuse of notation, m is treated as a state vector. Every possible solution to (4.16) is bounded and Lipschitz continuous, but not necessarily differentiable, which allows not only for the generation of the piecewise constant noise signals in Theorem 4.2.5 but also much richer admissible noise signals. Below, given a set $\mathcal{K} \subset \mathbb{R}^n$ and $\tau' \geq 0$, $\mathcal{R}^x_{\tau'}(\mathcal{K})$ denotes the reachable set of $\dot{x} = Ax$ from $\mathcal{K}$ up to $t = \tau'$ while $\mathcal{R}^{\xi}_{\tau'}(0)$ denotes the reachable set of $\dot{\xi}_1 = \mathrm{diag}_p(F_1)\xi_1 + \widetilde{L}_1$, $\dot{\xi}_2 = \mathrm{diag}_p(F_2)\xi_2 + \widetilde{L}_2$ from 0 also up to $t = \tau'$.

Theorem 4.2.9 *Suppose Assumption 4.1.1 holds and that $H \sum_{i=1}^{2} K_i \int_0^{\delta} \exp(F_i \tau) L_i d\tau - I$ is nonsingular. For each compact sets $\mathcal{K} \subset \mathbb{R}^n$ and $\mathcal{K}_{\hat{m}} \subset \mathbb{R}^p$, each $\varepsilon > 0$, and each $\tau' \geq 0$ there exists $\varsigma > 0$ such that if ΔA and ΔH satisfy*

$$\max\{|\Delta A|, |\Delta H|\} \max_{x \in \mathcal{R}^x_{\tau'}(\mathcal{K})} |x| \leq \frac{\varsigma}{\rho}$$

with

$$\rho = \max\{1, |L_1|, |L_2|, \max_{(\xi_1,\xi_2) \in \mathcal{R}^{\xi}_{\tau'}(0)} \{|T(\xi_1, \xi_2)\psi(\xi_1, \xi_2)|, |\psi(\xi_1, \xi_2)|\}\},$$

then the following property holds: for every solution $\widetilde{z}$ to $\widetilde{\mathcal{H}}$ with $\widetilde{\phi}(0,0) \in \mathcal{X}_{\xi} \cap S^{\star}$ there exists a solution z to $\mathcal{H}$ with $z(0,0) \in \mathcal{X}_{\xi} \cap S^{\star}$ such that $\widetilde{z}$ and z are (τ', ε)-close, where $\mathcal{X}_{\xi} = \mathcal{K} \times \mathcal{K} \times \mathcal{K} \times \mathbb{R}^{np} \times \mathbb{R}^{np} \times \mathcal{K}_{\hat{m}} \times [0, \delta]$.

Proof To establish the (τ', ε)-close property, we apply [73, Proposition 6.34]. To this end, note that under Assumption 4.1.1, Proposition 4.2.8 implies that $\mathcal{H}$ satisfies the hybrid basic conditions listed in (B1)-(B2) of Section 2.2. Denote by $\mathcal{H}_{\text{ex}}$ the interconnection between the plant in (1.1) and the noise model in (4.16), in which, at jumps of $\mathcal{H}$, m is mapped by the identity. This interconnection is autonomous and satisfies [73, Assumption 6.5] (which is the version of the hybrid basic conditions for the case of f and g being set valued). It follows from [73, Theorem 6.30] that $\mathcal{H}_{\text{ex}}$ is well posed; see [73, Definition 6.27] for a definition of well posedness.

Now, as we show next, every maximal solution (z, m) to $\mathcal{H}_{\text{ex}}$ is complete, i.e., it is pre-forward complete [73, Definition 6.12]. First, every maximal solution m to the exosystem (4.16) is bounded and complete. Moreover, m enters additively and linearly in f and g, in which the factors multiplying it are bounded. Since, at most after the first jump, the time between jumps is equal to δ, solutions to $\mathcal{H}$ from $S^\star$ do not escape to infinity in finite time when the measurement noise m is bounded. Denote by $T_C(z)$ the tangent cone of C at z. Then, for each $z(0,0) \in C \setminus D$ and $m(0,0) \in \Omega$,

$$T_C(z(0,0)) \cap f(z(0,0), m(0,0)) \neq \emptyset$$

and $g(D, m) \subset C$ for each $m \in \Omega$. Combining the above arguments it follows that only item (a) in [73, Proposition 6.10] holds, which, in turn, implies that every maximal solution to $\mathcal{H}_{\text{ex}}$ is complete.

Then, invoking [73, Proposition 6.34], there exists $\varsigma > 0$ such that for every solution $z_{\text{ex}}^{\varsigma}$ from $\mathcal{X}_\xi \cap S^*$ to an outer perturbation[6] of $\mathcal{H}_{\text{ex}}$ there exists a solution z_{ex} to $\mathcal{H}_{\text{ex}}$ from $\mathcal{X}_\xi \cap S^*$ such that $z_{\text{ex}}^{\varsigma}$ and z_{ex} are (τ', ε)-close. Since the mismatch between $\widetilde{f}$ and f in (4.14) and the mismatch between $\widetilde{g}$ and g in (4.15) are upper bounded by

$$\rho \max\{|\Delta A|, |\Delta H|\} \max_{x \in \mathcal{R}^x_{\tau'}(\mathcal{K})} |x|,$$

we have that if $|\Delta A|$ and $|\Delta H|$ are such that

$$\max\{|\Delta A|, |\Delta H|\} \max_{x \in \mathcal{R}^x_{\tau'}(\mathcal{K})} |x| \leq \frac{\varsigma}{\rho},$$

[6]See [73, Definition 6.27].

the claim follows by relating the solutions to $\mathcal{H}_{\rm ex}$ to $\mathcal{H}$ and those to the outer perturbation of $\mathcal{H}_{\rm ex}$ to $\widetilde{\mathcal{H}}$. ■

In simple terms, the above result establishes that the solutions resulting with ΔA and ΔH small enough do not differ much from those without such unmodeled dynamics. In particular, for piecewise constant measurement noise as in Theorem 4.2.5 and $\tau' > \delta$, the recurrent finite time convergence property in Theorem 4.2.5 is practically preserved up to $t = \tau'$.

4.3 Simulation results

Simulations illustrating the results in Section 4.2 are given next.

4.3.1 Piecewise-constant noise with unmodeled dynamics

For the plant in (1.1) with

$$A = \begin{bmatrix} 0 & 1 \\ -1 & 0 \end{bmatrix}, \quad H = \begin{bmatrix} 1 & 2 \\ 2 & 1 \end{bmatrix},$$

and parameters $\delta = 1$,

$$L_1 = \begin{bmatrix} -1.67 & 3.33 \\ 3.33 & -1.67 \end{bmatrix}, \quad L_2 = \begin{bmatrix} -2.67 & 5.33 \\ 5.33 & -2.67 \end{bmatrix},$$

then the invertibility of $H \sum_{i=1}^{2} K_i \int_0^\delta \exp(F_i\tau) L_i d\tau - I$ can be verified as

$$\det\left(H \sum_{i=1}^{2} K_i \int_0^\delta \exp(F_i\tau) L_i d\tau - I \right) \approx 0.01.$$

Moreover, L_1 and L_2 are such that F_1 and F_2 are Hurwitz. Hence, Assumption 4.1.1 holds. We perform simulations of the interconnection between the observer $\mathcal{H}_o$ and the plant with measurement noise $m(t) = \widetilde{c}_1 \chi_{B_1}(t) + \widetilde{c}_2 \chi_{B_2}(t) + \widetilde{c}_3 \chi_{B_3}(t)$ with $\widetilde{c}_1 = (0.3, 0.2)$, $\widetilde{c}_2 = (0.4, 0.4)$, $\widetilde{c}_3 = (0.2, 0.3)$, $B_1 = [0, 2.5)$, $B_2 = [2.5, 4.5)$, and $B_3 = [4.5, \infty)$, and from initial conditions $x(0,0) = (0.3, 0.4)$, $\hat{x}_1(0,0) = \hat{x}_2(0,0) = \hat{x}_0(0,0) = 0$, $\xi_1(0,0) = \xi_2(0,0) = 0$, and $\hat{m}(0,0) = 0$. Figures 4.3(a) and 4.3(b) show the estimation errors of the proposed observer (solid) and measurement noise with no unmodeled dynamics as well as those of Luenberger observer (dashed). Since the initial condition is in the set S, after the jump at $t = 1$ the estimation error of the proposed observer for each state component is zero. This illustrates Theorem 4.2.2. The noise changes at $t = 2.5$, which generates an increase of the error immediately. But once $t = 4$ (within 3δ after the first jump), the estimation error is again zero. This illustrates Theorem 4.2.5, indicating that $\widetilde{I}_1 = [1, 2.5)$.

Figures 4.3(c) and 4.3(d) show the estimation errors and measurement noise with unmodeled dynamics

$$\Delta A = \Delta A^\star := \begin{bmatrix} 0.01 & 0.01 \\ 0.01 & 0 \end{bmatrix},$$

$$\Delta H = \Delta H^\star := \begin{bmatrix} 0.002 & 0.015 \\ 0.011 & 0.003 \end{bmatrix}.$$

Although the finite-time convergence property is no longer preserved, the performance of the proposed observer is better than that of the Luenberger observer.

4.3.2 General noise with recursive jumps

Consider the same plant as defined in Section 4.3.1 with the hybrid observer $\mathcal{H}_o$ under the general measurement noise $m(t) = \widetilde{c}_1 \chi_{B_1}(t) + \widetilde{c}_2 \chi_{B_2}(t) + \widetilde{c}_3 \chi_{B_3}(t) +$

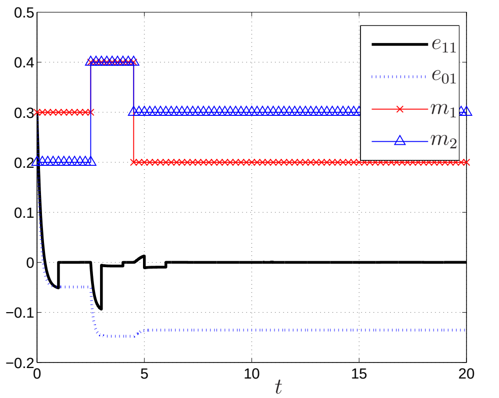

(a) Estimation error for first state component ($\Delta A = 0$ and $\Delta H = 0$).

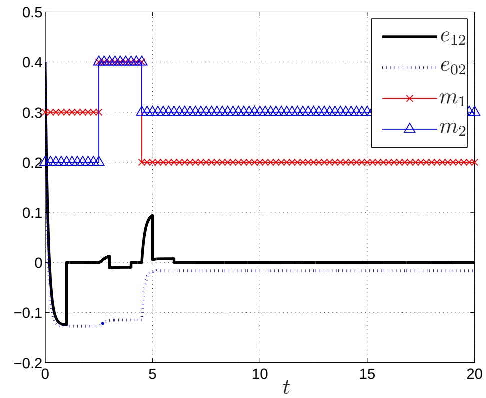

(b) Estimation error for second state component ($\Delta A = 0$ and ΔH=0).

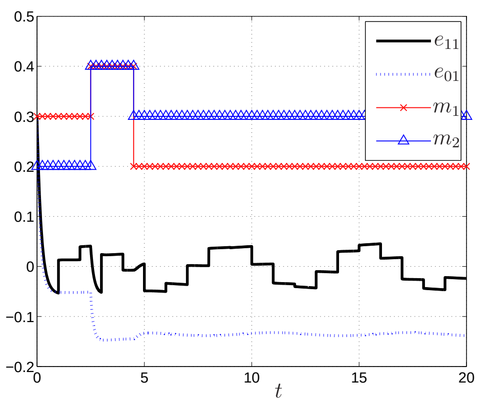

(c) Estimation error for first state component with nonzero unmodeled dynamics ($\Delta A = \Delta A^\star$ and $\Delta H = \Delta H^\star$).

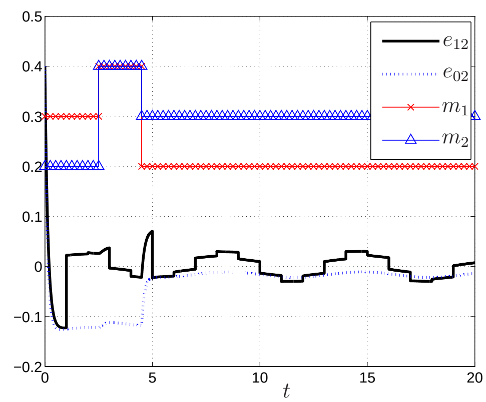

(d) Estimation error for second state component with nonzero unmodeled dynamics ($\Delta A = \Delta A^\star$ and $\Delta H = \Delta H^\star$).

Figure 4.3: State estimates ($\hat{x}_1 = (\hat{x}_{11}, \hat{x}_{12})$), measurement noise ($m = (m_1, m_2)$) and estimation error of the proposed observer ($e_1 = (e_{11}, e_{12}) = \hat{x}_1 - x$). (a) and (b) show the situation without unmodeled dynamics, while (c) and d are with unmodeled dynamics.

$0.05[\sin(t)\ \ \cos(t)]^\top$. Using the same gains L_1, L_2, $L_0 = L_2$, and $\delta = 1$ as in Section 4.3.1, a simulation result is shown in Figure 4.4 with initial conditions $x(0,0) = (0.3, 0.4)$, $\hat{x}_1(0,0) = \hat{x}_2(0,0) = \hat{x}_0(0,0) = 0$, $\xi_1(0,0) = \xi_2(0,0) = 0$, and $\hat{m}(0,0) = 0$. In Figure 4.4(a) and 4.4(b), black solid lines denote the estimation errors of the states from the proposed observer, blue dot-dashed lines denote estimate errors resulting from the Luenberger observer. As the figure shows, the proposed observer provides better estimates. This is also confirmed from Figure 4.4(c) and 4.4(d), where nonzero unmodeled dynamics are considered. Estimation errors of the proposed observer are closer to zero comparing to that of a Luenberger observer.

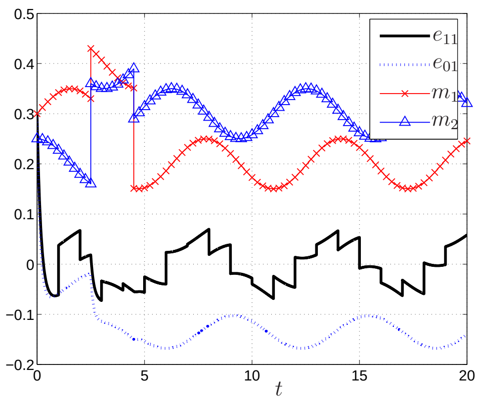

(a) Estimation error for first state component ($\Delta A = 0$ and $\Delta H = 0$).

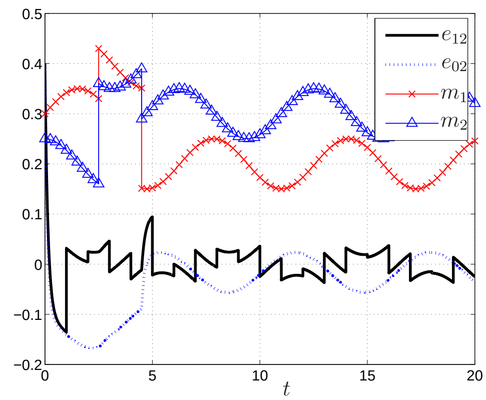

(b) Estimation error for second state component ($\Delta A = 0$ and ΔH=0).

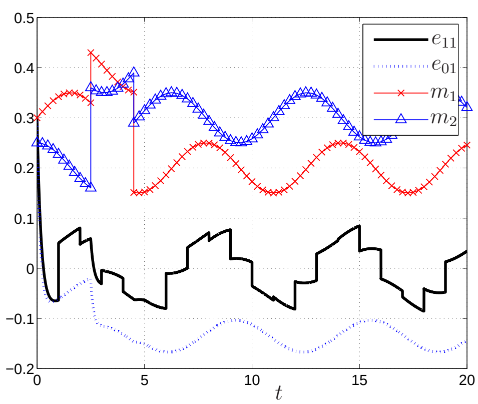

(c) Estimation error for first state component with nonzero unmodeled dynamics ($\Delta A = \Delta A^{\star}$ and $\Delta H = \Delta H^{\star}$).

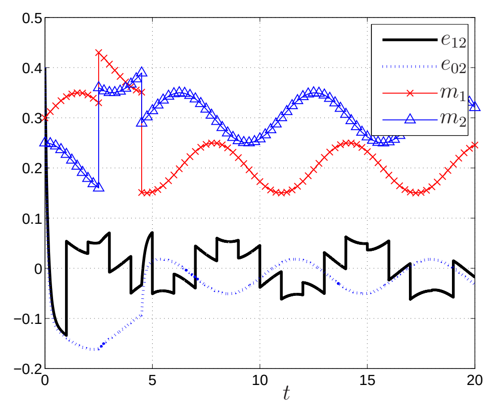

(d) Estimation error for second state component with nonzero unmodeled dynamics ($\Delta A = \Delta A^{\star}$ and $\Delta H = \Delta H^{\star}$).

Figure 4.4: State estimates ($\hat{x}_1 = (\hat{x}_{11}, \hat{x}_{12})$), measurement noise ($m = (m_1, m_2)$) and estimation error ($e_1 = (e_{11}, e_{12}) = \hat{x}_1 - x$). ($a$) and ($b$) show the situation without unmodeled dynamics, while (c) and d are with unmodeled dynamics.

4.3.3 An application to a mass-spring system

Example 4.3.1 *In this example, we consider a mechanical system which includes two masses that are connected by two springs as shown in Figure 4.5, where* M_1 *and* M_2 *are the masses, and they are considered as point masses that are located at positions* x_1 *and* x_2 *respectively. Moreover, the stiffness of the springs are denoted by* k_1 *and* k_2*, respectively. The viscous friction coefficient between the masses and the ground is assumed to be* c*. It is also assumed that the position of mass* M_1 *can be measured by a device with measurement noise* m*. The objective is to design an finite-time convergent observer to estimate the position of mass* M_2*.*

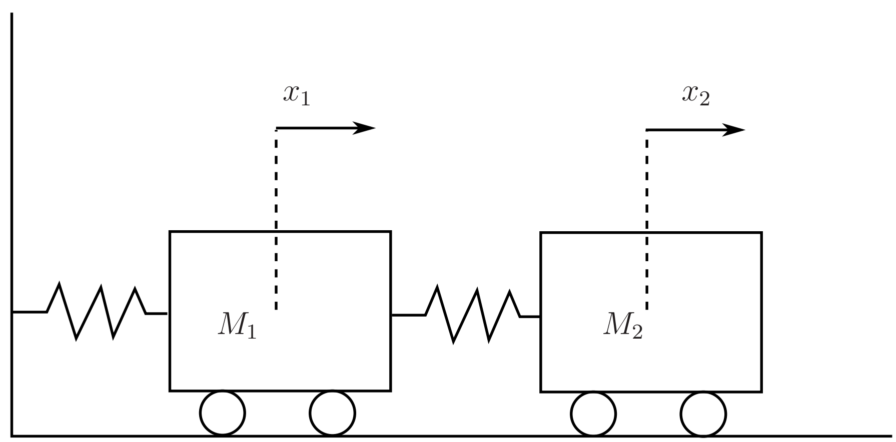

Figure 4.5: Mass-spring system

Consider the following parameters where $M_1 = 1$*,* $M_2 = 0.5$*,* $k_1 = 1$*,* $k_2 = 1$*,* $c = 1.5$*. Then, the state space realization*[7] *of the mass-spring system is given by*

$$\dot{x} = Ax + Bu$$

$$y = Hx + m,$$

[7]See [83, 31] for more details on the modeling and derivation.

where $x = (x_1, x_2, \dot{x}_1, \dot{x}_2)$ *and*

$$A = \begin{bmatrix} 0 & 0 & 1 & 0 \\ 0 & 0 & 0 & 1 \\ -2 & 1 & -1.5 & 0 \\ 2 & -2 & 0 & -3 \end{bmatrix}, \quad B = \begin{bmatrix} 0 \\ 0 \\ 1 \\ 0 \end{bmatrix}, \quad H = \begin{bmatrix} 1 \\ 0 \\ 0 \\ 0 \end{bmatrix}^\top, \tag{4.17}$$

where u *denotes the impulsive forces applied on the mass* M_1. *To focus on the observer design, we assume that* $u = 0$ *for the rest of this example.*

Now, we consider an observer with the form in (4.5). *Based on Theorem 4.2.5, we can design parameters as follows:*

$$\delta = 2, \quad L_1 = \begin{bmatrix} 0.5 \\ -0.3 \\ -1.4 \\ 2.6024 \end{bmatrix}, \quad L_2 = \begin{bmatrix} 21.5 \\ 480 \\ 145.75 \\ -118 \end{bmatrix}.$$

Then, a simulation is shown in Figure 4.6. The initial conditions are $x(0,0) =$

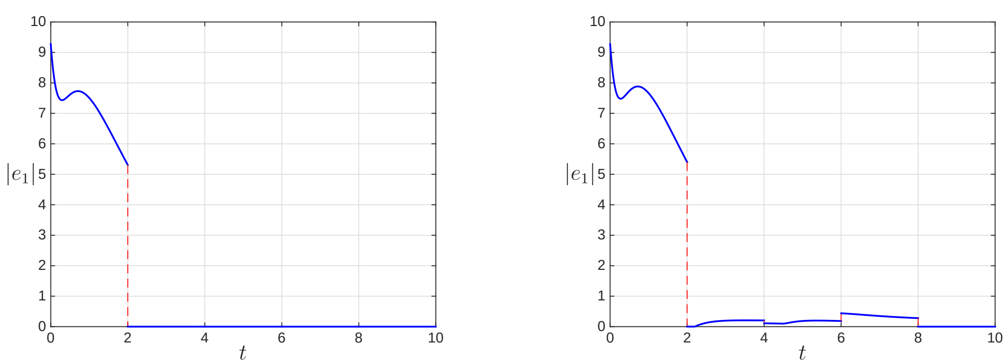

(a) Without measurement noise.

(b) With piece-wise constant measurement noise.

Figure 4.6: Finite-time convergent observer for a spring-mass system, where $e_1 = \hat{x}_1 - x$.

$(3,4,5,6)$, $\hat{x}_1(0,0) = \hat{x}_2(0,0) = 0$, $\xi_1(0,0) = \xi_2(0,0) = 0$, $\hat{m}(0,0) = 0$, $\tau(0,0) = 0$. *The corresponding measurement noise is given by* $m(t) = \widetilde{c}_1\chi_{B_1}(t) + \widetilde{c}_2\chi_{B_2}(t) + \widetilde{c}_3\chi_{B_3}(t)$ *with* $\widetilde{c}_1 = 0.4$, $\widetilde{c}_2 = 0.2$, $\widetilde{c}_3 = 0.4$, $B_1 = [0, 2.2)$, $B_2 = [2.2, 4.5)$, *and* $B_3 = [4.5, \infty)$. △

4.4 Summary

In this chapter, a robust finite-time hybrid observer consists of two interconnected sub-observers with impulsive behavior is discussed. When the measurement noise is an unknown piecewise-constant signal (time-varying bias, coarsely quantized noise, etc.), finite-time convergence is guaranteed under certain conditions. Furthermore, for generic measurement noise, the estimation error satisfies $\mathcal{KL}$-like bounds. Numerical results confirm the finite-time convergence and robustness of this observer.

Chapter 5

Distributed Estimation with Continuous Information Transmission

Motivated by the need of observers that are both robust to disturbances and guarantee fast convergence to zero of the estimation error, we propose an observer for linear time-invariant systems with noisy output that consists of the combination of N coupled observers over a connectivity graph. At each node of the graph, the output of these *interconnected observers* is defined as the average of the estimates obtained using local information. The convergence rate and the robustness to measurement noise of the proposed observer's output are characterized in terms of $\mathcal{KL}$ bounds. Several optimization problems are formulated to design the proposed observer so as to satisfy a given rate of convergence specification while minimizing the H_∞ gain from noise to estimates or the size of the connectivity graph. It is shown that that the interconnected observers relax the well-known tradeoff between rate of convergence and noise amplification, which is a property attributed to the proposed innovation term that, over the graph, couples the estimates between the individual observers. Sufficient conditions involving information of the plant only, assuring that the estimate obtained at each node of the graph outperforms the one obtained with a single, standard Luenberger observer are given. The results are illustrated in several examples throughout this chapter.

5.1 Observer structure and basic properties

Consider linear time-invariant systems in the form (1.1), the idea discussed in Section 1.2 can be generalized as follows. In particular, the general form of the proposed observer consists of N *interconnected observers* with output given by the average over a graph of the states of the individual observers.[1] Specifically, consider a network of N agents defined by a graph $\Gamma = (\mathcal{V}, \mathcal{E}, \mathcal{G})$. For the estimation of the plant's state, a local state observer using information from its neighbors is attached to each agent. More precisely, for each $i \in \mathcal{V}$, the agent i runs a local state observer given by

$$\dot{\hat{x}}_i = A\hat{x}_i - K_{ii}(\hat{y}_i - y_i) - \sum_{k \in \mathcal{N}(i)} K_{ik}(\hat{y}_k - y_k), \tag{5.1}$$

$$\hat{y}_i = H_i \hat{x}_i, \quad \bar{x}_i = \frac{1}{\mathrm{card}(\mathcal{N}(i))} \sum_{k \in \mathcal{N}(i)} \hat{x}_k, \tag{5.2}$$

where $\hat{x}_i$ denotes the state variable of the observer, $\bar{x}_i$ is the local estimate of the plant's state x, and y_i denotes the measurement of y in (1.1) taken by the i-th agent under measurement noise m_i, that is $y_i = Hx + m_i$. The information that the i-th agent obtains from its neighbors are the values of $\hat{x}_k$'s and y_k's for each $k \in \mathcal{N}(i)$. The collection of local state observers in (6.11) connected via the graph

[1] More general linear combinations defining $\bar{x}_i$ are possible, *i.e.*, $\bar{x}_i = \sum_{k \in \mathcal{N}(i)} \eta_k \hat{x}_k$ with $\eta_k \in \mathbb{R}$ for all k and $\sum_{k \in \mathcal{N}(i)} \eta_k = 1$.

Γ defines the proposed *interconnected observer*.

To analyze the properties of interconnected observers, define for each $i \in \mathcal{V}$, $e_i := \hat{x}_i - x$ and the associated vector $e := (e_1, \ldots, e_N)$. Furthermore, define the local estimation error $\bar{e}_i := \bar{x}_i - x$, the global estimation error vector $\bar{e} := (\bar{e}_1, \ldots, \bar{e}_N)$, and the noise vector $m := (m_1, \ldots, m_N)$. Then, it follows that

$$\begin{aligned} \dot{e}_i &= Ae_i - K_{ii}He_i - \sum_{k\in\mathcal{N}(i)} K_{ik}He_k + K_{ii}m_i + \sum_{k\in\mathcal{N}(i)} K_{ik}m_k, \\ \bar{e}_i &= \frac{1}{\text{card}(\mathcal{N}(i))} \sum_{k\in\mathcal{N}(i)} e_k, \end{aligned} \tag{5.3}$$

which can be rewritten in the compact form

$$\begin{aligned} \dot{e} &= (I_N \otimes A - (K_g * \overline{\mathcal{G}})H_g)e + (K_g * \overline{\mathcal{G}})m, \\ \bar{e} &= (D_{in}^{-1} \otimes I_n)(\overline{\mathcal{G}} \otimes I_n)e, \end{aligned} \tag{5.4}$$

where $\mathcal{G}$ is the adjacency matrix, D_{in} is the in-degree matrix,

$$K_g = \begin{bmatrix} K_{11} & K_{12} & \cdots & K_{1N} \\ K_{21} & K_{22} & \cdots & K_{2N} \\ \vdots & \vdots & \ddots & \vdots \\ K_{N1} & K_{N2} & \cdots & K_{NN} \end{bmatrix}, \tag{5.5}$$

$\overline{\mathcal{G}} = I_N + \mathcal{G}$, $H_g = I_N \otimes H$, and the Khatri-Rao product $K_g * \overline{\mathcal{G}}$ is such that K_g is treated as $N \times N$ block matrices with K_{ik}'s as blocks. Define

$$\begin{aligned} \mathcal{A} &:= I_N \otimes A - (K_g * \overline{\mathcal{G}})H_g, \\ \mathcal{B} &:= K_g * \overline{\mathcal{G}}, \\ \mathcal{C} &:= (D_{in}^{-1} \otimes I_n)(\overline{\mathcal{G}} \otimes I_n). \end{aligned} \tag{5.6}$$

Then, the transfer function[2] from measurement noise m to error $\bar{e}$ is given by $T(s) = \mathcal{C}(sI - \mathcal{A})^{-1}\mathcal{B}$. For the purpose of designing the proposed interconnected observer, each agent is self-connected, i.e., $(i, i) \in \mathcal{E}$. Therefore, we have $\mathrm{tr}(D_{in}) \geq N$.

Remark 5.1.1 *The matrix $I_N \otimes A$ is a block diagonal matrix with matrix A in each of the N diagonal blocks (of dimension $n \times n$). The matrix $K_g * \overline{\mathcal{G}}$ defines the gain matrix for the graph, while $(D_{in}^{-1} \otimes I_n)(\overline{\mathcal{G}} \otimes I_n)$ generates the estimation matrix for each agent by averaging the local estimates obtained from its neighbors.*

It can be verified that, under a detectability condition, interconnected observers can be designed so that the origin of the error system in (6.14) is (exponentially) stable.

Proposition 5.1.2 *For the plant* (1.1) *with measurement noise $m_i \equiv 0$ for each agent i, if the pair (H, A) is detectable, then, for any $N \in \mathbb{N}$, there exists a digraph Γ with adjacency matrix $\mathcal{G}$ and a gain K_g such that the matrix $\mathcal{A}$ is Hurwitz and the resulting system* (6.14) *has its origin exponentially stable.*

Proof For any $N \in \mathbb{N}$, consider $\mathcal{G} = I_N$. Then it follows that $\dot{e}_i = (A - K_{ii}H)e_i$ for each $i \in \mathcal{V}$. Under the assumption that the pair (H, A) is detectable, immediately we know that, for each $i \in \mathcal{V}$, there exists K_{ii} such that $A - K_{ii}H$ is Hurwitz. Therefore, the resulting $\mathcal{A}$ is Hurwitz. ■

[2] The transfer function T is called stable if all its poles have negative real part, the dominant pole for a stable transfer function is the pole with largest real part, the rate of convergence of a closed-loop system with stable transfer function is defined by the absolute value of real part of the dominant pole.

5.2 $\mathcal{KL}$ characterization of performance and robustness

In this section, the performance and robustness properties of observers are characterized in terms of $\mathcal{KL}$ bounds. More precisely, given an observer with estimation error e, we are interested in bounds of the form

$$|e(t)| \leq \beta(|e(0)|, t) + \varphi(|m|_\infty) \qquad \forall t \geq 0,$$

where $t \mapsto e(t)$ is a solution to the error system, β is a class-$\mathcal{K}L$ function, and φ is a class-$\mathcal{K}_\infty$ function. To establish and compare this property with that of the interconnected observers, the next result characterizes such bounds for the proposed observer so that it can be designed to outperform those due to a Luenberger observers.

Proposition 5.2.1 *For the plant* (1.1)*, assume the pair* (H, A) *is detectable. Let* $N \in \mathbb{N}$ *and a digraph* $\Gamma = (\mathcal{V}, \mathcal{E}, \mathcal{G})$ *be given. If there exists a gain* K_g *such that at least one of the following conditions are satisfied:*

1) The matrix $\mathcal{A}$ *is Hurwitz with distinct eigenvalues;*

2) The matrix $\mathcal{A}$ *is dissipative, i.e., for some* $\bar{\alpha} > 0$, $\mathcal{A}^\top + \mathcal{A} \leq -2\bar{\alpha}I$*;*

3) There exists $P = P^\top > 0$ *such that* $\mathrm{He}(\mathcal{A}, P) \leq -2\bar{\alpha}P$ *for some* $\bar{\alpha} > 0$*;*

then, there exist a class-$\mathcal{KL}$ *function* $\beta : \mathbb{R}_{\geq 0} \times \mathbb{R}_{\geq 0} \to \mathbb{R}_{\geq 0}$ *and a class-*$\mathcal{K}_\infty$ *function* $\varphi : \mathbb{R}_{\geq 0} \to \mathbb{R}_{\geq 0}$ *such that the solution* $\bar{e}$ *of* (6.14) *from any* $e(0) \in \mathbb{R}^{nN}$ *satisfies*

$$|\bar{e}(t)| \leq \beta(|e(0)|, t) + \varphi(|m|_\infty) \quad \forall t \in \mathbb{R}_{\geq 0}. \tag{5.7}$$

In particular, the functions β and φ can be chosen, for all $s, t \geq 0$, as follows: if 1) *holds, then,*

$$\beta(s,t)=\kappa(\mathcal{A})|\mathcal{C}|\exp(\alpha(\mathcal{A})t)s, \quad \varphi(s)=\kappa(\mathcal{A})\frac{|\mathcal{B}||\mathcal{C}|}{|\alpha(\mathcal{A})|}s; \tag{5.8}$$

if 2) *holds, then,*

$$\beta(s,t) = |\mathcal{C}| \exp(\mu(\mathcal{A})t)s, \quad \varphi(s) = \frac{|\mathcal{B}||\mathcal{C}|}{|\mu(\mathcal{A})|}s; \tag{5.9}$$

if 3) *holds, then,*

$$\beta(s,t) = \sqrt{c_p}|\mathcal{C}| \exp(-\lambda t)s, \quad \varphi(s) = c_p\frac{|\mathcal{B}||\mathcal{C}|}{|\lambda|}s, \tag{5.10}$$

with $\lambda = \frac{\bar{\alpha}\lambda_{\min}(P)}{\lambda_{\max}(P)}$ *and* $c_p = \frac{\lambda_{\max}(P)}{\lambda_{\min}(P)}$.

Proof For a Hurwitz matrix $\mathcal{A}$ with distinct eigenvalues, we have the following properties [75]:

P2.1 $|\exp(\mathcal{A}t)| \leq \kappa(\mathcal{A})\exp(\alpha(\mathcal{A})t), \ \forall t \geq 0$;

P2.2 Let $\Phi(t) = \exp(\mathcal{A}t)$ for all $t \in \mathbb{R}_{\geq 0}$, then $||\Phi||_1 \leq \frac{\kappa(\mathcal{A})}{|\alpha(\mathcal{A})|}$.

Then, the solution of system (6.14), given by

$$e(t) = \exp(\mathcal{A}t)e(0) + \int_0^t \exp(\mathcal{A}(t-\tau))\mathcal{B}m(\tau)d\tau,$$

can be bounded for all $t \geq 0$ as

$$|e(t)| \leq |\exp(\mathcal{A}t)||e(0)| + \left|\int_0^t \exp(\mathcal{A}(t-\tau))\mathcal{B}m(\tau)d\tau\right|. \tag{5.11}$$

Let $|\phi(t)| = \left|\int_0^t \exp(\mathcal{A}(t-\tau))\mathcal{B}m(\tau)d\tau\right|$, then

$$\begin{aligned} |\phi(t)| &\leq |\mathcal{B}| \int_0^t |\exp(\mathcal{A}(t-\tau))|\, d\tau\, |m|_\infty \\ &\leq |\mathcal{B}| \int_0^t |\exp(\mathcal{A}(\tau))|\, d\tau |m|_\infty \leq |\mathcal{B}|\, ||\Phi||_1\, |m|_\infty. \end{aligned} \tag{5.12}$$

Therefore, by using properties P2.1 and P2.2, inequality (5.11) can be simplified as

$$|e(t)| \leq \kappa(\mathcal{A}) \exp(\alpha(\mathcal{A})t)|e(0)| + \kappa(\mathcal{A}) \frac{|\mathcal{B}|}{|\alpha(\mathcal{A})|}|m|_\infty. \tag{5.13}$$

Furthermore,

$$|\bar{e}(t)| = |\mathcal{C}e(t)| \leq |\mathcal{C}||e(t)| \leq \kappa(\mathcal{A})|\mathcal{C}| \exp(\alpha(\mathcal{A})t)\, |e(0)| + \kappa(\mathcal{A}) \frac{|\mathcal{B}||\mathcal{C}|}{|\alpha(\mathcal{A})|}|m|_\infty.$$

Pick for $s,\ t \in \mathbb{R}_{\geq 0}$,

$$\beta(s,t) = \kappa(\mathcal{A})|\mathcal{C}| \exp(\alpha(\mathcal{A})t)s, \quad \varphi(s) = \kappa(\mathcal{A}) \frac{|\mathcal{B}||\mathcal{C}|}{|\alpha(\mathcal{A})|}s.$$

It follows that (5.7) holds.

When $\mathcal{A}$ is dissipative such that $\mathcal{A}^\top + \mathcal{A} \leq -2\alpha I$ for some $\alpha > 0$, following [75, Section 3.2], we have

P2.3 $\mathcal{A} + \mathcal{A}^\top \leq 2\mu(\mathcal{A})I$;

P2.4 $|\exp(\mathcal{A}t)| \leq \exp(\mu(\mathcal{A})t)$ for all $t \geq 0$;

P2.5 Let $\Phi(t) = \exp(\mathcal{A}t)$ for all $t \geq 0$. Then, $||\Phi||_1 \leq \frac{1}{|\mu(\mathcal{A})|}$.

Using properties P2.4 and P2.5, inequality (5.11) can be simplified as

$$|e(t)| \leq \exp(\mu(\mathcal{A})t)\,|e(0)| + \frac{|\mathcal{B}|}{|\mu(\mathcal{A})|}|m|_\infty.$$

Then, if follows that

$$|\bar{e}(t)| = |\mathcal{C}e(t)| \leq |\mathcal{C}||e(t)| \leq |\mathcal{C}|\exp(\mu(\mathcal{A})t)\,|e(0)| + \frac{|\mathcal{B}||\mathcal{C}|}{|\mu(\mathcal{A})|}|m|_\infty.$$

For each $s \in \mathbb{R}_{\geq 0}$ and $t \in \mathbb{R}_{\geq 0}$, define

$$\beta(s,t) = |\mathcal{C}|\exp(\mu(\mathcal{A})t)s, \quad \varphi(s) = \frac{|\mathcal{B}||\mathcal{C}|}{|\mu(\mathcal{A})|}s.$$

It follows that (5.7) holds. When there exists $P = P^\top > 0$ such that $\mathcal{A}^\top P + P\mathcal{A} \leq -2\alpha P$ for some $\alpha > 0$, consider the Lyapunov function $V(e) = e^\top Pe$. Then, V has the following properties:

P2.6 $\lambda_{\min}(P)|e|^2 \leq V(e) \leq \lambda_{\max}(P)|e|^2$;

P2.7 $\langle \nabla V(e), \mathcal{A}e \rangle \leq -2\alpha\lambda_{\min}(P)|e|^2$;

P2.8 $|\nabla V(e)| \leq 2\lambda_{\max}(P)|e|$.

Moreover, the derivative of the function $V(e) = e^\top Pe$ with respect to time is, for each $e \in \mathbb{R}^n$,

$$\dot{V}(e) = \langle \nabla V(e), \mathcal{A}e \rangle + \langle \nabla V(e), \mathcal{B}m \rangle. \tag{5.14}$$

Using properties P2.7 and P2.8 as well as the Cauchy-Schwarz inequality, we get that for each solution $t \mapsto e(t)$ to (6.14) and each $t \mapsto m(t)$

$$\dot{V}(e(t)) \leq -2\alpha\lambda_{\min}(P)|e(t)|^2 + 2\lambda_{\max}(P)|e(t)||\mathcal{B}||m(t)| \tag{5.15}$$

for all $t \geq 0$. To claim the desired bound on $e(t)$ from (5.15), using similar steps as those in the proof of [74, Theorem 5.1], we define $W(t) = \sqrt{V(e(t))}$. It can be shown that, for all values of $V(e(t))$,

$$D^{+}W(t) \leq -\frac{\alpha\lambda_{\min}(P)}{\lambda_{\max}(P)}W(t) + \frac{\lambda_{\max}(P)|\mathcal{B}|}{\sqrt{\lambda_{\min}(P)}}|m(t)|.$$

Then, by a comparison lemma (see, *e.g.*, [74, Lemma 3.4]), for all $t \geq 0$, $W(t)$ satisfies the inequality

$$W(t) \leq \exp(-\lambda t)W(0) + \frac{\lambda_{\max}(P)|\mathcal{B}|}{\sqrt{\lambda_{\min}(P)}}\int_0^t \exp(-\lambda(t-\tau))|m(\tau)|d\tau,$$

where $\lambda = \frac{\alpha\lambda_{\min}(P)}{\lambda_{\max}(P)}$ .Using property P2.6 and $W(t) = \sqrt{V(e(t))}$, it follows that for all $t > 0$,

$$|e(t)| \leq \sqrt{\frac{\lambda_{\max}(P)}{\lambda_{\min}(P)}}|e(0)|\exp(-\lambda t) + \frac{\lambda_{\max}(P)|\mathcal{B}|}{\lambda_{\min}(P)|\lambda|}|m|_{\infty}. \tag{5.16}$$

Then, it follows that

$$\begin{aligned} |\bar{e}(t)| &= |\mathcal{C}e(t)| \leq |\mathcal{C}||e(t)| \\ &\leq \sqrt{\frac{\lambda_{\max}(P)}{\lambda_{\min}(P)}}|\mathcal{C}||e(0)|\exp(-\lambda t) + \frac{\lambda_{\max}(P)|\mathcal{B}\|\mathcal{C}|}{\lambda_{\min}(P)|\lambda|}|m|_{\infty}. \end{aligned} \tag{5.17}$$

For every $s,\ t \in \mathbb{R}_{\geq 0}$, define

$$\beta(s,t) = \sqrt{\frac{\lambda_{\max}(P)}{\lambda_{\min}(P)}}|\mathcal{C}|\exp(-\lambda t)s, \quad \varphi(s) = \frac{\lambda_{\max}(P)|\tilde{B}||\mathcal{C}|}{\lambda_{\min}(P)|\lambda|}s.$$

Then, (5.7) holds. ■

Theorem 5.2.2 *For the plant* (1.1) *with the Luenberger observer* (1.3) *and the* *interconnected observers* (6.11)*, if there exists a matrix K_g such that at least one of the items* $1)-3)$ *of Proposition 5.2.1 holds, then there exists a class-$\mathcal{KL}$ function $\overline{\beta}$ and a class-$\mathcal{K}_\infty$ function $\overline{\varphi}$ such that the estimation error $\bar{e}$ resulting from the interconnected observers satisfy*

1) $|\bar{e}(t)| \leq \overline{\beta}(|e(0)|, t) + \overline{\varphi}(|m|_\infty) \qquad \forall t \geq 0$;

2) Given nonzero $e(0)$ *and* $e_L(0)$*, there exists* $t^\star \geq 0$ *such that*

$$\overline{\beta}(|e(0)|, t) < \beta_L(|e_L(0)|, t) \qquad \forall t > t^\star;$$

3) $\overline{\varphi}(s) < \varphi_0(s)$*, for all* $s \neq 0$*,* $s \in \mathbb{R}_{\geq 0}$*.*

Proof Recalling from (6.14) that $\overline{e} = \mathcal{C}e$, if follows that,

$$|\overline{e}(t)| = \left|\tilde{C}e(t)\right| \leq \frac{1}{N}\sum_{i=1}^{N}|e_i(t)| \leq \frac{\sqrt{N}}{N}|e(t)| \quad \forall t \geq 0,$$

where we have used the triangle inequality and properties of vector norms. With this property and Proposition 5.2.1, items 1)-3) are verified with $\bar{\beta}(s,t) = \frac{\sqrt{N}}{N}\beta(s,t)$ and $\bar{\varphi}(s) = \frac{\sqrt{N}}{N}\varphi(s)$ for all $s, t \geq 0$, where functions β and φ are defined accordingly as in Proposition 5.2.1 under associated assumptions. ■

Remark 5.2.3 *Note that the boundedness property in item* 2) *in Theorem 5.2.2 guarantees that the rate of convergence of the interconnected observers is faster or equal than that of a Luenberger observer by comparing the $\mathcal{KL}$ estimates they induce (which is a reasonable measure of performance when the $\mathcal{KL}$ functions are derived using similar bounding techniques).*

The $\mathcal{KL}$ bounds established in Proposition 5.2.1 characterize a worse case property of the estimation error of the proposed observer, which can be compared to that of a Luenberger observer via Theorem 5.2.2. The following example illustrates this point.

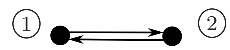

$\bar{x}_1 = \bar{x}_2 = \frac{1}{2}(\hat{x}_1 + \hat{x}_2)$

Figure 5.1: Two agents connected as a direct graph.

Example 5.2.4 *Consider the scalar example in* (1.5)*, an interconnected observer with* $N = 2$ *with an all-to-all graph as shown in Figure 5.1. In particular, the proposed observer takes the form*

$$\begin{aligned} \dot{\hat{x}}_1 &= a\hat{x}_1 - K_{11}(\hat{y}_1 - y) - K_{12}(\hat{y}_2 - y), \\ \dot{\hat{x}}_2 &= a\hat{x}_2 - K_{22}(\hat{y}_2 - y) - K_{21}(\hat{y}_1 - y), \\ \hat{y}_1 &= \hat{x}_1, \quad \hat{y}_2 = \hat{x}_2, \quad \bar{x}_1 = \bar{x}_2 = \frac{\hat{x}_1 + \hat{x}_2}{2}. \end{aligned} \tag{5.18}$$

It should be noted that averaging the estimates of two uncoupled single Luenberger observers (one at each agent) does not lead to both faster convergence rate and smaller steady state error. Consider the case when two agents are experiencing common noises $m_1 = m_2 = m$*. The transfer functions from* m *to* e_L *and from* m *to* $\overline{e}$ *(global) are given by*[3] $T_L(s) = \frac{K_L}{s-a+K_L}$ *and* $T(s) = \mathcal{C}(sI - \mathcal{A})^{-1}\mathcal{B}$*. The following result can be verified.*

Proposition 5.2.5 *Given* $a, K_L \in \mathbb{R}$ *such that* $a \neq 0$ *and* $a - K_L < 0$*, then there exist* $K_{11}, K_{22}, K_{12}, K_{21} \in \mathbb{R}$ *such that the rate of convergence of the observer* (6.11) *is no smaller than that of the one induced by the Luenberger observer and the* H_∞ *norm of* T *is smaller than the* H_∞ *norm of* T_L*, i.e.,* $||T||_\infty < ||T_L||_\infty$*.*

[3]For the particular choice of parameters $K_{11} = K_{22} = K_L$ and $K_{12} = K_{21} = 0$, $||T||_\infty = ||T_L||_\infty$.

It should be noted that averaging the estimates of two uncoupled single Luenberger observers (one at each agent) does not lead to both faster convergence rate and smaller steady state error. To perform a numerical comparison, we consider the case where $a = -0.5$ *and* $m : \mathbb{R}_{\geq 0} \to \mathbb{R}$ *is a continuous bounded function. A Luenberger observer is designed to achieve* $\sigma = 2.5$ *and* $\gamma_L = 0.8$*, which leads to* $K_L = 2$*. The interconnected observers are designed with error system* (6.14)*. Using Theorem 5.2.2, conditions* 2) *and* 3) *can be rewritten as*

$$\begin{aligned} \alpha(\widetilde{A}) &\leq a - K_L, \\ \frac{\sqrt{2}}{2}\frac{\sqrt{(K_{11}+K_{12})^2+(K_{22}+K_{21})^2}}{|\mu(\widetilde{A})|} &< \left|\frac{a}{a-K_L}\right|. \end{aligned} \tag{5.19}$$

From solving (5.19)*, we pick parameters* $K_{11} = 1.7896$*,* $K_{22} = 2.2278$*,* $K_{12} = 0.0538$*,* $K_{21} = -1.1633$*. It can be verified that the eigenvalues of* $\tilde{A}$ *according to this set of parameters are* $-2.5087 \pm 0.1208i$*. Moreover,* $\mu(\tilde{A}) = -1.9123$*.*

Now we perform simulations using these parameters and different measurement noises. With initial conditions $x(0) = 3$*,* $\overline{x}_1(0) = \overline{x}_2(0) = \overline{x}_L(0) = 5$*, the first simulation is run for measurement noise* $m(t) \equiv 0$ *and the resulting trajectories are shown in Figure 5.2(a). This figure shows that the interconnected observers converge at a faster rate compared to the Luenberger observer. In fact, item* 2) *of Theorem 5.2.2 holds with* $t^\star \approx 6.7s$*.*

Simulation results for $m(t) \equiv 0.3$ *are shown in Figure 5.2(b). The behavior of the interconnected observers with constant noise is similar to that of with zero noise. It is worth to note that there is an improvement of the steady-state error by the interconnected observers since* $\overline{e}^\star = 0.2272$*, while the Luenberger observer gives* $e_L^\star = 0.2400$*. As shown in Figure 5.2(b), at around* $t \approx 2s$*,* $\overline{e}$ *becomes closer to* 0 *than* $\overline{e}_L$ *thereafter. To further explore the performance of the interconnected observers, we also consider measurement noise with different frequencies, i.e., a*

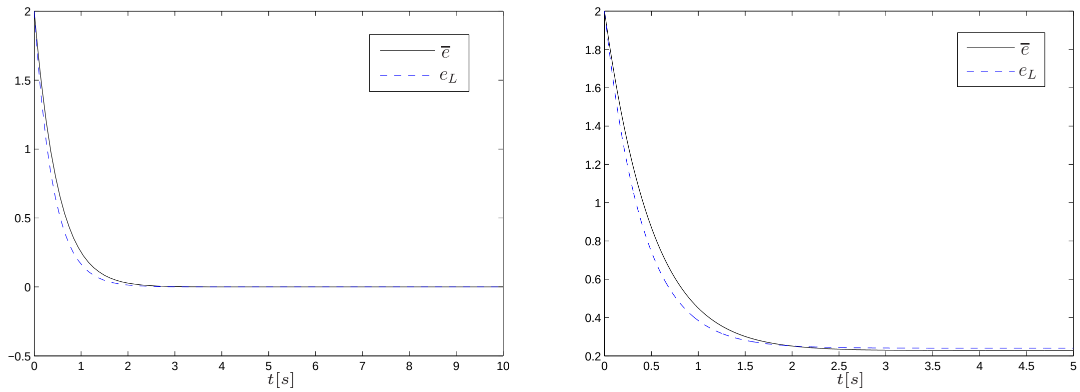

(a) $m(t) \equiv 0$.

(b) $m(t) \equiv 0.3$.

Figure 5.2: Comparisons of estimation errors of the proposed observer and that of a Luenberger observer for different measurement noises with $N = 2$.

low frequency noise $m(t) = 0.3 + 0.3\sin(20t)$ *and a high frequency noise* $m(t) = 0.3 + 0.3\sin(200t)$. *The advantage of the interconnected observers lies on the properties of damped oscillatory behavior and smaller mean value of estimation error. Specifically, a numerical comparison of the estimation errors after transient is reported in the first two columns of Table 5.1, which confirm the improvements guaranteed by the interconnected observers.* $\triangle$

Table 5.1: Comparison of estimation error ($\bar{e}$) of the observers with measurement noise of different frequencies.

observer type	low freq. noise		high freq. noise		H_∞ from m to $\bar{e}$	
	mean $\bar{e}$	std $\bar{e}$	mean $\bar{e}$	std $\bar{e}$	Thm. 5.2.2	Thm. 6.3.3
Luenberger's	0.2419	0.0211	0.2395	0.0022	0.8000	0.8000
Interconnected	0.2286	0.0154	0.2268	0.0016	0.7572	0.4953
Improved (%)	5.5	27.0	5.3	27.3	5.4	38.1

5.3 Design via feasibility/optimization problems

The interconnected observers in (6.11) can be designed by solving feasibility and optimization problems that minimize the H_∞ gain of the transfer function from measurement noise m to estimation error $\bar{e}$ (global) or $\bar{e}_i$ (local) under the rate of convergence constraint. To formulate such problems, following [76], the error system in (6.14) is rewritten as

$$\dot{e} = A_e e + u, \quad y_e = C_e e + m, \quad z_\infty = \mathcal{X} e, \tag{5.20}$$

where $A_e = I_N \otimes A,\ C_e = -I_N \otimes H$, and the "input" u is assigned via $u = M_u y_e$ with $M_u = K_g * \overline{\mathcal{G}}$. Note that z_∞ denotes the overall estimation error (or the local estimation error) of the interconnected observers, *i.e.*, $z_\infty = \overline{e}$ with $\mathcal{X} = \mathcal{C}$ (or $z_\infty = \overline{e}_i$ with $\mathcal{X} = \mathcal{C}_i$). In the s-domain, the transfer function from m to z_∞ for (5.20) can be written as

$$T(s) = \mathcal{X}\big(sI - \mathcal{A}\big)^{-1}\mathcal{B} + \mathcal{D}, \tag{5.21}$$

where $\mathcal{A} = A_e + M_u C_e, \mathcal{B} = M_u$, and $\mathcal{D} = 0$. Within this setting, feasibility (*i.e.*, inequalities) and optimization problems associated with the design of the interconnected observers are formulated in the following sections.

5.3.1 Rate of convergence and H_∞ gain in terms of matrix inequalities

To guarantee that the rate of convergence of the interconnected observers is better (or no worse) than than that of a Luenberger observer, the eigenvalues of the error system in (6.14) will be assigned to the left of the vertical line at $-\sigma$ in the s-plane, where σ is the rate of convergence for the Luenberger observer. Following [77], the error system (6.14) has all eigenvalues located at the left of $-\sigma$

in the s-plane if and only if there exists a matrix P_S such that

$$\mathrm{He}(\mathcal{A}, P_S) + 2\sigma P_S < 0,\ \ P_S = P_S^\top > 0. \tag{5.22}$$

Note that (5.22) is nonlinear because of the cross term $P_S(K_g * \overline{\mathcal{G}})$ obtained when expanding $P_S\mathcal{A}$. The following theorem provides an equivalent linear formulation and a sufficient condition for (5.22).

Proposition 5.3.1 *Condition* (5.22) *is satisfied if*

a) and only if $\mathrm{He}(A_e, P_S) + C_e^\top M_p^\top + M_p C_e + 2\sigma P_S < 0,\ \ P_S = P_S^\top > 0$, *in which case* $M_u = P_S^{-1} M_p$*;*

b) the graph is all-to-all connected and there exists $h_1, h_2 \in \mathbb{R}$ *such that the following conditions hold:*

b.1) $h_1 + h_2 \geq \sigma$*;*

b.2) $P_i = P_i^\top > 0$ *for each* $i \in \mathcal{V}$

b.3) $\mathrm{He}((A - K_{ii}C), P_i) + 2h_1 P_i < 0$ *for each* $i \in \mathcal{V}$*;*

b.4) $$\begin{bmatrix} 2h_2 P_1 & S_{12} & \cdots & S_{1N} \\ S_{12}^\top & 2h_2 P_2 & \cdots & S_{2N} \\ \vdots & \vdots & \ddots & \vdots \\ S_{1N}^\top & S_{2N}^\top & \cdots & 2h_2 P_N \end{bmatrix} < 0.$$

where $S_{ik} = -(K_{ki}H)^\top P_k - P_i K_{ik} H$*.*

Proof Letting $M_p = P_S M_u$, and using the definition of $\mathcal{A}$, inequality (5.22) can be written as

$$\mathrm{He}(A_e, P_S) + C_e^\top M_p^\top + M_p C_e + 2\sigma P_S < 0,$$

with $P_S = P_S^\top > 0$. This proves item a). Now, assuming $b.1$)-$b.3$) with $h_1, h_2 \in \mathbb{R}$, note that the inequalities in $b.3$) can be rewritten as

$$\operatorname{diag}(Q_1, \ldots, Q_N) + \operatorname{diag}(2h_1 P_1, \ldots, 2h_N P_N) < 0, \tag{5.23}$$

with $Q_i = \operatorname{He}((A - K_{ii}H), P_i)$ for each $i \in \mathcal{V}$. By $b.2$), symmetry of the inequalities (5.23) and $b.4$), and the definition of negative symmetric matrices, the sum of the left terms of (5.23) and $b.4$) satisfies

$$\begin{bmatrix} Q_1 & S_{12} & \cdots & S_{1N} \\ S_{12}^\top & Q_2 & \cdots & S_{2N} \\ \vdots & \vdots & \ddots & \vdots \\ S_{1N}^\top & S_{2N}^\top & \cdots & Q_N \end{bmatrix} + \begin{bmatrix} 2\bar{h}P_1 & 0 & \cdots & 0 \\ 0 & 2\bar{h}P_2 & \cdots & 0 \\ \vdots & \vdots & \ddots & \vdots \\ 0 & 0 & \cdots & 2\bar{h}P_N \end{bmatrix} < 0, \tag{5.24}$$

with $S_{ik} = -(K_{ki}H)^\top P_k - P_i K_{ik} H$ for $i, k \in \mathcal{V}$ and $k \neq i$ and $\bar{h} = h_1 + h_2$. Since $h_1 + h_2 \geq \sigma$, (5.22) is satisfied with $P_D = \operatorname{diag}(P_1, \ldots, P_N)$. ■

Proposition 5.3.2 *Conditions* $b.1$)-$b.4$) *in Proposition 5.3.1 hold if and only if there exist* $h_1,\ h_2, \in \mathbb{R},\ Y_i,\ W_{ik},\ P_i$ *for* $i, k \in \{1, 2, \ldots, N\}$ *and* $k \neq i$ *such that:*

a) $h_1 + h_2 \geq \sigma$,

b) $P_i = P_i^\top > 0$, *for each* $i \in \mathcal{V}$,

c) $\operatorname{He}(A, P_i) - H^\top Y_i^\top - Y_i H + 2h_1 P_i < 0$, *for each* $i \in \mathcal{V}$,

d) $$\begin{bmatrix} 2h_2P_1 & R_{12} & \cdots & R_{1N} \\ R_{21} & 2h_2P_2 & \cdots & R_{2N} \\ \vdots & \vdots & \ddots & \vdots \\ R_{N1} & R_{N2} & \cdots & 2h_2P_N \end{bmatrix} < 0,$$
where $R_{ik} = -H^\top W_{ki}^\top - W_{ik} H$.

The conditions b.3)-b.4) in Proposition 5.3.1 hold with $K_{ii} = P_i^{-1} Y_i$ *and* $K_{ik} = P_i^{-1} W_{ik}$ *for* $i, k \in \mathcal{V}$, $j \neq i$.

Proof Let $Y_i = P_i K_{ii}$ and $W_{ik} = P_i K_{ik}$ for $i, k \in \mathcal{V}$ and $k \neq i$, then, $b.3$)-$b.4$) in Proposition 5.3.1 can be rewritten as

$$\mathrm{He}(A, P_i) - H^\top Y_i^\top - Y_i H + 2h_1 P_i < 0$$

for each $i \in \{1, 2, \cdots, N\}$ and

$$\begin{bmatrix} 2h_2 P_1 & R_{12} & \cdots & R_{1N} \\ R_{21} & 2h_2 P_2 & \cdots & R_{2N} \\ \vdots & \vdots & \ddots & \vdots \\ R_{N1} & R_{N2} & \cdots & 2h_2 P_N \end{bmatrix} < 0,$$

respectively. Therefore, c) and d) of Proposition 5.3.2 hold. ■

5.3.2 Minimization of H_∞ norm under rate of convergence constraint with fixed connectivity graph

In this section, we consider the design of interconnected observer over a fixed digraph $\Gamma = (\mathcal{V}, \mathcal{E}, \mathcal{G})$. The design specifications of our interest are the rate of convergence and the H_∞ gain from noise m to estimation errors $\bar{e}$ or e_i, i.e., the $\mathcal{L}_2$ gain. In particular, to guarantee that the rate of convergence of the system (6.14) is better (or no worse) than that of a single Luenberger observer as in (1.3), the eigenvalues of the error system (6.14) will be assigned to the left of the vertical line at $-\sigma$ in the s-plane, where σ is the convergence rate for the Luenberger observer.

Theorem 5.3.3 *Given a plant as in* (1.1) *and a digraph* Γ*, the rate of convergence is larger than or equal to* σ *and the global* H_∞ *gain (respectively, the local* H_∞ *gain) from* m *to estimation error* $\bar{e}$ *in* (6.14) *(respectively,* $\bar{e}_i$ *in* (6.13)*) is minimized if and only if there exist matrices* K_g*,* P_S*, and* P_H *such that the following optimization problem has a solution:*

$$\inf \gamma \tag{5.25a}$$

$$s.t.\ \mathrm{He}(\mathcal{A}, P_S) + 2\sigma P_S < 0, \tag{5.25b}$$

$$\begin{bmatrix} \mathrm{He}(\mathcal{A}, P_H) & P_H \mathcal{B} & \mathcal{X}^\top \\ \mathcal{B}^\top P_H & -\gamma I & 0 \\ \mathcal{X} & 0 & -\gamma I \end{bmatrix} < 0, \tag{5.25c}$$

$$P_S = P_S^\top > 0,\ P_H = P_H^\top > 0, \tag{5.25d}$$

where $\mathcal{X} = \mathcal{C}$ *(respectively,* $\mathcal{X} = \mathcal{C}_i$ *and* $\mathcal{C}_i$ *is the sub-matrix of* $\mathcal{C}$ *from the* $(in - n + 1)$*-th row to the* (in)*-th row).*

Proof From [80, Theorem 2.41], the H_∞ gain for a system from input to output with realization $T_1(s) = C_1(sI - A_1)^{-1}B_1$ is less than or equal to γ if and only if there exists some $P_H = P_H^\top > 0$ such that

$$\begin{bmatrix} \mathrm{He}(A_1, P_H) & P_H B_1 & C_1^\top \\ B_1^\top P_H & -\gamma I & 0 \\ C_1 & 0 & -\gamma I \end{bmatrix} < 0, \tag{5.26}$$

Then, for system (6.14) with $T(s) = \mathcal{C}(sI - \mathcal{A})^{-1}\mathcal{B}$, we have that the global H_∞ gain from m to $\bar{e}$ is less than or equal to γ if and only if (5.26) holds with $A_1 = \mathcal{A}$, $B_1 = \mathcal{B}$ and $C_1 = \mathcal{C}$, which leads to (6.19c) with $\mathcal{X} = \mathcal{C}$. The same argument applies for $T_i(s) = \mathcal{C}_i(sI - \mathcal{A})^{-1}\mathcal{B}$ which leads to (6.19c) with $\mathcal{X} = \mathcal{C}_i$. Then, the proof finishes by adding constraint (5.22). ■

Remark 5.3.4 *For a fixed connectivity graph, the optimization problem in* (6.19) *can be solved offline. Moreover, due to the form of the observer at each node as in* (6.11)*, the information needed by each agent is what the neighbors provide through the connectivity graph. Therefore, the resulting observers for each agent are decentralized.*

Note that the optimization problem (6.19) is not jointly convex over the variables (P_S, P_H, M_u). Moreover, it is nonlinear because of the existence of cross terms $P_H M_u$ and $P_S M_u$. In order to remove the nonlinearities and make the two constraints jointly convex, following [76], we reformulate the problem by seeking common solutions of P_S and P_H, and changing variables to $M_p := PM_u$. Using item a) of Proposition 5.3.1 to rewrite the terms $\mathrm{He}(\mathcal{A}, P_S)$ and $\mathrm{He}(\mathcal{A}, P_H)$ in (6.19), we have the following result.

Theorem 5.3.5 *Given a plant as in* (1.1) *and a graph* Γ*, the rate of convergence is larger than or equal to* σ *and the global* H_∞ *gain (respectively, the local* H_∞ *gain) from* m *to estimation error* $\bar{e}$ *in* (6.14) *(respectively,* $\bar{e}_i$ *in* (6.13)*) is minimized if there exist* M_p *and* P *such that the following optimization problem (LMI) is feasible:*

$$\begin{aligned}
&\inf \gamma \\
&\textit{s.t.:}\ \mathrm{He}(A_e, P) + C_e^\top M_p^\top + M_p C_e + 2\sigma P < 0, \\
&\begin{bmatrix} \mathrm{He}(A_e, P) + C_e^\top M_p + M_p^\top C_e & M_p D_e & \mathcal{X}^\top \\ D_e^\top M_p^\top & -\gamma I & 0 \\ \mathcal{X} & 0 & -\gamma I \end{bmatrix} < 0, \\
&P = P^\top > 0,
\end{aligned}$$

where $\mathcal{X} = \mathcal{C}$ (respectively, $\mathcal{X} = \mathcal{C}_i$ and $\mathcal{C}_i$ is the sub-matrix of $\mathcal{C}$ from the $(in - n + 1)$-th row to the (in)-th row).

Remark 5.3.6 *The resulting observer gain matrix from Theorem 5.3.5 is given by $M_u = P^{-1}M_p$. By making the optimization problem linear and convex, a global optimizer is guaranteed. However, asking for common solution of $P_H = P_D$ may eliminate a better feasible solution to the original optimization problem in* (6.19).

Following [84, 85], it is possible to formulate an equivalent convex optimization problem to the one in Theorem 5.3.5 but with noncommon P_D and P_H matrices.

Proposition 5.3.7 *Given $\sigma \geq 0$, the rate of convergence of error system* (5.20) *is greater than or equal to σ and the H_∞ gain from m to $\bar{e}$ is less than or equal to γ if there exist real matrices P_S, P_H, Q_D, Q_H and real numbers $r_D > 0$, $r_H > 0$ such that the following optimization problem (LMI) is feasible:*

$$\inf \gamma$$

$$s.t. \quad \begin{bmatrix} \mathrm{He}(\mathcal{A}, Q_D) + 2\sigma P_S & P_S - Q_D^\top + r_D \mathcal{A}^\top Q_D \\ P_S - Q_D + r_D Q_D^\top \mathcal{A} & -r_D(Q_D + Q_D^\top) \end{bmatrix} < 0, \tag{5.27a}$$

$$\begin{bmatrix} \mathrm{He}(\mathcal{A}, Q_H) & P_S - Q_H^\top + r_H \mathcal{A}^\top Q_H & Q_H^\top \mathcal{B} & \mathcal{C}^\top \\ P_S - Q_H + r_H Q_H^\top \mathcal{A} & -r_H(Q_H + Q_H^\top) & r_H Q_H^\top \mathcal{B} & 0 \\ \mathcal{B}^\top Q_H & r_H \mathcal{B}^\top Q_H & -\gamma I & 0 \\ \mathcal{C} & 0 & 0 & -\gamma I \end{bmatrix} < 0, \tag{5.27b}$$

$$P_S = P_S^\top > 0, P_H = P_H^\top > 0. \tag{5.27c}$$

Proof The proof follows from [86, Theorem 1 and Theorem 2], see also [84, 85]. ■

Next, we provide an example to illustrate the results above.

Example 5.3.8 *We revisit the Example 5.2.4. To further indicate the improvement obtained by the proposed observer, we choose* $K_{11} = K_{22} = K_L = 2$*, and* $K_{21} = -0.5K_L = -1$*. The resulting local* H_∞ *gain from* m *to* $\bar{e}_1$ *is* 0.55*, which is smaller than that of the Luenberger observer, which is* 0.8*. If instead the connectivity graph in Figure 5.1 is considered, we can further optimize the parameters by solving the optimization problem* (6.19)*. Feasible parameters for* (6.19) *are found using the solver PENBMI [87]. For* $K_{11} \approx -6.7215$*,* $K_{22} \approx 10.7215$*,* $K_{12} \approx -13.2202$*,* $K_{21} \approx 5.7537$*, the resulting global* H_∞ *gain is* ≈ 0.5051*, which is* $\approx 36.86\%$ *smaller than that of Luenberger observer (which is* 0.8 *with* $K_L = 2$*). This improvement and the improvement obtained when using Theorem 5.2.2 are listed in the last two columns of Table 5.1.*

In fact, when the rate of convergence specification is $\sigma = 2.5$*, and the* H_∞ *gain from* m *to* $\bar{e}$ *is restricted to be less than or equal to* 0.8*, then, by letting* $K_{11} = 2$ *and* $K_{22} = 2$*, we can find the feasible region for* K_{12} *and* K_{21} *as shown in Figure 5.3(a). Moreover, if the rate of convergence is required to be* $\sigma = 3.0$ *with the same* H_∞ *constraint, then, by letting* $K_{11} = 2.5$ *and* $K_{22} = 2.5$*, we obtain the feasible region for* K_{12} *and* K_{21} *as shown in Figure 5.3(b). As the figure suggests, faster rate of convergence leads to a smaller feasible region for the observer parameters. More importantly, for a single Luenberger observer, there is no feasible solution for rate of convergence larger than or equal to* 3.0 *and global* H_∞ *gain less than* 0.8*.*

Now, for the same plant, consider digraphs with 6 *agents where the edges are defined as in Figure 5.4. In all cases, each agent is self connected. Let* M_1 *denote the number of non-self edges for agent* 1*, e.g., when* $M_1 = 0$ *as shown in*

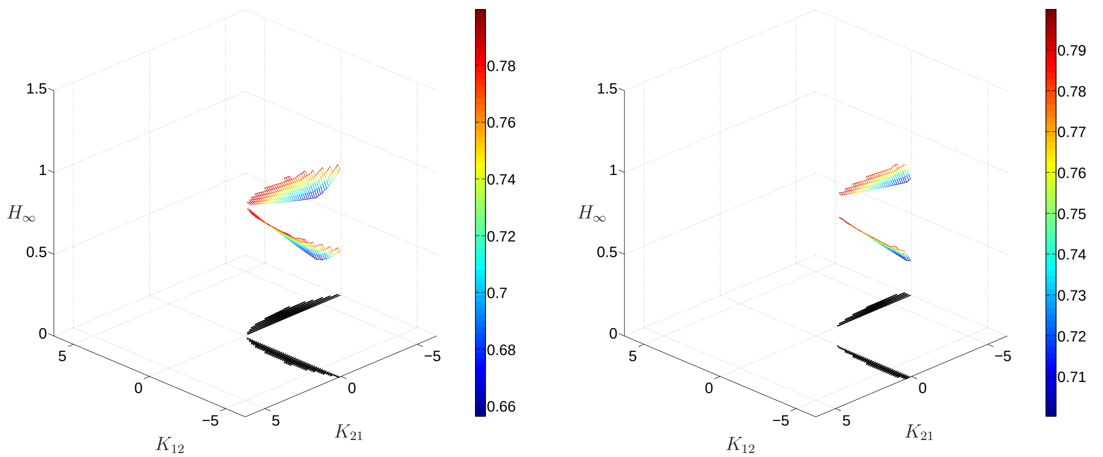

(a) Regions for rate of convergence equal 2.5 ($K_{12} = K_{21} = 2$).

(b) Regions for rate of convergence equal 3.0 ($K_{12} = K_{21} = 2.5$).

Figure 5.3: Feasible regions for observer parameters subject to different rate of convergence specification and global H_∞ gain less than 0.8.

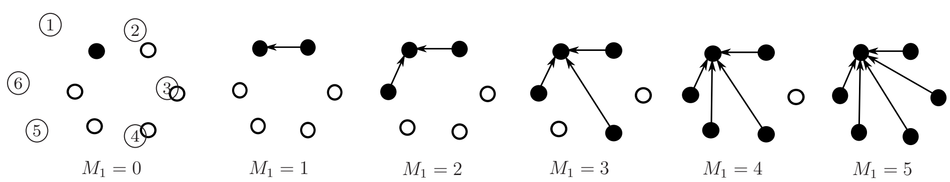

Figure 5.4: Different graph structures for agent 1 with $N = 6$.

Table 5.2: Comparison of local H_∞ norms from noise m to $\bar{e}_1$ with different number of incoming edges for agent 1.

	number of non-self edges (M_1)					
	0	1	2	3	4	5
local H_∞	0.80	0.45	0.34	0.28	0.25	0.22
improv. (%)	0.00	43.8	57.5	65.0	68.8	72.5

Figure 5.4, it is implied that $\overline{\mathcal{G}} = I_6$*, while when* $M_1 = 5$, $\overline{\mathcal{G}} = \begin{bmatrix} g_1 \\ g_2 \end{bmatrix}$, $g_1 = [1 \ 1_5^\top]$ *and* $g_2 = [0 \ I_5]$*. Let the rate of convergence specification be* $\sigma = 2.5$*. Then, the local* H_∞ *norms from noise* $m = (m_1, \ldots, m_6)$ *to estimation error* $\bar{e}_1$ *at agent 1 for the cases in Figure 5.4 are shown in Table 5.2. From case* $M_1 = 0$ *to case* $M_1 = 1$*, the improvement is significant; in fact, when an incoming edge is added to agent*

1, the local H_∞ is improved by 43.8% when compared to the case where a single Luenberger observer is used at agent 1. When two agents provide information to agent 1 ($M_1 = 2$), the improvement is approximately 57.5%, while when three and four agents communicate to agent 1, the improvement grows to approximately 65% and 69% ($M_1 = 4$), respectively. $\triangle$

Example 5.3.9 (second order plant) *First, we consider a second-order plant given as in (1.1) with*

$$A = \begin{bmatrix} -5/2 & 1/10 \\ 4/100 & -3 \end{bmatrix}, \quad H = \begin{bmatrix} 1 & 2 \end{bmatrix}.$$

For a given Luenberger observer with $K_L = [1.5 \quad -0.16]^\top$, its rate of convergence is -3.34 and its H_∞ norm from measurement noise m to estimation error e_L is equal 0.34. With the interconnected observers for $N = 2$ connected via an all-to-all connectivity graph, we obtain that the optimal global H_∞ norm from measurement noise m to estimation error $\bar{e}$ is approximately 0.05 and the optimal local H_∞ norm from m to $\bar{e}_1$ (or $\bar{e}_2$) is 0.03 with $M_u = [v_1 \; v_2]$, where $v_1 = [10.3834 \; -1.6019 \; -10.7581 \; 1.5963]^\top$ and $v_2 = [7.1992 \; -1.2410 \; -7.3028 \; 1.2426]^\top$. This is $\approx 85.29\%$ smaller than that of Luenberger observers.

Then, we consider a second-order plant with oscillatory behavior given as in (1.1) with

$$A = \begin{bmatrix} 0 & -1 \\ 1 & 0 \end{bmatrix}, \quad C = \begin{bmatrix} 1 & 0 \end{bmatrix}.$$

For a given Luenberger observer with $K_L = [2 \quad 0]^\top$, its rate of convergence is -1 and its H_∞ norm from measurement noise m to estimation error e_L is *equal* 2. *With the interconnected observers with* $N = 2$ *connected via an all-to-all connectivity graph, by formulating the problem according to* (5.20)*, the optimization problem in Theorem 6.3.3 is solved and the gain matrix is found as* $M_u = [v_1\ v_2]$*, where* $v_1 = [7.9503\ -9.9554\ -5.9424\ 9.0014]^\top$ *and* $v_2 = [-5.9324\ 9.1143\ 7.9605\ -9.8426]^\top$*. Its corresponding global* H_∞ *norm from* m *to* $\bar{e}$ *is* ≈ 1.4142 *and its local* H_∞ *norm from* m *to* $\bar{e}_1$ *(or* $\bar{e}_2$*) is* ≈ 1*. Comparing to the Luenberger observer, the global* H_∞ *norm is decreased by* $\approx 29.3\%$ *and the local* H_∞ *norm is decreased by* $\approx 50.0\%$*.* $\triangle$

The improvements on the local H_∞ gain guaranteed by the proposed interconnected observers in the examples above are justified by the fact that the sufficient condition given in the upcoming Section 5.4 are satisfied; see Theorem 5.4.1 and below it, where these examples are revisited.

5.3.3 Minimization of H_∞ norm under rate of convergence constraint with optimized connectivity graph

For interconnected observers whose digraph has not yet been specified, a natural question to ask is whether there exists a digraph that minimizes the number of links between agents for the given specifications. In applications, such minimizations could potentially lower the cost of a distributed system as it could reduce the number of agents and communication links. The following result provides a sufficient and necessary condition for such optimization problem.

Theorem 5.3.10 *For the error system* (6.14)*, the rate of convergence is larger than or equal to* σ *and the global* H_∞ *norm (respectively, the local* H_∞ *norm) from noise* m *to estimation error* $\bar{e}$ *in* (6.14) *(respectively,* $\bar{e}_i$ *in* (6.13)*) is less than or equal to* $\gamma^\star$ *over a digraph* Γ *with minimized number of edges if and only if there* *exist matrices K_g, $\mathcal{G}$, P_S, and P_H such that the following optimization problem has a solution:*

$$\inf \operatorname{tr}(D_{in}) \tag{5.28a}$$

$$s.t.\ \operatorname{He}(\mathcal{A}, P_S) + 2\sigma P_S < 0, \tag{5.28b}$$

$$\begin{bmatrix} \operatorname{He}(\mathcal{A}, P_H) & P_H\mathcal{B} & \mathcal{X}^\top \\ \mathcal{B}^\top P_H & -\gamma^\star I & 0 \\ \mathcal{X} & 0 & -\gamma^\star I \end{bmatrix} < 0, \tag{5.28c}$$

$$P_S = P_S^\top > 0,\ P_H = P_H^\top > 0, \tag{5.28d}$$

where $\mathcal{X} = \mathcal{C}$ (respectively, $\mathcal{X} = \mathcal{C}_i$).

Proof Following the proof of Theorem 6.3.3, the global H_∞ gain over a digraph Γ is less than or equal to $\gamma^\star$ if and only if (5.26) holds with $A_1 = \mathcal{A}$, $B_1 = \mathcal{B}$, $C_1 = \mathcal{C}$, $\gamma = \gamma^\star$ and $P_H = P_H^\top > 0$. The same argument applies to the local H_∞ gain. Moreover, the rate of convergence condition is satisfied if and only if (5.28b) holds. Since $\operatorname{tr}(D_{in}) = \sum_{i=1}^N \sum_{k=1}^N g_{ik}$, where $g_{ijk} = 1$ indicates there is an edge from node k to node i, then the number of edges of the graph is minimized if and only if $\operatorname{tr}(D_{in})$ is minimized. ■

The constraints in (5.28b) and (5.28c) are nonlinear and not jointly convex. By changing variables, the nonlinear constraints in (5.28b) and (5.28c) can be linearized as a function of Q and P.

Theorem 5.3.11 *For the error system* (6.14)*, the rate of convergence is larger than or equal to σ and the global H_∞ norm (respectively, the local H_∞ norm) from noise m to estimation error $\bar{e}$ in* (6.14) *(respectively, $\bar{e}_i$ in* (6.13)*) is less than or equal to $\gamma^\star$ over a digraph Γ with minimized number of communication links if* *there exist matrices K_g, $\mathcal{G}$, and P such that the following optimization problem is feasible:*

$$\inf \operatorname{tr}(D_{in}) \tag{5.29a}$$

$$s.t.\ \operatorname{He}(I_N \otimes A, P) - Z + 2\sigma P < 0, \tag{5.29b}$$

$$\begin{bmatrix} \operatorname{He}(I_N \otimes A, P) - Z & Q & \mathcal{X}^\top \\ Q^\top & -\gamma^\star I & 0 \\ \mathcal{X} & 0 & -\gamma^\star I \end{bmatrix} < 0, \tag{5.29c}$$

$$P = P^\top > 0, \tag{5.29d}$$

where $Q = P(K_g * \overline{\mathcal{G}})$, $Z = -Q(I_N \otimes H) - (I_N \otimes H)^\top Q^\top$, and $\mathcal{X} = \mathcal{C}$ (respectively, $\mathcal{X} = \mathcal{C}_i$).

Proof Let K_g, $\mathcal{G}$ and P be solutions of the optimization problem (5.29). Since the matrix $K_g * G^\top$ is such that $Q = P(K_g * \overline{\mathcal{G}})$, using $P = P^\top$ and the definition of $\mathcal{A}$ in (6.15), we have

$$\begin{aligned} &\operatorname{He}(I_N \otimes A, P) - Q(I_N \otimes H) - (I_N \otimes H)^\top Q^\top \\ &\quad = (I_N \otimes A)^\top P + P(I_N \otimes A) \\ &\qquad - (I_N \otimes H)^\top (K_g * \overline{\mathcal{G}})^\top P^\top - P(K_g * \overline{\mathcal{G}})(I_N \otimes H) \\ &\quad = \operatorname{He}(\mathcal{A}, P). \end{aligned}$$

Then, K_g, $\overline{\mathcal{G}}$, $P_S = P$ and $P_H = P$ satisfy (5.28). ■

Remark 5.3.12 *The results above define the graph via the resulting $\overline{\mathcal{G}}$. The resulting K_g and $\mathcal{G}$ from* (5.29) *satisfies $K_g * \overline{\mathcal{G}} = P^{-1}Q$, which may not be unique.*

Example 5.3.13 *Consider the scalar plant in* (1.5) *with* $a = -0.5$ *as in Example 5.3.8, and suppose that the rate of convergence specification is* $\sigma = 2.5$. *When using the graph that is all-to-all as shown in Figure 5.5(a), it is natural to ask the effect that the number of agents has on the improvement of the global* H_∞ *norm. As shown in Figure 5.5(b), the resulting global* H_∞ *gain is reduced as the number of agents* N *grows. These results are obtained following Theorem 5.3.10. The improvement is summarized in Table 5.3. Note that the improvement is less sig-*

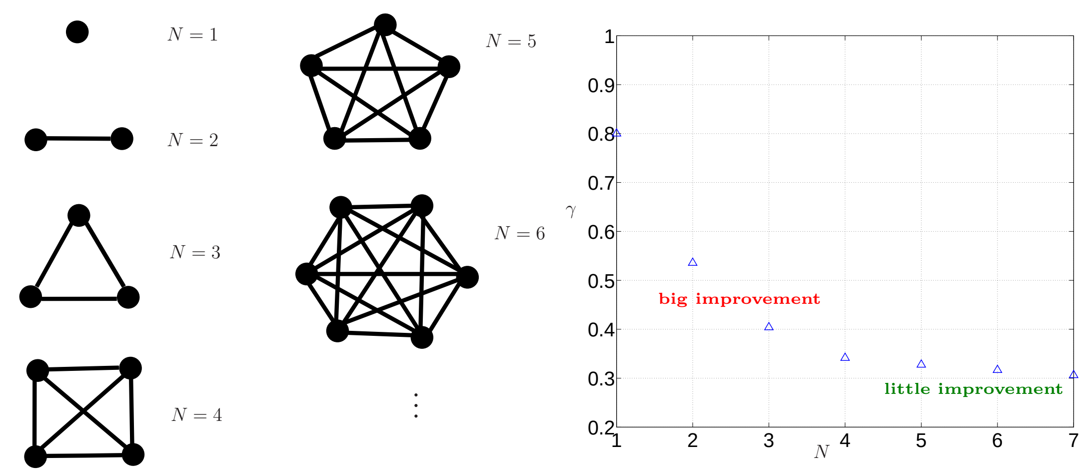

(a) Graph structures with all to all connections (self connection links are not shown).

(b) The global H_∞ norm from noise m to estimation error $\bar{e}$ with respect to the number of agents.

Figure 5.5: The influence of the number of agents on the H_∞ gain from noise m to estimation error $\bar{e}$.

Table 5.3: Comparison of global H_∞ norms from noise m to $\bar{e}$ with different number of agents under all-to-all connection.

	number of agents (N)						
	1	2	3	4	5	6	7
global H_∞	0.80	0.54	0.40	0.34	0.33	0.32	0.31
improv. (%)	0.00	32.5	50.0	57.5	58.8	60.0	61.3
local H_∞	0.80	0.38	0.24	0.23	0.21	0.20	0.19
improv. (%)	0.00	52.5	70.0	71.3	73.8	75.0	76.3

nificant for $N > 6$. *In particular, the table indicates that if the global* H_∞ *gain is* *required to be less than or equal to* 0.40*, then, as shown in Figure 5.5(b), the least number of agents needed is three* [4]*. For the same scalar plant with three interconnected observers, according to Theorem 5.3.10, we establish a relationship between* $\mathrm{tr}(D_{in})$ *and the global* H_∞ *gain from* m *to estimation error* $\bar{e}$ *in Table 5.4. In particular, for* $\mathrm{tr}(D_{in})$ *smaller than six, there is no improvement in the* H_∞ *gain when compared to that of Luenberger observers. Moreover, the table indicates that, with three interconnected observers, if the global* H_∞ *gain is required to be less than or equal to* 0.6*, then the minimum number of links required in the connectivity graph* Γ *is seven.* $\triangle$

Table 5.4: Comparison of global H_∞ norms from noise m to $\bar{e}$ with different connectivity graph with $N = 3$.

	$\mathrm{tr}(D_{in})$			
	6	7	8	9
global H_∞	0.64	0.53	0.43	0.40
improv. (%)	20.0	33.8	46.3	50.0

5.4 A sufficient condition guaranteeing smaller local H_∞ gain

In this section, we are interested in conditions on the plant (1.1) for which it is possible to design interconnected observers that, for a given rate of convergence σ, have local H_∞ gains smaller than when a single Luenberger observer is used at each agent. Note that the local H_∞ gain affects the quality of the estimates obtained at each node. These estimates can be computed efficiently and in a decentralized manner using local information, while computing the global estimate requires additional algorithms. The following result provides one such condition.

[4]The optimization problem related to the examples shown in this paper are solved by PENBMI [87].

Theorem 5.4.1 *Given $\sigma \geq 0$, suppose K_L is such that the eigenvalues of the error system* (1.4) *of the Luenberger observer* (1.3) *for the plant* (1.1) *are located in the region $\mathcal{D} = \{s \in \mathcal{C}_0 : Re(s) < -\sigma\}$, and the H_∞ gain from m to e_L is $\gamma_L > 0$. If there exist $\tilde{\alpha} \in \mathbb{R}$ and $P = P^\top > 0$ such that*

$$\begin{bmatrix} \mathrm{He}(A - K_L H, P) & P K_L H & -\tilde{\alpha} I_n \\ H^\top K_L^\top P & -I_n & (1+\tilde{\alpha}) I_n \\ -\tilde{\alpha} I_n & (1+\tilde{\alpha}) I_n & -I_n \end{bmatrix} < 0, \tag{5.30}$$

then, for every $N \in \mathbb{N},\ N > 1$, there exist a digraph Γ and a gain K_g for N interconnected observers in (6.11) *such that the error system* (6.14) *has its eigenvalues in $\mathcal{D}$ and the local H_∞ gain from m to associated $\bar{e}_i$ for all agents are less than or equal to γ_L. Moreover, for at least $N-1$ agents, the local H_∞ gain from m to associated $\bar{e}_i$ is strictly less than γ_L.*

Proof For any $N > 1$, let the digraph Γ have adjacency matrix such that

$$\overline{\mathcal{G}}_N = \begin{bmatrix} 1 & 0 \\ 1_{N-1} & I_{N-1} \end{bmatrix}. \tag{5.31}$$

This choice of $\overline{\mathcal{G}}$ indicates that agent 1 can share information with all other agents. Moreover, for each $i \in \mathcal{V}$, let T_i be the transfer function from m to $\bar{e}_i$. Take $N = 2$ and $K_{11} = K_{22} = K_L$, $K_{12} = 0$, and K_{21} to be determined later. Then, the interconnected observers in (6.11) reduce to

$$\begin{aligned} &\dot{\hat{x}}_1 = A\hat{x}_1 - K_L(\hat{y}_1 - y_1), \\ &\dot{\hat{x}}_2 = A\hat{x}_2 - K_L(\hat{y}_2 - y_2) - K_{21}(\hat{y}_1 - y_1), \\ &\hat{y}_1 = H\hat{x}_1,\ \hat{y}_2 = H\hat{x}_2, \quad \bar{x}_1 = \hat{x}_1,\ \bar{x}_2 = \frac{\hat{x}_1 + \hat{x}_2}{2}, \end{aligned} \tag{5.32}$$

with associated error system as in (6.14) with

$$\mathcal{A} = \begin{bmatrix} A - K_L H & 0 \\ -K_{21} H & A - K_L H \end{bmatrix}, \ \mathcal{B} = \begin{bmatrix} K_L & 0 \\ K_{21} & K_L \end{bmatrix}.$$

If K_L is such that (1.3) has its eigenvalues in $\mathcal{D}{=}\{s{\in}\mathcal{C}_0 : \ Re(s){<}{-}\sigma\}$, then, due to the block matrix form of $\mathcal{A}$, the eigenvalues of $\mathcal{A}$ are also in $\mathcal{D}$. Now, suppose (5.30) holds with $\alpha \in \mathbb{R}$ and $P = P^\top > 0$. Then, if (5.30) is treated as an H_∞ constraint, equivalently, we have

$$\left|\left| -\tilde{\alpha}(sI - \tilde{A}_L)^{-1} K_L H + (1 + \tilde{\alpha}) I \right|\right|_\infty < 1. \tag{5.33}$$

Therefore, the transfer function $T_2(s) = \mathcal{C}_2(sI - \mathcal{A})^{-1}\mathcal{B}$ satisfies

$$T_2 = \frac{1}{2}\begin{bmatrix} I & I \end{bmatrix} \begin{bmatrix} sI - \tilde{A}_L & 0 \\ K_{21} H & sI - \tilde{A}_L \end{bmatrix}^{-1} \begin{bmatrix} K_L & 0 \\ K_{21} & K_L \end{bmatrix}.$$

By using the inversion identity for a block matrix (inversion lemma), it follows that

$$\begin{bmatrix} sI{-}\tilde{A}_L & 0 \\ K_{21} H & sI - \tilde{A}_L \end{bmatrix}^{-1} = \begin{bmatrix} (sI{-}\tilde{A}_L)^{-1} & 0 \\ F & (sI{-}\tilde{A}_L)^{-1} \end{bmatrix},$$

where $F = -(sI - \tilde{A}_L)^{-1} K_{21} H (sI - \tilde{A}_L)^{-1}$ Then, by assigning $K_{21} = \tilde{\alpha} K_L$, T_2 can be simplified as

$$T_2 = \begin{bmatrix} \frac{1}{2} T_L - \frac{1}{2}\tilde{\alpha} T_L H T_L + \frac{1}{2}\tilde{\alpha} T_L & \frac{1}{2} T_L \end{bmatrix},$$

where $T_L(s) = (sI - \tilde{A}_L)^{-1}K_L$. Therefore, we obtain

$$||T_2||_\infty \leq \frac{1}{2}||(1+\tilde{\alpha})T_L - \tilde{\alpha}T_L H T_L||_\infty + \frac{1}{2}||T_L||_\infty.$$

Using (5.33), it follows that $||T_2||_\infty < ||T_L||_\infty = \gamma_L$. Now consider for any $N > 1, N \in \mathbb{N}$, with digraph whose adjacency matrix is such that $\mathcal{G} + I_N = \overline{\mathcal{G}}_N$, it follows that the transfer function T_i from noise m to $\bar{e}_i$ satisfies $T_i = T_2$ for all $i \in \mathcal{V}, i \neq 1$. Therefore, $||T_i||_\infty < \gamma_L$ for all $i \in \mathcal{V}, i \neq 1$. ∎

Note that condition (5.30) is a property on the plant for a given K_L; basically, an H_∞ inequality as in (6.19c). Next, we illustrate this condition in the examples throughout the paper.

Example 5.4.2 *For the scalar plant* (1.5) *with the Luenberger observer* (1.3)*, the transfer function in the s-domain from m to e_L is given by $T_L(s) = \frac{K_L}{s-a+K_L}$. Since* (5.30) *is an LMI with respect to P and $\tilde{\alpha}$, its feasibility can be easily verified, e.g., for $a = -0.5$ and $K_L = 2$, $P = 0.47$ and $\tilde{\alpha} = -0.5$ solve* (5.30)*. Therefore, for the plant* (1.5)*, there exist interconnected observers such that at least $N-1$ local H_∞ gains are smaller than $\gamma_L = 0.8$ with $K_L = 2$. This justifies the improvement shown in the motivational example as in Table 5.1.* △

Example 5.4.3 *We revisit the systems in Example 5.3.9. For the first system discussed in Example 5.3.9, the improvement is justified by the fact that condition* (5.30) *in Theorem 5.4.1 holds with $\tilde{\alpha} = -0.3241$ and $P = 0.1I$. While for the other second-order plant with oscillatory behavior, the improvement is justified by the fact that condition* (5.30) *in Theorem 5.4.1 holds with $\tilde{\alpha} = 0.8631$ and $P = [w_1\ w_2]$ with $w_1 = [0.1839\ 0.0117]^\top$ and $w_2 = [0.0117\ 0.1722]^\top$.* △

5.5 Consensus of the estimates in the nominal case

The results in the previous section enable the design of interconnected observers as in (6.11) that meet specifications involving the rate of convergence, H_∞ gains, and connectivity graphs. The local estimate could further be employed to determine a global estimate over the connectivity graph. Such an estimate can be obtained using consensus algorithms, in which case it will consists of a consensus problem of time-varying signals. When measurement noise is zero, the algorithm in [43] can already be employed when generalized to the case of vector inputs. To this end, we attach to each agent an agreement vector ξ_i and employ the following distributed algorithm to guarantee that each ξ_i asymptotically approaches the average of the local estimates, namely, $\frac{1}{N}\sum_{j=1}^{N}\hat{x}_j(t)$:

$$\begin{aligned}
\dot{\xi}_i^k &= -\beta_1(\xi_i^k - \hat{x}_i^k) - \beta_2\sum_{j=1}^{N}\ell_{ij}\xi_j^k - v_i^k + \dot{\hat{x}}_i^k, \\
\dot{v}_i^k &= \beta_1\beta_2\sum_{j=1}^{N}\ell_{ij}\xi_i^k,
\end{aligned} \tag{5.34}$$

for $i \in \mathcal{V}$, $1 \le k \le n$, where $\xi_i = (\xi_i^1, \ldots, \xi_i^k, \ldots, \xi_i^n)$; $\hat{x}_i$'s are the estimates generated by agent i using the local observer in (6.11), v_i is the auxiliary variable, and ℓ_{ij}'s are elements of the Laplacian $\mathcal{L}$ associated with the digraph Γ. The constants $\beta_1, \beta_2 \in \mathbb{R}$ are parameters to be determined.

To analyze the convergence and stability of algorithm (6.12), following [43], it is rewritten as

$$\begin{aligned}
\dot{\delta} &= -\beta_1\delta - \beta_2(\mathcal{L}\otimes I_n)\delta - w, \\
\dot{w} &= \beta_1\beta_2(\mathcal{L}\otimes I_n)\delta - \Pi_{nN}(\ddot{\hat{x}} + \beta_1\dot{\hat{x}}),
\end{aligned} \tag{5.35}$$

where $\delta = (\delta_1, \delta_2, \ldots, \delta_N)$, $\delta_i = \xi_i - \frac{1}{N}\sum_{j=1}^{N} \hat{x}_j, i \in \mathcal{V}$, $w = v - \Pi_{nN}(\dot{\hat{x}} + \beta_1 \hat{x})$, and $\Pi_{nN} := I_{nN} - \frac{1}{nN} 1_{nN} 1_{nN}^\top$. Following [43, Lemma 4.3], we obtain the following property.

Lemma 5.5.1 *For the plant in* (1.1)*, assume the digraph Γ is strongly connected and weight balanced, where $\hat{x}_i$ has the dynamics given in* (6.11) *with $m_i \equiv 0$. Moreover, assume there exists K_g in* (6.15) *such that $\mathcal{A}$ is Hurwitz. Then, for any $x(0), \hat{x}_i(0), \xi_i(0) \in \mathbb{R}^n$, $\beta_1 > 0$, $\beta_2 > 0$, and $v_i(0) \in \mathbb{R}^n$ such that $\sum_{i=1}^{N} v_i(0) = 0$, we have*

$$\lim_{t\to\infty} \left(\xi_i(t) - \frac{1}{N}\sum_{j=1}^{N} \hat{x}_j(t) \right) = 0$$

for all $i \in \mathcal{V}$.

Proof Consider the k-th element of $\hat{x}_i$ as $\hat{x}_i^k$ with the algorithm in (6.12). Let $\delta^k = (\delta_1^k, \delta_2^k, \ldots, \delta_N^k)$, $w^k = (w_1^k, w_2^k, \ldots, w_N^k)$, $v^k = (v_1^k, v_2^k, \ldots, v_N^k)$ and $\hat{x}^k = (\hat{x}_1^k, \hat{x}_2^k, \ldots, \hat{x}_N^k)$. We can rewrite (6.12) as

$$\dot{\delta}^k = -\beta_1 \delta^k - \beta_2 \mathcal{L} \delta^k - w^k, \tag{5.36}$$

$$\dot{w}^k = \beta_1 \beta_2 \mathcal{L} \delta^k - \Pi_N(\ddot{\hat{x}}^k + \beta_1 \dot{\hat{x}}^k), \tag{5.37}$$

where

$$\delta_i^k = \xi_i^k - \frac{1}{N}\sum_{j=1}^{N} \hat{x}_j^k, i \in \mathcal{V},$$

$$w^k = v^k - \Pi_N(\dot{\hat{x}}^k + \beta_1 \hat{x}^k).$$

Then, we obtain

$$\begin{bmatrix} \dot{\delta}^k \\ \dot{w} \end{bmatrix} = A_k \begin{bmatrix} \delta^k \\ w \end{bmatrix} - \begin{bmatrix} 0 \\ \Pi_N(\ddot{\hat{x}}^k + \beta_1 \dot{\hat{x}}^k) \end{bmatrix}, \tag{5.38}$$

where

$$A_k = \begin{bmatrix} -\beta_1 I_N - \beta_2 \mathcal{L} & -I_N \\ \beta_1 \beta_2 \mathcal{L} & 0 \end{bmatrix}. \tag{5.39}$$

Applying [43, Lemma 4.3], we have

$$\lim_{t\to\infty} \left(\xi_i^k(t) - \frac{1}{N} \sum_{j=1}^{N} \hat{x}_j^k(t) \right) = 0$$

for all $i \in \mathcal{V}$. Furthermore, this is true for all $k \in \{1, 2, \ldots, n\}$. Therefore, the lemma is proved. ■

When the measurement noise m is not zero, due to the linear dynamics, we conjecture that the algorithm in (6.12) has an ISS like property with respect to m, similar to the $\mathcal{KL}$ bound in (5.7). Along with Theorem 5.4.1, such a property could potentially be used to characterize the improvement of the global H_∞ guaranteed by the interconnected observers.

5.6 Summary

While it may be possible to get further improvement by designing the gains of the interconnected observers as in the design of Kalman filters, it should be noted that the tradeoff between performance and robustness affects general Kalman filters. In contrast to standard observers for linear time-invariant systems, interconnected observers have the capability of attaining fast rate of convergence rate without necessarily jeopardizing robustness to measurement noise in the H_∞ sense. The comparison between $\mathcal{KL}$ bounds between interconnected and Luenberger observers leads to checkable conditions that can be used for design – though potentially conservative. When solved for specific systems, the stated feasibility and optimization problems lead to significant improvements, when compared to single Luenberger observers. Such improvement is guaranteed by the satisfaction of an LMI condition. While the optimization of the number of internal observers and the connectivity graph are not necessarily linear and convex, numerical results for a particular plant indicate that the improvement obtained in robustness is significant only up to a finite number of such internal observers.

Chapter 6

Dynamic Consensus for Distributed Estimation

Motivated by the design of distributed observers with good performance and robustness to measurement and communication noise, the problem of obtaining a global estimate, over a graph, of a common process is considered. In this chapter, we propose a global consensus algorithm that satisfies a pre-specified rate of convergence and has optimized robustness to both communication and measurement noise. At each node of the graph, a local (linear) observer and a consensus variable are updated employing information received from neighbors. The convergence rate and the robustness to communication and measurement noise of the proposed consensus algorithm are characterized in terms of $\mathcal{KL}$ bounds as well as in terms of (nonlinear and linear) optimization problems. The stability and robustness properties of the proposed algorithm are shown analytically and validated numerically.

6.1 A motivational example

Consider the plant in (1.5). It is shown in previous chapter that a distributed state observer can be designed to satisfy a pre-specified rate of convergence constraint and have an optimized H_∞ gain from measurement noise to estimation error. In this example, we consider two connected agents are such that agent 1 can transmit information to agent 2, but agent 2 cannot send data to agent 1, as shown in Figure 6.1. Following [88], a distributed state observer takes the form[1]

$$
\begin{aligned}
&\dot{\hat{x}}_1 = a\hat{x}_1 - K_{11}(\hat{y}_1 - y_1),\\
&\dot{\hat{x}}_2 = a\hat{x}_2 - K_{22}(\hat{y}_2 - y_2) - K_{21}(\hat{x}_1^\sigma - y_1^\sigma),\\
&\hat{y}_1 = \hat{x}_1, \quad \hat{y}_2 = \hat{x}_2, \quad y_1 = x + m_1, \quad y_2 = x + m_2,\\
&\hat{x}_1^\sigma = \hat{x}_1 + \sigma_{11}, \quad y_1^\sigma = y_1 + \sigma_{12},\\
&\bar{x}_1 = \hat{x}_1, \quad \bar{x}_2 = \frac{1}{2}(\hat{x}_1 + \hat{x}_2),
\end{aligned}
\tag{6.1}
$$

where, for each $i \in \{1, 2\}$, $\hat{x}_i$ is a state associated to agent i, $\hat{y}_i$ is the output of agent i, $\hat{x}_1^\sigma$ is the corrupted version of $\hat{x}_1$ due to communication noise that is received at agent 2, m_i is the measurement noise when agent i takes measurements of the plant's state x, and σ_{11}, σ_{12} are the communication noises that affect $\hat{x}_1$ and

[1] In (6.1), the terms $a\hat{x}_i - K_{ii}(\hat{y}_i - y_i)$ follow from the definitions of injection terms for Luenberger observers. The term $-K_{21}(\hat{x}_1^\sigma - y_1^\sigma)$ is an innovative injection term that utilizes information of agent 1 and dynamically couples the first and second equation in (6.1).

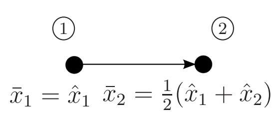

Figure 6.1: Graph connectivity of two agents, self link is not shown.

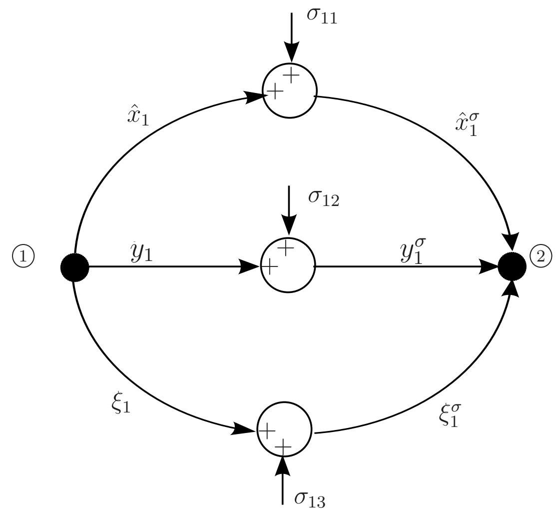

Figure 6.2: Information over the network under the effect of communication noise.

y_1, respectively, as shown in Figure 6.2. Variables $\bar{x}_1, \bar{x}_2$ provide local estimates at agent 1 and 2, respectively. The gains K_{11}, K_{21}, K_{22} are to be determined. Note that m_i's are assumed to be independent. As agent 1 sends information of $\hat{x}_1, y_1$ to agent 2, the information is also influenced by communication noise, namely, agent 2 receives the corrupted version of $\hat{x}_1$ and y_1, given by $\hat{x}_1^\sigma = \hat{x}_1 + \sigma_{11}$ and $y_1^\sigma = y_1 + \sigma_{12}$, respectively.

By defining $e_i = \hat{x}_i - x$, $\tilde{e}_i = \bar{x}_i - x$, for each $i \in \{1, 2\}$, $m = (m_1, m_2)$, $\tilde{e} = (\tilde{e}_1, \tilde{e}_2)$ and $e = (e_1, e_2)$, we can rewrite system (6.1) in the form

$$\begin{aligned} \dot{e} &= A_e e + B_1 m + B_2 \begin{bmatrix} \sigma_{11} \\ \sigma_{12} \end{bmatrix}, \\ \tilde{e} &= C_e e, \end{aligned} \tag{6.2}$$

where

$$A_e = \begin{bmatrix} a - K_{11} & 0 \\ -K_{21} & a - K_{22} \end{bmatrix}, \quad C_e = \begin{bmatrix} 1 & 0 \\ 1/2 & 1/2 \end{bmatrix},$$

$$B_1 = \begin{bmatrix} K_{11} & 0 \\ K_{21} & K_{22} \end{bmatrix}, \quad B_2 = \begin{bmatrix} 0 & 0 \\ -K_{21} & K_{21} \end{bmatrix}.$$

The quantity $\frac{1}{2}(\hat{x}_1 + \hat{x}_2)$ provides a global estimate of x, namely, the average of the estimate at each agent. However, not every agent in the network can compute this quantity. In the particular example considered, agent 1 is not capable of computing it since it does not receive $\hat{x}_2$.

In this chapter, a decentralized consensus algorithm is proposed to guarantee a pre-specified rate of convergence constraint as well as robustness to measurement and communication noise. For the particular distributed state observer leading to (6.2), our consensus algorithm is given by

$$\dot{\xi}_1 = \dot{\hat{x}}_1 - \alpha_1(\xi_1 - \hat{x}_1), \tag{6.3a}$$

$$\dot{\xi}_2 = \dot{\hat{x}}_2 - \alpha_2(\xi_2 - \hat{x}_2) - \omega_{21}(\xi_2 - \xi_1^\sigma) - \theta_{21}(\hat{x}_2 - \hat{x}_1^\sigma), \tag{6.3b}$$

$$\xi_1^\sigma = \xi_1 + \sigma_{13}, \tag{6.3c}$$

where ξ_1 and ξ_2 are consensus variables attached to agent 1 and agent 2, respectively, and $\alpha_1, \alpha_2, \omega_{21}, \theta_{21}$ are parameters to be designed. The transmission of information ξ_1 is also corrupted by communication noise which is denoted by σ_{13}, i.e., the signal ξ_1^σ shown in Figure 6.2. By defining $\delta_i = \xi_i - \frac{1}{2}(\hat{x}_1 + \hat{x}_2)$ for each

$i \in \{1,2\}$, we can rewrite (6.3) as

$$\begin{aligned}\dot{\delta}_1 &= -\alpha_1\delta_1 + \frac{1}{2}\alpha_1(e_1 - e_2) + \frac{1}{2}(\dot{e}_1 - \dot{e}_2),\\ \dot{\delta}_2 &= -(\alpha_2 + \omega_{21})\delta_2 + \omega_{21}\delta_1 + \left(\frac{1}{2}\alpha_2 - \theta_{21}\right)(e_2 - e_1)\\ &\quad + \frac{1}{2}(\dot{e}_2 - \dot{e}_1) + \omega_{21}\sigma_{13} + \theta_{21}\sigma_{11}.\end{aligned} \tag{6.4}$$

Let $\delta = (\delta_1, \delta_2)$ and $\sigma = (\sigma_{11}, \sigma_{12}, \sigma_{13})$. To see the effect of noises m and σ, assume m and σ are constant, i.e., $m_1 \equiv m_2 \equiv m^\star$ and $\sigma_{11} = \sigma_{12} = \sigma_{13} \equiv \sigma^\star$. Then, the steady state of (6.2) and (6.4) is given by

$$\delta^\star = \begin{bmatrix} 0 \\ \dfrac{\omega_{21} + \theta_{21}}{\alpha_2 + \omega_{21}} \end{bmatrix} \sigma^\star + \begin{bmatrix} \bar{c}_1 \\ \bar{c}_2 \end{bmatrix} m^\star, \tag{6.5}$$

$$e^\star = -\begin{bmatrix} \dfrac{K_{11}}{a - K_{11}} \\ \dfrac{K_{21}a + K_{22}(a - K_{11})}{(a - K_{11})(a - K_{22})} \end{bmatrix} m^\star, \tag{6.6}$$

where

$$\bar{c}_1 = \frac{a(K_{21} + K_{22} - K_{11})}{2(K_{11} - a)(K_{22} - a)}, \tag{6.7}$$

$$\bar{c}_2 = \frac{a(\alpha_2 - \omega_{21} - 2\theta_{21})(K_{11} - K_{21} - K_{22})}{2(\alpha_2 + \omega_{21})(K_{11} - a)(K_{22} - a)}. \tag{6.8}$$

Suppose K_{11} and K_{22} are fixed in order to satisfy a rate of convergence constraint[2], i.e., $K_{11} = K_{22}$. Then, by choosing $K_{21} = \frac{(K_{11}-a)K_{22}}{a}$, we have $e_2^\star = 0$. To make the steady state error $(\delta^\star, e^\star)$ corresponding to measurement noise $m^\star$ zero, we

[2]Note that since A_e is a lower triangular matrix, the eigenvalues of A_e are given by $a - K_{11}$ and $a - K_{22}$.

pick

$$\alpha_2 - \omega_{21} - 2\theta_{21} = 0. \tag{6.9}$$

A simulation of this scenario is shown in Figure 6.3(a), where the effect of measurement noise is shown. On the other hand, to make the steady-state error corresponding to communication noise $\sigma^\star$ zero, we pick

$$\omega_{21} + \theta_{21} = 0. \tag{6.10}$$

A simulation of this scenario is shown in Figure 6.3(b), where the effect of measurement noise is depicted. However, note that if equalities (6.9) and (6.10) are simultaneously satisfied, then $\alpha_2 = -\omega_{21}$. In this case, the system in (6.4) has an eigenvalue at zero, which does not lead to an exponentially convergent (to zero) state δ. In fact, this dilemma is generic and similar to the typical tradeoff between convergence rate and robustness to measurement noise for an observer, see, e.g., [22, 21, 24]. The idea behind the proposed consensus algorithm illustrated in the example above generalizes to the case where N agents can measure the plant's output over a graph. The purpose of the next two sections is making this precise.

6.2 A dynamic consensus algorithm for distributed state observers

6.2.1 Problem statement

Our goal is to design a consensus algorithm such that each agent achieves consensus on the average of all local estimates provided by a distributed state

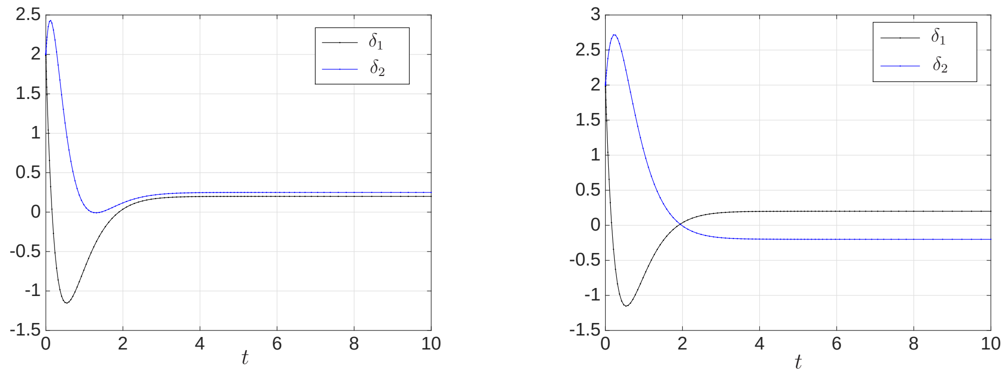

(a) Parameters are such that $\alpha_2 - \omega_{21} - 2\theta_{21} = 0$, in particular, $\alpha_1 = \alpha_2 = 2.5$, $\omega_{21} = 1.5$, $\theta_{21} = 0.5$.

(b) Parameters are such that $\omega_{21}+\theta_{21} = 0$, in particular, $\alpha_1 = \alpha_2 = 2.5$, $\omega_{21} = 1.5$, $\theta_{21} = -1.5$.

Figure 6.3: Comparison of steady state error according to different design strategies. Parameters are $a = -0.5$, $K_{11} = K_{22} = 2$, $K_{21} = \frac{(K_{11}-a)K_{22}}{a}$, $m_1 = m_2 = \sigma_{11} = \sigma_{12} = \sigma_{13} = 0.5$.

observer under communication and measurement noise. For this purpose, we adapt the distributed state observer from [88], for the plant in (1.1) and over a network of N agents connected via a digraph Γ, in which each agent has a local state observer that uses measurements of the plant and of its neighbors. After adding communication noise, which is particular to the problem studied in this paper, for each $i \in \mathcal{V}$, the agent i runs a local state observer given by

$$\dot{\hat{x}}_i = A\hat{x}_i - K_{ii}(\hat{y}_i - y_i) - \sum_{k\in\mathcal{V}} g_{ik}K_{ik}(H_k\hat{x}_k^\sigma - y_k^\sigma), \tag{6.11a}$$

$$\hat{x}_i^\sigma = \hat{x}_i + \sigma_{i1}, \quad y_i^\sigma = y_i + \sigma_{i2}, \tag{6.11b}$$

$$\bar{x}_i = \frac{1}{1+d^{in}(i)}\sum_{k=1}^{N} g_{ik}\hat{x}_k, \quad \hat{y}_i = H_i\hat{x}_i \tag{6.11c}$$

where $\hat{x}_i$ denotes the state variable of the observer, $\bar{x}_i$ denotes the local estimate of x at agent i, K_{ik}'s are estimation gains to be designed, y_i denotes the measurement of y in (1.1) taken by the i-th agent with measurement noise m_i, that is,

$$y_i = H_i x + m_i \in \mathbb{R}^{p_i},$$

where p_i is the dimension of the measurement taken at the i-th agent. The information that the i-th agent obtains from its neighbors is given by $\hat{x}_k^\sigma$ and y_k^σ for each $k \in \mathcal{N}(i)$, which correspond to the values of $\hat{x}_k$ and y_k corrupted by communication noise σ_{i1} and σ_{i2}, respectively. The collection of local state observers in (6.11) connected via the digraph Γ defines a *distributed state observer* [88].

While convergence of the local estimates was characterized in [88], the algorithm therein does not provide a mechanism to obtain a globally agreed quantity of the estimate of x (neither for the nominal case nor when noise in the measurements are present). Unless the graph is all-to-all connected, not every agent can compute $\frac{1}{N}\sum_{k=1}^{N}\hat{x}_k(t)$. To make the quantity $\frac{1}{N}\sum_{k=1}^{N}\hat{x}_k(t)$ accessible to each agent, a possible solution is to use a dynamic consensus algorithm: obtain information from neighbors and make an internal state of each agent approach the quantity $\frac{1}{N}\sum_{k=1}^{N}\hat{x}_k(t)$ asymptotically. Note that this quantity converges to zero when A is Hurwitz, the observers are convergent, and noise signals are zero.

6.2.2 Distributed consensus algorithm

In this paper, we propose a *distributed consensus algorithm for the local estimates* $\hat{x}_i$. Following (6.3), the algorithm is given by

$$\dot{\xi}_i = \dot{\hat{x}}_i - \alpha_i(\xi_i - \hat{x}_i) - \sum_{k \in \mathcal{V}} g_{ik}\omega_{ik}(\xi_i - \xi_k^\sigma) - \sum_{k \in \mathcal{V}} g_{ik}\theta_{ik}(\hat{x}_i - \hat{x}_k^\sigma), \tag{6.12a}$$

$$\xi_i^\sigma = \xi_i + \sigma_{i3}, \tag{6.12b}$$

where, for each $i \in \mathcal{V}$, $\xi_i \in \mathbb{R}^n$ is the consensus variable attached to agent i; $\alpha_i, \omega_{ik}, \theta_{ik}$ are constant gains; and ξ_i^σ is the communication noise (σ_{i3}) corrupted value of ξ_i. Note that the algorithm uses information of $\dot{\hat{x}}_i$, ξ_i as well as information received from its neighbors, i.e., ξ_k^σ, $\hat{x}_k^\sigma$ for each $k \in \mathcal{N}(i)$. In particular, ξ_k^σ is defined in (6.11), and the transmissions of ξ_i are corrupted by communication noise σ_{i3}, where $\hat{x}_i$'s are the estimates generated by agent i using the local observer in (6.11a). For each $i, k \in \mathcal{V}$, the gains $\alpha_i, \omega_{ik}, \theta_{ik} \in \mathbb{R}$ are design parameters.

To analyze the interconnection between (6.11) and (6.12), for each $i \in \mathcal{V}$, define $e_i := \hat{x}_i - x$ and the associated vector $e := (e_1, \dots, e_N)$, and $\tilde{e}_i := \bar{x}_i - x$ and the associated vector $\tilde{e} := (\tilde{e}_1, \dots, \tilde{e}_N)$. Furthermore, define $\delta_i = \xi_i - \frac{1}{N}\sum_{k=1}^{N} \hat{x}_k$ and $\delta = (\delta_1, \cdots, \delta_N)$, the measurement noise vector $m := (m_1, \dots, m_N)$, and the communication noise vector $\sigma = (\sigma_{11}, \dots, \sigma_{N1}, \sigma_{12}, \dots, \sigma_{N2}, \sigma_{13}, \dots, \sigma_{N3})$. Then, it follows that

$$\dot{e}_i = Ae_i - K_{ii}H_ie_i - \sum_{k\in\mathcal{V}} g_{ik}K_{ik}H_ke_k + K_{ii}m_i + \sum_{k\in\mathcal{V}} g_{ik}K_{ik}m_k - \sum_{k\in\mathcal{V}} g_{ik}K_{ik}H_k\sigma_{k1} \tag{6.13a}$$

$$+ \sum_{k\in\mathcal{V}} g_{ik}K_{ik}\sigma_{k2},$$

$$\dot{\delta}_i = -\alpha_i\delta_i - \sum_{k\in\mathcal{V}} g_{ik}w_{ik}(\delta_i - \delta_k) + \frac{1}{N}\sum_{k\in\mathcal{V}}(\dot{e}_i - \dot{e}_k + \alpha_i(e_i - e_k)) - \sum_{k\in\mathcal{V}} g_{ik}\theta_{ik}(e_i - e_k) \tag{6.13b}$$

$$+ \sum_{k\in\mathcal{V}} g_{ik}(\omega_{ik}\sigma_{k3} + \theta_{ik}\sigma_{k1}),$$

which can be rewritten in the compact form

$$\dot{e} = A_e e + B_1 m + B_2 \sigma, \tag{6.14a}$$

$$\dot{\delta} = A_\delta \delta + A_c e + B_3 m + B_4 \sigma, \tag{6.14b}$$

$$\tilde{e} = C_e e, \tag{6.14c}$$

where

$$\begin{aligned}
&A_e = I_N \otimes A - (\mathcal{K} * \overline{\mathcal{G}}) H_g, \quad C_e = (\bar{D}_{in}^{-1} * \overline{\mathcal{G}}) \otimes I_n, \\
&B_1 = \mathcal{K} * \overline{\mathcal{G}}, \quad \overline{\mathcal{G}} = \mathcal{G} + I_N, \quad \bar{\Pi}_N = \Pi_N \otimes I_n, \\
&B_2 = \begin{bmatrix} -(\mathcal{K} * \mathcal{G}) H_g & \mathcal{K} * \mathcal{G} & 0_{nN \times nN} \end{bmatrix}, \\
&A_\delta = -(\mathrm{diag}(\alpha) + \mathcal{L}_\omega) \otimes I_n, \quad \bar{D}_{in} = D_{in} + I_N, \\
&A_c = \bar{\Pi}_N (A_e + \mathrm{diag}(\alpha) \otimes I_n) - \mathcal{L}_\theta \otimes I_n, \\
&B_3 = \bar{\Pi}_N B_1, \quad \mathcal{G}_\theta = \mathcal{G} * \Theta, \quad \mathcal{G}_\omega = \mathcal{G} * \Omega, \\
&B_4 = \bar{\Pi}_N B_2 + \begin{bmatrix} \mathcal{G}_\theta \otimes I_n & 0_{nN \times nN} & \mathcal{G}_\omega \otimes I_n \end{bmatrix}, \\
&\mathcal{L}_\omega = \mathrm{diag}(\mathcal{G}_\omega 1_N) - \mathcal{G}_\omega, \quad \mathcal{L}_\theta = \mathrm{diag}(\mathcal{G}_\theta 1_N) - \mathcal{G}_\theta, \\
&H_g = \mathrm{diag}(H_1, H_2, \cdots, H_N),
\end{aligned}$$

and gains

$$\mathcal{K} = \{K_{ik}\}_{N \times N}, \quad \Omega = \{\omega_{ik}\}_{N \times N}, \quad \Theta = \{\theta_{ik}\}_{N \times N},$$

where $\mathcal{G}$ is the adjacency matrix, D_{in} is the in-degree matrix, the Khatri-Rao product $\mathcal{K} * \overline{\mathcal{G}}$ is such that $\mathcal{K}$ is treated as $N \times N$ block matrices with K_{ik}'s as blocks. By defining

$$\mathcal{A} := \begin{bmatrix} A_e & 0 \\ A_c & A_\delta \end{bmatrix}, \quad \mathcal{B}_1 := \begin{bmatrix} B_1 \\ B_3 \end{bmatrix}, \quad \mathcal{B}_2 := \begin{bmatrix} B_2 \\ B_4 \end{bmatrix}, \tag{6.15}$$

and the total error $\bar{e} = (e, \delta)$, the interconnection in (6.14) can be written as

$$\dot{\bar{e}} = \mathcal{A}\bar{e} + \mathcal{B}_1 m + \mathcal{B}_2 \sigma. \tag{6.16}$$

Remark 6.2.1 *$I_N \otimes A$ defines a block diagonal matrix with matrix A in each of the N blocks (of dimension $n \times n$). The matrix $\mathcal{K} * \overline{\mathcal{G}}$ defines the gain matrix for the graph, while $C_e = (\bar{D}^{-1} * \overline{\mathcal{G}}) \otimes I_n$ generates the estimation matrix for each agent by averaging the local estimates obtained from its neighbors. When the estimation algorithm in* (6.13) *is properly designed, A_e is Hurwitz and e converges to zero asymptotically. It further implies that, due to the property of A_δ, the steady state of δ in* (6.14b) *depends on the supremum of "inputs" e, σ and m.*

6.3 Design using optimization formulation

6.3.1 Decoupled design

The design of the closed-loop system in (6.16) can be decomposed into two steps. The distributed state observer in (6.11) can be designed first, while the distributed consensus algorithm in (6.12) is designed after. In this section, we discuss several particular optimization problems for such decoupled design procedure.

For the distributed consensus in (6.12), the design specifications of interest are the rate of convergence and the H_∞ gain from communication noise σ and from measurement noise m to the consensus error δ. In particular, to guarantee a particular rate of convergence of system (6.14), the eigenvalues of the error system (6.14) will be assigned to the left of the vertical line at $-h$ in the s-plane, where $h > 0$ is the convergence rate specification. Following [77], the eigenvalues of the matrix A_δ are located in the region $\mathcal{R} := \{s \in \mathbb{C} : Re(s) < -h\}$ if and only if there exists a matrix $P_S = P_S^\top > 0$ such that

$$A_\delta^\top P_S + P_S A_\delta + 2hP_S < 0. \tag{6.17}$$

Recall from the motivational example in Section 6.1 that there is a tradeoff when choosing parameters to reduce the effect of measurement noise and communication noise simultaneously. To determine the performance of our distributed consensus algorithm (6.12), we introduce the criterion of global H_∞ gain from noise vector (m, σ) to consensus error vector δ. Recall that finding the H_∞ gain of a transfer function $T(s) = \mathcal{C}(sI - \mathcal{A})\mathcal{B} + \mathcal{D}$ is equivalent to the feasibility of a certain matrix inequality.

Then, we can establish the following optimization problem for the design of the distributed consensus algorithm according to a pre-specified global H_∞ gain from (m, σ) to δ.

Proposition 6.3.1 *Given a plant as in* (1.1) *and a digraph* Γ*, the global* H_∞ *gain of the transfer function from* (m, σ) *to* δ *in* (6.16) *is less than or equal to* γ *if and only if the following inequality is feasible for some* $P_H = P_H^\top > 0$*:*

$$\begin{bmatrix} \mathrm{He}(\mathcal{A}, P_H) & P_H\mathcal{B} & \mathcal{C}^\top \\ \mathcal{B}^\top P_H & -\gamma I & 0 \\ \mathcal{C} & 0 & -\gamma I \end{bmatrix} < 0, \tag{6.18}$$

where $\mathcal{B} := [\mathcal{B}_1\ \mathcal{B}_2]$, *and* $\mathcal{C} := [0\ \ 1] \otimes I_{nN}$.

Proof The proof follows using Lemma 3.2.2 where the transfer function of interest is $\mathcal{C}(sI - \mathcal{A})^{-1}\mathcal{B}$. ■

Remark 6.3.2 *The global H_∞ gain from (m, σ) to δ determines the overall effect of the total noise (m, σ) on the distributed consensus of local estimates provided by* (6.12)*. To determine the effect of the noise (m, σ) on the local estimate δ_i, the H_∞ gain from (m, σ) to δ_i can also be characterized in* (6.18) *by replacing $\mathcal{C}$ with $\mathcal{C}_i$, where $\mathcal{C}_i$ is the sub-matrix of $\mathcal{C}$ from the $(in-n+N+1)$-th row to the $(in+N)$-th row.*

Then, by combining the rate of convergence constraint in (6.17) and the H_∞ constraint in (6.18), we can perform the synthesis of the distributed consensus algorithm of global estimates in (6.12) using the following result.

Theorem 6.3.3 *For the plant in* (1.1) *with distributed state observer* (6.11) *and distributed consensus algorithm* (6.12)*, given a digraph Γ, and a gain $\mathcal{K}$ such that $\mathcal{A}$ is Hurwitz, the rate of convergence of* (6.14) *is larger than or equal to $h > 0$ and the H_∞ gain from (m, σ) to δ in* (6.14) *is minimized if and only if there exist matrices α, Θ, Ω, P_S, and P_H such that the following optimization problem is feasible:*

$$\min \gamma \tag{6.19a}$$

$$s.t.\ \mathrm{He}(A_\delta, P_S) + 2hP_S < 0, \tag{6.19b}$$

$$\begin{bmatrix} \mathrm{He}(\mathcal{A}, P_H) & P_H\mathcal{B} & \mathcal{C}^\top \\ \mathcal{B}^\top P_H & -\gamma I & 0 \\ \mathcal{C} & 0 & -\gamma I \end{bmatrix} < 0, \tag{6.19c}$$

$$P_S = P_S^\top > 0,\ P_H = P_H^\top > 0. \tag{6.19d}$$

Proof The proof follows using (6.17) and Proposition 6.3.1. ■

Remark 6.3.4 *The problem in* (6.19) *can be solved offline by using, e.g., [87], and the resulting observers along with the consensus algorithm are decentralized. Note that the two constraints in* (6.19b) *and* (6.19c) *are nonlinear due to the fact that* Ω *in* A_δ *is multiplied by* P_S *and* P_H *in the operation of* $\mathrm{He}(A_\delta, P_S)$ *and* $\mathrm{He}(\mathcal{A}, P_H)$*, respectively. Moreover, if the local* H_∞ *gain from noise* (m, σ) *to* δ_i *at agent* i *is of interest, then, the matrix* $\mathcal{C}$ *in* (6.19c) *can be replaced by* $\mathcal{C}_i$*. When the effect of communication noise (measurement noise, respectively) is of major concern, the matrix* $\mathcal{B}$ *in* (6.19) *can be replaced by* $\mathcal{B}_2$ *(*$\mathcal{B}_1$*, respectively).*

Next, we provide an example to illustrate the results above.

Example 6.3.5 *Consider the plant in* (1.5) *with* $a = -0.5$*, and the motivational example with two agents connected as in Figure 6.1. Suppose that the distributed state observers in* (6.2) *is designed to satisfy a rate of convergence equal to* 2.5 *with parameters* $K_{11} = K_{22} = 2$*,* $K_{12} = 0$ *and* $K_{21} = -4.7$*. Then, we can design the distributed consensus algorithm of local estimates by solving* (6.19)*. The resulting gains are*

$$\alpha = (7.14, 14.24),\ \Omega = \begin{bmatrix} 0 & 0 \\ 0.52 & 0 \end{bmatrix},\ \Theta = \begin{bmatrix} 0 & 0 \\ -3.6 & 0 \end{bmatrix}.$$

The resulting H_∞ *gain from* (m, σ) *to* δ *is approximately* 3.17*. If instead, these two agents are all-to-all connected, then, by solving* (6.19)*, the resulting gains are*

$$\alpha = (3.5, 2.5),\ \Omega = \begin{bmatrix} 0 & -0.88 \\ 0.28 & 0 \end{bmatrix},\ \Theta = \begin{bmatrix} 0 & 0.79 \\ 0.06 & 0 \end{bmatrix},$$

and the resulting H_∞ gain from (m, σ) to δ is approximately 1.65. $\triangle$

6.3.2 Joint observer-consensus design

As shown in Example 6.3.5, when K_{11}, K_{21}, K_{22} for the distributed state observer are fixed, the effect of measurement and communication noise on the estimation error e are fixed. In such a case, we can only tune the performance of the distributed consensus algorithm. On the other hand, we can simultaneously design the consensus algorithm in (6.12) and the estimation algorithm in (6.11). In particular, for a fixed graph Γ, we can design $\mathcal{K}$, α, Θ, Ω simultaneously.

For such a design, note that $\mathcal{A}$ is a lower block triangular matrix, so its eigenvalues consist of the eigenvalues of A_e and of A_δ. Imposing a rate of convergence on $\mathcal{A}$ is equivalent to imposing it on both A_δ and A_e. In other words, the eigenvalues of a matrix $\mathcal{A}$ are located in the region $\mathcal{D} := \{s \in \mathbb{C} : Re(s) < -h\}$ if and only if there exist matrices $P_1 = P_1^\top > 0$ and $P_2 = P_2^\top > 0$ such that

$$\mathrm{He}(A_\delta, P_1) + 2hP_1 < 0, \tag{6.20a}$$

$$\mathrm{He}(A_e, P_2) + 2hP_2 < 0. \tag{6.20b}$$

Then, we can establish the following result for a joint observer-consensus design.

Theorem 6.3.6 *For the plant in* (1.1) *with the distributed state observer* (6.11) *and the distributed consensus algorithm* (6.12)*, given a digraph* Γ*, the rate of convergence of* (6.16) *is larger than or equal to* h *and the* H_∞ *gain from* σ *to consensus error* δ *in* (6.14) *is minimized if and only if there exist matrices* $\mathcal{K}$*,* α*,*

Θ, Ω, P_1, P_2 and P_H such that the following optimization problem is feasible:

$$\min \gamma$$

$$s.t.\ \mathrm{He}(A_\delta, P_1) + 2hP_1 < 0, \tag{6.21a}$$

$$\mathrm{He}(A_e, P_2) + 2hP_2 < 0, \tag{6.21b}$$

$$\begin{bmatrix} \mathrm{He}(\mathcal{A}, P_H) & P_H\mathcal{B}_2 & ([0\ 1] \otimes I_{nN})^\top \\ \mathcal{B}_2^\top P_H & -\gamma I & 0 \\ [0\ 1] \otimes I_{nN} & 0 & -\gamma I \end{bmatrix} < 0, \tag{6.21c}$$

$$P_1 = P_1^\top > 0,\ P_2 = P_2^\top > 0,\ P_H = P_H^\top > 0. \tag{6.21d}$$

Proof The proof follows using (6.20) and Lemma 3.2.2 where the transfer function of interest for (6.21c) is $(I_{nN} \otimes [0\ 1])(sI - \mathcal{A})^{-1}\mathcal{B}_2$. ■

Example 6.3.7 *Consider Example 6.3.5 with $a = -0.5$ and a rate of convergence constraint equal to 2.5. Now, we let $\mathcal{K}$ be the gain to be chosen. By solving (6.21), we obtain*

$$\alpha = (2.50, 4.22), \quad \Omega = \begin{bmatrix} 0 & 0 \\ 1.35 & 0 \end{bmatrix},$$

$$\Theta = \begin{bmatrix} 0 & 0 \\ 0.35 & 0 \end{bmatrix}, \quad \mathcal{K} = \begin{bmatrix} 2 & 0 \\ 0.55 & 2 \end{bmatrix}.$$

The resulting H_∞ gain from (m, σ) to δ is approximately 0.82, which is a significant improvement over a gain equal to 3.17 obtained in Example 6.3.5. On the other hand, consider the same plant with two agents that are all-to-all connected, *then, by solving* (6.21)*, the resulting gains are*

$$\alpha = (10.98, 10.98), \quad \Omega = \begin{bmatrix} 0 & 1.32 \\ 1.32 & 0 \end{bmatrix},$$
$$\Theta = \begin{bmatrix} 0 & 3.31 \\ 3.31 & 0 \end{bmatrix}, \quad \mathcal{K} = \begin{bmatrix} 2.95 & 0.95 \\ 0.95 & 2.95 \end{bmatrix},$$

the resulting H_∞ gain from (m, σ) to δ is approximately 0.32*, and the resulting H_∞ gain from m to $\tilde{e}$ is approximately* 0.88*.* △

Recall from the motivational example that when measurement noise is assumed to be zero, the optimal strategy to reduce the effect of communication noise is to not communicate at all. However, such a strategy also eliminates the possibility of reducing the effect of measurement noise, which is a key capability of distributed state observers. The following result provides one way to formulate a design with a pre-specified H_∞ gain from m to $\tilde{e}$.

Theorem 6.3.8 *For the plant in* (1.1) *with estimation system in* (6.11) *and consensus algorithm in* (6.12)*, given a digraph Γ, the rate of convergence of* (6.16) *is larger than or equal to h, the H_∞ gain from m to estimation error $\tilde{e}$ in* (6.14) *is no larger than $\gamma^\star$ and the H_∞ gain from σ to consensus error δ in* (6.14) *is minimized if and only if there exist matrices $\mathcal{K}$, α, Θ, Ω, P_1, P_2, P_H, and P_e such* *that the following optimization problem is feasible:*

$$
\begin{aligned}
&\min \gamma \\
s.t.\ &\mathrm{He}(A_\delta, P_1) + 2hP_1 < 0, && \text{(6.22a)}\\
&\mathrm{He}(A_e, P_2) + 2hP_2 < 0, && \text{(6.22b)}\\
&\begin{bmatrix} \mathrm{He}(\mathcal{A}, P_H) & P_H\mathcal{B}_2 & ([0\ 1]\otimes I_{nN})^\top \\ \mathcal{B}_2^\top P_H & -\gamma I & 0 \\ [0\ 1]\otimes I_{nN} & 0 & -\gamma I \end{bmatrix} < 0, && \text{(6.22c)}\\
&\begin{bmatrix} \mathrm{He}(A_e, P_e) & P_eB_1 & C_e^\top \\ B_1^\top P_e & -\gamma^\star I & 0 \\ C_e & 0 & -\gamma^\star I \end{bmatrix} < 0, && \text{(6.22d)}\\
&P_1 = P_1^\top > 0,\ P_2 = P_2^\top > 0, && \text{(6.22e)}\\
&P_H = P_H^\top > 0,\ P_e = P_e^\top > 0. && \text{(6.22f)}
\end{aligned}
$$

Proof The proof follows using (6.20) and Lemma 3.2.2, where (6.22c) corresponds to transfer function $(I_{nN}\otimes[0\ 1])(sI-\mathcal{A})^{-1}\mathcal{B}_2$ and (6.22d) corresponds to transfer function $(C_e\otimes[1\ 0])(sI-\mathcal{A})^{-1}B_1$. ■

Remark 6.3.9 *Note that the constraints defined in* (6.22a) *and* (6.22c) *are non-linear due to the fact that* Ω *in* A_δ *is multiplied with* P_1, P_H *in the operation of* $\mathrm{He}(A_\delta, P_1)$ *and* $\mathrm{He}(\mathcal{A}, P_H)$*, respectively. The constraints defined in* (6.22b) *and* (6.22d) *are also nonlinear and not jointly convex due to the products* $P_2\mathcal{K}$ *and* $P_e\mathcal{K}$*. With the structure of the distributed state observer in* (6.11)*, the* H_∞ *gain* $\gamma^\star$ *from* m *to estimation error* $\tilde{e}$ *can be chosen much smaller than that of a Luenberger observer as in [88].*

Example 6.3.10 *Consider the plant in* (1.5) *with* $a = -0.5$*, and a distributed state observer with two agents connected via an all-to-all connectivity graph. The specifications of interest are convergence rate greater than or equal to* 2.5 *and* H_∞ *gain from* m *to* $\tilde{e}$ *no larger than* 0.6 *(which is smaller than* 0.88 *obtained in Example 6.3.7). By solving* (6.22)*, we obtain*

$$\alpha = (13.75, 93.80), \quad \Omega = \begin{bmatrix} 0 & 8.52 \\ 0.34 & 0 \end{bmatrix},$$

$$\Theta = \begin{bmatrix} 0 & 1.55 \\ 7.96 & 0 \end{bmatrix}, \quad \mathcal{K} = \begin{bmatrix} 1.11 & -5.77 \\ 0.14 & 2.90 \end{bmatrix}.$$

The resulting H_∞ *gain from* σ *to* δ *is approximately* 1.52*, and the resulting* H_∞ *gain from* (m, σ) *to* δ *is approximately* 2.34*.* $\triangle$

6.4 Summary

The proposed distributed consensus algorithm for distributed state observers has the capability of attaining fast rate of convergence without necessarily jeopardizing robustness to measurement and communication noise in the H_∞ sense. An optimization-based design method is proposed to separately and jointly determine the parameters of distributed state observer and the proposed distributed consensus algorithm. Furthermore, the resulting distributed consensus algorithm is exponentially stable and robust to measurement and communication noise.

Chapter 7

Distributed Estimation with Intermittent Information Transmission

In this chapter, the problem of robustly estimating the state x of a continuous-time plant from intermittent measurements of functions of its output over a network of N agents is considered. The nominal model governing the state x is given by a linear time-invariant system, which, under perturbations, assumes the form

$$\dot{x} = Ax + \delta(x, t) \tag{7.1}$$

where δ is an unknown function and $t \geq 0$ denotes ordinary time. The i-th agent in the network receives a measurement y_i at time instances t_s^i, $s \in \{1, 2, \ldots\}$, defining the incoming information events for that agent. The nominal model for y_i is a linear function of the state, while the perturbed case takes the form

$$y_i = H_i x + \varphi_i(x, t) \tag{7.2}$$

where φ_i is an unknown function. The event times t_s^i are independently defined for each agent; the only restriction imposed on communication times is that they must satisfy

$$t_{s+1}^i - t_s^i \in [T_1^i, T_2^i] \qquad \forall s \in \{1, 2, \ldots\} \tag{7.3}$$

where T_1^i and T_2^i are nominal parameters that define the lower and upper bounds, respectively, of the time allowed to elapse between consecutive communication events and are such that $T_2^i \geq T_1^i > 0$. Hence, the event times t_s^i can potentially be determined by a random variable taking values in the interval $[T_1^i, T_2^i]$. The parameters T_1^i and T_2^i are assumed to be known but are not necessarily the same for each agent. Furthermore, these parameters may be further perturbed.

7.1 Observer configuration

We propose a distributed hybrid observer that is capable of asymptotically reconstructing the state of the plant x locally, at each agent, with stability and by only exchanging information from the plant and its neighbors at communication events as introduced above. In the nominal case, the algorithm guarantees the estimates of x to globally converge with an exponential rate. In the presence of unknown perturbations, the algorithm guarantees that such property is preserved, semiglobally and practically, when the perturbations are small enough, while when bounds on certain perturbations are known, the said global exponential stability is fully recovered. Our distributed hybrid observer assures such properties by running a decentralized algorithm that, at the i-th agent, generates an estimate of the state x, which is denoted $\hat{x}_i$, and an information fusion quantity, which is denoted η_i. These state variables are continuously updated by a differential equation, which takes the general form

$$\dot{\hat{x}}_i = A\hat{x}_i + \eta_i \tag{7.4}$$

$$\dot{\eta}_i = f_{oi}(\hat{x}_i, \eta_i) \tag{7.5}$$

when no information is received, while when information is received, the states $\hat{x}_i$ and η_i are updated according to

$$\hat{x}_i^+ = \hat{x}_i \tag{7.6}$$

$$\eta_i^+ = \sum_{k \in \mathcal{V}} g_{ik} G_{oi}^k(\hat{x}_i, \hat{x}_k, y_i, y_k) \tag{7.7}$$

where $\mathcal{V} := \{1, 2, \ldots, N\}$ defines the set of all agents; g_{ik} defines a connectivity graph, namely, $g_{ik} = 1$ if the k-th agent can share information to agent i and $g_{ik} = 0$ otherwise; the map f_{oi} defines the continuous evolution of the information fusion state and the map G_{oi}^k defines the impulsive update law when new information is collected from the plant and the k-th neighbor.[1] The information fusion state η_i is injected into the continuous dynamics of the local estimate $\hat{x}_i$ and, at communication events, injects new information impulsively – the right-hand side of (7.7) is the "innovation term" of the proposed observer. The continuous and discrete dynamics in (7.4) and (7.7), respectively, along with a proper autonomous model triggering the communication events, define a hybrid observer at each agent as well as hybrid dynamical system modeling the entire networked system.

The nondeterministic time-invariant hybrid system model of the network in (7.88b) conveniently captures the event times in [61, 89, 68], which lead to a time-varying system and make analysis more difficult. Similar hybrid models were used in [69]. When $f_{oi} = 0$ for all $i \in \mathcal{V}$, the hybrid information fusion strategy

[1]The actual forms of f_{oi} and G_{oi}^k are discussed in next two sections.

in (7.89)-(7.90) falls into the category of zero-order sample-and-hold control; see, e.g., [90] and [91]. Note that the work in [90] and [91] pertain to single-agent systems and that robustness properties of the observer therein are not studied.

7.2 Synchronous communication events

In this section, we look at a simpler case where all timers τ_i's are synchronous. Moreover, $T_1^i = T_1$ and $T_2^i = T_2$ for all $i \in \mathcal{V}$.

7.2.1 Hybrid modeling

When all timers τ_i's are synchronous, i.e., each agents are receiving information in a global fashion, the communication events among all agents are triggered by a common timer τ_s whose dynamics are given by

$$\dot{\tau}_s = -1 \qquad \tau_s \in [0, T_2], \tag{7.8a}$$

$$\tau_s^+ \in [T_1, T_2] \qquad \tau_s = 0. \tag{7.8b}$$

For each $i \in \mathcal{V}$, denote the local estimation error $e_i = \hat{x}_i - x$, it follows that the continuous dynamics of e_i and η_i are given by

$$\dot{e}_i = Ae_i + \eta_i, \tag{7.9}$$

$$\dot{\eta}_i = h_i \eta_i, \tag{7.10}$$

for each $\tau_s \in [0, T_2]$, and, when $\tau_s = 0$, the discrete dynamics are

$$e_i^+ = e_i, \tag{7.11}$$

$$\eta_i^+ = K_{ii} H_i e_i + \sum_{k \in \mathcal{V}} g_{ik} K_{ik} H_k e_k + \gamma \sum_{k \in \mathcal{V}} g_{ik}(e_i - e_k). \tag{7.12}$$

$e = (e_1, e_2, \cdots, e_N)$ and $\eta = (\eta_1, \eta_2, \cdots, \eta_N)$, it follows that

$$\dot{e} = (I_N \otimes A)e + \eta,$$

$$\dot{\eta} = H_\eta \eta,$$

for each $\tau_s \in [0, T_2]$, while when $\tau_s = 0$,

$$e^+ = e, \tag{7.13}$$

$$\eta^+ = (K_g H_g * (I_N + \mathcal{G}) + \gamma \mathcal{L} \otimes I_n)e, \tag{7.14}$$

Then, in the (e, η) coordinates, the closed-loop system can be written as a hybrid system $\mathcal{H}_s = (C_s, f_s, D_s, G_s)$ with state $\chi_s = (\sigma, \tau) \in \mathcal{X}_s := \mathbb{R}^{nN} \times \mathbb{R}^{nN} \times [0, T_2]$ with $\sigma = (e, \eta)$, and data given by

$$f_s(\chi_s) := (A_f \sigma, -1) \qquad \forall \chi_s \in C_s \tag{7.15}$$

$$G_s(\chi_s) := (A_g \sigma, [T_1, T_2]) \qquad \forall \chi_s \in D_s, \tag{7.16}$$

where $C_s := \mathcal{X}_s$, $D_s := \mathbb{R}^{nN} \times \mathbb{R}^{nN} \times \{0\}$,

$$A_f := \begin{bmatrix} I_N \otimes A & I_{nN} \\ 0 & H_\eta \end{bmatrix}, \tag{7.17}$$

$$A_g := \begin{bmatrix} I_{nN} & 0 \\ K_g H_g * (I_N + \mathcal{G}) + \gamma \mathcal{L} \otimes I_n & 0 \end{bmatrix}, \tag{7.18}$$

and $H_\eta = \mathrm{diag}(h_1, h_2, \ldots, h_N) \otimes I_n$. In this case, the set of interest is

$$\mathcal{A} = \{0_{nN}\} \times \{0_{nN}\} \times [0, T_2]. \tag{7.19}$$

Remark 7.2.1 *Due to the jumps being triggered by the timer τ with dynamics (7.8) reaching zero, the hybrid time domain of any maximal solution to $\mathcal{H}_s$ satisfies the following property. For any given $\phi \in \mathcal{S}_{\mathcal{H}_s}$, $T_1 \leq t_{j+1} - t_j \leq T_2$ for all $j \geq 1$ and $0 \leq t_1 \leq T_2$, and*

$$(j-1)T_1 \leq t \leq (j+1)T_2 \qquad \forall\ j \geq 1 \tag{7.20}$$

for all $(t, j) \in \mathrm{dom}\,\phi$. $\square$

The following result provides a sufficient condition for uniform global asymptotic stability of $\mathcal{A}$.

Theorem 7.2.2 *Let $0 < T_1 \leq T_2$ be given. Suppose there exist matrices $K_g \in \mathbb{R}^{nN \times p}$ and $P \in \mathbb{R}^{2nN \times 2nN}$ such that $P = P^\top > 0$ and*

$$A_g^\top \exp(A_f^\top \nu) P \exp(A_f \nu) A_g - P < 0 \tag{7.21}$$

for all $\nu \in [T_1, T_2]$. Then, the set $\mathcal{A}$ in (7.19) is UGAS for the hybrid system $\mathcal{H}_s$.

Proof Consider the Lyapunov function candidate $V : \mathcal{X}_s \to \mathbb{R}_{\geq 0}$ given by

$$V(\chi_s) = \sigma^\top \exp(A_f^\top \tau_s) P \exp(A_f \tau_s) \sigma \tag{7.22}$$

By using the property that $|\chi_s|_\mathcal{A}^2 = |\sigma|^2$, it follows that

$$\alpha_1 |\chi_s|_\mathcal{A}^2 \leq V(\chi_s) \leq \alpha_2 |\chi_s|_\mathcal{A}^2 \tag{7.23}$$

for all $\chi_s \in C_s$, where

$$\alpha_1 = \min_{\nu \in [0, T_2]} \underline{\lambda} \left(\exp(A_f^\top \nu) P \exp(A_f \nu) \right), \tag{7.24}$$

$$\alpha_2 = \max_{\nu \in [0, T_2]} \overline{\lambda} \left(\exp(A_f^\top \nu) P \exp(A_f \nu) \right), \tag{7.25}$$

Since the gradient of V is given by

$$\nabla V(\chi_s) = (2 \exp(A_f^\top \tau_s) P \exp(A_f \tau_s) \sigma, \sigma^\top \exp(A_f^\top \tau_s) \mathrm{He}(A_f, P) \exp(A_f \tau_s) \sigma),$$

for each $\chi_s \in C_s$, we have

$$\begin{aligned} \langle \nabla V(\chi_s), f_s(\chi_s) \rangle &= 2\sigma^\top \exp(A_f^\top \tau_s) P \exp(A_f \tau_s) A_f \sigma \\ &\quad - \sigma^\top \exp(A_f^\top \tau_s) \mathrm{He}(A_f, P) \exp(A_f \tau_s) \sigma \\ &= 0, \end{aligned} \tag{7.26}$$

where we used the property $\exp(A_f \tau_s) A_f = A_f \exp(A_f \tau_s)$. Moreover, for each $\chi_s \in D_s$, by using the data in (7.16) and condition (7.21), for each $\tilde{g} \in G_s(\chi_s)$

where $\tilde{g} = (A_g\sigma, \nu)$ and $\nu \in [T_1, T_2]$,

$$\begin{aligned} V(\tilde{g}) - V(\chi_s) &= \sigma^\top A_g^\top \exp(A_f^\top \nu) P \exp(A_f \nu) A_g \sigma - \sigma^\top P \sigma \\ &= \sigma^\top \left(A_g^\top \exp(A_f^\top \nu) P \exp(A_f \nu) A_g - P \right) \sigma \\ &< 0. \end{aligned} \tag{7.27}$$

Note that every solution $\phi \in \mathcal{S}_{\mathcal{H}_s}$ is complete and for each $(t, j) \in \operatorname{dom} \phi$, using (7.20), we have that for any $T > 0$, $t + j \geq T$ implies

$$j \geq T - t \geq T - (j+1)T_2.$$

Therefore, $t + j \geq T$ implies $j \geq \frac{T}{T_2+1} - \frac{T_2}{T_2+1}$. Then, from the inequalities in (7.26) and (7.27), by using [73, Proposition 3.24], we have that the set $\mathcal{A}$ is UGAS for $\mathcal{H}_s$. ■

Remark 7.2.3 *Note that when condition* (7.21) *holds, Theorem 7.2.2 guarantees that e and η converges to zero asymptotically. Recalling that $e_i = \hat{x}_i - x$, this implies that $\hat{x}_i$ converges to x asymptotically for all $i \in \mathcal{V}$. Furthermore, due to the multiplication of the parameters ν, P, and K_g in the first term of* (7.21)*, it might be difficult to efficiently check* (7.21) *numerically. In the next section, we develop constructive LMI-like conditions for the design of parameters to guarantee this condition. It is worth pointing out that condition* (7.21) *is satisfied if, for all $\nu \in [T_1, T_2]$, the eigenvalues of* $\exp(A_f \nu) A_g$ *are contained in the unit circle.* □

Note that the pair (H_i, A) is not explicitly assumed to be detectable in this work. In fact, as we will show in the following example, even when (H_i, A) are not detectable for each $i \in \mathcal{V}$, we can still guarantee UGAS of $\mathcal{A}$ by satisfying (7.21).

Example 7.2.4 *Consider an oscillatory plant as in* (7.1) *with*

$$A = \begin{bmatrix} 0 & -1 \\ 1 & 0 \end{bmatrix}. \tag{7.28}$$

Consider the case of two agents that are all-to-all connected, namely,

$$\mathcal{G} = \begin{bmatrix} 0 & 1 \\ 1 & 0 \end{bmatrix}.$$

Let the measurements of x *at agent* 1 *be*

$$y_1 = H_1 x, \quad H_1 = [1 \ \ 0]$$

and the measurements at agent 2 *be*

$$y_2 = H_2 x, \quad H_2 = [0 \ \ 1].$$

Let $T_1 = 0.5$ *and* $T_2 = 1$. *By solving inequality*[2] (7.21) *in Theorem 7.2.2, we obtain the following parameters:*

$$K_{11} = \begin{bmatrix} -0.5 & -0.2 \end{bmatrix}^\top, \quad K_{12} = \begin{bmatrix} -0.2 & -0.2 \end{bmatrix}^\top,$$
$$K_{21} = \begin{bmatrix} 0.2 & 0.3 \end{bmatrix}^\top, \quad K_{22} = \begin{bmatrix} -0.1 & -0.5 \end{bmatrix}^\top,$$

[2] Note that the inequality in (7.21) is not linear. The tool developed in [87] provides a way to solve it.

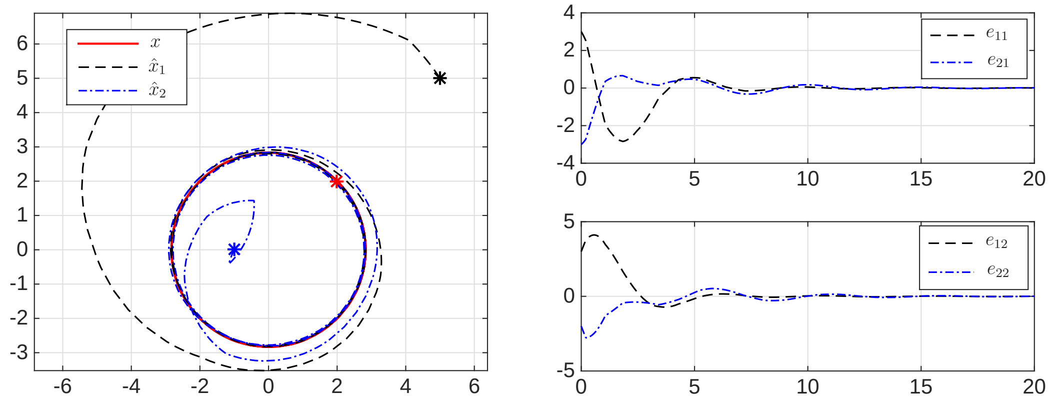

(a) Phase plots of $x, \hat{x}_1, \hat{x}_2$ from initial conditions that are denoted by $*$.

(b) Estimation error, where $x = (x_1, x_2)$, $\hat{x}_i = (\hat{x}_{i1}, \hat{x}_{i2})$, $e_{i1} = \hat{x}_{i1} - x_1$, $e_{i2} = \hat{x}_{i2} - x_2$, for $i \in \{1, 2\}$.

Figure 7.1: Phase plots of $x, \hat{x}_1$ and $\hat{x}_2$ as well as estimation errors e_1 and e_2 for two all-to-all connected agents using the observer in Example 7.2.4. Initial conditions are $x(0,0) = (2,2)$, $\hat{x}_1(0,0) = (5,5)$, $\hat{x}_2(0,0) = (-1,0)$, $\eta_1(0,0) = (1,1)$, $\eta_2(0,0) = (-1,-1)$, $\tau(0,0) = 0.2$.

with $\gamma = -0.1$. *An appropriate choice of* P *is*

$$P \approx \begin{bmatrix} 24.84 & -4.57 & 0.08 & 0.43 & 1.17 & 0.89 & -0.80 & -1.90 \\ -4.57 & 23.11 & 2.91 & -1.20 & -2.48 & -0.38 & 1.16 & 0.53 \\ 0.08 & 2.91 & 24.07 & 3.17 & 1.55 & 0.73 & -0.07 & 0.67 \\ 0.44 & -1.20 & 3.17 & 21.79 & 1.63 & 0.62 & -0.47 & 1.35 \\ 1.17 & -2.48 & 1.55 & 1.63 & 14.01 & -1.17 & 1.33 & 0.46 \\ 0.89 & -0.38 & 0.73 & 0.62 & -1.17 & 16.77 & 0.44 & 0.14 \\ -0.80 & 1.13 & -0.07 & -0.48 & 1.33 & 0.44 & 16.49 & -0.95 \\ -1.90 & 0.53 & 0.67 & 1.35 & 0.46 & 0.14 & -0.95 & 14.36 \end{bmatrix}.$$

A simulation with these parameters is shown in Figure 7.1. The estimates $\hat{x}_1$ *and* $\hat{x}_2$ *converge to* x *asymptotically as guaranteed by Theorem 7.2.2.* [3]

[3]Code at `https://github.com/HybridSystemsLab/ObsSyncTimes2nd`.

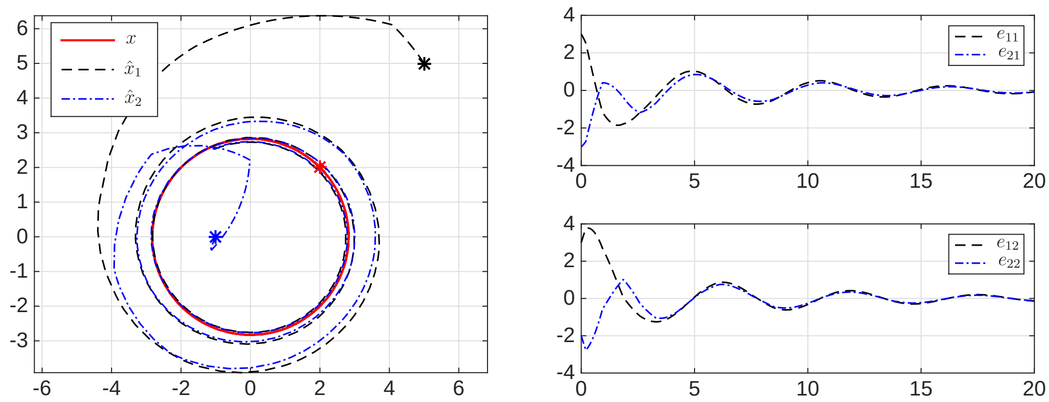

(a) Phase plots of $x, \hat{x}_1, \hat{x}_2$ from initial conditions that are denoted by $*$.

(b) Estimation errors for both components.

Figure 7.2: Phase plots and estimation errors for the observer in Example 7.2.4. The gain used is $\gamma = -0.4$ while the rest of the parameters are the same as those used for the simulations in Figure 7.1.

More interestingly, consider the scenario where agent 1 *loses the capability of receiving measurements, i.e.,* $H_1 = 0$*. A simulation with same initial conditions and gains as those in Figure 7.1 is shown in Figure 7.6. As suggested from the simulation, it can be seen that even though the agent has measurement* $y_1 \equiv 0$*, through the consensus-like term (the third term in* (7.90)*), the components* $\hat{x}_1$ *and* $\hat{x}_2$ *reach consensus first and then converge to* x *asymptotically. This highlights further a benefit of the third term in the dynamics of* η *in* (7.90)*. In fact, the third term enforces consensus between the estimates* $\hat{x}_1$ *and* $\hat{x}_2$*. Another benefit of using this term will be seen in the next example.* $\triangle$

Next, we consider a scenario with two connected agents, where, if communication between these two agent is not possible, they cannot estimate the state of the plant individually. However, when the information is shared between them, our observer guarantees that the state of each agent converges to the state of the plant asymptotically.

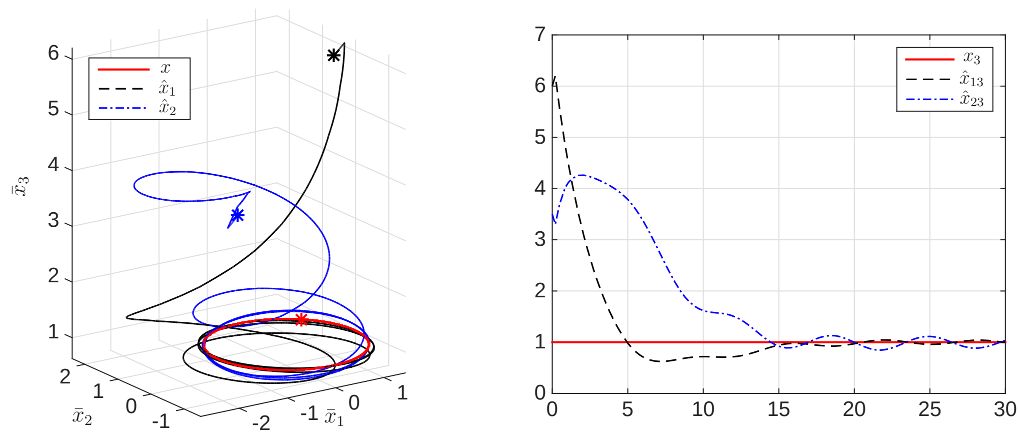

(a) Phase plots of $x, \hat{x}_1, \hat{x}_2$ from initial conditions that are denoted by $*$.

(b) Estimation error for the third state component.

Figure 7.3: Phase portrait and estimation errors for the third state component for the system in Example 7.2.5, where $x = (x_1, x_2, x_3)$, $\hat{x}_i = (\hat{x}_{i1}, \hat{x}_{i2}, \hat{x}_{i3})$, $e_{ik} = \hat{x}_{ik} - x_k$, for $i \in \{1, 2\}, k \in \{1, 2, 3\}$. Initial conditions are $x(0,0) = (1,1,1)$, $\hat{x}_1(0,0) = (1,0,6)$, $\eta_1(0,0) = (1,1,1)$, $\hat{x}_2(0,0) = (-1,0,3.5)$, $\eta_2(0,0) = (-1,-1,-1)$, $\tau(0,0) = 0.2$.

Example 7.2.5 *Consider a plant in* $\mathbb{R}^3$ *with oscillatory dynamics for* (x_1, x_2) *and trivial dynamics for* x_3*, i.e.,*

$$A = \begin{bmatrix} 0 & -1 & 0 \\ 1 & 0 & 0 \\ 0 & 0 & 0 \end{bmatrix}. \tag{7.29}$$

Consider the case of two agents that are all-to-all connected and measure x *according to* (7.2) *with*

$$H_1 = [0 \;\; 0 \;\; 1], \quad H_2 = [1 \;\; 1 \;\; 0].$$

Since the pairs (H_1, A) *and* (H_2, A) *are not detectable, neither agent can estimate the full state of the plant by running an observer that does not use information from the other agent. However, when communication between agents is allowed,* *our observer would be able to reconstruct x. In fact, given $T_1 = 0.2$ and $T_2 = 0.4$, by solving condition (7.21), we obtain the following parameters:*

$$
\begin{aligned}
K_{11} &= \begin{bmatrix} -0.5 & -0.2 & -0.1 \end{bmatrix}^\top, \qquad & K_{12} &= \begin{bmatrix} -0.2 & -0.2 & -0.5 \end{bmatrix}^\top, \\
K_{21} &= \begin{bmatrix} 0.2 & 0.3 & 0.3 \end{bmatrix}^\top, \qquad & K_{22} &= \begin{bmatrix} -0.1 & -0.5 & 0.2 \end{bmatrix}^\top,
\end{aligned}
$$

and gain $\gamma = -0.4$. The simulation shown in Figure 7.7 indicates that the estimates $\hat{x}_1$ and $\hat{x}_2$ converge to x asymptotically. Figure 7.7(a) shows the trajectory of $x = (x_1, x_2, x_3)$, and the observer states $\hat{x}_1 = (\hat{x}_{11}, \hat{x}_{12}, \hat{x}_{13})$, $\hat{x}_2 = (\hat{x}_{21}, \hat{x}_{22}, \hat{x}_{23})$. Figure 7.7(b) shows their third components, denoted x_3, $\hat{x}_{13}$ and $\hat{x}_{23}$. [4] $\triangle$

Similarly, by defining the variable

$$\theta_i = \sum_{k \in \mathcal{V}} g_{ik} G^k_{oi}(\hat{x}_i, \hat{x}_k, y_i, y_k) - \eta_i$$

and $\theta = (\theta_1, \theta_2, \ldots, \theta_N)$, the system in coordinates e and θ can be written as a hybrid system $\mathcal{H}_\theta = (C_\theta, f_\theta, D_\theta, G_\theta)$ with state $\chi_\theta = (\sigma_\theta, \tau) \in \mathcal{X}_s$, $\sigma_\theta = (e, \theta)$, and data given by

$$f_\theta(\chi_\theta) := (A_{f\theta}\sigma_\theta, -1)$$

for each $\chi_\theta \in C_\theta := \mathbb{R}^{nN} \times \mathbb{R}^{nN} \times [0, T_2]$, and

$$G_\theta(\chi_\theta) := (A_{g\theta}\sigma_\theta, [T_1, T_2])$$

[4] Code at `https://github.com/HybridSystemsLab/ObsSyncTimes3rd`.

when $\chi_\theta \in D_\theta := \mathbb{R}^{nN} \times \mathbb{R}^{nN} \times \{0\}$, where $A_{f\theta}$ is given in (7.94) and

$$A_{g\theta} = \begin{bmatrix} I_{nN} & 0 \\ 0 & 0 \end{bmatrix}. \tag{7.30}$$

Since the state e denotes the estimation error, the variable θ denotes the difference between the current information fusion state (η) and the new value of the fusion state (η^+), we are also interested in guaranteeing asymptotic stability of the set $\mathcal{A}$ defined in (7.19). In these new coordinates, we establish the following result.

Theorem 7.2.6 *Let $0 < T_1 \leq T_2$ be given. Suppose there exist $\delta > 0$ and matrices $K_g \in \mathbb{R}^{nN \times p}$, $P, Q \in \mathbb{R}^{nN \times nN}$ satisfying $P = P^\top > 0$, $Q = Q^\top > 0$, and*

$$\begin{bmatrix} \mathrm{He}(A_\theta, P) & -P + \exp(\delta\nu) A_\theta^\top \mathcal{K}^\top Q \\ \star & -\exp(\delta\nu)(\delta Q + \mathrm{He}(\mathcal{K}, Q)) \end{bmatrix} < 0 \tag{7.31}$$

for all $\nu \in [0, T_2]$. Then, the set $\mathcal{A}$ in (7.19) is UGAS for the hybrid system $\mathcal{H}_\theta$.

Proof Consider the Lyapunov function candidate $V : \mathcal{X}_s \to \mathbb{R}_{\geq 0}$ given by

$$V(\chi_\theta) = e^\top P e + \exp(\delta\tau)\theta^\top Q \theta, \tag{7.32}$$

it follows that

$$\alpha_1 |\chi_\theta|_{\mathcal{A}}^2 \leq V(\chi_\theta) \leq \alpha_2 |\chi_\theta|_{\mathcal{A}}^2 \tag{7.33}$$

for all $\chi_\theta \in C_\theta$, where

$$\alpha_1 = \min\{\underline{\lambda}(P), \underline{\lambda}(Q)\}, \tag{7.34}$$

$$\alpha_2 = \max\{\overline{\lambda}(P), \exp(\delta T_2)\overline{\lambda}(Q)\}. \tag{7.35}$$

Since the gradient of V is given by

$$\nabla V(\chi_\theta) = (2Pe, 2\exp(\delta\tau)Q\theta, \delta\exp(\delta\tau)\theta^\top Q\theta),$$

for each $\chi_\theta \in C_\theta$, we have

$$\begin{aligned}\langle \nabla V(\chi_\theta), f_\theta(\chi_\theta)\rangle &= e^\top \mathrm{He}(A_\theta, P)e - 2e^\top P\theta + 2\exp(\delta\tau)\theta^\top Q\mathcal{K}A_\theta e \\ &\quad - \exp(\delta\tau)\theta^\top \mathrm{He}(\mathcal{K}, Q)\theta - \delta\exp(\delta\tau)\theta^\top Q\theta \\ &= \begin{bmatrix} e \\ \theta \end{bmatrix}^\top \begin{bmatrix} \mathrm{He}(A_\theta, P) & -P + \exp(\delta\tau)A_\theta^\top \mathcal{K}^\top Q \\ -P + \exp(\delta\tau)Q\mathcal{K}A_\theta & -\exp(\delta\tau)(\delta Q + \mathrm{He}(\mathcal{K}, Q)) \end{bmatrix} \begin{bmatrix} e \\ \theta \end{bmatrix}.\end{aligned} \tag{7.36}$$

Therefore, by using (7.31), we have

$$\langle \nabla V(\chi_\theta), f_\theta(\chi_\theta)\rangle < 0 \quad \forall \chi_\theta \in C_\theta \setminus \mathcal{A} \tag{7.37}$$

Moreover, for each $\chi_\theta \in D_\theta$, for each $\tilde{g} \in G_\theta(\chi_\theta)$,

$$V(\tilde{g}) - V(\chi_\theta) = -\theta^\top Q\theta \leq 0 \tag{7.38}$$

Note that every solution $\phi \in \mathcal{S}_{\mathcal{H}_\theta}$ is complete and for $(t, j) \in \operatorname{dom} \phi$, by using (7.20), we have that for any $T > 0$, $t + j \geq T$ implies

$$t \geq \frac{T_1}{1+T_1} T - \frac{T_1}{1+T_1}.$$

From the inequalities in (7.37) and (7.38), by using [73, Proposition 3.27], we have that the set $\mathcal{A}$ is UGAS for $\mathcal{H}_\theta$. ■

Remark 7.2.7 *Note that the condition in* (7.31) *is different than the condition in* (7.95)*, the latter requires the matrix* $\widetilde{Q}(\nu)$ *to be block diagonal, while the former does not.*

Note that the condition in (7.31) needs to be checked over a closed interval $[0, T_2]$, which is a difficult task. The following result relaxes this requirement.

Proposition 7.2.8 *Let* $T_2 > 0$ *be given. The inequality in* (7.31) *holds for each* $\nu \in [0, T_2]$ *if there exist* $\delta > 0$ *and matrices* $P, Q \in \mathbb{R}^{nN \times nN}$ *satisfying* $P = P^\top > 0$, $Q = Q^\top > 0$,

$$E_1 := \begin{bmatrix} \operatorname{He}(A_\theta, P) & -P + A_\theta^\top \mathcal{K}^\top Q \\ \star & -\delta Q - \operatorname{He}(\mathcal{K}, Q) \end{bmatrix} < 0, \tag{7.39}$$

$$E_2 := \begin{bmatrix} \operatorname{He}(A_\theta, P) & -P + \exp(\delta T_2) A_\theta^\top \mathcal{K}^\top Q \\ \star & -\exp(\delta T_2)(\delta Q + \operatorname{He}(\mathcal{K}, Q)) \end{bmatrix} < 0. \tag{7.40}$$

Proof Given $T_2 > 0$ and $\delta > 0$, define the function $r : [0, T_2] \to [0, 1]$ as

$$r(\nu) = \frac{\exp(\delta T_2) - \exp(\delta \nu)}{\exp(\delta T_2) - 1}$$

for all $\nu \in [0, T_2]$. Then, it can be verified that for each $\nu \in [0, T_2]$

$$\exp(\delta\nu) = r(\nu) + (1 - r(\nu)) \exp(\delta T_2). \tag{7.41}$$

Then, by using this relationship, the matrix function in (7.31) can be written as

$$\begin{bmatrix} \mathrm{He}(A_\theta, P) & -P + \exp(\delta\nu) A_\theta^\top \mathcal{K}^\top Q \\ \star & -\exp(\delta\nu)(\delta Q + \mathrm{He}(\mathcal{K}, Q)) \end{bmatrix} = r(\nu)E_1 + (1 - r(\nu))E_2 \tag{7.42}$$

for each $\nu \in [0, T_2]$, where E_1 is given in (7.39) and E_2 is given in (7.40). Therefore, it follows that when (7.39) and (7.40) hold, (7.31) is satisfied. ■

Example 7.2.9 *Consider the network estimation problem in Example 7.2.4. Using the same parameters K_{11}, K_{12}, K_{21}, K_{22} and γ therein, it can be verified that* (7.39) *and* (7.40) *hold for $\delta = 10$ and a maximum value of $T_2 \approx 0.4$. As expected, replacing condition* (7.31) *by* (7.39) *and* (7.40)*, which is a relaxation of* (7.31)*, the largest T_2 allowed becomes smaller.* △

Remark 7.2.10 *Note that the matrices E_1 and E_2 involve the multiplication of $Q\mathcal{K}A_\theta$, which contains cross terms involving Q, K_g, and γ. The presence of these terms makes the problem nonlinear and difficult to solve numerically. This difficulty motivates the LMI conditions established in the next section.* □

7.2.2 Design of parameters via LMIs

Since the conditions established in Theorem 7.2.2 and in Theorem 7.2.6 are nonlinear and need to be checked for infinitely many points, they are potentially difficult to be solved numerically. In this section, we develop constructive conditions that can efficiently be checked numerically.

Following the idea in [92], condition (7.21) can be relaxed as shown in the following result.

Proposition 7.2.11 *Let $0 < T_1 \leq T_2$, $\Gamma = (\mathcal{V}, \mathcal{E}, \mathcal{G})$ and $\gamma \in \mathbb{R}$ be given. The matrices K_g and $P = P^\top > 0$ satisfy condition (7.21) for each $\nu \in [T_1, T_2]$ if there exist matrices $\mathcal{F}_1, \mathcal{F}_2 \in \mathbb{R}^{nN \times nN}$ such that, for each $\nu \in [T_1, T_2]$,*

$$\begin{bmatrix} -\mathrm{He}(\mathcal{F}, I) & \begin{bmatrix} \mathcal{F}_1 & 0 \\ \gamma \mathcal{F}_2 \widetilde{L} + \widetilde{\mathcal{F}}_2 \widetilde{H}_g & 0 \end{bmatrix} & \exp(A_f^\top \nu) P \\ \star & -P & 0 \\ \star & \star & -P \end{bmatrix} < 0, \qquad (7.43)$$

where A_f is given in (7.17), $H_g = \mathrm{diag}(H_1, H_2, \ldots, H_N)$, $\widetilde{\mathcal{F}}_2 = \mathcal{F}_2 K_g$, $\mathcal{F} = \mathrm{diag}(\mathcal{F}_1, \mathcal{F}_2)$, $\widetilde{L} = \mathcal{L} \otimes I_n$ and $\widetilde{H}_g = H_g * (I_N + \mathcal{G})$.

Proof Let

$$X = \begin{bmatrix} \exp(A_f^\top \nu) P \exp(A_f \nu) & 0 \\ 0 & -P \end{bmatrix}, N_Y = \begin{bmatrix} A_g \\ I \end{bmatrix}, N_Z = \begin{bmatrix} 0 \\ I \end{bmatrix}. \qquad (7.44)$$

Then, condition (7.21) can be written as

$$N_Y^\top X N_Y < 0 \qquad (7.45)$$

while the positive definiteness requirement for P is equivalent to

$$N_Z^\top X N_Z < 0. \qquad (7.46)$$

Note that the columns of N_Y form the basis of the null space of

$$Y = \begin{bmatrix} -I & A_g \end{bmatrix}, \tag{7.47}$$

and the columns of N_Z form the basis of the null space of

$$Z = \begin{bmatrix} I & 0 \end{bmatrix}. \tag{7.48}$$

Thus, by using the projection lemma [93], inequalities (7.45) and (7.46) are satisfied if and only if there exists a matrix $\widetilde{\mathcal{F}} \in \mathbb{R}^{nN \times nN}$ such that

$$Y^\top \widetilde{\mathcal{F}} Z + Z^\top \widetilde{\mathcal{F}}^\top Y + X = \begin{bmatrix} \exp(A_f^\top \nu) P \exp(A_f \nu) - \mathrm{He}(\widetilde{\mathcal{F}}, I) & \widetilde{\mathcal{F}} A_g \\ \star & -P \end{bmatrix} < 0.$$

Moreover, we have

$$\begin{aligned} &\begin{bmatrix} \exp(A_f^\top \nu) P \exp(A_f \nu) - \mathrm{He}(\widetilde{\mathcal{F}}, I) & \widetilde{\mathcal{F}} A_g \\ \star & -P \end{bmatrix} \\ &\qquad = \begin{bmatrix} -\mathrm{He}(\widetilde{\mathcal{F}}, I) & \tilde{\mathcal{F}} A_g \\ \star & -P \end{bmatrix} + \begin{bmatrix} \exp(A_f^\top \nu) \\ 0 \end{bmatrix} P \begin{bmatrix} \exp(A_f^\top \nu) \\ 0 \end{bmatrix}^\top \end{aligned}$$

Using Schur complement, we further have

$$\begin{bmatrix} -\mathrm{He}(\widetilde{\mathcal{F}}, I) & \tilde{\mathcal{F}} A_g & \exp(A_f^\top \nu) \\ \star & -P & 0 \\ \star & \star & -P^{-1} \end{bmatrix} < 0. \tag{7.49}$$

Then, by pre and post multiplying by $\mathrm{diag}(I, I, P)$, we have

$$\begin{bmatrix} -\mathrm{He}(\widetilde{\mathcal{F}}, I) & \widetilde{\mathcal{F}} A_g & \exp(A_f^\top \nu) P \\ \star & -P & 0 \\ \star & \star & -P \end{bmatrix} < 0. \tag{7.50}$$

Recall A_g from (7.18), by choosing $\widetilde{\mathcal{F}} = \mathrm{diag}(\mathcal{F}_1, \mathcal{F}_2)$, we have

$$\begin{aligned} \widetilde{\mathcal{F}} A_g &= \begin{bmatrix} \mathcal{F}_1 & 0 \\ 0 & \mathcal{F}_2 \end{bmatrix} \begin{bmatrix} I_{nN} & 0 \\ K_g H_g * (I_N + \mathcal{G}) + \gamma \mathcal{L} \otimes I_n & 0 \end{bmatrix} \\ &= \begin{bmatrix} \mathcal{F}_1 & 0 \\ \mathcal{F}_2 K_g H_g * (I_N + \mathcal{G}) + \gamma \mathcal{F}_2 \mathcal{L} \otimes I_n & 0 \end{bmatrix} \\ &= \begin{bmatrix} \mathcal{F}_1 & 0 \\ \gamma \mathcal{F}_2 \widetilde{L} + \widetilde{\mathcal{F}}_2 \widetilde{H}_g & 0 \end{bmatrix}. \end{aligned}$$

Then the result follows. ■

Remark 7.2.12 *Note that for fixed ν and γ, condition* (7.43) *is a LMI with respect to the parameters $\mathcal{F}_1, \mathcal{F}_2$ and $\widetilde{\mathcal{F}}_2$. In fact, the feasibility problem* (7.43) *can be solved efficiently by applying the polytopic embedding approach, see, e.g., [92, Corollary 1]. In particular, the embedding approach provides a way to handle the term* $\exp(A_f \nu)$ *and only requires to check condition* (7.43) *over a discrete and bounded set, i.e., a finite number of inequalities.* □

Next, we propose design methods based on the conditions in Proposition 7.2.8. First, note that the matrix $A_{f\theta}$ in (7.30) can be written in the form $A_{f\theta} = \widetilde{A}_1 \widetilde{A}_2$, where

$$\widetilde{A}_1 = \begin{bmatrix} I & 0 \\ \mathcal{K} & I \end{bmatrix}, \quad \widetilde{A}_2 = \begin{bmatrix} A_\theta & -I_{nN} \\ 0 & 0 \end{bmatrix}. \tag{7.51}$$

We have the following result.

Proposition 7.2.13 *Let $T_2 > 0$ be given. The positive definite symmetric matrices $P, Q \in \mathbb{R}^{nN\times nN}$, the constants $\delta > 0$, $\gamma \in \mathbb{R}$, and the matrix $K_g \in \mathbb{R}^{nN\times p}$ satisfy conditions*[5] (7.39) *and* (7.40) *if and only if there exist matrices $\mathcal{O}_i, \mathcal{T}_i \in \mathbb{R}^{nN\times nN}, i \in \mathbb{N}, 1 \le i \le 6$, such that*

$$\begin{bmatrix} \mathrm{He}(\Omega_1, I_{2nN}) & \Omega_2 + \widetilde{P}_1 \\ \star & \widetilde{Y} + \mathrm{He}(\Omega_3, I_{2nN}) \end{bmatrix} < 0, \tag{7.52}$$

$$\begin{bmatrix} \mathrm{He}(\Lambda_1, I_{2nN}) & \Lambda_2 + \widetilde{P}_2 \\ \star & \widetilde{Z} + \mathrm{He}(\Lambda_3, I_{2nN}) \end{bmatrix} < 0, \tag{7.53}$$

where

$$\begin{aligned} &\widetilde{P}_1 = \mathrm{diag}(P, Q), \quad \widetilde{Z} = \mathrm{diag}(0_{nN}, -\delta \exp(\delta T_2) Q), \\ &\widetilde{P}_2 = \mathrm{diag}(P, \exp(\delta T_2) Q), \quad \widetilde{Y} = \mathrm{diag}(0_{nN}, -\delta Q), \end{aligned} \tag{7.54}$$

[5]For simplicity, $H_\eta = 0$.

and

$$\Omega_1 = \begin{bmatrix} -\mathcal{O}_1 + \mathcal{K}^\top \mathcal{O}_4 & -\mathcal{O}_2 + \mathcal{K}^\top \mathcal{O}_5 \\ -\mathcal{O}_4 & -\mathcal{O}_5 \end{bmatrix} \tag{7.55}$$

$$\Omega_2 = \begin{bmatrix} \mathcal{O}_1^\top A_\theta - \mathcal{O}_3 + \mathcal{K}^\top \mathcal{O}_6 & -\mathcal{O}_1^\top \\ \mathcal{O}_2^\top A_\theta - \mathcal{O}_6 & -\mathcal{O}_2^\top \end{bmatrix} \tag{7.56}$$

$$\Omega_3 = \begin{bmatrix} A_\theta^\top \mathcal{O}_3 & 0 \\ -\mathcal{O}_3 & 0 \end{bmatrix} \tag{7.57}$$

$$\Lambda_1 = \begin{bmatrix} -\mathcal{T}_1 + \mathcal{K}^\top \mathcal{T}_4 & -\mathcal{T}_2 + \mathcal{K}^\top \mathcal{T}_5 \\ -\mathcal{T}_4 & -\mathcal{T}_5 \end{bmatrix} \tag{7.58}$$

$$\Lambda_2 = \begin{bmatrix} \mathcal{T}_1^\top A_\theta - \mathcal{T}_3 + \mathcal{K}^\top \mathcal{T}_6 & -\mathcal{T}_1^\top \\ \mathcal{T}_2^\top A_\theta - \mathcal{T}_6 & -\mathcal{T}_2^\top \end{bmatrix} \tag{7.59}$$

$$\Lambda_3 = \begin{bmatrix} A_\theta^\top \mathcal{T}_3 & 0 \\ -\mathcal{T}_3 & 0 \end{bmatrix}. \tag{7.60}$$

Proof Let

$$N_{\mathcal{W}} = \begin{bmatrix} A_{f\theta} \\ I \end{bmatrix}, \widetilde{\mathcal{Y}} = \begin{bmatrix} 0 & \widetilde{P}_1 \\ \star & \widetilde{Y} \end{bmatrix}, \widetilde{\mathcal{Z}} = \begin{bmatrix} 0 & \widetilde{P}_2 \\ \star & \widetilde{Z} \end{bmatrix}, N_{\mathcal{Y}} = \begin{bmatrix} 0 \\ I \end{bmatrix}. \tag{7.61}$$

Then, inequality (7.39) can be written as

$$E_1 = N_{\mathcal{W}}^\top \widetilde{\mathcal{Y}} N_{\mathcal{W}} < 0, \quad N_{\mathcal{Y}}^\top \widetilde{\mathcal{Y}} N_{\mathcal{Y}} < 0, \tag{7.62}$$

and inequality (7.40) can be written as

$$E_2 = N_{\mathcal{W}}^\top \widetilde{\mathcal{Z}} N_{\mathcal{W}} < 0, \quad N_{\mathcal{Y}}^\top \widetilde{\mathcal{Z}} N_{\mathcal{Y}} < 0. \tag{7.63}$$

Moreover, the columns of $N_{\mathcal{W}}$ (respectively, $N_{\mathcal{Y}}$) form the basis of the null space of $\mathcal{W}$ (respectively, $\mathcal{Y}$), where $\mathcal{W}$ and $\mathcal{Y}$ are given by

$$\mathcal{W} = \begin{bmatrix} -\widetilde{A}_1^{-1} & \widetilde{A}_2 \end{bmatrix} = \begin{bmatrix} -I & 0 & A_\theta & -I_{nN} \\ \mathcal{K} & -I & 0 & 0 \end{bmatrix}, \tag{7.64}$$

and

$$\mathcal{Y} = \begin{bmatrix} I_{nN} & 0_{nN} & 0_{nN} & 0_{nN} \\ 0_{nN} & I_{nN} & 0_{nN} & 0_{nN} \\ 0_{nN} & 0_{nN} & I_{nN} & 0_{nN} \end{bmatrix}. \tag{7.65}$$

Then, using the projection lemma [93], inequalities (7.62) and (7.63) are equivalent to the existence of two matrices $\mathcal{O}, \mathcal{T} \in \mathbb{R}^{2nN \times 3nN}$ such that

$$\widetilde{\mathcal{Y}} + \mathcal{W}^\top \mathcal{O} \mathcal{Y} + \mathcal{Y}^\top \mathcal{O}^\top \mathcal{W} < 0, \tag{7.66}$$

$$\widetilde{\mathcal{Z}} + \mathcal{W}^\top \mathcal{T} \mathcal{Y} + \mathcal{Y}^\top \mathcal{T}^\top \mathcal{W} < 0. \tag{7.67}$$

Therefore, by letting

$$\mathcal{O} = \begin{bmatrix} \mathcal{O}_1 & \mathcal{O}_2 & \mathcal{O}_3 \\ \mathcal{O}_4 & \mathcal{O}_5 & \mathcal{O}_6 \end{bmatrix}, \quad \mathcal{T} = \begin{bmatrix} \mathcal{T}_1 & \mathcal{T}_2 & \mathcal{T}_3 \\ \mathcal{T}_4 & \mathcal{T}_5 & \mathcal{T}_6 \end{bmatrix}, \tag{7.68}$$

we have

$$\mathcal{W}^\top \mathcal{O} \mathcal{Y} + \mathcal{Y}^\top \mathcal{O}^\top \mathcal{W} + \widetilde{\mathcal{Y}} = \begin{bmatrix} \mathrm{He}(\Omega_1, I) & \Omega_2 + \widetilde{P}_1 \\ \star & \widetilde{Y} + \mathrm{He}(\Omega_3, I) \end{bmatrix}, \tag{7.69}$$

which leads to (7.52). The proof of (7.53) follows similarly. ■

By the transformation in Proposition 7.2.13, it can be seen that in the new set of inequalities (7.52) and (7.53), the cross term $\mathcal{K}\mathcal{K}$ from the multiplication of $\mathcal{K}A_\theta$ in (7.39) and (7.40) vanishes. In fact, the conditions (7.52) and (7.53) lead to several designs by choosing the matrices $\mathcal{O}_i, \mathcal{T}_i \in \mathbb{R}^{nN\times nN}$ properly. The following result illustrates one particular such design when the graph is all-to-all connected.

Corollary 7.2.14 *Let $T_2 > 0$ be given. The set $\mathcal{A}$ is UGAS for $\mathcal{H}_\theta$ if there exist $\delta > 0$, $\gamma \in \mathbb{R}$ and positive definite symmetric matrices $P, Q \in \mathbb{R}^{nN\times nN}$, $\mathcal{Q} \in \mathbb{R}^{nN\times p}$, and $\mathcal{R} \in \mathbb{R}^{nN\times nN}$ such that*

$$\begin{bmatrix} \mathrm{He}(\mathcal{Z}_1, I_{2nN}) & \mathcal{Z}_2 + \widetilde{P}_1 \\ \star & Y + \mathrm{He}(\mathcal{Z}_3, I_{2nN}) \end{bmatrix} < 0, \tag{7.70}$$

$$\begin{bmatrix} \mathrm{He}(\mathcal{Z}_1, I_{2nN}) & \mathcal{Z}_2 + \widetilde{P}_2 \\ \star & Z + \mathrm{He}(\mathcal{Z}_3, I_{2nN}) \end{bmatrix} < 0, \tag{7.71}$$

where $\widetilde{P}_1, \widetilde{P}_2, Y, Z$ are in (7.54), and

$$\mathcal{Z}_1 = \begin{bmatrix} -\mathcal{R} + H_g^\top \mathcal{Q} + \widetilde{\mathcal{L}}^\top \mathcal{R} & H_g^\top \mathcal{Q} + \widetilde{\mathcal{L}}^\top \mathcal{R} \\ -\mathcal{R} & -\mathcal{R} \end{bmatrix}, \tag{7.72}$$

$$\mathcal{Z}_2 = \begin{bmatrix} \mathcal{R}^\top \widetilde{A} + \mathrm{He}(\mathcal{Q}, H_g) + \mathrm{He}(\mathcal{R}, \widetilde{\mathcal{L}}) - \mathcal{R} & -\mathcal{R} \\ -\mathcal{R} & 0 \end{bmatrix}, \tag{7.73}$$

$$\mathcal{Z}_3 = \begin{bmatrix} \widetilde{A}^\top \mathcal{R} + H_g^\top \mathcal{Q} + \widetilde{\mathcal{L}}^\top \mathcal{R} & 0 \\ -\mathcal{R} & 0 \end{bmatrix}, \tag{7.74}$$

$\widetilde{A} = I_N \otimes A$, $\widetilde{\mathcal{L}} = \gamma \mathcal{L} \otimes I_n$, $K_g^\top = \mathcal{Q}\mathcal{R}^{-1}$.

Proof When the graph is all-to-all connected, we have $(K_g H_g) * (I_N + \mathcal{G}) = K_g H_g$. By choosing $O_1 = O_3 = O_4 = O_5 = O_6 = \mathcal{R}$ and $T_1 = T_3 = T_4 = T_5 = T_6 = \mathcal{R}$, and $K_g^\top = \mathcal{R}^{-1}\mathcal{Q}$, $O_2 = T_2 = 0$, conditions (7.52) and (7.53) reduce to (7.70) and (7.71), respectively. ■

Example 7.2.15 *For the system in Example 7.2.4 and for given $T_2 = 0.4$, it can be verified that the inequalities* (7.70) *and* (7.71) *can be solved by choosing $\delta = 10$ and $\gamma = -0.2$, the resulting gain is*

$$K_g^\top \approx \begin{bmatrix} -1.11 & -0.43 & -0.41 & -0.09 \\ 0.09 & -0.41 & 0.43 & -1.11 \end{bmatrix}.$$

Note that (7.70) *and* (7.71) *are LMIs that can be solved efficiently.* △

7.2.3 Robustness to measurement and communication noise

In this section, we investigate the scenario when the measurements y_i's are noisy, i.e., for each $i \in \mathcal{V}$, $\tilde{y}_i = y_i + m_i$, where $m_i : \mathbb{R}_{\geq 0} \to \mathbb{R}^{p_i}$ denotes the measurement noise on the information received by agent i. Moreover, when agent i receives information (including $\hat{x}_k, y_k$) from agent k ($k \in \mathcal{N}(i)$), it is also affected by channel noise, i.e., $\tilde{x}_k^i = \hat{x}_k + c_i^x$ and $\tilde{y}_k^i = \tilde{y}_k + c_i^y$, where $c_i = (c_i^x, c_i^y) : \mathbb{R}_{\geq 0} \to \mathbb{R}^{n+p_i}$ is the channel noise when agent i receives information from its neighbors. Then, according to the design in (7.89)-(7.90), the noise is injected through the update law of η_i, that is,

$$\dot{\eta}_i = 0 \tag{7.75}$$

when $\tau \in [0, T_2]$, and

$$\eta_i^+ = K_{ii} H_i e_i + \sum_{k \in \mathcal{V}} g_{ik}(K_{ik} H_k e_k + e_i - e_k) + \zeta_i \tag{7.76}$$

when $\tau = 0$, where

$$\begin{aligned}\zeta_i &= -K_{ii}m_i + \sum_{k\in\mathcal{V}} g_{ik}K_{ik}(H_k c_i^x - c_i^y - m_k) - \gamma \sum_{k\in\mathcal{V}} g_{ik}c_i^x. \\ &= K_{ii}m_i - \sum_{k\in\mathcal{V}} g_{ik}K_{ik}m_k + \sum_{k\in\mathcal{V}} g_{ik}(K_{ik}H_k - \gamma I)c_i^x - \sum_{k\in\mathcal{V}} g_{ik}K_{ik}c_i^y.\end{aligned}$$

Then, the closed-loop system in (7.15) and (7.16) with added noise can be written in the following compact form:

$$\dot{\chi} = f_s(\chi) := (A_f\sigma, -1) \qquad \chi \in C_s, \tag{7.77}$$

$$\chi^+ \in G_s(\chi, \zeta) := (A_g\sigma + \zeta, [T_1, T_2]) \qquad \chi \in D_s, \tag{7.78}$$

where A_f and A_g are given in (7.17) and (7.18), respectively,

$$\begin{aligned}\zeta &= (0, K_m m + K_c c), \\ K_m &= -K_g * (I + \mathcal{G}), \\ K_c &= \begin{bmatrix}(K_g H_g - \gamma I) * \mathcal{G} & -K_g * \mathcal{G}\end{bmatrix},\end{aligned}$$

$m = (m_1, m_2, \ldots, m_N)$, $c = (c^x, c^y)$, $c^x = (c_1^x, c_2^x, \ldots, c_N^x)$, and $c^y = (c_1^y, c_2^y, \ldots, c_N^y)$.[6] For this perturbed hybrid system, we have the following result.

Theorem 7.2.16 *Let $0 < T_1 \leq T_2$ be given. Suppose there exist matrices $K_g \in \mathbb{R}^{nN\times p}$ and $P \in \mathbb{R}^{2nN\times 2nN}$ such that $P = P^\top > 0$ and condition (7.21) holds. Then, the set $\mathcal{A}$ is ISS with respect to measurement noise and communication*

[6]Note that the Khatri-Rao product $-K_g * (I + \mathcal{G})$ is such that the (i,k)-th entry K_{ik} of K_g is multiplied by the (i,k)-th scalar entry of the matrix $I + \mathcal{G}$ for all $i, k \in \mathcal{V}$.

noise, i.e., each $\phi \in \mathcal{S}_{\mathcal{H}_s}$ *satisfies, for any* $(t, j) \in \operatorname{dom}\phi$,

$$|\phi(t, j)|_{\mathcal{A}} \leq \max\left\{\sqrt{2\frac{\alpha_2}{\alpha_1}}\lambda_d^{j/2}|\phi(0, 0)|_{\mathcal{A}}, \widetilde{\gamma}_m(j)|m|_\infty, \widetilde{\gamma}_c(j)|c|_\infty\right\}, \tag{7.79}$$

where $\lambda_d = 1 - \frac{\mu}{\alpha_2} + \epsilon \in (0, 1)$, $\widetilde{\gamma}_m(j) = 2\sqrt{\frac{\rho}{\alpha_1}\frac{1-\lambda_d^j}{1-\lambda_d}}|K_m|$, $\widetilde{\gamma}_c(j) = 2\sqrt{\frac{\rho}{\alpha_1}\frac{1-\lambda_d^j}{1-\lambda_d}}|K_c|$, $\rho = \frac{1}{\epsilon\alpha_1}w_1 + w_2$, $\epsilon \in \left(0, \frac{\mu}{\alpha_2}\right)$, $\mu \in \left(0, \min\left\{\alpha_2, -\hat{\beta}\right\}\right)$,

$$\begin{aligned}
\alpha_1 &= \min_{\nu\in[0,T_2]} \underline{\lambda}\left(\exp(A_f^\top\nu)P\exp(A_f\nu)\right),\\
\alpha_2 &= \max_{\nu\in[0,T_2]} \overline{\lambda}\left(\exp(A_f^\top\nu)P\exp(A_f\nu)\right),\\
w_1 &= \max_{\nu\in[T_1,T_2]} |\exp(A_f^\top\nu)P\exp(A_f\nu)A_g|^2,\\
w_2 &= \max_{\nu\in[T_1,T_2]} |\exp(A_f^\top\nu)P\exp(A_f\nu)|,\\
\hat{\beta} &= \max_{\nu\in[T_1,T_2]} \overline{\lambda}(\exp(\delta\nu)A_g^\top\exp(A_f^\top\nu)P\exp(A_f\nu)A_g - P).
\end{aligned}$$

Proof Consider the Lyapunov function candidate $V : \mathcal{X}_s \to \mathbb{R}_{\geq 0}$ given by

$$V(\chi) = \sigma^\top \exp(A_f^\top\tau)P\exp(A_f\tau)\sigma \tag{7.80}$$

where $\delta > 0$ and $P^\top = P > 0$. Following the proof of Theorem 7.2.2, it follows that

$$\alpha_1|\chi|_{\mathcal{A}}^2 \leq V(\chi) \leq \alpha_2|\chi|_{\mathcal{A}}^2 \tag{7.81}$$

for all $\chi \in C_s$, where α_1 and α_2 are given by (7.24) and (7.25). Then, during flows, we have

$$\langle\nabla V(\chi), f_s(\chi)\rangle = 0 \quad \forall\chi \in C_s \tag{7.82}$$

Moreover, for each $\chi \in D_s \setminus \mathcal{A}$, by using (7.144) and (7.145), for each $\tilde{g} \in G_s(\chi, \zeta)$ where $\tilde{g} = (A_g\sigma + \zeta, \nu)$ and $\nu \in [T_1, T_2]$,

$$\begin{aligned}
V(G_s(\chi)) - V(\chi) &= (A_g\sigma + \zeta)^\top \exp(A_f^\top \nu) P \exp(A_f \nu)(A_g\sigma + \zeta) - \sigma^\top P \sigma \\
&= \sigma^\top \left(A_g^\top \exp(A_f^\top \nu) P \exp(A_f \nu) A_g - P \right) \sigma \\
&\quad + \zeta^\top \exp(A_f^\top \nu) P \exp(A_f \nu) \zeta \\
&\quad + 2\zeta^\top \exp(A_f^\top \nu) P \exp(A_f \nu) A_g \sigma.
\end{aligned}$$

Using Young's inequality, we have

$$\begin{aligned}
2\zeta^\top \exp(A_f^\top \nu) P \exp(A_f \nu) A_g \sigma &= 2 \left(A_g^\top \exp(A_f^\top \nu) P \exp(A_f \nu) \zeta \right)^\top \sigma \\
&\leq \frac{1}{\epsilon \alpha_1} \left| A_g^\top \exp(A_f^\top \nu) P \exp(A_f \nu) \zeta \right|^2 + \epsilon \alpha_1 |\sigma|^2.
\end{aligned}$$

Therefore,

$$\begin{aligned}
V(G_s(\chi)) - V(\chi) &\leq -\mu \sigma^\top \sigma + \epsilon \alpha_1 \sigma^\top \sigma + \zeta^\top \exp(A_f^\top \nu) P \exp(A_f \nu) \zeta \\
&\quad + \frac{1}{\epsilon \alpha_1} \zeta^\top \exp(A_f^\top \nu) P \exp(A_f \nu) A_g A_g^\top \exp(A_f^\top \nu) P \exp(A_f \nu) \zeta \\
&\leq - \left(\frac{\mu}{\alpha_2} - \epsilon \right) V(\chi) + \rho \zeta^\top \zeta
\end{aligned}$$

where

$$\mu \in \left(0, \min \left\{ \alpha_2, - \max_{\nu \in [T_1, T_2]} \overline{\lambda} \left(A_g^\top \exp(A_f^\top \nu) P \exp(A_f \nu) A_g - P \right) \right\} \right),$$

$\epsilon \in \left(0, \frac{\mu}{\alpha_2}\right)$, $\rho = \frac{1}{\epsilon\alpha_1} w_1 + w_2$ and

$$w_1 = \max_{\nu \in [T_1, T_2]} \left|\exp(A_f^\top \nu) P \exp(A_f \nu) A_g\right|^2, \tag{7.83}$$

$$w_2 = \max_{\nu \in [T_1, T_2]} \left|\exp(A_f^\top \nu) P \exp(A_f \nu)\right|. \tag{7.84}$$

Note that by the choice of μ and ϵ,

$$0 < 1 - \frac{\mu}{\alpha_2} + \epsilon < 1.$$

Then, given a solution $\phi \in \mathcal{S}_{\mathcal{H}_s}$, we have that for all $(t, j) \in \operatorname{dom} \phi$ such that $t \in [t_j, t_{j+1}]$,

$$V(\phi(t, j)) = V(\phi(t_j, j)) \tag{7.85}$$

and

$$V(\phi(t_{j+1}, j + 1)) \leq \lambda_d V(\phi(t_{j+1}, j)) + \rho|\zeta|_\infty^2 \tag{7.86}$$

where $\lambda_d = 1 - \frac{\mu}{\alpha_2} + \epsilon \in (0, 1)$. Therefore, by recursively applying the above two inequalities, we have, for each $(t, j) \in \operatorname{dom} \phi$,

$$|\phi(t, j)|_\mathcal{A}^2 \leq \frac{\alpha_2}{\alpha_1} \lambda_d^j |\phi(0, 0)|_\mathcal{A}^2 + \frac{\rho}{\alpha_1} \frac{1 - \lambda_d^j}{1 - \lambda_d} |\zeta|_\infty^2. \tag{7.87}$$

Since $|\zeta|_\infty^2 \leq 2|K_m|^2 |m|_\infty^2 + 2|K_c|^2 |c|_\infty^2$, it follows that, for each $(t, j) \in \operatorname{dom} \phi$,

$$|\phi(t, j)|_\mathcal{A} \leq \max\left\{\sqrt{2\frac{\alpha_2}{\alpha_1}} \lambda_d^{j/2} |\phi(0, 0)|_\mathcal{A}, 2\sqrt{\frac{\rho}{\alpha_1} \frac{1 - \lambda_d^j}{1 - \lambda_d}} |K_m||m|_\infty, 2\sqrt{\frac{\rho}{\alpha_1} \frac{1 - \lambda_d^j}{1 - \lambda_d}} |K_c||c|_\infty\right\}$$

■

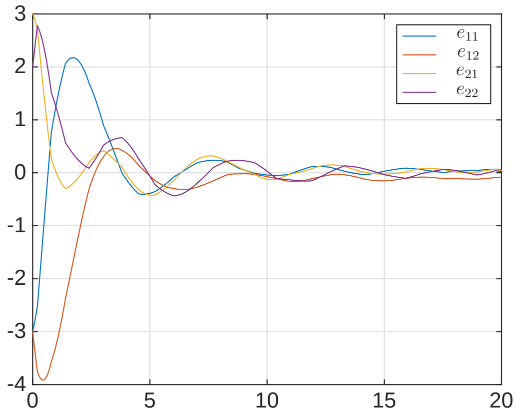

(a) Noise magnitude $a = 0.2$.

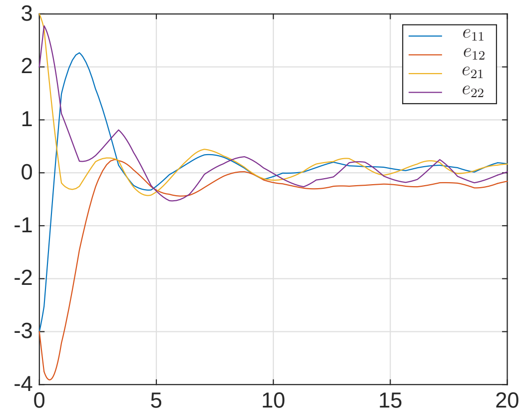

(b) Noise magnitude $a = 0.4$.

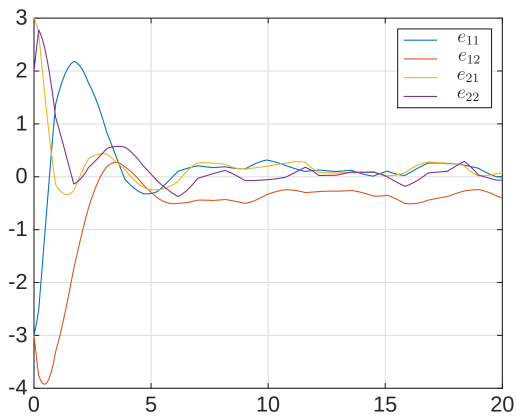

(c) Noise magnitude $a = 0.6$.

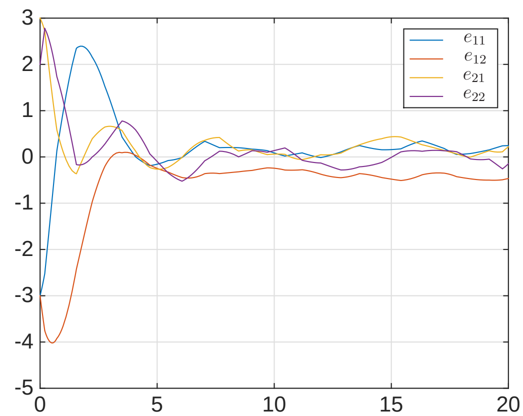

(d) Noise magnitude $a = 0.8$.

Figure 7.4: Effect of measurement and communication noise for the system in Example 7.2.17.

Example 7.2.17 *To show the effect of communication noise and measurement noise, we revisit Example 7.2.4. Moreover, we consider the communication noise and measurement noise is generated randomly and with values in* $[0, a]$*, where* $a \in \mathbb{R}_{\geq 0}$*. With the same set of parameters, four simulations are shown in Figure 7.4. It can be seen that the steady-state estimation error increases with the size of the measurement and communication noises.* $\triangle$

Remark 7.2.18 *Since the hybrid system* $\mathcal{H}_s$ *satisfies the hybrid basic conditions* *and, under the conditions in Theorem 7.2.2, the compact set $\mathcal{A}$ is UGAS for $\mathcal{H}_s$, it follows from [73, Lemma 7.20] that the stability of $\mathcal{A}$ is robust to general small perturbations.* $\square$

7.3 Asynchronous and heterogeneous communication events

7.3.1 Hybrid modeling

Consider N agents that are connected via a directed graph and where each agent runs a local observer of the state x of the linear time-invariant plant in (7.1). Each local observer uses its own measurement and information received from its neighbors. Due to the impulsive nature of such communication mechanism, the communication events are triggered by a decreasing timer τ_i. Namely, τ_i decreases and upon reaching zero it is reset to a point in $[T_1^i, T_2^i]$. Such dynamics of τ_i at agent i can be modeled by a hybrid system given by

$$\dot{\tau}_i = -1 \qquad \tau_i \in [0, T_2^i], \tag{7.88a}$$

$$\tau_i^+ \in [T_1^i, T_2^i] \qquad \tau_i = 0. \tag{7.88b}$$

This hybrid system generates any possible sequence of time instances $\{t_s^i\}_{s=1}^{\infty}$ at which events occur and satisfy (7.3). Note that T_1^i and T_2^i may not be equal for each $i \in \mathcal{V}$, in this way the intervals which observer can update their estimates may be vastly different. Consider the case of $N = 2$, then, at jumps, the timer states τ_1, τ_2 are reset by $\tau_1^+ \in [T_1^1, T_2^1]$ when $\tau_1 = 0$ and $\tau_2^+ \in [T_1^1, 2T_2^1]$ when $\tau_2 = 0$, for such a jump map, τ_1 could potentially jump twice as fast as τ_2.

In this paper, we consider the following dynamics for η_i defining a specific hybrid information fusion strategy:

$$f_{oi}(\hat{x}_i, \eta_i) = h_i \eta_i \tag{7.89}$$

for all $(\hat{x}_i, \eta_i) \in \mathbb{R}^n \times \mathbb{R}^n$, and, for all $(\hat{x}_i, \hat{x}_k, y_i, y_k) \in \mathbb{R}^n \times \mathbb{R}^n \times \mathbb{R}^{p_i} \times \mathbb{R}^{p_k}$,

$$G^k_{oi}(\hat{x}_i, \hat{x}_k, y_i, y_k) = \frac{1}{d_i^{in}} K_{ii} y_i^e + K_{ik} y_k^e + \gamma(\hat{x}_i - \hat{x}_k) \tag{7.90}$$

where, for each $i, k \in \mathcal{V}$, $y_i^e = H_i \hat{x}_i - y_i$, $K_{ik} \in \mathbb{R}^{n \times p_k}$, and $\gamma \in \mathbb{R}$ are the gain matrices for the i-th agent. Note that due to the specific update law in (7.90) and the definition of g_{ik}, the second term in (7.90) uses the output error of each k-th agent that is a neighborhood of the i-th agent, and the third term in (7.90) uses the difference between the estimates $\hat{x}_i$ and $\hat{x}_k$. These are the quantities that are transmitted at communication events. For simplicity, for the rest of the section, we will assume that $\delta \equiv 0$ and $\varphi_i \equiv 0$ for all $i \in \mathcal{V}$, the scenario when they are nonzero are discussed in Section 7.4.

Remark 7.3.1 *When $h_i = 0$ for all $i \in \mathcal{V}$, the hybrid information fusion strategy proposed in* (7.89)-(7.90) *falls into the category of zero-order sample-and-hold control; see, e.g., [90] and [91]. Note that the work in [90] and [91] pertain to single-agent systems and that robustness to measurement and communication noise is not studied.* □

Remark 7.3.2 *Note that the maps f_{oi} and G_{oi} enable a rich choices of dynamics for the variable η_i, although not pursued in this paper due to space limitation, one can potentially choose a sliding mode-like dynamics, for example, see [94].*

Inspired by the idea in [95], let $e_i = \hat{x}_i - x$ and $e = (e_1, \cdots, e_N)$, $\theta = (\theta_1, \cdots, \theta_N)$, $\tau = (\tau_1, \cdots, \tau_N)$, and

$$\theta_i = K_{ii} y_i^e + \sum_{k \in \mathcal{V}} g_{ik} K_{ik} y_k^e + \gamma \sum_{k \in \mathcal{V}} g_{ik}(e_i - e_k) - \eta_i. \tag{7.91}$$

Then, the resulting closed-loop system is given by the interconnection between the plant in (7.1), all local observers and the dynamics of the information fusion state in (7.4)-(7.7). In particular, the resulting system in coordinates e, θ and τ can be written as a hybrid system $\mathcal{H} = (C, f, D, G)$ with state $\chi = (\sigma, \tau) \in \mathcal{X} := \mathbb{R}^{nN} \times \mathbb{R}^{nN} \times \mathcal{T}_0$, where $\mathcal{T}_0 = [0, T_2^1] \times \cdots \times [0, T_2^N]$, $\sigma = (e, \theta)$, and has data given by

$$f(\chi) := (A_{f\theta}\sigma, -\mathbf{1}_N) \tag{7.92}$$

for each $\chi \in C = \mathcal{X}$, and

$$G(\chi) := \{G_i(\chi) : \chi \in D_i, i \in \mathcal{V}\} \tag{7.93}$$

when $\chi \in D = \bigcup_{i \in \mathcal{V}} D_i$, $D_i = \{\chi \in C : \tau_i = 0\}$,

$$G_i(\chi) = \begin{bmatrix} e \\ (\theta_1, \theta_2, \cdots, \theta_{i-1}, 0, \theta_{i+1}, \cdots, \theta_N) \\ (\tau_1, \tau_2, \cdots, \tau_{i-1}, [T_1^i, T_2^i], \tau_{i+1}, \cdots, \tau_N) \end{bmatrix},$$

where

$$A_{f\theta} = \begin{bmatrix} A_\theta & -I_{nN} \\ \mathcal{K}\widetilde{A}_\theta & -\widetilde{\mathcal{K}} \end{bmatrix}, \tag{7.94}$$

$A_\theta = I_N \otimes A + \mathcal{K}$, $\widetilde{A}_\theta = A_\theta - H_\eta$, $\mathcal{K} = K_g H_g * (I_N + \mathcal{G}) + \gamma \mathcal{L} \otimes I_n$, and $\widetilde{\mathcal{K}} = \mathcal{K} - H_\eta$, the matrices $H_g = \mathrm{diag}(H_1, H_2, \ldots, H_N)$ and $H_\eta = \mathrm{diag}(h_1 I_n, h_2 I_n, \ldots, h_N I_n)$ are block diagonal and $K_g \in \mathbb{R}^{nN \times p}$ is a $N \times N$ block matrix with the (i,k)-th entry given by $K_{ik} \in \mathbb{R}^{n \times p_k}$ for all $i, k \in \mathcal{V}$ with $p = \sum_{i \in \mathcal{V}} p_i$. Note that the operation "$*$" denotes the Khatri-Rao product, where the matrix $K_g H_g$ is treated as a $N \times N$ block matrix. As the objective of each agent is to estimate the state x of the plant, i.e., for each $i \in \mathcal{V}$, make $\hat{x}_i$ converge to x asymptotically, and since η_i approaches zero as e_i approaches zero, the set of interest is defined as $\mathcal{A} = \{0_{nN}\} \times \{0_{nN}\} \times \mathcal{T}_0$.

Remark 7.3.3 *The dynamics in* (7.90) *requires the transmission of measurements y_i's and estimates $\hat{x}_i$'s through the network. As we will show later (Example 7.3.9), the transmission of $\hat{x}_i$'s are essential as when certain agents does not have enough information directly from measurements, the consensus term $\gamma(\hat{x}_i - \hat{x}_k)$ enables the reconstruction of state x. Similar arguments apply to the transmission of y_i's.*

Remark 7.3.4 *Note that the flow set C and the jump set D are closed. Moreover, the flow map f is continuous and the jump map and the jump map G is outer semicontinuous* [7]. *Therefore, the hybrid system $\mathcal{H}$ satisfies the hybrid basic conditions. Note that satisfying the hybrid basic conditions implies that the hybrid system $\mathcal{H}$ is well-posed and, with asymptotic stability of a compact set, leads to robustness to small enough perturbations; see Section 7.4.1 for more information.*

7.3.2 Properties of solutions

As mentioned in Section 7.1, solutions to general hybrid systems $\mathcal{H}$ can evolve continuously and/or discretely depending on the continuous and discrete dynamics

[7] A set-valued mapping $G : \mathbb{R}^n \rightrightarrows \mathbb{R}^n$ is outer semicontinuous if its graph $\{(x, y) : x \in \mathbb{R}^n,\ y \in G(x)\}$ is closed; see [73, Lemma 5.10].

and the sets where those dynamics apply. We treat the number of jumps as an independent variable j and the time of flow by the independent variable t.

Due to the fact that the timer variables being zero is the only trigger of the jump map, properties on the domain of solutions can be characterized in the following results.

Lemma 7.3.5 *Given $0 < T_1^i \leq T_2^i$ for all $i \in \mathcal{V}$. Every $\phi \in \mathcal{S}_{\mathcal{H}}$ satisfies the following:*

1. *ϕ is complete, i.e., $\operatorname{dom}\phi$ is unbounded in both t and j directions;*

2. *for each $(t, j) \in \operatorname{dom}\phi$, $\frac{j}{2N}\min_{i\in\mathcal{V}} T_1^i \leq t \leq \frac{j}{N}\max_{i\in\mathcal{V}} T_2^i$.*

Proof For any given $\phi \in \mathcal{S}_{\mathcal{H}}$, for any $(t, j) \in \operatorname{dom}\phi$, note that within $\min_{i\in\mathcal{V}} T_1^i$ window, at most all of the N timers can be triggered twice, therefore, $\frac{j}{2N}\min_{i\in\mathcal{V}} T_1^i \leq t$. Similarly, within $\max_{i\in\mathcal{V}} T_2^i$ window, all N timers jump at least once, then, $t \leq \frac{j}{N}\max_{i\in\mathcal{V}} T_2^i$. To see the completeness of maximal solutions to $\mathcal{H}$, note that for any $\chi \in C \setminus D$, we have $\mathbb{T}_{C\setminus D}(\chi) \cap f(\chi) \neq \emptyset$. [8] Moreover, when $\chi \in C \cap D$, solutions cannot be extended via flow. Furthermore, $G(D) \subset C \cup D$. Therefore, according to [73, Proposition 6.10], the maximal solution ϕ is complete. ■

7.3.3 Sufficient conditions for global exponential stability

In this section, we establish sufficient conditions that guarantee the GES property of the set $\mathcal{A}$ for $\mathcal{H}$. Then, we have the following result.

Theorem 7.3.6 *Let $0 < T_1^i \leq T_2^i$ be given for all $i \in \mathcal{V}$. Suppose N agents are connected via a digraph $\Gamma = (\mathcal{V}, \mathcal{E}, \mathcal{G})$. Moreover, suppose there exist $\delta > 0$*

[8] $\mathbb{T}(\chi)$ denotes the tangent cone to the set $C \setminus D$ at χ, see [73, Definition 5.12].

and matrices $K_g \in \mathbb{R}^{nN\times p}$, $P \in \mathbb{R}^{nN\times nN}, Q_i \in \mathbb{R}^{n\times n}$ *satisfying* $P = P^\top > 0$, $Q_i = Q_i^\top > 0$ *for all* $i \in \mathcal{V}$, *and*

$$\begin{bmatrix} \mathrm{He}(A_\theta, P) & -P + \widetilde{A}_\theta^\top \mathcal{K}^\top \widetilde{Q}(\nu) \\ \star & -\delta\widetilde{Q}(\nu) - \mathrm{He}(\widetilde{\mathcal{K}}, \widetilde{Q}(\nu)) \end{bmatrix} < 0 \tag{7.95}$$

for all $\nu = (\nu_1, \nu_2, \ldots, \nu_N) \in \mathcal{T}_0$, *where* $\widetilde{Q}(\nu) = \mathrm{diag}\left(\widetilde{Q}_1(\nu_1), \widetilde{Q}_2(\nu_2), \cdots, \widetilde{Q}_N(\nu_N)\right)$ *and* $\widetilde{Q}_i(\nu_i) = \exp(\delta\nu_i)Q_i$ *for each* $i \in \mathcal{V}$. *Then, the set* $\mathcal{A}$ *is GES for the hybrid system* $\mathcal{H}$.

Proof Consider the Lyapunov function candidate $V : \mathcal{X} \to \mathbb{R}_{\geq 0}$ given by

$$V(\chi) = e^\top P e + \theta^\top \widetilde{Q}(\tau)\theta. \tag{7.96}$$

It follows that

$$\alpha_1 |\chi|^2_{\mathcal{A}} \leq V(\chi) \leq \alpha_2 |\chi|^2_{\mathcal{A}} \tag{7.97}$$

for all $\chi \in C$, where

$$\alpha_1 = \min\left\{\underline{\lambda}(P), \underline{\lambda}\left(\widetilde{Q}(0)\right)\right\}, \tag{7.98}$$

$$\alpha_2 = \max\left\{\overline{\lambda}(P), \overline{\lambda}\left(\widetilde{Q}(T_2)\right)\right\}. \tag{7.99}$$

Since the gradient of V is given by

$$\nabla V(\chi) = \left(2Pe, 2\widetilde{Q}(\tau)\theta, \delta\,\mathrm{diag}(\theta)\widetilde{Q}(\tau)\,\mathrm{diag}(\theta)\mathbf{1}_N\right),$$

where $\operatorname{diag}(\theta) = \operatorname{diag}(\theta_1, \theta_2, \dots, \theta_N)$. Then, for each $\chi \in C$, we have

$$\begin{aligned}
\langle \nabla V(\chi), f_a(\chi) \rangle &= e^\top \operatorname{He}(A_\theta, P)e - 2e^\top P\theta + 2\theta^\top \widetilde{Q}(\tau)\mathcal{K}\widetilde{A}_\theta e \\
&\quad - \theta^\top \operatorname{He}(\widetilde{\mathcal{K}}, \widetilde{Q}(\tau))\theta - \delta\theta^\top \widetilde{Q}(\tau)\theta \\
&= \begin{bmatrix} e \\ \theta \end{bmatrix}^\top \begin{bmatrix} \operatorname{He}(A_\theta, P) & -P + \widetilde{A}_\theta^\top \mathcal{K}^\top \widetilde{Q}(\tau) \\ -P + \widetilde{Q}(\tau)\mathcal{K}\widetilde{A}_\theta & -\delta\widetilde{Q}(\tau) - \operatorname{He}(\widetilde{\mathcal{K}}, \widetilde{Q}(\tau)) \end{bmatrix} \begin{bmatrix} e \\ \theta \end{bmatrix}.
\end{aligned}$$

Therefore, by using (7.95), we have

$$\langle \nabla V(\chi), f(\chi) \rangle < -\beta |\chi|_{\mathcal{A}}^2, \quad \forall \chi \in C \setminus \mathcal{A}, \tag{7.100}$$

where $\beta = -\overline{\lambda}(\mathcal{M})$ and

$$\mathcal{M} = \begin{bmatrix} \operatorname{He}(A_\theta, P) & -P + \widetilde{A}_\theta^\top \mathcal{K}^\top \widetilde{Q}(\tau) \\ -P + \widetilde{Q}(\tau)\mathcal{K}\widetilde{A}_\theta & -\delta\widetilde{Q}(\tau) - \operatorname{He}(\widetilde{\mathcal{K}}, \widetilde{Q}(\tau)) \end{bmatrix}. \tag{7.101}$$

Moreover, for each $\chi = (e, \theta, \tau) \in D$ and for each $g \in G(\chi)$, there exists at least one component of τ, say, the i-th component, such that $\tau_i = 0$. Then, at jumps we have

$$V(g) - V(\chi) \leq -\theta_i^\top Q_i \theta_i \leq 0 \tag{7.102}$$

Then, for a given $\phi \in \mathcal{S}_{\mathcal{H}}$, for any $(t, j) \in \operatorname{dom}\phi$ and let $0 = t_0 \leq t_1 \leq \cdots \leq t_{j+1} \leq t$ satisfy

$$\operatorname{dom}\phi \bigcap ([0, t_{j+1}] \times \{0, \dots, j\}) = \bigcup_{s=0}^{j} [t_s, t_{s+1}] \times \{s\}.$$

For each $s \in \{0, \ldots, j\}$ and almost all $r \in [t_s, t_{s+1}]$, $\phi(r, i) \in C$. Then, (7.95) implies that, for each $s \in \{0, \ldots, j\}$ and for almost all $r \in [t_s, t_{s+1}]$,

$$\frac{d}{dr}V(\phi(r,i)) \leq -\beta|\phi(r,i)|^2_{\mathcal{A}} \leq -\frac{\beta}{\alpha_2}V(\phi(r,i)). \tag{7.103}$$

Integrating both sides of this inequality yields

$$V(\phi(t_{s+1}, s)) \leq \exp\left(-\frac{\beta}{\alpha_2}(t_{s+1} - t_s)\right)V(\phi(t_s, s)) \quad \forall s \in \{0, \ldots, j\}. \tag{7.104}$$

Similarly, for each $s \in \{1, \ldots, j\}$, $\phi(t_s, s-1) \in D$, and thus

$$V(\phi(t_s, s)) - V(\phi(t_s, s-1)) \leq 0 \quad \forall s \in \{1, \ldots, j\}. \tag{7.105}$$

The last two displayed inequalities imply that

$$V(\phi(t,j)) \leq \exp\left(-\frac{\beta}{\alpha_2}t\right)V(\phi(0,0)). \tag{7.106}$$

Therefore, by using (7.97), for any $(t, j) \in \operatorname{dom}\phi$,

$$\phi(t,j) \leq \sqrt{\frac{\alpha_2}{\alpha_1}}\exp\left(-\frac{\beta}{2\alpha_2}t\right)|\phi(0,0)|_{\mathcal{A}}. \tag{7.107}$$

From Lemma 7.3.5, we have that $t \geq \frac{j}{2N}T_1$ which implies that

$$\begin{aligned}
\phi(t,j) &\leq \sqrt{\frac{\alpha_2}{\alpha_1}}\exp\left(-\frac{\beta}{2\alpha_2}t\right)|\phi(0,0)|_{\mathcal{A}} \\
&\leq \sqrt{\frac{\alpha_2}{\alpha_1}}\exp\left(-\frac{\beta}{2\alpha_2}\left(\frac{1}{2}t + \frac{T_1}{4N}j\right)\right)|\phi(0,0)|_{\mathcal{A}} \\
&\leq \sqrt{\frac{\alpha_2}{\alpha_1}}\exp\left(-\frac{\beta}{4\alpha_2}\min\left\{1, \frac{T_1}{2N}\right\}(t+j)\right)|\phi(0,0)|_{\mathcal{A}}
\end{aligned}$$

Furthermore, the set $\mathcal{A}$ is GES for $\mathcal{H}$. ■

Note that condition (7.95) needs to be checked over a closed set $\mathcal{T}_0$, which might be a difficult task. The following result relaxes this requirement.

Proposition 7.3.7 *Let $T_2^i > 0$ be given for each $i \in \mathcal{V}$. The inequality in (7.95) holds if there exists $\delta > 0$ and matrices $K_g \in \mathbb{R}^{nN\times p}$, $P \in \mathbb{R}^{nN\times nN}, Q_i \in \mathbb{R}^{n\times n}$ satisfying $P = P^\top > 0$, $Q_i = Q_i^\top > 0$ for all $i \in \mathcal{V}$ such that*

$$\begin{bmatrix} \mathrm{He}(A_\theta, P) & -P+\widetilde{A}_\theta^\top \mathcal{K}^\top Q \\ \star & -\delta Q - \mathrm{He}(\widetilde{\mathcal{K}}, Q) \end{bmatrix} < 0, \tag{7.108}$$

$$\begin{bmatrix} \mathrm{He}(A_\theta, P) & -P+\widetilde{A}_\theta^\top \mathcal{K}^\top \overline{E} Q \\ \star & -(\delta \overline{E} Q+\mathrm{He}(\widetilde{\mathcal{K}}, \overline{E} Q)) \end{bmatrix} < 0, \tag{7.109}$$

where $Q = \mathrm{diag}(Q_1, \ldots, Q_N)$ and $\overline{E} = \mathrm{diag}(\exp(\delta T_2^1), \ldots, \exp(\delta T_2^N)) \otimes I_n$.

Proof Given $T_2^i > 0$ for all $i \in \mathcal{V}$ and $\delta > 0$, for each $i \in \mathcal{V}$, define a function $r_i : [0, T_2^i] \to [0, 1]$ as

$$r_i(\nu_i) = \frac{\exp(\delta\nu_i) - \exp(\delta T_2^i)}{1 - \exp(\delta T_2^i)}$$

for all $\nu_i \in [0, T_2^i]$. Then, it can be verified that, for any $i \in \mathcal{V}$ and for any $\nu_i \in [0, T_2^i]$,

$$\exp(\delta\nu_i) = r_i(\nu_i) + (1 - r_i(\nu_i)) \exp(\delta T_2^i). \tag{7.110}$$

Therefore, for each $\nu \in \mathcal{T}_0$,

$$\widetilde{Q}(\nu) = \overline{R}(\nu)\widetilde{Q}(0) + (I - \overline{R}(\nu))\widetilde{Q}(\overline{T}_2), \tag{7.111}$$

where $\nu = (\nu_1, \nu_2, \cdots, \nu_N)$, $\overline{T}_2 = (T_2^1, \ldots, T_2^N)$ and

$$\overline{R}(\nu) = \mathrm{diag}(r_1(\nu_1), \cdots, r_N(\nu_N)) \otimes I_n. \tag{7.112}$$

Then, inequality (7.95) can be rewritten as

$$\begin{bmatrix} \mathrm{He}(A_\theta, P) & -P + \widetilde{A}_\theta^\top \mathcal{K}^\top Q(\nu) \\ -P + Q(\nu)\mathcal{K}\widetilde{A}_\theta & -\delta Q(\nu) - \mathrm{He}(\widetilde{\mathcal{K}}, Q(\nu)) \end{bmatrix} = \overline{R}(\nu)E_1 + (I - \overline{R}(\nu))E_2,$$

$$= \mathcal{B}_1(\nu)E_1\mathcal{B}_1(\nu) + \mathcal{B}_2(\nu)E_2\mathcal{B}_2(\nu)$$

where

$$E_1 = \begin{bmatrix} \mathrm{He}(A_\theta, P) & -P + \widetilde{A}_\theta^\top \mathcal{K}^\top \widetilde{Q}(0) \\ -P + \widetilde{Q}(0)\mathcal{K}\widetilde{A}_\theta & -\delta\widetilde{Q}(0) - \mathrm{He}(\widetilde{\mathcal{K}}, \widetilde{Q}(0)) \end{bmatrix}, \tag{7.113}$$

$$E_2 = \begin{bmatrix} \mathrm{He}(A_\theta, P) & -P + \widetilde{A}_\theta^\top \mathcal{K}^\top \widetilde{Q}(\overline{T}_2) \\ -P + \widetilde{Q}(\overline{T}_2)\mathcal{K}\widetilde{A}_\theta & -(\delta\widetilde{Q}(\overline{T}_2) + \mathrm{He}(\widetilde{\mathcal{K}}, \widetilde{Q}(\overline{T}_2))) \end{bmatrix}, \tag{7.114}$$

$$\mathcal{B}_1(\nu) = \mathrm{diag}\left(\sqrt{r_1(\nu_1)}, \sqrt{r_2(\nu_2)}, \cdots, \sqrt{r_N(\nu_N)}\right) \otimes I_n, \tag{7.115}$$

$$\mathcal{B}_1(\nu) = \mathrm{diag}\left(\sqrt{1 - r_1(\nu_1)}, \sqrt{1 - r_2(\nu_2)}, \cdots, \sqrt{1 - r_N(\nu_N)}\right) \otimes I_n. \tag{7.116}$$

By using (7.108) and (7.109), $E_1 < 0$ and $E_2 < 0$ and (7.95) holds for each $\nu \in \mathcal{T}_0$.

■

Example 7.3.8 *Consider an oscillatory plant with data given by*

$$A = \begin{bmatrix} 0 & -1 \\ 1 & 0 \end{bmatrix}. \tag{7.117}$$

Consider the case of two agents that are all-to-all connected, namely,

$$\mathcal{G} = \begin{bmatrix} 0 & 1 \\ 1 & 0 \end{bmatrix}.$$

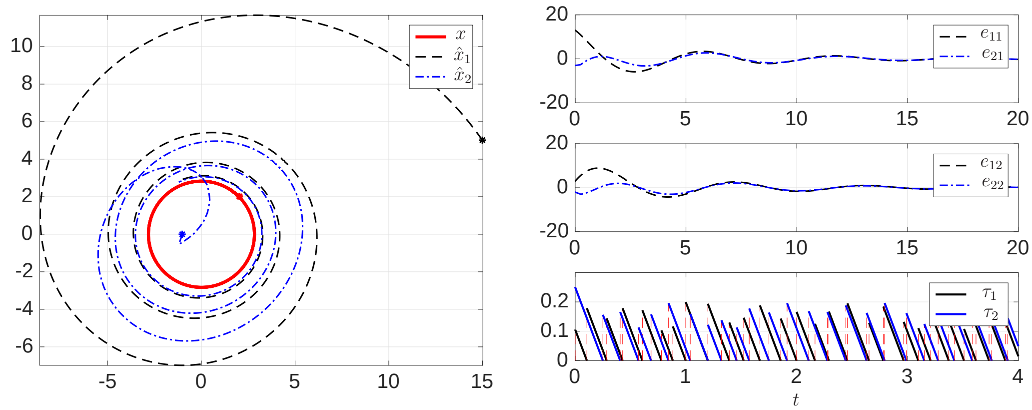

(a) Phase plots of $x, \hat{x}_1, \hat{x}_2$ from initial conditions that are denoted by $*$.

(b) Estimation error and timer states, where $x = (x_1, x_2)$, $\hat{x}_i = (\hat{x}_{i1}, \hat{x}_{i2})$, $e_{i1} = \hat{x}_{i1} - x_1$, $e_{i2} = \hat{x}_{i2} - x_2$, for $i \in \{1, 2\}$.

Figure 7.5: Phase plots of $x, \hat{x}_1$ and $\hat{x}_2$ as well as estimation errors e_1 and e_2 for two all-to-all connected agents using the observer in Example 7.3.8. Initial conditions are $x(0,0) = (2,2)$, $\hat{x}_1(0,0) = (5,5)$, $\hat{x}_2(0,0) = (-1,0)$, $\eta_1(0,0) = (1,1)$, $\eta_2(0,0) = (-1,-1)$, $\tau_1(0,0) = 0.1$ and $\tau_2(0,0) = 0.25$.

Let the measurements of x at agent 1 be

$$y_1 = H_1 x, \quad H_1 = [1 \quad 0]$$

and the measurements at agent 2 be

$$y_2 = H_2 x, \quad H_2 = [0 \quad 1].$$

By solving inequalities[9] (7.108) *and* (7.109) *in Proposition 7.3.11, we obtain the following parameters:*

$$K_{11} = \begin{bmatrix} -0.5 & -0.2 \end{bmatrix}^\top, \quad K_{12} = \begin{bmatrix} -0.2 & -0.2 \end{bmatrix}^\top,$$
$$K_{21} = \begin{bmatrix} 0.2 & 0.3 \end{bmatrix}^\top, \quad K_{22} = \begin{bmatrix} -0.1 & -0.5 \end{bmatrix}^\top,$$

[9]Note that the inequality in (7.108) and (7.109) are not linear. The tool developed in [87] provides a way to solve it.

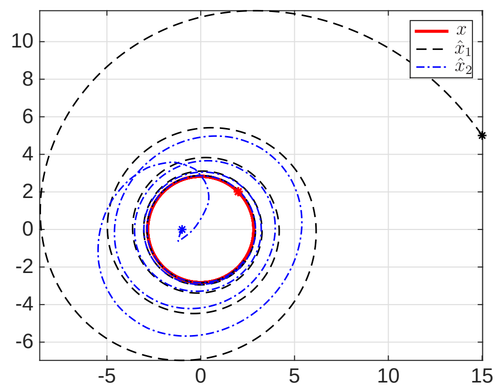

(a) Phase plots of $x, \hat{x}_1, \hat{x}_2$ from initial conditions that are denoted by $*$.

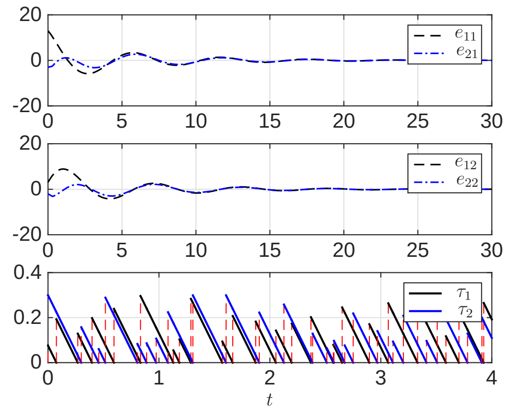

(b) Estimation errors for both components and two timer states.

Figure 7.6: Phase plots and estimation errors for the observer in Example 7.3.8. The gain used is $\gamma = -0.4$ while the rest of the parameters are the same as those used for the simulations in Figure 7.5.

with $h_1 = h_2 = 0$, $\gamma = -0.1$, $T_2^1 = T_2^2 = 0.2$, $\delta = 10$. *A simulation with these parameters is shown in Figure 7.5. The estimates* $\hat{x}_1$ *and* $\hat{x}_2$ *converge to* x *asymptotically as guaranteed by Proposition 7.3.11.*[10]

More interestingly, consider the scenario where agent 1 *loses the capability of receiving measurements, i.e.,* $H_1 = 0$. *A simulation with same initial conditions and gains as those in Figure 7.5 is shown in Figure 7.6. As suggested from the simulation, it can be seen that even though the agent has measurement* $y_1 \equiv 0$, *through the consensus-like term (the third term in* (7.90)*), the components* $\hat{x}_1$ *and* $\hat{x}_2$ *reach consensus first and then converge to* x *asymptotically. This highlights further a benefit of the third term in the dynamics of* η *in* (7.90). *In fact, the third term enforces consensus between the estimates* $\hat{x}_1$ *and* $\hat{x}_2$. *Another benefit of using this term will be seen in the next example.* $\triangle$

Next, we consider a situation with two connected agents, where, if communication between them is not possible, they cannot estimate the state of the plant

[10] Code at `https://github.com/HybridSystemsLab/ObsSyncTimes2ndAsyn`.

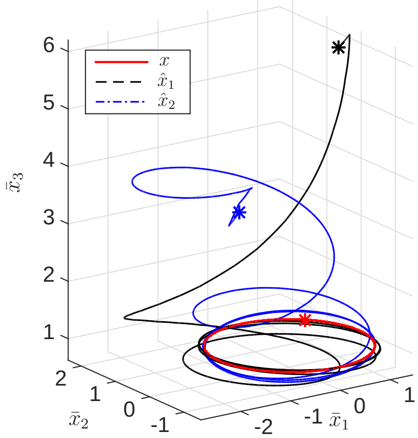

(a) Phase plots of $x, \hat{x}_1, \hat{x}_2$ from initial conditions that are denoted by $*$.

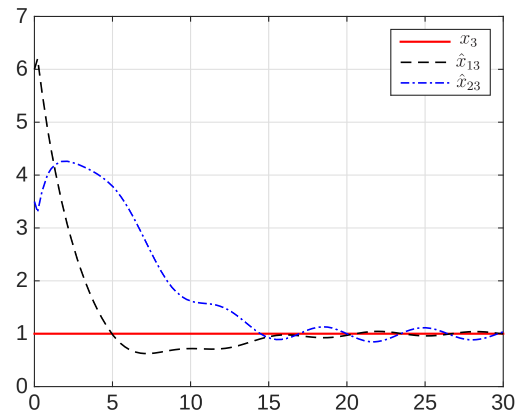

(b) Estimation error for the third state component.

Figure 7.7: Phase portrait and estimation errors for the third state component for the system in Example 7.3.9, where $x = (x_1, x_2, x_3)$, $\hat{x}_i = (\hat{x}_{i1}, \hat{x}_{i2}, \hat{x}_{i3})$, $e_{ik} = \hat{x}_{ik} - x_k$, for $i \in \{1, 2\}, k \in \{1, 2, 3\}$. Initial conditions are $x(0, 0) = (1, 1, 1)$, $\hat{x}_1(0, 0) = (1, 0, 6)$, $\eta_1(0, 0) = (1, 1, 1)$, $\hat{x}_2(0, 0) = (-1, 0, 3.5)$, $\eta_2(0, 0) = (-1, -1, -1)$, $\tau_1(0, 0) = 0.2$ and $\tau_2(0, 0) = 0$.

individually. However, when the information is shared between them, our observer guarantees that the state of each agent converges to the state of the plant asymptotically.

Example 7.3.9 *Consider a plant with state $x = (x_1, x_2, x_3) \in \mathbb{R}^3$ that has oscillatory dynamics for (x_1, x_2) and trivial dynamics for x_3, in particular,*

$$A = \begin{bmatrix} 0 & -1 & 0 \\ 1 & 0 & 0 \\ 0 & 0 & 0 \end{bmatrix}. \tag{7.118}$$

Consider the case of two agents that are all-to-all connected and measure x according to (7.2) *with*

$$H_1 = [0 \;\; 0 \;\; 1], \quad H_2 = [1 \;\; 1 \;\; 0].$$

Since the pairs (H_1, A) and (H_2, A) are not detectable, neither agent can estimate the full state of the plant by running an observer that does not use information from the other agent. However, when communication between agents is allowed, our observer would be able to reconstruct x. In fact, given $T_1 = 0.2$ and $T_2 = 0.4$, by solving conditions in (7.108) and (7.109), we obtain the following parameters:

$$K_{11} = \begin{bmatrix} -0.5 & -0.2 & -0.1 \end{bmatrix}^\top, \qquad K_{12} = \begin{bmatrix} -0.2 & -0.2 & -0.5 \end{bmatrix}^\top,$$
$$K_{21} = \begin{bmatrix} 0.2 & 0.3 & 0.3 \end{bmatrix}^\top, \qquad K_{22} = \begin{bmatrix} -0.1 & -0.5 & 0.2 \end{bmatrix}^\top,$$

$h_1 = h_2 = 0$, $\delta = 10$, and gain $\gamma = -0.4$. The simulation shown in Figure 7.7 indicates that the estimates $\hat{x}_1$ and $\hat{x}_2$ converge to x asymptotically. Figure 7.7(a) shows the trajectory of $x = (x_1, x_2, x_3)$, and the observer states $\hat{x}_1 = (\hat{x}_{11}, \hat{x}_{12}, \hat{x}_{13})$, $\hat{x}_2 = (\hat{x}_{21}, \hat{x}_{22}, \hat{x}_{23})$. Figure 7.7(b) shows their third components, denoted x_3, $\hat{x}_{13}$ and $\hat{x}_{23}$. [11] *Note that even though the data in this example would satisfy the conditions in [56], in our setting the information is arriving at different times, which makes the reconstruction of the state not possible with the results therein.*

$\triangle$

Example 7.3.10 *Consider a plant with state $x = (x_1, x_2, x_3) \in \mathbb{R}^3$ that has unstable dynamics, in particular,*

$$A = \begin{bmatrix} 0.1 & 0 & 0 \\ 0 & 0.1 & 0 \\ 0 & 0 & 0.1 \end{bmatrix}. \tag{7.119}$$

[11] Code at `https://github.com/HybridSystemsLab/ObsSyncTimes3rdAsyn`.

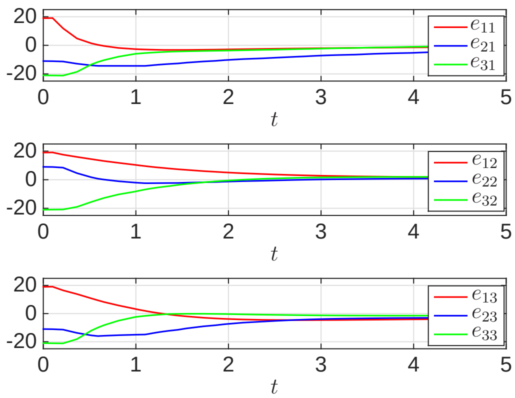

(a) Estimation error for each components.

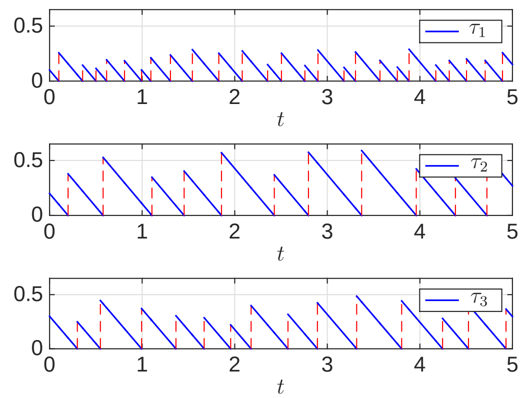

(b) Trajectories of timer states.

Figure 7.8: Trajectories for Example 7.3.10, for $i \in \{1, 2, 3\}$, the estimate $\hat{x}_i = (\hat{x}_{i1}, \hat{x}_{i2}, \hat{x}_{i3})$, and the estimation error $e_i = (e_{i1}, e_{i2}, e_{i3}) = \hat{x}_i - x_i$.

Consider the case of three agents that are circularly connected with

$$\mathcal{G} = \begin{bmatrix} 0 & 1 & 0 \\ 0 & 0 & 1 \\ 1 & 0 & 0 \end{bmatrix}$$

and measure x according to (7.2) *with*

$$H_1 = \begin{bmatrix} 1 & 0 & 0 \end{bmatrix}, \quad H_2 = \begin{bmatrix} 0 & 1 & 0 \end{bmatrix}, \quad H_3 = \begin{bmatrix} 0 & 0 & 1 \end{bmatrix}.$$

Since the pairs (H_i, A)*'s are not detectable for all $i \in \mathcal{V}$, neither agent can estimate the full state of the plant by running an observer that does not use information from the other agent. Note that, even though agent* 1 *can access both y_1 and y_2 when $\tau_1 = 0$, the combination of measurements* $(H_1 + H_2, A)$ *is also not detectable. However, when communication between agents is allowed over the network with adjacency matrix $\mathcal{G}$, each agent would be able to reconstruct x. In fact, given* $T_1^2 = 0.3$, $T_2^2 = 0.6$ *and* $T_3^2 = 0.5$, *by solving conditions in* (7.108) *and* (7.109),

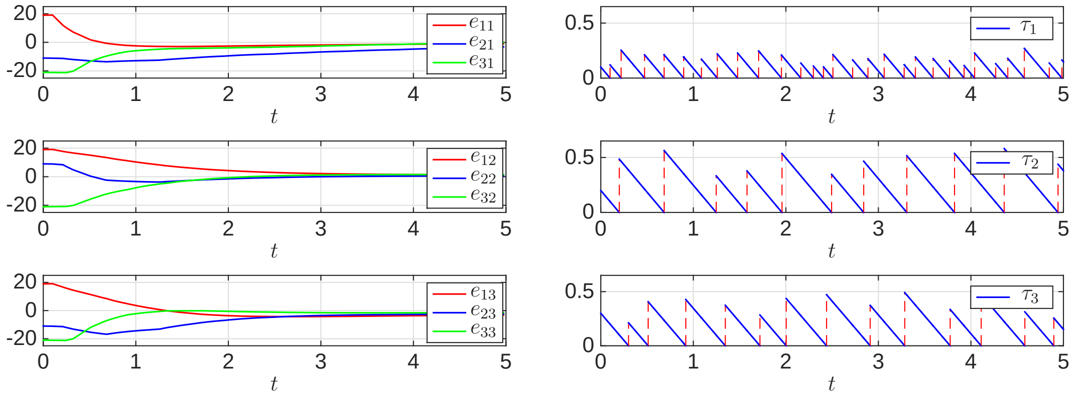

(a) Estimation error for each components. (b) Trajectories of timer states.

Figure 7.9: Trajectories for Example 7.3.10, for $i \in \{1,2,3\}$, the estimate $\hat{x}_i = (\hat{x}_{i1}, \hat{x}_{i2}, \hat{x}_{i3})$, and the estimation error $e_i = (e_{i1}, e_{i2}, e_{i3}) = \hat{x}_i - x_i$.

we obtain the following parameters:

$$K_{11} = \begin{bmatrix} -1.5 & -0.3 & 0 \end{bmatrix}^\top, \qquad K_{12} = \begin{bmatrix} 0 & -0.2 & -0.2 \end{bmatrix}^\top,$$
$$K_{22} = \begin{bmatrix} 0 & -1.5 & 1.2 \end{bmatrix}^\top, \qquad K_{23} = \begin{bmatrix} 0.2 & -0.3 & 0 \end{bmatrix}^\top,$$
$$K_{31} = \begin{bmatrix} -0.2 & 0 & -0.3 \end{bmatrix}^\top, \qquad K_{33} = \begin{bmatrix} -1.1 & 0 & -1.2 \end{bmatrix}^\top,$$

$h_1 = -2.2, h_2 = -2.1, h_3 = -2.1$, $\delta = 10$, *and gain* $\gamma = -0.8$. *The simulation shown in Figure 7.8 indicates that the estimates* $\hat{x}_i$*'s converge to* x *asymptotically. Note that even though the data in this example would satisfy the conditions in [56], in our setting the information is arriving at different times, which makes the reconstruction of the state not possible with the results therein.*

More interestingly, for $i \in \{1,2,3\}$, *when a timer* $\tau_i = 0$, *if the information* y_k *is not available anymore for* $k \in \mathcal{N}(i)$, *then the second term in* (7.90) *vanishes, namely,* $K_{ik} = 0$ *for* $k \in \mathcal{N}(i)$. *It can be verified that the same set of parameters with* $K_{12} = K_{23} = K_{31} = 0$ *also satisfies the conditions in* (7.108) *and* (7.109). *A* *simulation of this scenario is in Figure 7.9.* △

We can further relax the conditions in Proposition 7.3.11 as follows.

Proposition 7.3.11 *Let $T_2^i > 0$ be given for each $i \in \mathcal{V}$. The inequality in* (7.95) *holds if there exists $\delta > 0$ and matrices $K_g \in \mathbb{R}^{nN\times p}$, $P \in \mathbb{R}^{nN\times nN}, Q_i \in \mathbb{R}^{n\times n}$ satisfying $P = P^\top > 0$, $Q_i = Q_i^\top > 0$ for all $i \in \mathcal{V}$ such that*

$$\begin{bmatrix} \mathrm{He}(A_\theta, P) & -P + \widetilde{A}_\theta^\top \mathcal{K}^\top Q \\ \star & -\delta Q - \mathrm{He}(\widetilde{\mathcal{K}}, Q) \end{bmatrix} < 0, \tag{7.120}$$

$$\begin{bmatrix} \mathrm{He}(A_\theta, P) & -P + \exp(\delta T_2^{\max}) \widetilde{A}_\theta^\top \mathcal{K}^\top Q \\ \star & -\exp(\delta T_2^{\max})(\delta Q + \mathrm{He}(\widetilde{\mathcal{K}}, Q)) \end{bmatrix} < 0, \tag{7.121}$$

where $Q = \mathrm{diag}(Q_1, \ldots, Q_N)$ and $T_2^{\max} = \max_{i\in\mathcal{V}} T_2^i$.

Proof First, note that if the inequality in (7.95) holds for all $\nu = (\nu_1, \nu_2, \ldots, \nu_N) \in [0, T_2^{\max}]^N$, it holds for all $\nu = (\nu_1, \nu_2, \ldots, \nu_N) \in \mathcal{T}_0$. Then, the result follows by applying Proposition 7.3.11. ■

Remark 7.3.12 *In practice, one may want to search for parameters to maximize the allowable value for $T_2^{\max}$ that satisfies* (7.121)*. By doing so, information is allowed to be transmitted at low frequency which in turn reduce the energy consumed, but may take longer for the estimates to converge to the plant dynamics.*

7.3.4 Nominal design of parameters via LMIs

Motivated by the fact that the conditions in (7.108) and (7.109) are nonlinear, in this section, we propose design methods in terms of LMIs. Below, we will use the fact that the matrix $A_{f\theta}$ in (7.94) can be written in the form $A_{f\theta} = \widetilde{A}_1\widetilde{A}_2$, where

$$\widetilde{A}_1 = \begin{bmatrix} I & 0 \\ \mathcal{K} & I \end{bmatrix}, \quad \widetilde{A}_2 = \begin{bmatrix} A_\theta & -I_{nN} \\ -\mathcal{K}H_\eta & H_\eta \end{bmatrix}. \tag{7.122}$$

We have the following result.

Proposition 7.3.13 *Let $T_2^i > 0$ be given. The positive definite symmetric matrices $P, Q \in \mathbb{R}^{nN\times nN}$, the constants $\delta > 0$, $\gamma \in \mathbb{R}$, and the matrices H_η and $K_g \in \mathbb{R}^{nN\times p}$ satisfy conditions* (7.108) *and* (7.109) *if and only if there exist matrices $\mathcal{O}_i, \mathcal{T}_i \in \mathbb{R}^{nN\times nN}, i \in \mathbb{N}, 1 \le i \le 6$, such that*

$$\begin{bmatrix} \mathrm{He}(\Omega_1, I_{2nN}) & \Omega_2 + \widetilde{P}_1 \\ \star & \widetilde{Y} + \mathrm{He}(\Omega_3, I_{2nN}) \end{bmatrix} < 0, \tag{7.123}$$

$$\begin{bmatrix} \mathrm{He}(\Lambda_1, I_{2nN}) & \Lambda_2 + \widetilde{P}_2 \\ \star & \widetilde{Z} + \mathrm{He}(\Lambda_3, I_{2nN}) \end{bmatrix} < 0, \tag{7.124}$$

where

$$\begin{aligned} \widetilde{P}_1 &= \mathrm{diag}(P, Q), \quad \widetilde{Z} = \mathrm{diag}(0_{nN}, -\delta\overline{E}Q), \\ \widetilde{P}_2 &= \mathrm{diag}(P, \overline{E}Q), \quad \widetilde{Y} = \mathrm{diag}(0_{nN}, -\delta Q), \end{aligned} \tag{7.125}$$

and

$$\Omega_1 = \begin{bmatrix} -\mathcal{O}_1 + \mathcal{K}^\top \mathcal{O}_4 & -\mathcal{O}_2 + \mathcal{K}^\top \mathcal{O}_5 \\ -\mathcal{O}_4 & -\mathcal{O}_5 \end{bmatrix}$$

$$\Omega_2 = \begin{bmatrix} \mathcal{O}_1^\top A_\theta - \mathcal{O}_3 + \mathcal{K}^\top \mathcal{O}_6 - \mathcal{O}_4^\top \mathcal{K} H_\eta & -\mathcal{O}_1^\top + \mathcal{O}_4^\top H_\eta \\ \mathcal{O}_2^\top A_\theta - \mathcal{O}_6 - \mathcal{O}_5^\top \mathcal{K} H_\eta & -\mathcal{O}_2^\top + \mathcal{O}_5^\top H_\eta \end{bmatrix}$$

$$\Omega_3 = \begin{bmatrix} A_\theta^\top \mathcal{O}_3 - H_\eta^\top \mathcal{K}^\top \mathcal{O}_6 & 0 \\ -\mathcal{O}_3 + H_\eta \mathcal{O}_6 & 0 \end{bmatrix}$$

$$\Lambda_1 = \begin{bmatrix} -\mathcal{T}_1 + \mathcal{K}^\top \mathcal{T}_4 & -\mathcal{T}_2 + \mathcal{K}^\top \mathcal{T}_5 \\ -\mathcal{T}_4 & -\mathcal{T}_5 \end{bmatrix}$$

$$\Lambda_2 = \begin{bmatrix} \mathcal{T}_1^\top A_\theta - \mathcal{T}_3 + \mathcal{K}^\top \mathcal{T}_6 - \mathcal{T}_4^\top \mathcal{K} H_\eta & -\mathcal{T}_1^\top + \mathcal{T}_4^\top H_\eta \\ \mathcal{T}_2^\top A_\theta - \mathcal{T}_6 - \mathcal{T}_5^\top \mathcal{K} H_\eta & -\mathcal{T}_2^\top + \mathcal{T}_5^\top H_\eta \end{bmatrix}$$

$$\Lambda_3 = \begin{bmatrix} A_\theta^\top \mathcal{T}_3 - H_\eta^\top \mathcal{K}^\top \mathcal{T}_6 & 0 \\ -\mathcal{T}_3 + H_\eta \mathcal{T}_6 & 0 \end{bmatrix}.$$

Proof Let

$$N_{\mathcal{W}} = \begin{bmatrix} A_{f\theta} \\ I \end{bmatrix}, \widetilde{\mathcal{Y}} = \begin{bmatrix} 0 & \widetilde{P}_1 \\ \star & \widetilde{Y} \end{bmatrix}, \widetilde{\mathcal{Z}} = \begin{bmatrix} 0 & \widetilde{P}_2 \\ \star & \widetilde{Z} \end{bmatrix}, N_{\mathcal{Y}} = \begin{bmatrix} 0_{nN} & 0_{nN} & 0_{nN} & I_{nN} \end{bmatrix}^\top. \tag{7.126}$$

Then, inequality (7.108) can be written as

$$E_1 = N_{\mathcal{W}}^\top \widetilde{\mathcal{Y}} N_{\mathcal{W}} < 0, \quad N_{\mathcal{Y}}^\top \widetilde{\mathcal{Y}} N_{\mathcal{Y}} < 0, \tag{7.127}$$

and inequality (7.109) can be written as

$$E_2 = N_{\mathcal{W}}^\top \widetilde{\mathcal{Z}} N_{\mathcal{W}} < 0, \quad N_{\mathcal{Y}}^\top \widetilde{\mathcal{Z}} N_{\mathcal{Y}} < 0. \tag{7.128}$$

Moreover, the columns of $N_{\mathcal{W}}$ (respectively, $N_{\mathcal{Y}}$) form the basis of the null space of $\mathcal{W}$ (respectively, $\mathcal{Y}$), where $\mathcal{W}$ and $\mathcal{Y}$ are given by

$$\mathcal{W} = \begin{bmatrix} -\widetilde{A}_1^{-1} & \widetilde{A}_2 \end{bmatrix} = \begin{bmatrix} -I & 0 & A_\theta & -I_{nN} \\ \mathcal{K} & -I & -\mathcal{K}H_\eta & H_\eta \end{bmatrix}, \tag{7.129}$$

and

$$\mathcal{Y} = \begin{bmatrix} I_{nN} & 0_{nN} & 0_{nN} & 0_{nN} \\ 0_{nN} & I_{nN} & 0_{nN} & 0_{nN} \\ 0_{nN} & 0_{nN} & I_{nN} & 0_{nN} \end{bmatrix}. \tag{7.130}$$

Then, using the projection lemma [93], inequalities (7.127) and (7.128) are equivalent to the existence of two matrices $\mathcal{O}, \mathcal{T} \in \mathbb{R}^{2nN \times 3nN}$ such that

$$\widetilde{\mathcal{Y}} + \mathcal{W}^\top \mathcal{O} \mathcal{Y} + \mathcal{Y}^\top \mathcal{O}^\top \mathcal{W} < 0, \tag{7.131}$$

$$\widetilde{\mathcal{Z}} + \mathcal{W}^\top \mathcal{T} \mathcal{Y} + \mathcal{Y}^\top \mathcal{T}^\top \mathcal{W} < 0. \tag{7.132}$$

Therefore, by letting

$$\mathcal{O} = \begin{bmatrix} \mathcal{O}_1 & \mathcal{O}_2 & \mathcal{O}_3 \\ \mathcal{O}_4 & \mathcal{O}_5 & \mathcal{O}_6 \end{bmatrix}, \quad \mathcal{T} = \begin{bmatrix} \mathcal{T}_1 & \mathcal{T}_2 & \mathcal{T}_3 \\ \mathcal{T}_4 & \mathcal{T}_5 & \mathcal{T}_6 \end{bmatrix}, \tag{7.133}$$

we have

$$\mathcal{W}^\top \mathcal{O}\mathcal{Y} + \mathcal{Y}^\top \mathcal{O}^\top \mathcal{W} + \widetilde{\mathcal{Y}} = \begin{bmatrix} \mathrm{He}(\Omega_1, I) & \Omega_2 + \widetilde{P}_1 \\ \star & \widetilde{Y} + \mathrm{He}(\Omega_3, I) \end{bmatrix}, \tag{7.134}$$

which leads to (7.108). The proof of (7.109) follows similarly. ■

By the transformation in Proposition 7.3.13, it can be seen that in the new set of inequalities (7.123) and (7.124), the cross term $\mathcal{K}\mathcal{K}$ from the multiplication of $\mathcal{K}A_\theta$ in (7.108) and (7.109) vanishes. In fact, the conditions (7.123) and (7.124) lead to several designs by choosing the matrices $\mathcal{O}_i, \mathcal{T}_i \in \mathbb{R}^{nN\times nN}$ properly. The following result illustrates one particular such design when the graph is all-to-all connected.

Corollary 7.3.14 *Let $T_2^i > 0$ be given. The set $\mathcal{A}$ is GES for $\mathcal{H}$ if there exist $\delta > 0$, $\gamma \in \mathbb{R}$ and positive definite symmetric matrices $P \in \mathbb{R}^{nN\times nN}, Q_i \in \mathbb{R}^{n\times n}$ for all $i \in \mathcal{V}$, $\mathcal{Q} \in \mathbb{R}^{nN\times p}$, and $\mathcal{R} \in \mathbb{R}^{nN\times nN}$ such that*

$$\begin{bmatrix} \mathrm{He}(\mathcal{Z}_1, I_{2nN}) & \mathcal{Z}_2 + \widetilde{P}_1 \\ \star & Y + \mathrm{He}(\mathcal{Z}_3, I_{2nN}) \end{bmatrix} < 0, \tag{7.135}$$

$$\begin{bmatrix} \mathrm{He}(\mathcal{Z}_1, I_{2nN}) & \mathcal{Z}_2 + \widetilde{P}_2 \\ \star & Z + \mathrm{He}(\mathcal{Z}_3, I_{2nN}) \end{bmatrix} < 0, \tag{7.136}$$

where $Q = \mathrm{diag}(Q_1, \ldots, Q_N)$ *and* $\widetilde{P}_1, \widetilde{P}_2, Y, Z$ *are in* (7.125), *and*

$$\mathcal{Z}_1 = \begin{bmatrix} -\mathcal{R} + H_g^\top \mathcal{Q} + \widetilde{\mathcal{L}}^\top \mathcal{R} & H_g^\top \mathcal{Q} + \widetilde{\mathcal{L}}^\top \mathcal{R} \\ -\mathcal{R} & -\mathcal{R} \end{bmatrix}, \tag{7.137}$$

$$\mathcal{Z}_2 = \begin{bmatrix} \mathcal{R}^\top \widetilde{A} + \mathrm{He}(\mathcal{Q}, H_g) + \mathrm{He}(\mathcal{R}, \widetilde{\mathcal{L}}) - \mathcal{R} - \mathcal{Q}^\top H_g H_\eta - \mathcal{R}^\top \widetilde{\mathcal{L}} H_\eta & -\mathcal{R}^\top (I - H_\eta) \\ -\mathcal{R} - \mathcal{Q}^\top H_g H_\eta - \mathcal{R}^\top \widetilde{\mathcal{L}} H_\eta & \mathcal{R}^\top H_\eta \end{bmatrix}, \tag{7.138}$$

$$\mathcal{Z}_3 = \begin{bmatrix} \widetilde{A}^\top \mathcal{R} + H_g^\top \mathcal{Q} + \widetilde{\mathcal{L}}^\top \mathcal{R} - H_\eta H_g^\top \mathcal{Q} - H_\eta \widetilde{\mathcal{L}}^\top R & 0 \\ -\mathcal{R} + H_\eta \mathcal{R} & 0 \end{bmatrix}, \tag{7.139}$$

$\widetilde{A} = I_N \otimes A$, $\widetilde{\mathcal{L}} = \gamma \mathcal{L} \otimes I_n$, $K_g^\top = \mathcal{Q}\mathcal{R}^{-1}$.

Proof By choosing $\mathcal{O}_1 = \mathcal{O}_3 = \mathcal{O}_4 = \mathcal{O}_5 = \mathcal{O}_6 = \mathcal{R}$ and $\mathcal{T}_1 = \mathcal{T}_3 = \mathcal{T}_4 = \mathcal{T}_5 = \mathcal{T}_6 = \mathcal{R}$, and $K_g^\top = \mathcal{R}^{-1}\mathcal{Q}$, $\mathcal{O}_2 = \mathcal{T}_2 = 0$, conditions (7.123) and (7.124) reduce to (7.135) and (7.136), respectively. ■

Example 7.3.15 *For the system in Example 7.3.8 and for given* $T_2 = 0.4$, *it can be verified that the inequalities* (7.135) *and* (7.136) *can be solved by choosing* $h_1 = h_2 = 0$, $\delta = 10$ *and* $\gamma = -0.2$, *the resulting gain is*

$$K_g^\top \approx \begin{bmatrix} -1.11 & -0.43 & -0.41 & -0.09 \\ 0.09 & -0.41 & 0.43 & -1.11 \end{bmatrix}.$$

Note that (7.135) *and* (7.136) *are LMIs that can be solved efficiently.* △

Remark 7.3.16 *The inequalities in* (7.120) *and* (7.121) *can be transformed into LMIs similarly as done in Proposition 7.3.13 and Corollary 7.3.14.*

7.4 Robustness properties and design

In this section, we consider the effect of general perturbations and unmodeled dynamics on the plant. In such a setting, the perturbed plant is given in (7.1) and the measurements taken by agent i is given by (7.2), where the functions $\delta : \mathbb{R}^n \times \mathbb{R}_{\geq 0} \to \mathbb{R}^n$ and $\varphi_i : \mathbb{R}^n \times \mathbb{R}_{\geq 0} \to \mathbb{R}^{p_i}$ are unknown functions that captures the unmodeled dynamics and measurement noises. Moreover, when agent i receives information (including $\hat{x}_k, y_k$) from agent k ($k \in \mathcal{N}(i)$), it is also affected by channel noise, i.e., $\tilde{x}_k^i = \hat{x}_k + c_i^x$ and $\tilde{y}_k^i = y_k + c_i^y$, where $c_i = (c_i^x, c_i^y) : \mathbb{R}_{\geq 0} \to \mathbb{R}^{n+p_i}$ is the channel noise when agent i receives information from its neighbors. Furthermore, we consider a skew on the rate of the timers, i.e.,

$$\dot{\tau}_i = -1 + \varsigma_i \qquad \tau_i \in [0, T_2 + \vartheta_i(\tau_i)], \tag{7.140a}$$

$$\tau_i^+ \in [T_1 - \vartheta_i(\tau_i), T_2 + \vartheta_i(\tau_i)] \qquad \tau_i = 0. \tag{7.140b}$$

where $\varsigma_i : \mathbb{R}_{\geq 0} \to (-\infty, 1)$ is the skew on the timer dynamics for τ_i and $\vartheta_i : \mathbb{R}_{\geq 0} \to \left[\frac{T_1 - T_2}{2}, T_1\right)$ perturb the threshold values of τ_i. Then, according to the design in (7.89)-(7.90), the perturbed dynamics of η_i is,

$$\dot{\eta}_i = h_i \eta_i \tag{7.141}$$

when $\tau_i \in [0, T_2 + \vartheta_i(\tau_i)]$, and

$$\begin{aligned} \eta_i^+ = K_{ii} H_i e_i + \sum_{k \in \mathcal{V}} g_{ik} (K_{ik} H_k e_k + \gamma e_i - \gamma e_k) + \zeta_i \\ - K_{ii} \varphi_i(x, t) - \sum_{k \in \mathcal{V}} g_{ik} K_{ik} \varphi_k(x, t) \end{aligned} \tag{7.142}$$

when $\tau_i = 0$, where

$$\zeta_i(x,t) = -K_{ii}\varphi_i(x,t) + \sum_{k\in\mathcal{V}} g_{ik}K_{ik}(H_k c_i^x - c_i^y - \varphi_k(x,t)) - \gamma \sum_{k\in\mathcal{V}} g_{ik}c_i^x.$$

Then, by letting

$$\theta_i = K_{ii}H_i e_i + \sum_{k\in\mathcal{V}} g_{ik}(K_{ik}H_k e_k + \gamma e_i - \gamma e_k) - \eta_i,$$

the resulting hybrid system $\widetilde{\mathcal{H}} = (C, \widetilde{f}, D, \widetilde{G})$ with state $\chi = (\sigma, \tau) = (e, \theta, \tau)$ is given by

$$\widetilde{f}(\chi) := f(\chi) + (-\mathbf{1}_N\delta(x,t), -\widetilde{\mathcal{K}}\mathbf{1}_N\delta(x,t), \varsigma)$$

when $\chi \in C := \mathbb{R}^{nN} \times \mathbb{R}^{nN} \times \mathcal{T}$, where

$$\mathcal{T} = [0, T_2 + \vartheta_1(\tau_1)] \times [0, T_2 + \vartheta_2(\tau)] \times \cdots \times [0, T_2 + \vartheta_N(\tau_N)],$$

and $\varsigma = (\varsigma_1, \varsigma_2, \ldots, \varsigma_N)$. Moreover, when $\chi \in D := \bigcup_{i\in\mathcal{V}} D_{ai}$, $D_{ai} = \{\chi \in C : \tau_i = 0\}$,

$$G_p(\chi, \zeta) := \{G_i(\chi, \zeta) : \chi \in D_i, i \in \mathcal{V}\}$$

and

$$G_{ai}(\chi,\zeta) = \begin{bmatrix} e \\ (\theta_1, \theta_2, \cdots, \theta_{i-1}, -\zeta_i(x,t), \theta_{i+1}, \cdots, \theta_N) \\ (\tau_1, \tau_2, \cdots, \tau_{i-1}, [T_1^i - \vartheta_i(\tau_i), T_2^i + \vartheta_i(\tau_i)], \tau_{i+1}, \cdots, \tau_N) \end{bmatrix},$$

where $\zeta(x,t) = (\zeta_1(x,t), \dots, \zeta_N(x,t))$, $\varphi(x,t) = (\varphi_1(x,t), \dots, \varphi_N(x,t))$ and

$$\begin{aligned}
\zeta(x,t) &= K_m \varphi(x,t) + K_c c, \\
K_m &= -K_g * (I + \mathcal{G}), \\
K_c &= \begin{bmatrix} (K_g H_g - \gamma I) * \mathcal{G} & -K_g * \mathcal{G} \end{bmatrix},
\end{aligned}$$

$m = (m_1, m_2, \dots, m_N)$, $c = (c^x, c^y)$, $c^x = (c_1^x, c_2^x, \dots, c_N^x)$, and $c^y = (c_1^y, c_2^y, \dots, c_N^y)$.[12]

7.4.1 Robustness properties with respect to small perturbations

Motivated by Remark 7.3.4, in this section, we focus on the generic robustness property to small perturbations. Below, given a set $S_c \subset \mathbb{R}^n$, $\mathcal{R}^x(S_c)$ denotes the reachable set of $\dot{x} = Ax$ from S_c. Then, we can establish the following result.

Theorem 7.4.1 *Given $T_2^i \geq T_1^i > 0$, suppose the gains K_g, γ, h_i for all $i \in \mathcal{V}$ are chosen such that the set $\mathcal{A}$ is GES for the unperturbed hybrid system $\mathcal{H}$. Then, $\mathcal{A}$ is semiglobally practically robustly $\mathcal{KL}$ asymptotically stable[13] for $\mathcal{H}$, i.e., there exists $\beta \in \mathcal{KL}$ such that for every compact set $S_c \subset \mathcal{X}$ and every $\varepsilon > 0$, there exists $\rho^\star \in (0, \infty)$ such that if*

$$\max_{i \in \mathcal{V}} \{\overline{\rho}_1, \overline{\rho}_2, |c|_\infty, |\varsigma|_\infty\} \leq \rho^\star, \tag{7.143}$$

where $\overline{\rho}_1 = \max_{x \in \mathcal{R}^x(S_c), t \in \mathbb{R}_{\geq 0}} |\varphi(x,t)|$, $\overline{\rho}_2 = \max_{x \in \mathcal{R}^x(S_c), t \in \mathbb{R}_{\geq 0}} |\delta(x,t)|$, then, every $\phi \in \mathcal{S}_{\widetilde{\mathcal{H}}}(S_c)$ satisfies $|\phi(t,j)|_{\mathcal{A}} \leq \beta(|\phi(0,0)|_{\mathcal{A}}, t+j) + \varepsilon$ for all $(t,j) \in \operatorname{dom} \phi$.

[12]Note that the Khatri-Rao product $-K_g * (I + \mathcal{G})$ is such that the (i,k)-th entry K_{ik} of K_g is multiplied by the (i,k)-th scalar entry of the matrix $I + \mathcal{G}$ for all $i, k \in \mathcal{V}$.

[13]See [73, Definition 7.18] for a definition.

Proof Consider the hybrid system $\mathcal{H}$ and a continuous function $\rho : \mathbb{R}^{nN} \times \mathbb{R}^{nN} \times \mathcal{T} \to \mathbb{R}_{\geq 0}$, the ρ-perturbation of $\mathcal{H}$, denoted $\mathcal{H}_\rho$, is the hybrid system

$$\begin{cases} \chi \in C_\rho & \dot{\chi} \in F_\rho(\chi) \\ \chi \in D_\rho & \chi^+ \in G_\rho(\chi) \end{cases}$$

where

$$\begin{aligned} C_\rho &= \{\chi \in \mathcal{X} : (\chi + \rho(\chi)\mathbb{B}) \cap C \neq \emptyset\}, \\ F_\rho(\chi) &= \overline{\mathrm{con}} f((\chi + \rho(\chi)\mathbb{B}) \cap C) + \rho(\chi)\mathbb{B} \quad \forall \chi \in \mathcal{X}, \\ D_\rho &= \{\chi \in \mathcal{X} : (\chi + \rho(\chi)\mathbb{B}) \cap D \neq \emptyset\}, \\ G_\rho(\chi) &= \{v \in \mathcal{X} : v \in g + \rho(g)\mathbb{B}, g \in G((\chi + \rho(\chi)\mathbb{B}) \cap D)\} \quad \forall \chi \in \mathcal{X}. \end{aligned}$$

Since the set $\mathcal{A}$ is GES for $\mathcal{H}$, it is also UGAS for $\mathcal{H}$. Moreover, since the hybrid system $\mathcal{H}$ satisfies the hybrid basic conditions, by [73, Theorem 6.8] $\mathcal{H}_\rho$ is nominally well-posed and, moreover, by [73, Proposition 6.28] is well-posed. Then, [73, Theorem 7.20] implies that $\mathcal{A}$ is semiglobally practically robustly $\mathcal{KL}$ asymptotically stable for $\mathcal{H}$. Namely, for every compact $S_c \subset \mathcal{X}$ and every $\varepsilon > 0$, there exists $\widetilde{\rho} \in (0, 1)$ such that every $\phi \in \mathcal{S}_{\mathcal{H}_{\widetilde{\rho}\rho}}(S_c)$ satisfies $|\phi(t, j)|_\mathcal{A} \leq \beta(|\phi(0, 0)|_\mathcal{A}, t + j) + \varepsilon$ for all $(t, j) \in \mathrm{dom}\,\phi$. Then, the results follow by picking $\rho^\star > 0$ such that

$$\max\{1, |K_m| + |K_c|, |\widetilde{\mathcal{K}}\mathbf{1}_N|\}\rho^\star \leq \widetilde{\rho}$$

and relating solutions to $\widetilde{\mathcal{H}}$ and solutions to $\mathcal{H}_{\widetilde{\rho}\rho}$. ■

In simple terms, the above result establishes that the solutions resulting hybrid system ($\widetilde{\mathcal{H}}$) with small enough perturbations do not differ much from the unperturbed system ($\mathcal{H}$).

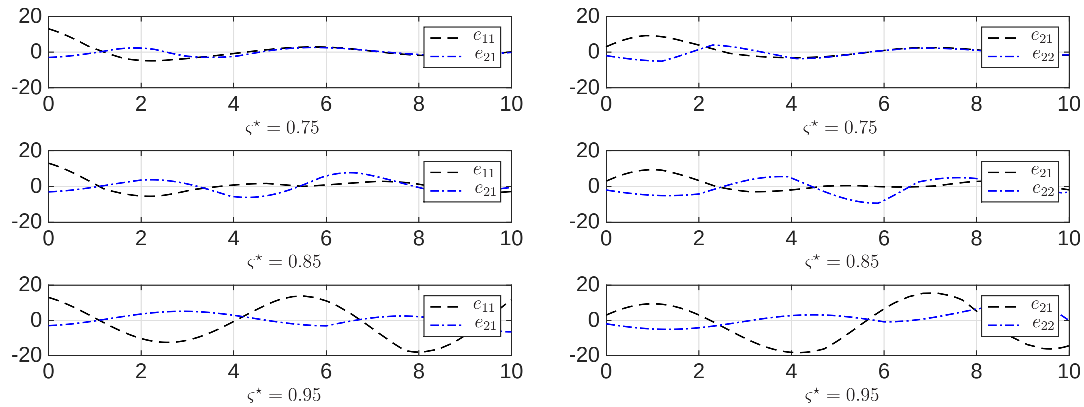

(a) Estimation error for the first state component

(b) Estimation error for the second state component.

Figure 7.10: Estimation error under different choice of perturbation $\varsigma^\star$.

Remark 7.4.2 *In general, though not pursued here, the result in Theorem 7.4.1 is also applicable to the case when the measurement and communication noise have specific statistical properties, such as Gaussian noise. Furthermore, if the proposed observer includes an estimate of nonlinear term* δ*, which is possible by adding* $\hat{\delta}(\hat{x})$ *to the right hand side of equation* (7.4)*, then under the usual assumptions in the literature [89], precisely, the one in Lemma 2.1, we can bound the difference between* δ *and* $\hat{\delta}$ *by*

$$|\delta(x) - \hat{\delta}(x + x^\star)| \leq L|x^\star| + L_0$$

for all $x, x^\star \in \mathbb{R}^n$*, where* $L, L_0 \in \mathbb{R}_{\geq 0}$*. Moreover, for such robustified observer, a result following the lines of the proofs in Theorem 7.3.6 guaranteeing asymptotic stability of the zero estimation error holds.*

The following examples illustrates a particular perturbation from skewed clock.

Example 7.4.3 *Consider the system in Example 7.3.8 with same set of parameters. Furthermore, we consider a particular perturbation where* $\delta(x,t) \equiv 0$*,* $\varphi_1(x,t) = \varphi_2(x,t) \equiv 0$*,* $\vartheta_i(\tau_i) \equiv 0$ *for all* $\tau_i \in [0, T_2^i]$ *and* $\varsigma_1 = \varsigma_2 = \varsigma^\star$ *where*

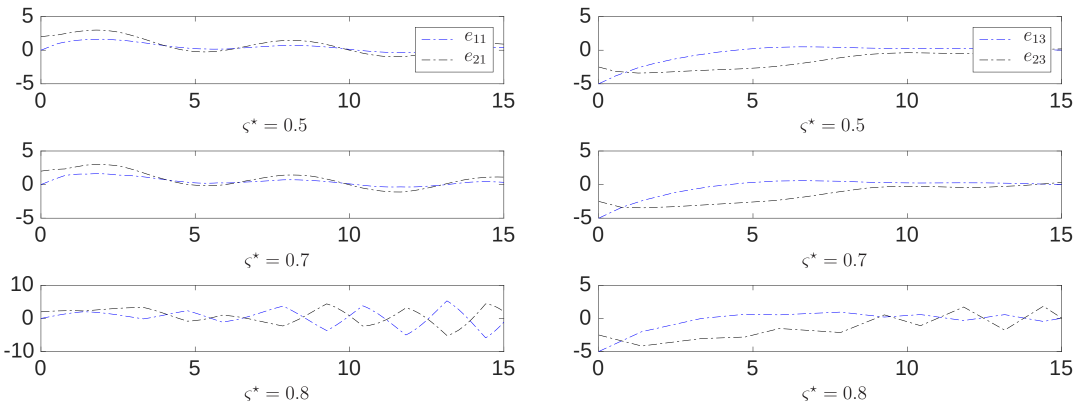

(a) Estimation error for the first state component

(b) Estimation error for the second state component.

Figure 7.11: Estimation error under different choice of perturbation $\varsigma^\star$.

$\varsigma^\star \in (-\infty, 1)$ *is a constant. From the Figure 7.10, we can see that with larger and larger perturbations of* $\varsigma^\star$*, the estimation error becomes larger and larger, this further motivates a particular robustness analysis when each agent has its own* T_1 *and* T_2 *thresholds due to different perturbations. More details can be found in Section 7.4.3.* $\triangle$

Example 7.4.4 *Consider the system in Example 7.3.9 with same set of parameters. Furthermore, we consider a particular perturbation where* $\delta(x,t) \equiv 0$, $\varphi_1(x,t) = \varphi_2(x,t) \equiv 0$, $\vartheta_i(\tau_i) \equiv 0$ *for all* $\tau_i \in [0, T_2^i]$ *and* $\varsigma_1 = \varsigma_2 = \varsigma^\star$ *where* $\varsigma^\star \in (-\infty, 1)$ *is a constant. From the Figure 7.11, we can see that with larger and larger perturbations of* $\varsigma^\star$*, the estimation error becomes larger and larger, this further motivates a particular robustness analysis when each agent has its own* T_1 *and* T_2 *thresholds due to different perturbations. More details can be found in Section 7.4.3.* $\triangle$

7.4.2 Robustness to measurement and communication noise

In this section, we consider the hybrid system $\widetilde{\mathcal{H}}$ where only the communication noise and channel noise are present. Namely, $\delta \equiv 0$, $\varsigma_i \equiv 0$, $\vartheta_i \equiv 0$, for all $i \in \mathcal{V}$, and the function φ_i reduces to a function m_i, i.e., $m_i(t) = \varphi_i(x,t)$ for all $t \in \mathbb{R}_{\geq 0}$. Therefore, the closed-loop system $\widetilde{\mathcal{H}}$ with added noise can be written in the following compact form:

$$\dot{\chi} = f(\chi) := (A_{f\theta}\sigma, -\mathbf{1}_N) \qquad \chi \in C, \tag{7.144}$$

$$\chi^+ \in G(\chi,\zeta) := \{G_i(\chi,\zeta) : \chi \in D_i, i \in \mathcal{V}\} \qquad \chi \in D \tag{7.145}$$

where $C := \mathbb{R}^{nN} \times \mathbb{R}^{nN} \times [0, T_2]$, $D = \bigcup_{i\in\mathcal{V}} D_{ai}$, $D_i = \{\chi \in C : \tau_i = 0\}$,

$$G_i(\chi,\zeta) = \begin{bmatrix} e \\ (\theta_1, \theta_2, \cdots, \theta_{i-1}, -\zeta_i, \theta_{i+1}, \cdots, \theta_N) \\ (\tau_1, \tau_2, \cdots, \tau_{i-1}, [T_1, T_2], \tau_{i+1}, \cdots, \tau_N) \end{bmatrix},$$

where $\zeta = (\zeta_1, \ldots, \zeta_N)$ and

$$\begin{aligned} \zeta &= K_m m + K_c c, \\ K_m &= -K_g * (I + \mathcal{G}), \\ K_c &= \begin{bmatrix} (K_g H_g - \gamma I) * \mathcal{G} & -K_g * \mathcal{G} \end{bmatrix}, \end{aligned}$$

$m = (m_1, m_2, \ldots, m_N)$, $c = (c^x, c^y)$, $c^x = (c^x_1, c^x_2, \ldots, c^x_N)$, and $c^y = (c^y_1, c^y_2, \ldots, c^y_N)$.[14]

For a given hybrid system $\mathcal{H}$, we are interested in set $\mathcal{A}$ being input to state stable with respect to measurement and communication noise, which is defined, in general, as follows:

[14]Note that the Khatri-Rao product $-K_g * (I + \mathcal{G})$ is such that the (i,k)-th entry K_{ik} of K_g is multiplied by the (i,k)-th scalar entry of the matrix $I + \mathcal{G}$ for all $i, k \in \mathcal{V}$.

Definition 7.4.5 *Given a compact set $\mathcal{A}$. The hybrid system $\mathcal{H} = (C, f, D, G)$ with state x and input u and data given by*

$$\dot{x} = f(x,u) \quad \forall (x,u) \in C \tag{7.146}$$

$$x^+ \in G(x,u) \quad \forall (x,u) \in D \tag{7.147}$$

is input-to-state stable (ISS) with respect to $\mathcal{A}$ if there exist $\beta \in \mathbb{KL}$ and $\gamma \in \mathbb{K}$ such that, for each $\phi(0,0) \in \mathbb{R}^n$, every solution pair $(\phi, u) \in \mathcal{S}_{\mathcal{H}}$ satisfies

$$|\phi(t,j)|_{\mathcal{A}} \leq \max\{\beta(|\phi(0,0)|_{\mathcal{A}}, t+j), \gamma(|u|_\infty)\}$$

for each $(t,j) \in \operatorname{dom}\phi$.

Before we present the ISS result, we first establish the following property which will be used to prove the ISS result.

Proposition 7.4.6 *Consider a hybrid system $\mathcal{H} = (C, f, D, G)$ with state $x \in \mathbb{R}^n$. Suppose there exists a continuous function $V : \mathbb{R}^n \to \mathbb{R}_{\geq 0}$ such that*

$$\langle V(x), \tilde{f} \rangle \leq -aV(x) \qquad \forall x \in C, \tilde{f} \in f(x) \tag{7.148}$$

$$V(g) \leq V(x) + b \qquad \forall x \in D, g \in G(x) \tag{7.149}$$

where $a, b \geq 0$. Moreover, suppose there exist scalars $0 < T_1 \leq T_2$ and $N \in \mathbb{Z}_{\geq 1}$ such that each $\phi \in \mathcal{S}_{\mathcal{H}}$ satisfies

$$t_{(j+1)N} - t_{jN} \in [T_1, T_2] \tag{7.150}$$

for all $j \in \mathbb{N}$ such that $(t_{(j+1)N}, (j+1)N), (t_{jN}, jN) \in \operatorname{dom}\phi$, then, the function

V satisfies

$$V(\phi(t,j)) \leq e^{-at} V(\phi(0,0)) + Nb \sum_{s=0}^{\tilde{j}} e^{-asT_1}, \tag{7.151}$$

for all $(t,j) \in \operatorname{dom}\phi$, where $\tilde{j} = \left\lfloor \frac{j}{N} \right\rfloor$.

Proof Given a $\phi \in \mathcal{S}_{\mathcal{H}}$, pick any $(t,j) \in \operatorname{dom}\phi$ and let $0 = t_0 \leq t_1 \leq \cdots \leq t_{j+1} \leq t$ satisfy

$$\operatorname{dom}\phi \bigcap ([0, t_{j+1}] \times \{0, \ldots, j\}) = \bigcup_{s=0}^{j} [t_s, t_{s+1}] \times \{s\}.$$

For each $s \in \{0, \ldots, j\}$ and almost all $r \in [t_s, t_{s+1}]$, $\phi(r,i) \in C$. Then, (7.95) implies that, for each $s \in \{0, \ldots, j\}$ and for almost all $r \in [t_s, t_{s+1}]$, from (7.148) we have that

$$\frac{d}{dr} V(\phi(r,i)) \leq -\beta |\phi(r,i)|^2_{\mathcal{A}} \leq -aV(\phi(r,i)). \tag{7.152}$$

while integrating both sides leads to

$$V(\phi(t_{s+1}, s)) \leq \left(e^{-a(t_{s+1} - t_s)}\right) V(\phi(t,s)) \tag{7.153}$$

for each $s \in \{0, \ldots, j\}$. Similarly, for each $s \in \{1, \ldots, j\}$, $\phi(t_s, s-1) \in D$, and thus

$$V(\phi(t_s, s)) \leq V(\phi(t_s, s-1)) + b. \tag{7.154}$$

Due to the last two displayed inequalities, we have, for each $(t,j) \in \operatorname{dom}\phi$ with

$t \geq t_j$, that

$$\begin{aligned} V(\phi(t,j)) &\leq e^{-at}V(\phi(0,0)) + b\sum_{s=1}^{j} e^{-a(t-t_s)} \\ &\leq e^{-at}V(\phi(0,0)) + b\sum_{s=1}^{j} e^{-a(t_j-t_s)}. \end{aligned}$$

Due to the increasing sequence of times $t_1 \leq t_2 \leq t_3 \leq \cdots \leq t_j$, we have that there must exist a integer $\tilde{j}$ which defines the maximum multiple of N, i.e., $\tilde{j} = \lfloor \frac{j}{N} \rfloor$. Then, we can group the sum $\sum_{s=1}^{j} e^{-a(t_j-t_s)}$ as follows:

$$\sum_{s=1}^{j} e^{-a(t_j-t_s)} = \sum_{s=0}^{\tilde{j}-1}\sum_{k=1}^{N} e^{-a(t_j-t_{sN+k})} + \sum_{k=\tilde{j}N+1}^{j} e^{-a(t_j-t_k)}.$$

Note that for each $s \in \{0, \ldots, \tilde{j}-1\}$, we have

$$\max_{t_{sN+k}, k\in\{1,\ldots,N-1\}} \sum_{k=1}^{N} e^{-a(t_j-t_{sN+k})} = \sum_{k=1}^{N} e^{-a(t_j-t_{(s+1)N})} = Ne^{-a(t_j-t_{(s+1)N})},$$

which corresponds to the maximizer satisfying $t_{sN+k} = t_{(s+1)N}$ for all $k \in \{1, \ldots, N-1\}$. Therefore, it follows that

$$\begin{aligned} \sup_{\phi\in\mathcal{S}_{\mathcal{H}}, (t_j,j)\in\operatorname{dom}\phi} \sum_{s=1}^{j} e^{-a(t_j-t_s)} \leq & \sup_{\phi\in\mathcal{S}_{\mathcal{H}}, (t_j,j)\in\operatorname{dom}\phi} \sum_{s=0}^{\tilde{j}-1} \max_{t_{sN+k}, k\in\{1,\ldots,N-1\}} \sum_{k=1}^{N} e^{-a(t_j-t_{sN+k})} \\ & + \sup_{\phi\in\mathcal{S}_{\mathcal{H}}, (t_j,j)\in\operatorname{dom}\phi} \sum_{k=\tilde{j}N+1}^{j} e^{-a(t_j-t_k)} \\ \leq & \sup_{\phi\in\mathcal{S}_{\mathcal{H}}, (t_j,j)\in\operatorname{dom}\phi} \sum_{s=0}^{\tilde{j}-1} Ne^{-a(t_j-t_{(s+1)N})} + N, \\ \leq & \sup_{\phi\in\mathcal{S}_{\mathcal{H}}, (t_j,j)\in\operatorname{dom}\phi} \sum_{s=0}^{\tilde{j}-1} Ne^{-a(t_{\tilde{j}N}-t_{(s+1)N})} + N, \end{aligned}$$

where we used the property that $j - \tilde{j}N < N$. From the assumption on the hybrid time domain in (7.150), it follows that

$$t_{(s+1)N} - t_{sN} \in [T_1, T_2],$$

for all $(t_{sN}, sN), (t_{(s+1)N}, (s+1)N) \in \operatorname{dom} \phi$ with $\phi \in \mathcal{S}_{\mathcal{H}}$, which implies that for each $s \in \{0, 1, \ldots, \tilde{j} - 1\}$,

$$t_{\tilde{j}N} - t_{sN} \in [(\tilde{j} - s)T_1, (\tilde{j} - s)T_2].$$

Therefore,

$$\sup_{\phi \in \mathcal{S}_{\mathcal{H}}, (t_j, j) \in \operatorname{dom} \phi} N \sum_{s=0}^{\tilde{j}-1} e^{-a(t_{\tilde{j}N} - t_{(s+1)N})} + N \leq \sum_{s=1}^{\tilde{j}} e^{asT_1} + N = N \sum_{s=0}^{\tilde{j}} e^{asT_1}$$

where $\tilde{j} = \left\lfloor \frac{j}{N} \right\rfloor$. Therefore, for each $(t, j) \in \operatorname{dom} \phi$, V satisfies

$$V(\phi(t, j)) \leq e^{-at} V(\phi(0, 0)) + Nb \sum_{s=0}^{\tilde{j}} e^{-asT_1}$$

for $\tilde{j} = \left\lfloor \frac{j}{N} \right\rfloor$ which concludes the proof. ■

For this perturbed hybrid system, we have the following result.

Theorem 7.4.7 *Let* $0 < T_1 \leq T_2$ *be given. Suppose there exist matrices* $K_g \in \mathbb{R}^{nN \times p}$ *and* $P \in \mathbb{R}^{2nN \times 2nN}$ *such that* $P = P^\top > 0$ *and condition* (7.95) *holds. Then, the set* $\mathcal{A}$ *is ISS with respect to measurement noise and communication noise, i.e., there exists* $E_s > 0$ *such that for each* $\phi \in \mathcal{S}_{\mathcal{H}_s}$ *and for any* $(t, j) \in$

$\operatorname{dom}\phi$,

$$|\phi(t,j)|_{\mathcal{A}} \leq \max\left\{\sqrt{2\frac{\alpha_2}{\alpha_1}}\exp\left(-\frac{1}{2}\widetilde{\beta}t\right)|\phi(0,0)|_{\mathcal{A}}, \widetilde{\gamma}_m|m|_\infty, \widetilde{\gamma}_c|c|_\infty\right\}, \tag{7.155}$$

where $\widetilde{\beta} = \frac{\beta}{\alpha_2}$ *and* $\widetilde{\alpha} = \frac{1}{1-\exp(-\frac{\beta}{\alpha_2 N}T_2)}$, $\widetilde{\gamma}_m = 2\sqrt{\frac{E_j}{\alpha_1}\overline{\lambda}(Q)}|K_m|$, $\widetilde{\gamma}_c = 2\sqrt{\frac{E_j}{\alpha_1}\overline{\lambda}(Q)}|K_c|$, $E_j = N\left(\frac{e^{aT_1}-e^{-aT_1\lfloor\frac{j}{N}\rfloor}}{e^{aT_1}-1}\right)$,

$$\alpha_1 = \min\left\{\underline{\lambda}(P), \underline{\lambda}\left(\widetilde{Q}(0)\right)\right\}, \quad \alpha_2 = \max\left\{\overline{\lambda}(P), \overline{\lambda}\left(\widetilde{Q}(T_2)\right)\right\}.$$

Proof Consider the Lyapunov function candidate $V : \mathcal{X} \to \mathbb{R}_{\geq 0}$ given by

$$V(\chi) = e^\top P e + \theta^\top \widetilde{Q}(\tau)\theta. \tag{7.156}$$

Following the proof of Theorem 7.3.6, it follows that

$$\alpha_1|\chi|^2_{\mathcal{A}} \leq V(\chi) \leq \alpha_2|\chi|^2_{\mathcal{A}} \tag{7.157}$$

for all $\chi \in C$, where α_1 and α_2 are given by (7.98) and (7.99). Then, as similar in the proof in the proof of Theorem 7.3.6, during flows, by using (7.95), we have

$$\langle\nabla V(\chi_a), f_a(\chi_a)\rangle < -\beta|\chi_a|^2_{\mathcal{A}}, \quad \forall\chi_a \in C_a \setminus \mathcal{A}_a, \tag{7.158}$$

where $\beta = -\overline{\lambda}(\mathcal{M})$ and

$$\mathcal{M} = \begin{bmatrix} \operatorname{He}(A_\theta, P) & -P + \widetilde{A}_\theta^\top \mathcal{K}^\top \widetilde{Q}(\tau) \\ -P + \widetilde{Q}(\tau)\mathcal{K}\widetilde{A}_\theta & -\delta\widetilde{Q}(\tau) - \operatorname{He}(\widetilde{\mathcal{K}}, \widetilde{Q}(\tau)) \end{bmatrix}. \tag{7.159}$$

Moreover, for each $\chi_a = (e,\theta,\tau) \in D_a$ and for each $g_a \in G_a(\chi_a)$, there exists at least one component of τ, say, the i-th component, such that $\tau_i = 0$. Then, at jumps we have

$$\begin{aligned} V(g_a) - V(\chi_a) &\leq -\theta_i^\top Q_i \theta_i + \zeta_i^\top Q_i \zeta_i \\ &\leq \zeta^\top Q \zeta. \end{aligned}$$

Then, from Proposition 7.4.6, with $a = \frac{\beta}{\alpha_2}$ and $b = \overline{\lambda}(Q)$, we have that

$$V(\phi(t,j)) \leq \exp\left(-\frac{\beta}{\alpha_2} t\right) V(\phi(0,0)) + \overline{\lambda}(Q) N \sum_{s=1}^{n} e^{-asT_1} |\zeta|_\infty^2$$

note that the $\sum_{s=0}^{n} e^{-asT_1} = \left(\frac{e^{aT_1} - e^{-anT_1}}{e^{aT_1}-1}\right)$. Defining $E_j = N\left(\frac{e^{aT_1} - e^{-aT_1 \lfloor \frac{j}{N} \rfloor}}{e^{aT_1}-1}\right)$ and with (7.157), we have that

$$|\phi(t,j)|_{\mathcal{A}}^2 \leq \frac{\alpha_2}{\alpha_1} \exp\left(-\frac{\beta}{\alpha_2} t\right) |\phi(0,0)|_{\mathcal{A}}^2 + \frac{1}{\alpha_1} \overline{\lambda}(Q) E_j |\zeta|_\infty^2.$$

Since $|\zeta|_\infty^2 \leq 2|K_m|^2 |m|_\infty^2 + 2|K_c|^2 |c|_\infty^2$, it follows that, for each $(t,j) \in \operatorname{dom} \phi$,

$$|\phi(t,j)|_{\mathcal{A}} \leq \max\left\{ \sqrt{2\frac{\alpha_2}{\alpha_1}} \exp\left(-\frac{1}{2}\frac{\beta}{\alpha_2} t\right) |\phi(0,0)|_{\mathcal{A}}, 2\sqrt{\frac{E_j}{\alpha_1}\overline{\lambda}(Q)} |K_m| |m|_\infty, 2\sqrt{\frac{E_j}{\alpha_1}\overline{\lambda}(Q)} |K_c| |c|_\infty \right\}.$$

■

7.4.3 Robustness properties with respect to T_1^i and T_2^i perturbations

In a real world application, the bounds on update communication times may not be explicitly known. Moreover, these update times may not be unique for each agent as is assumed in the previous section. Therefore, we consider the affect of perturbations on to the parameters T_1^i and T_2^i for the time sequences in (7.3).

In this section, we consider the case of $\widetilde{\mathcal{H}}$ with $\delta = 0$, $\varphi_i = 0$ and $\varsigma_i = 0$ and when ϑ_i is a known skew of timer states, i.e., $\vartheta_i \in [\vartheta_{1i}, \vartheta_{2i}]$. With these assumptions, we have that the timer dynamics of $\widetilde{\mathcal{H}}$ are given by

$$\begin{aligned} \dot{\tau}_i &= -1 & \tau_i &\in [0, T_2^i + \vartheta_{2i}], \\ \tau_i^+ &\in [T_1^i + \vartheta_{1i}, T_2^i + \vartheta_{2i}] & \tau_i &= 0. \end{aligned}$$

Then, we have the following results.

Corollary 7.4.8 *Let $0 < T_1^i \leq T_2^i$ be given for each $i \in \mathcal{V}$. Suppose N agents are connect via a digraph $\Gamma = (\mathcal{V}, \mathcal{E}, \mathcal{G})$. The set $\{0_{nN}\} \times \{0_{nN}\} \times \mathcal{T}$ is GES for the hybrid system $\mathcal{H}_\vartheta$ if there exists $\delta > 0$ and matrices $K_g \in \mathbb{R}^{nN \times p}, P = P^\top \in \mathbb{R}^{nN \times nN}, Q_i = Q_i^\top \in \mathbb{R}^{n \times n}$ for each $i \in \mathcal{V}$ and*

$$\begin{bmatrix} \mathrm{He}(A_\theta, P) & -P + \widetilde{A}_\theta^\top \mathcal{K}^\top \widetilde{Q}(\nu) \\ \star & -\delta \widetilde{Q}(\nu) - \mathrm{He}(\widetilde{\mathcal{K}}, \widetilde{Q}(\nu)) \end{bmatrix} < 0 \qquad (7.160)$$

holds for each $\nu \in \mathcal{T}$.

Proof The proof follows from applying Proposition 7.3.6. ∎

From Corollary 7.4.8, we have that the nominal system $\mathcal{H}$ is robust to some perturbation on the maximum update time parameter. Furthermore, if we have a solution for $\mathcal{H}$ that satisfies the conditions in Theorem 7.3.6 for $\mathcal{A}$ to be GES, then a solution to Proposition 7.3.11 is also known. Using the boundary condition idea in Proposition 7.3.11, we can use the following corollary to check the condition in Corollary 7.4.8 over a larger interval. Namely, we have the following:

Corollary 7.4.9 *Let $0 < T_1^i \leq T_2^i$ be given for all $i \in \mathcal{V}$. Suppose the assumptions in Proposition 7.3.11 hold. The inequality in* (7.160) *holds if there exists $\delta > 0$*

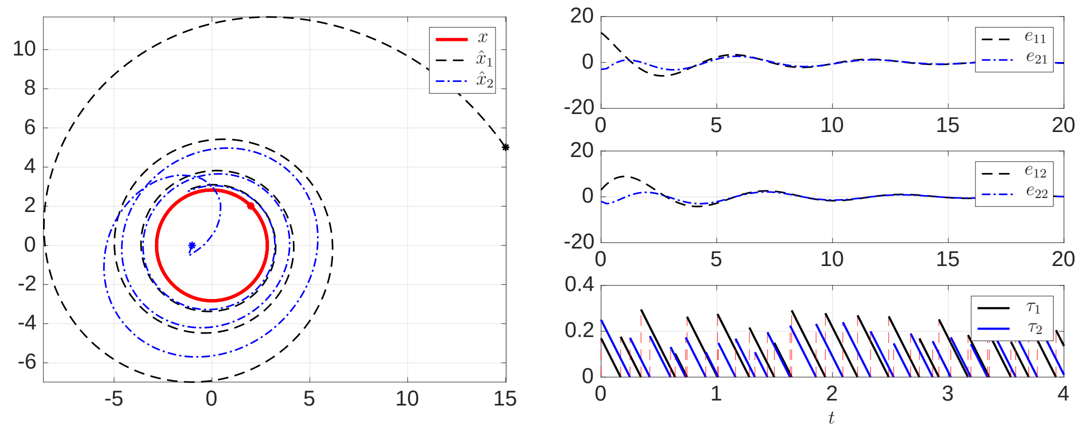

(a) Phase plots of $x, \hat{x}_1, \hat{x}_2$ from initial conditions that are denoted by $*$.

(b) Estimation error and timer states, where $x = (x_1, x_2)$, $\hat{x}_i = (\hat{x}_{i1}, \hat{x}_{i2})$, $e_{i1} = \hat{x}_{i1} - x_1$, $e_{i2} = \hat{x}_{i2} - x_2$, for $i \in \{1, 2\}$.

Figure 7.12: Phase plots of $x, \hat{x}_1$ and $\hat{x}_2$ as well as estimation errors e_1 and e_2 for two all-to-all connected agents using the observer in Example 7.3.8. Initial conditions are $x(0,0) = (2,2)$, $\hat{x}_1(0,0) = (15,5)$, $\hat{x}_2(0,0) = (-1,0)$, $\eta_1(0,0) = (1,1)$, $\eta_2(0,0) = (-1,-1)$, $\tau_1(0,0) = 0$ $\tau_2(0,0) = 0.3$.

and matrices $K_g \in \mathbb{R}^{nN \times p}, P = P^\top \in \mathbb{R}^{nN \times nN}, Q_i = Q_i^\top \in \mathbb{R}^{n \times n}$ *for each* $i \in \mathcal{V}$ *and*

$$\begin{bmatrix} \mathrm{He}(A_\theta, P) & -P + \exp(\delta\nu)\widetilde{A}_\theta^\top \mathcal{K}^\top \widetilde{Q} \\ \star & -\exp(\delta\nu)(\delta\widetilde{Q} + \mathrm{He}(\widetilde{\mathcal{K}}, \widetilde{Q})) \end{bmatrix} < 0 \tag{7.161}$$

where $Q = \mathrm{diag}(Q_1, Q_2, \ldots, Q_N)$ *and* $\nu \in \{0, T_2^{\max} + \max_{i \in \mathcal{V}} \vartheta_{2i}\}$.

Proof The proof follows from applying Proposition 7.3.11. ■

Example 7.4.10 *From Example 7.3.8 we can extend the reset times of the agents by letting* $\vartheta_{1i} = 0$ *for each* i *and* $\vartheta_{21} = 0.1$ *and* $\vartheta_{22} = .05$. *Which effectively adjusts the upper boundary of reset times for each agent to be unique, namely* $\tau_1 \in [0, 0.3]$ *and* $\tau \in [0, 0.25]$. *Since the parameters found in Example 7.3.8 satisfy Proposition 7.3.11 and with condition* (7.161) *begin satisfied for* $\nu = 0.3$, *then Corollary 7.4.9 is satisfied.* △

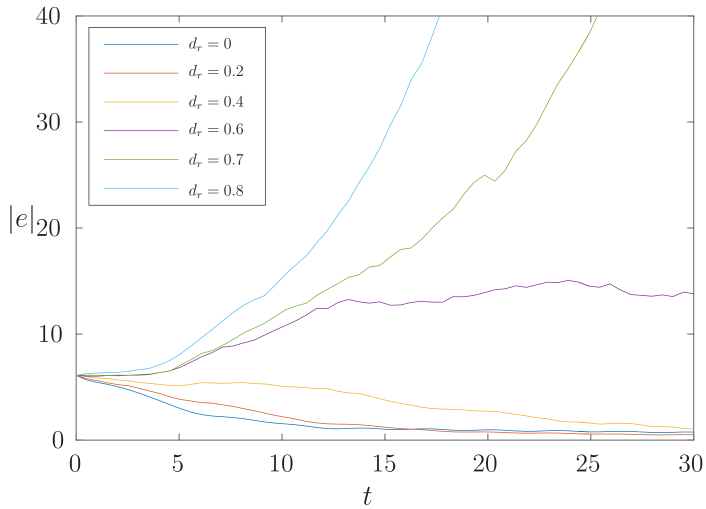

Figure 7.13: The relationship between the dropout rate d_r and the corresponding average estimation error $|e|$ for 20 solutions and projected onto the flow time t.

7.4.4 Robustness to information dropout

In this section, we consider the robustness property with respect to information dropping during transmission over the network. In particular, we assume the package dropping satisfies the following assumption.

Assumption 7.4.11 *(The Independent and Identically Distributed (I.I.D) Bernoulli model) A Bernoulli random variable b_k indicates whether the packet with index k is received correctly. If it goes through the network successfully, then $b_k = 1$, otherwise, $b_k = 0$. For any value of $k \in \mathbb{Z}_{\geq 1}$, b_k is I.I.D with probability distribution $\mathcal{P}(b_k = 1) = d_r$ and $\mathcal{P}(b_k = 0) = 1 - d_r$, where $d_r \in [0, 1]$.*

Note that this model is one of the simplest and often used model for packet dropping in large-scale networks, see, e.g. [96]. A simulation of the proposed observer subject this model of package dropping is discussed in the following example.

Example 7.4.12 *Consider the system in Example 7.3.9 with same set of param-*

eters. Twenty simulations of the relationship between the dropout rate and the corresponding estimation error $|e|$ is shown in Figure 7.13. Note that with higher and higher value of d_r, the estimation error fails to converge to zero over the simulation window. △

On the other hand, if further information of the package dropping can be obtained, for example, if one knows that for the overall network, at most $k^\star$ packages could be dropped consecutively, then, we can use the following result to justify the design of parameters.

Corollary 7.4.13 *Let $0 < T_1^i \leq T_2^i$ be given for all $i \in \mathcal{V}$. Moreover, suppose at most $k^\star$ packages could be dropped consecutively. Then, the set $\mathcal{A}$ is GES if there exists $\delta > 0$ and matrices $K_g \in \mathbb{R}^{nN\times p}, P = P^\top \in \mathbb{R}^{nN\times nN}, Q_i = Q_i^\top \in \mathbb{R}^{n\times n}$ for each $i \in \mathcal{V}$ such that if there exists $\delta > 0$ and matrices $K_g \in \mathbb{R}^{nN\times p}$, $P \in \mathbb{R}^{nN\times nN}, Q_i \in \mathbb{R}^{n\times n}$ satisfying $P = P^\top > 0$, $Q_i = Q_i^\top > 0$ for all $i \in \mathcal{V}$ such that*

$$\begin{bmatrix} \mathrm{He}(A_\theta, P) & -P+\widetilde{A}_\theta^\top \mathcal{K}^\top Q \\ \star & -\delta Q - \mathrm{He}(\widetilde{\mathcal{K}}, Q) \end{bmatrix} < 0, \tag{7.162}$$

$$\begin{bmatrix} \mathrm{He}(A_\theta, P) & -P+\exp(\delta k T_2^{\max})\widetilde{A}_\theta^\top \mathcal{K}^\top Q \\ \star & -\exp(\delta k T_2^{\max})(\delta Q+\mathrm{He}(\widetilde{\mathcal{K}}, Q)) \end{bmatrix} < 0, \tag{7.163}$$

where $Q = \mathrm{diag}(Q_1, \ldots, Q_N)$ and $T_2^{\max} = \max_{i\in\mathcal{V}} T_2^i$.

Proof The proof follows from applying Proposition 7.3.11. ■

7.5 Summary

In this chapter, we provided a complete solutions to the state estimation a distributed state observer under intermittent information communication is proposed. In contrast to classic observers for linear time-invariant systems, a node with enough information from its neighbors can estimate the plant state even without detectability or even taking measurements of the plant output. Sufficient conditions that guarantee global exponential stability of the convergence of estimation error to zero are presented. Moreover, design methods via LMI-like conditions are also proposed, enabling the design of parameters numerically. Furthermore, a rigorous robustness analysis and design was performed of the stability under certain conditions with respect to communication and measurement noises are studied in terms of ISS.

Chapter 8

Conclusion and Future Directions

In this thesis, the problem of designing distributed state observers with constant gains to guarantee the rate of convergence and robustness was addressed. Three main fundamental aspects are considered. One relies on continuous information transmission and guarantees the zero estimation error set to be uniformly asymptotically stable. The second one generates estimates that converge to the plant's state in finite-time even under piece-wise constant noises. The last one addresses the design of distributed state observers when measurements and information are only available asynchronously and intermittently over networks.

When information is available continuously, unique advantages of interconnected observers over Luenberger observer is shown analytically and numerically. Moreover, optimization problem based on LMIs are formulated for synthesis to corporate multi-objectives designs including rate of convergence, H_∞ and etc. In addition, a consensus algorithm is designed to enable each agent to compute the global average of all local estimates.

When rate of convergence is prioritized in the design specifications, a robust finite-time observer consists of two coupled Luenberger observers is developed. It generates estimates that converge to the plant's state in a preset finite-time regardless of initial conditions. Such finite-time convergence property is preserved when the measurement noise is piece-wise constant.

When information over the network is transmitted in an intermittent fashion, the design methods and tools in continuous-time or discrete-time domain do not apply directly. A hybrid distributed estimation frame work is proposed. Sufficient conditions to guarantee GES of the zero estimation error set are given by constructive LMIs, which grants efficient design of parameters. Furthermore, a comprehensive study on robustness with respect to unmodeled dynamics, measurement noise, skewed clock rates, and perturbations on event thresholds are carried.

Regarding future research directions, many extensions of the generic estimation framework presented in this dissertation consists of N interconnected local observers are promising and can be considered. With significant advantages under this structure shown throughout the thesis, one direction lies on relaxation of constant gains and parameters to time-varying ones. In particular, one could consider Kalman-like updating laws for each individual observer, demonstrations of such design are available in literatures, see, e.g., [39]. In fact, multi-objective synthesis with time-varying gains is still a challenging and open question. Another interesting extension originates from the need of finite-time stability in network systems. When the plant is LTI, sliding-mode like techniques can be employed, e.g., [97]. Moreover, when information transmission over networks are restricted, the analog version of these problems are also subjected to further development. Note that in this work, new information is used through an information fusion state η. One could consider updating the local estimates $\hat{x}_i$'s directly when new information arrives via networks.

On the other hand, as two communication graphs (continuous and intermittent) are considered, other type of communication graphs or realistic graphs for certain applications could be considered. Note that for the intermittent interconnected observers within this work, each agent is collecting information from all neighbors intermittently. One can consider a “dual” problem where each agent broadcasts its local information whenever accessible, see, e.g., [98] which employs such model in consensus design of multi-agent systems. More interestingly, one may consider event-based communication protocol in the sense that an agent only communicate with its connected neighbors when necessary (determined by the event functions). Evaluation of the performance and robustness properties of designed observers over various communication networks/protocols would be essential for applications.

In addition, generalizing the framework for more complicated plants also extends its applicability. The challenge appears when the plant or each node in the network exhibits both continuous and discrete behavior (hybrid systems). In this scenario, a comprehensive studied notation itself is still an open question. A preliminary work of defining such stability notion for hybrid systems and its analysis is presented in [99]. Furthermore, due to the potential mismatch of domains of definition for solutions, see. e.g., [100], one may consider other stability notions like incremental stability as to characterize the overall behavior of the networks and to design observers.

Bibliography

[1] N. A. Chaturvedi, R. Klein, J. Christensen, J. Ahmed, and A. Kojic. Algorithms for advanced battery-management systems. *IEEE Control Systems*, 30(3):49–68, June 2010.

[2] C. Unterrieder, R. Priewasser, S. Marsili, and M. Huemer. Battery State Estimation Using Mixed Kalman/Hinfinity, Adaptive Luenberger and Sliding Mode Observer. *IEEE Vehicle Power and Propulsion Conference (VPPC)*, pages 71–76, October 2013.

[3] G. L. Plett. Extended kalman filtering for battery management systems of lipb-based HEV battery packs: Part 1. background. *Journal of Power Sources*, 134(2):252 – 261, 2004.

[4] S. J. Moura, N. Chaturvedi, and M. Krstić. Adaptive Partial Differential Equation Observer for Battery State-of-Charge/State-of-Health Estimation Via an Electrochemical Model. *Journal of Dynamic Systems, Measurement, and Control*, 136(1):1–11, October 2013.

[5] J. B. Rawlings and B. R. Bakshi. Particle filtering and moving horizon estimation. *Computers & Chemical Engineering*, 30:1529 – 1541, 2006.

[6] C. V. Rao, J. B. Rawlings, and J. H. Lee. Constrained linear state estimation - a moving horizon approach. *Automatica*, 37(10):1619 – 1628, 2001.

[7] J. B. Mare and J. A. De Dona. Moving horizon estimation of constrained nonlinear systems by carleman approximations. In *Proc. of 45th IEEE Conference on Decision and Control*, pages 2147–2152, Dec 2006.

[8] E. L. Haseltine and J. B. Rawlings. Critical evaluation of extended kalman filtering and moving-horizon estimation. *Industrial & Engineering Chemistry Research*, 44(8):2451–2460, 2005.

[9] H. Wang and S. Daley. Actuator fault diagnosis: an adaptive observer-based technique. *IEEE Transactions on Automatic Control*, 41(7):1073–1078, Jul 1996.

[10] J. Su, W. Chen, and B. Li. Disturbance observer based fault diagnosis. In *Proc of 33rd Chinese Control Conference (CCC)*, pages 3024–3029, July 2014.

[11] D. Luenberger. An introduction to observers. *IEEE Transactions on Automatic Control*, 16(6):596–602, December 1971.

[12] H. Kwakernaak and R. Silvan. *Linear Optimal Control Systems*. John WIley & Sons, Inc., 1972.

[13] S. Boyd, L. El Ghaoui, E. Feron, and V. Balakrishnan. *Linear Matrix Inequalities in Systems and Control Theory*. Siam, 1994.

[14] J. Jung, K. Huh, H. K. Fathy, and J. L. Stein. Optimal robust adaptive observer design for a class of nonlinear systems via an H-infinity approach. In *Proc of American Control Conference*, pages 3637–3642, June 2006.

[15] H. Li and M. Fu. A linear matrix inequality approach to robust H-infinity filtering. *IEEE Transactions on Signal Processing*, 45(9):2338–2350, 1997.

[16] H. J. Marquez. A frequency domain approach to state estimation. *Journal of the Franklin Institute*, 340(2):147–157, 2003.

[17] B. Egardt. *Stability of adaptive controllers*. Springer Verlag, 1979.

[18] P. Ioannou and J. Sun. *Robust adaptive control*. Prentice Hall, 1996.

[19] A. Astolfi and L. Praly. Global complete observability and output-to-state stability imply the existence of a globally convergent observer. *Mathematics of Control, Signals, and Systems (MCSS)*, 18(1):32–65, 2006.

[20] V. Andrieu, L. Praly, and A. Astolfi. High gain observers with updated gain and homogeneous correction terms. *Automatica*, 45(2):422 – 428, 2009.

[21] J. H. Ahrens and H. K. Khalil. High-gain observers in the presence of measurement noise: A switched-gain approach. *Automatica*, 45(4):936–943, 2009.

[22] L. K. Vasiljevic and H. K. Khalil. Differentiation with high-gain observers the presence of measurement noise. In *45th IEEE Conference on Decision and Control*, pages 4717–4722, Dec. 2006.

[23] A. A. Ball and H. K. Khalil. Analysis of a nonlinear high-gain observer in the presence of measurement noise. In *Proc. of American Control Conference*, pages 2584–2589, July 2011.

[24] R. G. Sanfelice and L. Praly. On the performance of high-gain observers with gain adaptation under measurement noise. *Automatica*, 47(10):2165–2176, 2011.

[25] H. Lei, J. Wei, and W. Lin. A global observer for observable autonomous

systems with bounded solution trajectories. In *Proc. of 44th IEEE Conference on Decision and Control*, pages 1911–1916, Dec. 2005.

[26] H. Shim, A. Tanwani, and Z. Ping. Back-and-forth operation of state observers and norm estimation of estimation error. In *Proc. of 51st IEEE Conference on Decision and Control*, pages 3221–3226, Dec 2012.

[27] T. Raff and F. Allgower. An impulsive observer that estimates the exact state of a linear continuous-time system in predetermined finite time. In *Proc. of Mediterranean Conference on Control and Automation*, pages 1–3, 2007.

[28] R. Engel and G. Kreisselmeier. A continuous-time observer which converges in finite time. *IEEE Transactions on Automatic Control*, 47(7):1202–1204, 2002.

[29] T. Raff, P. Menold, C. Ebenbauer, and F. Allgower. A finite time functional observer for linear systems. In *Proc. of 44th IEEE Conference on Decision and Control*, pages 7198–7203, Dec. 2005.

[30] T. Raff, F. Lachner, and F. Allgower. A finite time unknown input observer for linear systems. In *Proc. of 14th Mediterranean Conference on Control and Automation*, pages 1–5, June 2006.

[31] T. Raff and F. Allgöwer. An observer that converges in finite time due to measurement-based state updates. In 41, editor, *IFAC World Congress*, volume 2, pages 2693 – 2695, Seoul, Korea, 2008.

[32] W. Perruquetti, T. Floquet, and E. Moulay. Finite-time observers: Application to secure communication. *IEEE Transactions on Automatic Control*, 53(1):356–360, 2008.

[33] Y. Shen and X. Xia. Semi-global finite-time observers for nonlinear systems. *Automatica*, 44(12):3152–3156, 2008.

[34] T. Menard, E. Moulay, and W. Perruquetti. A global high-gain finite-time observer. *IEEE Transactions on Automatic Control*, 55(6):1500–1506, 2010.

[35] Y. Shen, Y. Huang, and J. Gu. Global finite-time observers for lipschitz nonlinear systems. *IEEE Transactions on Automatic Control*, 56(2):418–424, 2011.

[36] J. Cortes. Distributed Kriged Kalman filter for spatial estimation. *IEEE Transactions on Automatic Control*, 54(12):2816–2827, 2009.

[37] P. Alriksson and A. Rantzer. Distributed Kalman filtering using weighted averaging. In *Proc. of 17th International Symposium on Mathematical Theory of Networks and Systems*, 2006.

[38] R. Carli, A. Chiuso, L. Schenato, and S. Zampieri. Distributed Kalman filtering based on consensus strategies. *IEEE Journal on Selected Areas in Communications*, 26(4):622–633, 2008.

[39] R. Olfati-Saber. Distributed Kalman filter with embedded consensus filters. In *Proc. of 44th IEEE Conference on Decision and Control, European Control Conference.*, pages 8179–8184, 2005.

[40] R. Olfati-Saber. Distributed Kalman filtering for sensor networks. In *Proc. of 46th IEEE Conference on Decision and Control*, pages 5492–5498, 2007.

[41] D. P. Spanos, R Olfati-Saber, and R. M. Murray. Approximate distributed Kalman filtering in sensor networks with quantifiable performance. In *Proc. of 4th International Symposium on Information Processing in Sensor Networks*, Piscataway, NJ, USA, 2005. IEEE Press.

[42] Y. Zhao, Z. Duan, G. Wen, and G. Chen. Distributed H_∞ consensus of multi-agent systems: a performance region-based approach. *International Journal of Control*, 85(3):332–341, 2012.

[43] S. Martinez S. S. Kia, J. Cortes. Dynamical average consensus under limited control authority and privacy requirements. *International Journal of Robust and Nonlinear Control*, 2013.

[44] Y. Hong, G. Chen, and L. Bushnell. Distributed observers design for leader-following control of multi-agent networks. *Automatica*, 44(3):846–850, 2008.

[45] S. Wang and W. Ren. On the consistency and confidence of distributed dynamic state estimation in wireless sensor networks. In *Proc. 54th IEEE Conference on Decision and Control*, pages 3069–3074, Osaka, Japan, December 2015.

[46] A. T. Kamal, J. A. Farrell, and A. K. Roy-Chowdhury. Information weighted consensus filters and their application in distributed camera networks. *IEEE Transactions on Automatic Control*, 58(12):3112–3125, Dec 2013.

[47] R. Olfati-Saber, J. A. Fax, and R. M. Murray. Consensus and cooperation in networked multi-agent systems. *Proceedings of the IEEE*, 95(1):215–233, Jan 2007.

[48] W. Ren and E. Atkins. Distributed multi-vehicle coordinated control via local information exchange. *International Journal of Robust and Nonlinear Control*, 17(10-11):1002–1033, 2007.

[49] M. Mesbahi and M. Egerstedt. *Graph theoretic methods in multiagent networks.* Princeton University Press, 2010.

[50] D. P. Spanos, R. Olfati-Saber, and R. M. Murray. Dynamic consensus on mobile networks. In *IFAC world congress*, pages 1–6. Prague Czech Republic, 2005.

[51] Z. Li, Z. Duan, and G. Chen. Dynamic consensus of linear multi-agent systems. *Control Theory & Applications, IET*, 5(1):19–28, 2011.

[52] R. A. Freeman, P. Yang, and K. M. Lynch. Stability and convergence properties of dynamic average consensus estimators. In *Proc. of IEEE Conference on Decision and Control*, pages 398–403, 2006.

[53] L. Xiao, S. Boyd, and S. J. Kim. Distributed average consensus with least-mean-square deviation. *Journal of Parallel and Distributed Computing*, 67(1):33–46, 2007.

[54] R. Olfati-Saber. Kalman-consensus filter: Optimality, stability, and performance. In *Proc. of IEEE Conference on Decision and Control, held jointly with the Chinese Control Conference.*, pages 7036–7042, 2009.

[55] S. Kar and J. M. F. Moura. Distributed consensus algorithms in sensor networks with imperfect communication: Link failures and channel noise. *IEEE Transactions on Signal Processing*, 57(1):355–369, 2009.

[56] S. Park and N. C. Martins. Necessary and sufficient conditions for the stabilizability of a class of LTI distributed observers. *Proceedings of the IEEE Conference on Decision and Control*, pages 7431–7436, 2012.

[57] W. Zhang, L. Yu, and G. Feng. Optimal linear estimation for networked systems with communication constraints. *Automatica*, 47(9):1992 – 2000, 2011.

[58] D. Dačić and D. Nešić. Observer design for wired linear networked control systems using matrix inequalities. *Automatica*, 44(11):2840 – 2848, 2008.

[59] F. Dörfler, F. Pasqualetti, and F. Bullo. Continuous-time distributed observers with discrete communication. *IEEE Journal on Selected Topics in Signal Processing*, 7(2):296–304, 2013.

[60] P. Naghshtabrizi and J. P. Hespanha. Designing an observer-based controller for a network control system. In *Proc. of the 44th IEEE Conference on Decision and Control*, pages 848–853, Dec 2005.

[61] R. Postoyan and D. Nešić. A Framework for the Observer Design for Networked Control Systems. *IEEE Transactions on Automatic Control*, 57(5):1309–1314, 2012.

[62] L. Schenato, B. Sinopoli, M. Franceschetti, K. Poolla, and S. S. Sastry. Foundations of control and estimation over lossy networks. *Proceedings of the IEEE*, 95(1):163–187, Jan 2007.

[63] L. Shi, L. Xie, and R. M. Murray. Kalman filtering over a packet-delaying network: A probabilistic approach. *Automatica*, 45(9):2134 – 2140, 2009.

[64] F. S. Cattivelli and A. H. Sayed. Diffusion strategies for distributed kalman filtering and smoothing. *IEEE Transactions on Automatic Control*, 55(9):2069–2084, Sept 2010.

[65] T. Ahmed-Ali, I. Karafyllis, and F. Lamnabhi-Lagarrigue. Global exponential sampled-data observers for nonlinear systems with delayed measurements. *Systems & Control Letters*, 62(7):539 – 549, 2013.

[66] M. Farza, M. M'Saad, M. L. Fall, E. Pigeon, O. Gehan, and K. Busawon.

Continuous-discrete time observers for a class of mimo nonlinear systems. *IEEE Transactions on Automatic Control*, 59(4):1060–1065, April 2014.

[67] T. N. Dinh, V. Andrieu, M. Nadri, and U. Serres. Continuous-discrete time observer design for lipschitz systems with sampled measurements. *IEEE Transactions on Automatic Control*, 60(3):787–792, March 2015.

[68] F. Mazenc, V. Andrieu, and M. Malisoff. *Continuous-Discrete Observers for Time-Varying Nonlinear Systems: A Tutorial on Recent Results*, chapter 25, pages 181–188. 2015.

[69] F. Ferrante, F. Gouaisbaut, R. G. Sanfelice, and S. Tarbouriech. State Estimation of Linear Systems in the Presence of Sporadic Measurements. *Automatica*, page to appear, 2016.

[70] H. H. Rosenbrock. *Computer-Aided Control System Design*. Academic Press, 1974.

[71] M. Green and D. JN. Limebeer. *Linear robust control*. Courier Dover Publications, 1995.

[72] R. E. Kalman and R. S. Bucy. New results in linear filtering and prediction theory. *Journal of Fluids Engineering*, 83(1):95–108, March 1961.

[73] R. Goebel, R.G. Sanfelice, and A. Teel. *Hybrid Dynamical Systems, Modeling, Stability, and Robustness*. Princeton University Press, 2012.

[74] H. K. Khalil. *Nonlinear Systems*. Pearson Education, Inc, 2002.

[75] M. J. Corless; A. E. Frazho. *Linear Systems and Control: An Operator Perspective*. New York: Marcel Dekker, 2003.

[76] C. Scherer, P. Gahinet, and M. Chilali. Multiobjective output-feedback control via lmi optimization. *Automatic Control, IEEE Transactions on*, 42(7):896–911, jul 1997.

[77] M. Chilali and P. Gahinet. H_∞ design with pole placement constraints: an LMI approach. *Automatic Control, IEEE Transactions on*, 41(3):358–367, mar 1996.

[78] P. Bernhard T. Barsar. *H^∞-Optimal Control and Related Minmax Design Problems: A Dynamic Game Approach*. Birkhauser Boston, 1995.

[79] B. D. O. Anderson and S. Vongpanitlerd. *Network Analysis*. Englewood Cliffs, NJ: Prentice-Hall, 1973.

[80] C. Scherer. *The Riccati inequality and state-space H_∞-optimal control*. PhD thesis, University Wurzburg, Germany, 1990.

[81] J. Willems. Least squares stationary optimal control and the algebraic riccati equation. *Automatic Control, IEEE Transactions on*, 16(6):621–634, dec 1971.

[82] R.G. Sanfelice. Input-output-to-state stability tools for hybrid systems and their interconnections. *IEEE Transactions on Automatic Control*, 59(5):1360–1366, May 2014.

[83] T. Iwasaki. Robust performance analysis for systems with structured uncertainty. *International Journal of Robust and Nonlinear Control*, 6(2):85–99, 1996.

[84] Y. Ebihara and T. Hagiwara. New dilated LMI characterizations for continuous-time multiobjective controller synthesis. *Automatica*, 40(11):2003–2009, 2004.

[85] Y. Ebihara and T. Hagiwara. A dilated LMI approach to robust performance analysis of linear time-invariant uncertain systems. *Automatica*, 41(11):1933–1941, 2005.

[86] W. Xie. Multi-objective H_∞/α-stability controller synthesis of LTI systems. *IET Control Theory & Applications*, 2:51–55(4), January 2008.

[87] M. Kocvara and M. Stingl. Pennon: A code for convex nonlinear and semidefinite programming. *Optimization Methods and Software*, 18(3):317–333, 2003.

[88] Y. Li and R. G. Sanfelice. Interconnected observers for robust decentralized estimation with performance guarantees and optimized connectivity graph. *IEEE Transactions on Control of Network Systems*, PP(99):1–1, 2015.

[89] T. Ahmed-Ali, I. Karafyllis, and F. Lamnabhi-Lagarrigue. Global exponential sampled-data observers for nonlinear systems with delayed measurements. *Systems and Control Letters*, 62(7):539–549, 2013.

[90] P. Naghshtabrizi, J. P. Hespanha, and A. R. Teel. Exponential stability of impulsive systems with application to uncertain sampled-data systems. *Systems & Control Letters*, 57(5):378 – 385, 2008.

[91] T. Raff, M. Kogel, and F. Allgower. Observer with sample-and-hold updating for Lipschitz nonlinear systems with nonuniformly sampled measurements. In *Proc. American Control Conference*, pages 5254–5257, June 2008.

[92] F. Ferrante, F. Gouaisbaut, R. G. Sanfelice, and S. Tarbouriech. An Observer with Measurement-triggered Jumps for Linear Systems with Known Input. Rapport LAAS n13537. 2013. hal-00911851v1, October 2013.

[93] G. Pipeleers, B. Demeulenaere, J. Swevers, and L. Vandenberghe. Extended LMI characterizations for stability and performance of linear systems. *Systems & Control Letters*, 58(7):510 – 518, 2009.

[94] Y. Cao, W. Ren, and Z. Meng. Decentralized finite-time sliding mode estimators and their applications in decentralized finite-time formation tracking. *Systems & Control Letters*, 59(9):522 – 529, 2010.

[95] F. Ferrante, F. Gouaisbaut, R. G. Sanfelice, and S. Tarbouriech. A hybrid observer with a continuous intersample injection in the presence of sporadic measurements. In *Proc. 54th IEEE Conference on Decision and Control*, pages 5654–5659, Dec 2015.

[96] Z. Jin, V. Gupta, and Richard M. Murray. State estimation over packet dropping networks using multiple description coding. *Automatica*, 42(9):1441–1452, 2006.

[97] S. Yu and X. Long. Finite-time consensus for second-order multi-agent systems with disturbances by integral sliding mode. *Automatica*, 54:158 – 165, 2015.

[98] G. S. Seyboth, D. V. Dimarogonas, and K. H. Johansson. Event-based broadcasting for multi-agent average consensus. *Automatica*, 49(1):245 – 252, 2013.

[99] Y. Li and R. G. Sanfelice. Results on finite time stability for a class of hybrid systems. In *Proc. of American Control Conference*, 2016 (to appear).

[100] Y. Li, S. Phillips, and R. G. Sanfelice. Basic properties and characterizations of incremental stability prioritizing flow time for a class of hybrid systems. *Systems & Control Letters*, 90:7 – 15, 2016.

Appendix A

Publications

Journal articles/book chapters

1. Y. Li and R. G. Sanfelice. Interconnected observers for linear systems to improve rate of convergence and robustness to measurement noise. *IEEE Transactions on Control and Network Systems*, vol. 3, no. 1, pp. 1-11, March 2016.

2. Y. Li, S. Phillips and R. G. Sanfelice. Basic properties and characterizations of incremental stability prioritizing flow time for a class of hybrid systems. *Systems and Control Letters*, vol. 90, pp. 7-15, April 2016.

3. Y. Li and R. G. Sanfelice. A finite-time convergent observer with robustness to piecewise-constant measurement noise. *Automatica*, vol. 57, pp. 222-230, July 2015.

4. Y. Li and R. G. Sanfelice. Necessary and sufficient conditions for incremental graphical asymptotic stability for hybrid systems. *Springer (book chapter)*, 2016 (2nd Revision).

5. Y. Li and R. G. Sanfelice. Results on Finite Time Stability for A Class of Hybrid Systems. *Automatica*, 2016 (In preparation).

6. Y. Li, S. Phillips and R. G. Sanfelice. A Hybrid Distributed Observer for Linear Systems Under Intermittent Information with Robustness. *IEEE Transaction on Automatic Control*, 2016 (In preparation).

7. Y. Li, X. Lou and R. G. Sanfelice. Results on Stability and Robustness of Hybrid Limit Cycles for A Class of Hybrid Systems. *IEEE Transaction on Automatic Control*, 2016 (In preparation).

Conference papers (selected)

1. Y. Li and R. G. Sanfelice. A decentralized consensus algorithm for distributed state observers with robustness guarantees. In *Proc. of American Control Conference*, 2016.

2. Y. Li and R. G. Sanfelice. Results on finite time stability for a class of hybrid systems. In *Proc. of American Control Conference*, 2016.

3. X. Lou, Y. Li and R. G. Sanfelice. Results on stability and robustness of hybrid limit cycles for a class of hybrid systems. In *Proc. of IEEE Conference on Decision and Control*, 2015.

4. Y. Li and R. G. Sanfelice. On necessary and sufficient conditions for incremental stability of hybrid systems using the graphical distance between solutions. In *Proc. of IEEE Conference on Decision and Control*, 2015.

5. X. Lou, Y. Li and R. G. Sanfelice. On robust stability of limit cycles for hybrid systems with multiple jumps. In *Proc. of IFAC Analysis and Design of Hybrid Systems*, 2015.

6. Y. Li, S. Phillips and R. G. Sanfelice. Results on incremental stability for hybrid systems. In *Proc. of IEEE Conference on Decision and Control*, 2014.

7. Y. Li and R. G. Sanfelice. Robust distributed state observers with performance guarantees and optimized communication graph. In *Proc. of American Control Conference*, 2014 (Finalist for Best Student Paper Award).

8. Y. Li and R. G. Sanfelice. A robust finite-time convergent hybrid observer for linear systems. In *Proc. of IEEE Conference on Decision and Control*, 2013.

9. Y. Li and R. G. Sanfelice. A coupled pair of Luenberger observers for linear systems to improve rate of convergence and robustness to measurement noise. In *Proc. of American Control Conference*, 2013.

Recent submissions

1. Y. Li, S. Phillips and R. G. Sanfelice. On distributed intermittent observers for linear time-invariant systems with robustness. In *Proc. of IFAC NOLCOS*, 2016 (to appear).

2. S. Phillips, Y. Li and R. G. Sanfelice. On distributed intermittent consensus for first-order systems with robustness. In *Proc. of IFAC NOLCOS*, 2016 (to appear).